

# **OPTIMAL SHAPE DESIGN USING TRANSLATION INVARIANT COST FUNCTIONALS IN FLUID DYNAMICS**

by

**HENRY KASUMBA**

A thesis submitted to the  
Institute of Mathematics and Scientific Computing  
in conformity with the requirements for  
the degree of Doctorate of Science

Karl-Franzens University Graz,  
Austria

October- 2010

FIRST ADVISOR: PROF. DR. KARL KUNISCH  
SECOND ADVISOR: PROF. DR. GÜNTER BRENN



## ABSTRACT

In this thesis, shape design optimization problems for stationary viscous incompressible flows using translation invariant cost functionals are investigated. Two different study cases are considered. The first involving stationary incompressible Navier-Stokes equations in a bounded domain as PDE constraints and the second involving stationary incompressible Navier-Stokes equations in a domain with a free surface. With respect to the former, analytical expressions for the shape design sensitivity involving different cost functionals are derived rigorously in a generalized framework using the adjoint method and the material derivative concept. Numerical discretizations of the primal (flow), adjoint problems and as well as the analytical expressions for the shape design sensitivity are achieved using the Galerkin FEM method. Channel flow problems with a bump as a moving boundary and with an obstacle are taken as test examples. The shape of the bump is represented by Bezier curves of order 3 is optimized in order to minimize the vortices in the flow field. Numerical results are provided in various graphical forms for relatively low Reynolds numbers. Striking differences are found for the optimal shape control corresponding to the 3 different cost functionals, which constitute different quantifications of vorticity. With respect to the latter, design sensitivity involving different cost functionals are derived using a formal Lagrangian framework. Numerical discretization is again achieved with Galerkin FEM method. The optimization problem is solved in its original setting, that is to find a solution to free surface problem first and then to proceed to the upper level represented by the minimization of the cost functional. Since the free surface problem has to be solved several times for varying interface, an efficient method for solving the free surface problem is developed. Numerical results are presented which indicate the robustness of the proposed algorithm for solving this coupled problem.

Key words: Shape optimization, Free surface flow, Vorticity quantification.



## **ACKNOWLEDGMENTS**

The writing of this thesis has been one of the most significant challenges I have ever had to face. Without support, patience and guidance of the following people, this study would not have been completed. It is to them that I owe my deepest gratitude.

- My supervisor Professor Karl Kunisch. His wisdom, knowledge and commitment to highest standards inspired and motivated me. Moreover I want to thank him for giving me the opportunity to get in touch with international research groups.
- Professor Günter Brenn who undertook the role of my second advisor. His rigorous knowledge of fluid mechanics helped me quite a lot.
- Professor G. Haase for his tremendous help during my enrollment as a student, his guidance on the curriculum, as well as his invitation to the social events especially the unforgettable Glühwien in winter season.
- Dr. A. Laurain for his many helpful discussions on shape optimization. Prof. S. Keeling and Markus Müller for their cooperation.
- Professors G. Peichl and J. Haslinger for their willingness to be co-reporters on this work.
- My wife, son, parents, brother and sisters who have always supported, encouraged and believed in me, in all my endeavors.

Last I would like to acknowledge the financial support of FWF, without which, this research would not have been possible.

Karl-Franzens University Graz

October , 2010

Henry Kasumba



## NOMENCLATURE

$\mathbb{R}, \mathbb{R}^d$	Set of real numbers and set of vectors $\mathbf{x} = (x_i)_{i=1,\dots,d}$ , $x_i \in \mathbb{R}$
$d$	Space dimension
$u$	Scalar valued function
$\mathbf{u}, \mathbf{u}_h$	Vector valued function and its finite element approximation
$\mathbf{A}$	System matrix $\mathbf{A} \in \mathbb{R}^{m \times m}$
$\mathbf{A}^T$	Transpose of system matrix $\mathbf{A} \in \mathbb{R}^{m \times m}$
$\det \mathbf{A}$	Determinant of the matrix $\mathbf{A}$
$\mathbf{A}^{-T}$	Transpose of inverse of matrix $\mathbf{A}$
$X, X^*$	Generic Hilbert space and its dual.
$\langle \cdot, \cdot \rangle_{X, X^*}$	Duality pairing between $X$ and $X^*$
$(\cdot, \cdot)_X, \ \cdot\ _X$	The inner product in $X$ and the associated norm
$\mathcal{L}(X, Y)$ ( $\mathcal{L}(X)$ )	The set of bounded linear operators from $X$ to $Y$ (if $X = Y$ )
$\Omega, \Gamma = \partial\Omega$	Bounded domain (open and connected subset of $\mathbb{R}^2$ ) with sufficiently smooth boundary $\Gamma = \partial\Omega$ .
$I_d$	The identity operator.
$\Gamma_f$	Part of the boundary $\Gamma$ to be optimized.
$\Gamma_{fs}$	Part of the boundary $\Gamma$ with a free surface
$\mathbf{n}$	Normal unit (outward) direction with respect to the boundary
$\Gamma = \partial\Omega$ of some domain $\Omega$ .	
$\nabla$	Gradient, $\nabla \mathbf{u} := \left( \frac{\partial u_j}{\partial x_i} \right)_{i,j=1,\dots,d}$
$\operatorname{div} \mathbf{u}$	The divergence of the vector $\mathbf{u}$ in rectangular coordinates: $\operatorname{div} \mathbf{u} = \frac{\partial u_1}{\partial x_1} + \cdots + \frac{\partial u_n}{\partial x_n}$
$\mathbf{u} \cdot \nabla$	The nonlinear operator in the Navier-Stokes equations: $\mathbf{u} \cdot \nabla = u_1 \frac{\partial}{\partial x_1} + u_2 \frac{\partial}{\partial x_1}$

$\nabla \mathbf{u} : \nabla \mathbf{v}$	Tensor product, $\nabla \mathbf{u} : \nabla \mathbf{v} := \left( \sum_{i,j=1}^d \frac{\partial u_j}{\partial x_i} \frac{\partial v_j}{\partial x_i} \right) \in \mathbb{R}$
$A := B$	$A$ is defined by expression $B$ .
$u_x$	All subscripts indicate partial derivatives, e.g., $u_x = \frac{\partial u}{\partial x}$
$K$	Triangulation of domain $\Omega$ such that $\bar{\Omega} = \cup_{j=1}^N K_j$ .
$P^j(K), j = 1, 2..$	Polynomial of degree $j$ over a triangulation $K$ .
$H^m(\Omega)$	See section 2.1.1
$Re$	The Reynolds number of a flow.
BVP	Boundary value problem.
FEM	Finite element method.
PDE	Partial differential equation.
State	This is the solution to the PDE constraints for the optimization problem.

# CONTENTS

<b>1</b>	<b>Introduction</b>	<b>1</b>
1.1	Motivation . . . . .	1
1.2	Objectives . . . . .	3
1.3	Contributions . . . . .	4
1.4	Organization of thesis . . . . .	4
<b>2</b>	<b>PDE constrained-optimization problem in a bounded domain</b>	<b>7</b>
2.1	Setting of the state problem . . . . .	7
2.2	Optimization problem . . . . .	18
<b>3</b>	<b>Solving shape optimization problems</b>	<b>35</b>
3.1	Sensitivity analysis . . . . .	35
3.2	The Eulerian derivative . . . . .	39
3.3	The Eulerian derivative of the 3 cost functionals . . . . .	47
3.4	Solution approaches . . . . .	61
<b>4</b>	<b>Finite element approximation and discretization</b>	<b>73</b>
4.1	Weak formulation . . . . .	74
4.2	Approximation using mixed finite elements . . . . .	75
<b>5</b>	<b>Numerical solutions of reference problems</b>	<b>85</b>
5.1	Shape optimization of flow in a channel with a bump . . . . .	86
5.2	Shape optimization of an irrotational flow in a channel with a bump . . . . .	95
5.3	Flow in a channel with an obstacle . . . . .	99

<b>6 Free surface PDE constrained shape optimization</b>	<b>107</b>
6.1 The free surface problem . . . . .	107
6.2 Optimization problem . . . . .	120

## Appendices

<b>7 Computational details</b>	<b>141</b>
7.1 Componentwise splitting of vector matrices . . . . .	141
7.2 Computation of the local stiffness matrices . . . . .	143
7.3 Derivative of a finite element solution . . . . .	148
7.4 Numerical integration . . . . .	150

## LIST OF FIGURES

2.1 Domains for test problems . . . . .	17
2.2 Geometric constraints for test problems . . . . .	19
2.3 The Hausdorff distance $\delta(A, B)$ . . . . .	26
3.1 Domain . . . . .	36
3.2 Constrained perturbation of a circle . . . . .	71
3.3 Constrained perturbation of a circle (domain mesh) . . . . .	72
5.1 Domain for test problem 1 . . . . .	86
5.2 Test case geometries . . . . .	87
5.3 Discretized computational geometries . . . . .	88
5.4 Plot of distribution of vertical and horizontal components of velocity . . . . .	88
5.5 Vector plot of velocity vectors $u_1$ and $u_2$ . . . . .	89
5.6 Initial and final domain . . . . .	90
5.7 Velocity on final geometry . . . . .	90
5.8 History of three cost functionals during minimization of tracking type cost . . . . .	91
5.9 Initial and final design . . . . .	91
5.10 History of three cost functionals during minimization of curl type cost . . . . .	92
5.11 Initial geometry, flow field and final flow field with $J_2$ . . . . .	92
5.12 Illustration figure . . . . .	92
5.13 Initial geometry, flow field and final flow field with $J_3$ . . . . .	94
5.14 History of three cost functionals during minimization of cost $J_3$ . . . . .	94
5.15 Flow on initial geometry . . . . .	96
5.16 Final geometry and history of cost $J_1$ . . . . .	97
5.17 Final geometry and history of cost $J_2$ . . . . .	98
5.18 Domain for test problem 2 . . . . .	99

5.19	Direct numerical simulation geometries . . . . .	100
5.20	Discretized computational geometries . . . . .	100
5.21	Vector plots of flow field patterns . . . . .	100
5.22	Vector plot of velocity field on initial and optimal geometry . . . . .	101
5.23	Zoomed velocity field on initial and optimal geometry . . . . .	102
5.24	Vector plot of velocity field on initial and optimal geometry . . . . .	102
5.25	Zoomed velocity field and streamlines on the optimal geometry . . . . .	103
5.26	Vector plot of velocity field on initial and optimal geometry . . . . .	104
5.27	Zoomed velocity field on initial and optimal geometry . . . . .	104
6.1	Model domain . . . . .	108
6.2	Conditions at a free surface formed by an interface between two fluids . . . . .	110
6.3	Computational geometry . . . . .	118
6.4	Snapshots of velocity field at different iteration numbers . . . . .	119
6.5	Snapshots of velocity field at different iteration numbers . . . . .	119
6.6	Flow field at different values for the depth $d$ . . . . .	134
6.7	Variation of the cost functions with the depth $d$ . . . . .	134
6.8	Streamlines corresponding to flows at different depths . . . . .	134
6.9	Flow field at different values for the angles $\theta_i$ . . . . .	135
6.10	Variation of the cost functions with wall angles ( $\theta_i > 90^\circ$ ) . . . . .	135
6.11	Variation of the cost functions with wall angles ( $\theta_i < 90^\circ$ ) . . . . .	135
6.12	Admissible domains . . . . .	136
6.13	Snapshots of optimized geometries using the three costs $J_1$ , $J_2$ and $J_3$ . . . . .	137
6.14	Zoom of $\alpha_{opt}$ for $J_2$ and $J_3$ . . . . .	137
6.15	Convergence history using the three costs $J_1$ , $J_2$ and $J_3$ . . . . .	138
6.16	Snapshots of optimized geometries using the three costs $J_1$ , $J_2$ and $J_3$ . . . . .	139
7.1	Typical triangulation . . . . .	149

## **LIST OF TABLES**

- 5.1 The values of the cost functions on the three geometries . . . . . 101



# 1

## INTRODUCTION

In this thesis we consider optimal shape design problems. These are problems in the field of optimal control of partial differential equations. Typically we have a system governed by a partial differential equation whose solution  $u_\Omega$  depends on some variable geometric shape  $\Omega$ . The problem is to minimize a given cost functional over the set  $\mathcal{U}_{ad}$  of all admissible geometric shapes with a smooth or piecewise smooth boundary. Such problems arise for example in the optimal design of structures such as bridges, where one attempts to minimize compliance of the structure due to known loads and given material constraints. Here we consider shape optimization problems in the field of fluid mechanics. The typical constraints are therefore, the instationary Navier-Stokes equations. Solving the instationary Navier-Stokes equations is a challenging task, both theoretically and with regard to computational effort. On the other hand numerical optimization is frequently based on an iterative process every step of which requires several solutions of the instationary Navier-Stokes system or its linearization. For this reason, we have restricted our study to two dimensional stationary problems.

### 1.1 Motivation

The problem we consider in this thesis is inspired by the process of continuous casting of steel. Today, nearly 95% of crude steel is produced by continuous casting. Given increasing demands related to quality of steel products, further optimization of the processes involved in continuous casting is required e.g., process improvements in metallurgical reactors like ladle, tundish and mould. To this end, it is important to analyze the fluid flow and mixing behavior that result from various processing parameters.

Large vortex structures that appear in different metallurgical reactors influence the flotation and separation of non-metallic inclusions and therefore the steel quality. These large vortex structures are partly due to the shape of metallurgical reactors. Different shapes produce different kinds of

flows. Therefore the optimal vortex control by means of the shape of these metallurgical reactors is important to ensure a good quality output. However, to quantify the control objective, which is to minimize the large vortex structures, one needs a good choice of objective functional and this is not an ***obvious*** task. Specifically the quantification of a 'vortex' is still an active research area in the fluid mechanics community itself, see e.g., [Haller 2001], and this research had very little impact on optimal control so far.

### 1.1.1 The objective functional

An important topic in the field of optimal control of partial differential equation is the choice of appropriate cost functional which is used to quantify the control objective. This functional depends on the state variables  $(\mathbf{u}, p)$ , where  $\mathbf{u}$  and  $p$  are the velocity and pressure of the fluid respectively and in our case on the control parameters describing the shape of the domain. Typical cost functionals that are in use today for vortex reduction, are based on tracking-type functionals or minimization of the curl of the velocity field, i.e.,

$$J_1(\mathbf{u}) = \frac{1}{2} \int_{\tilde{\Omega}} |\mathbf{u}(x) - \mathbf{u}_d(x)|^2 dx, \quad J_2(\mathbf{u}) = \frac{1}{2} \int_{\tilde{\Omega}} |\operatorname{curl} \mathbf{u}(x)|^2 dx, \quad (1.1)$$

where  $\tilde{\Omega} \subset \Omega$  describes the subset of  $\Omega$  over which vortex reduction is desired and  $\mathbf{u}_d$  stands for a given desired flow field which contains some of the expected features of the controlled flow field without the undesired vortices. The tracking type cost functional  $J_1$  has a disadvantage that it does not attempt to quantify the vortices in the flow in terms of intrinsic properties of the velocity field  $\mathbf{u}$  or pressure  $p$  [Hintermüller 2004]. Moreover, this functional has the disadvantage that it is not invariant under changes of frames which move at a constant speed relative to each other. Functionals which allow such a property are referred to as **Galilean invariant**. Turning to the cost functional  $J_2$ , it is important to note that vorticity  $\operatorname{curl} \mathbf{u}(x)$  is Galilean invariant (see e.g., [Martinec , Chapter 5] for more details). Therefore, as an advantage, this cost functional is Galilean invariant. By using this functional, vortices in the flow can be thought of as regions of high vorticity magnitude. However, there is no universal threshold over which vorticity is to be considered high [Haller 2005]. More alarmingly, vorticity magnitude ( $|\operatorname{curl} \mathbf{u}|$ ) may also be high in parallel shear flows where no vortices are present [Jeong 1995]. Due to the draw backs with cost functionals  $J_1$  and  $J_2$ , another vortex definition is introduced in [Blackburn 1996], [Chong 1990]. Research in [Blackburn 1996], [Chong 1990], suggests that vortex cores are related to regions with complex eigenvalues of the velocity gradient tensor  $\nabla \mathbf{u}$ . This vortex definition is Galilean invariant [Haller 2001], [Jeong 1995]. From the linear-dynamic system point of view [Kaplan 1967], this definition suggests that a local streamline pattern is closed or spirals in a reference frame moving with the particle. In 2D, eigenvalues of  $\nabla \mathbf{u}$  are complex if  $\det \nabla \mathbf{u} > 0$

[Jeong 1995], and this suggests to choose ([Hintermüller 2004])

$$J_3(u) = \int_{\tilde{\Omega}} \max(0, \det \nabla \mathbf{u}(x)) dx. \quad (1.2)$$

Since  $J_3$  is based on a Galilean invariant vortex definition, it is a **Galilean invariant cost functional**. From the mathematical point of view,  $J_3$  penalizes the complex eigenvalues of the velocity gradient tensor  $\nabla \mathbf{u}(x)$  which are responsible for the swirling motion. However, due to the max-operation, the cost functional in (1.2) is not differentiable and hence we introduce the smoothing function  $g_3 \in C^2(\mathbb{R})$  defined, e.g, by

$$g_3(t) = \begin{cases} 0, & t \leq 0 \\ t^3/(t^2 + 1), & t > 0, \end{cases}$$

such that

$$J_3(u) = \int_{\tilde{\Omega}} g_3(\det \nabla \mathbf{u}(x)) dx. \quad (1.3)$$

## 1.2 Objectives

A first step towards investigating Galilean invariant cost-functionals for optimal vortex control in fluids was carried out in [Hintermüller 2004] for a driven-cavity problem, and later in [Kunisch 2007] for a flow around an obstacle. In [Kunisch 2007], striking differences were found for the optimal controls corresponding to the three different cost functionals expressed in (1.1)-(1.3). Our major goal is therefore to systematically analyze optimal shapes corresponding to the minimization of functionals (1.1)-(1.3). A comparison of optimal shapes corresponding to the three functionals in (1.1)-(1.3) is also of paramount importance.

### 1.2.1 The fundamental theoretical issues

In order to provide an adequate answer to the fundamental research question, three related fundamental theoretical issues have been isolated. These seek to determine the following:

- (a) First issue: Analyzing existence of solutions for a possibly wide class of feasible domains.
- (b) Second issue: Fixing necessary optimality conditions, allowing for an effective determination of the optimal domains;
- (c) Third issue: Development of numerical methods for approximate determination of optimal shapes by solving the optimality conditions or by optimizing the shape functionals under given constraints, with the use of appropriate computational methods.

We shall explore these issues in detail in the remainder of this thesis.

## 1.3 Contributions

A formal derivation of shape derivative of a general cost functional  $J$  can be found in the literature (see, e.g., [Sokolowski 1992], [Delfour 2001]). In the present work the computation of the shape derivative of  $J$  under minimal regularity assumptions is presented. The technique employed was first suggested in [Ito 2006] and then used in [Haslinger 2009] and allows to compute the shape derivative of the mapping  $\Omega \mapsto J(\Omega)$  without using the chain rule. In [Ito 2006], a cost functional of the form  $J(u, \Omega) = \int_{\Omega} j_1(u)$  was considered. In this work, a generalized cost functional of the form  $J(u, \Omega) = \int_{\Omega} j_1(C_{\gamma}u)$  is considered, where  $C_{\gamma}$  is an affine operator:

$$C_{\gamma}: u(\cdot) \mapsto Cu(\cdot) + \gamma(\cdot) \quad \gamma \in L^2(\Omega)$$

satisfying some properties to be specified later. Further more, flows often encountered in nature and engineering practice involve a separation of the the fluid with air. Due to over determined boundary conditions at the separating boundary, this leads to the free surface flow problem. The boundary of the free surface is not known a priori and its part of the problem. This boundary can be located by several techniques as we shall see later. In this work, however, we have dealt with a much more complicated problem namely, with the control of the shape of the flow domain  $\Omega$  containing a fluid with a free surface. Such an optimization problem has been treated for the Bernoulli problem in [Toivanen 2008] and has not been considered previously for the free surface flows governed by the Navier-stokes equations. Furthermore in [Toivanen 2008], sensitivity analysis was performed on a discretized problem. In this work, we have carried out the sensitivity analysis on the continuous free surface problem formulation . We solve the optimization problem by finding a solution to the free surface problem first and then proceed to the upper level represented by the minimization of the cost functional. Since the free surface problem as a state constraint has to be solved several times for varying interfaces, we used a fixed point type method to solve the problem. This method converges linearly [Cuvelier 1990](equivalent to the rate of convergence of a shape optimization method, which requires calculation of shape derivatives which is really only feasible for fairly simple systems).

## 1.4 Organization of thesis

The remainder of this work is organized as follows. In Chapter 2, a PDE constrained shape optimization problem in a bounded domain is introduced. A summary of important results from

functional analysis necessary for establishing existence and uniqueness of solutions to general boundary value problems is set forth. The existence and uniqueness of solutions first to the state, then to the adjoint equations and finally to the optimization problem are established.

In Chapter 3, a framework for establishing sensitivity analysis of a general optimization problem under minimal regularity requirements is presented. Several techniques that make use of sensitivity information to solve the shape optimization problem are briefly introduced. The method that we follow in this work is afterwards discussed in detail.

In Chapter 4, the numerical discretizations of the state and adjoint problems as well as the analytical expressions for the shape design sensitivity are achieved using the Galerkin FEM method. The solvability and well-posedness of the resulting discrete algebraic systems is discussed.

In Chapter 5, the numerical solutions to different reference problems are presented. The numerical results are provided in various graphical forms for relatively low Reynolds numbers. A comparison of optimal shapes corresponding to the three cost functions is made.

In Chapter 6, the shape optimization of a flow domain with a free surface is presented. The design sensitivities involving different cost functionals are derived using a formal Lagrangian framework. The technique for solving the free surface problem as a PDE constraint is discussed. An algorithm for solving the optimization problem is then set forth. Finally several numerical examples are presented.

In Chapter 7, some conclusive remarks and a summary of this work are given.



# 2

## PDE CONSTRAINED-OPTIMIZATION PROBLEM IN A BOUNDED DOMAIN

This chapter introduces the PDE constraint and optimization problems considered in this work. In particular, the PDE takes the form of stationary incompressible Navier-Stokes equations defined on a parameter-dependent domain. First, we give the classical formulation of the Navier-Stokes equations which in this case, take the meaning of the state problem. We then present the necessary notation and framework to provide the existence and uniqueness of weak solutions for the state problem. Different test problems that will be used in this work are then stated and the optimization problems are introduced. Finally, the existence of the solution to a specific optimization problem is analyzed. Readers who are already familiar with the topic may find the details of this chapter helpful to solidify their understanding of the mathematical concepts used in the derivation of sensitivity equations in the following chapter.

### 2.1 Setting of the state problem

We consider a stationary incompressible fluid flow in a domain  $\Omega \subset \mathbb{R}^2$  governed by the following system of equations

$$\begin{cases} -\eta \Delta \mathbf{u} + \rho \mathbf{u} \cdot \nabla \mathbf{u} + \nabla p = \mathbf{F}, & \text{in } \Omega, \\ \operatorname{div} \mathbf{u} = 0, & \text{in } \Omega, \end{cases} \quad (2.1)$$

where  $\eta$  is the dynamic viscosity and  $\rho$  representing the density of the fluid. The first equation is the balance of momentum from Newton's second law. The other relationship is the equation of continuity, where zero on the right-hand side states that the fluid is incompressible.

The Navier-Stokes system is the basis for computational modeling of the flow of an incompressible Newtonian fluid, such as air or water. Finding effective approximation methods for this system is at the heart of a broad range of engineering applications, from airplane design to nuclear

reactor safety evaluation. It is also the basic model for weather prediction, so is firmly embedded in everyday life. In (2.1)  $\mathbf{u}$  represents the velocity of the fluid and  $p$  represents the pressure. The convection term  $\mathbf{u} \cdot \nabla \mathbf{u}$  is simply the vector obtained by taking the convective derivative of each velocity component in turn, that is,  $\mathbf{u} \cdot \nabla \mathbf{u} := (\mathbf{u} \cdot \nabla) \mathbf{u}$ . The fact that this term is nonlinear is what makes life interesting. Conditions under which equations (2.1) have a unique stable solution will be a key feature of this chapter. The use of mixed approximation methods leads to nonlinear algebraic systems of equations which can only be solved using iteration. Two such strategies, namely Picard iteration and Newton iteration, are discussed later. The technique of solving the linearized equations that arise at each level of the nonlinear iteration will be considered in later chapters.

The boundary value problem that is considered is the system (2.1) posed on a two-dimensional domain  $\Omega$ , together with boundary conditions on  $\partial\Omega = \partial\Omega_D \cup \partial\Omega_N$  given by

$$\mathbf{u} = \mathbf{g} \text{ on } \partial\Omega_D, \quad \eta \frac{\partial \mathbf{u}}{\partial \mathbf{n}} - p \cdot \mathbf{n} = 0 \text{ on } \partial\Omega_N, \quad (2.2)$$

where  $\mathbf{n}$  denotes the outward-pointing normal to the boundary. If the velocity is specified everywhere on the boundary, that is, if  $\partial\Omega = \partial\Omega_D$ , then the pressure solution to the Navier-Stokes problem (2.1) is only unique up to a hydrostatic constant. The presence of the convection term in (2.1) means that layers in the solution are likely to arise. Having a quantitative measure of the relative contributions of convection and viscous diffusion is very useful. This can be achieved by normalizing the system (2.1) with respect to the size of the domain and the magnitude of the velocity. To this end, let  $U$  and  $L$  represent, respectively, the characteristic velocity and length of the flow governed by (2.1), (2.2), [Kundu 1990, Chapter 2]. We introduce the variables

$$\mathbf{u}^* = \mathbf{u}/U, \quad x^* = x/L,$$

as well as a properly scaled pressure  $p^*$  and a properly scaled forces  $\mathbf{f}^*$ , (see equation (2.4) below). Assuming constant density, the equations then become

$$\begin{cases} -\frac{1}{Re} \Delta \mathbf{u}^* + \mathbf{u}^* \cdot \nabla \mathbf{u}^* + \nabla p^* = \mathbf{f}^*, & \text{in } \Omega, \\ \operatorname{div} \mathbf{u}^* = 0 & \text{in } \Omega, \end{cases} \quad (2.3)$$

where the magnitude of the viscous forces are measured by the dimensionless Reynolds number

$$Re = \frac{UL\rho}{\eta}.$$

The relationship between the dimensionless pressure and volume forces respectively, are

$$\begin{cases} p^* = \frac{p}{\rho U^2}, \\ \mathbf{f}^* = \mathbf{F} \frac{L}{\rho U^2}. \end{cases} \quad (2.4)$$

For simplicity of notation, from now on we shall drop the asterisk-notation in (2.3) to write

$$\begin{cases} -\eta \Delta \mathbf{u} + \mathbf{u} \cdot \nabla \mathbf{u} + \nabla p = \mathbf{f} \text{ in } \Omega, \quad \eta = \frac{1}{Re}, \\ \operatorname{div} \mathbf{u} = 0 \text{ in } \Omega. \end{cases} \quad (2.5)$$

### 2.1.1 Basic definitions, notations and inequalities

In this section we summarize some of the basic notation and results concerning the necessary functional spaces, norms and trace operators. Specifically we describe some technical details of Sobolev spaces which are the natural spaces of functions in which to solve variational formulations of the Navier-Stokes equations (2.5) that will become important in the following subsections and in later chapters.

#### 2.1.1.1 Notation

Vector-valued functions are indicated by bold letters. A typical point in  $\mathbb{R}^d$  is denoted by  $x = (x_1, \dots, x_d)$ ; its norm  $|x|_{\mathbb{R}^d} = (\sum_{j=1}^d x_j^2)^{1/2}$ . Two notations for the inner product in  $\mathbb{R}^d$ ,  $d \in \mathbb{N}$ , shall be used, namely  $(x, y)$  respectively  $x \cdot y$ . The latter shall be used in case of nested inner products.

If  $\alpha = (\alpha_1, \dots, \alpha_d)$  is a  $d$ -tuple of nonnegative integers  $\alpha_j$ , we call  $\alpha$  a multi-index and denote by  $x^\alpha$  the monomial  $x_1^{\alpha_1} \cdots x_d^{\alpha_d}$ , which has degree  $|\alpha| = \sum_{j=1}^d \alpha_j$ . Also, if  $f : \mathbb{R}^d \mapsto \mathbb{R}$  is a smooth function, and  $\alpha = (\alpha_1, \dots, \alpha_d)$  is a multi-index, we define

$$\partial^\alpha f(x) = \frac{\partial^{|\alpha|} f}{\partial x_1^{\alpha_1} \cdots \partial x_d^{\alpha_d}}.$$

For a vector valued function  $\mathbf{u}$ , the gradient of  $\mathbf{u}$  denoted by  $\nabla \mathbf{u}$  is a second order tensor defined as follows

$$\nabla \mathbf{u} := \left( \frac{\partial u_j}{\partial x_i} \right)_{i,j=1,\dots,d}, \quad (2.6)$$

while the Jacobian of  $\mathbf{u}$  is the transpose of the gradient. The inner product between  $\mathbf{u}$  and  $\nabla \mathbf{u}$  denoted by  $\mathbf{u} \cdot \nabla \mathbf{u}$  is defined by

$$\mathbf{u} \cdot \nabla \mathbf{u} := \left( \sum_{i=1}^d u_i \frac{\partial u_j}{\partial x_i} \right)_{j=1,\dots,d} \in \mathbb{R}^d, \quad (2.7)$$

which represents the nonlinear term in the Navier-Stokes equation (2.5). The divergence of a vector field  $\mathbf{u}$  denoted by  $\operatorname{div} \mathbf{u}$  is defined as

$$\operatorname{div} \mathbf{u} := \sum_{i=1}^d \frac{\partial u_i}{\partial x_i}, \quad (2.8)$$

while the curl of a vector field  $\mathbf{u} = (u_1, u_2) \in \mathbb{R}^2$  denoted by  $\operatorname{curl} \mathbf{u}$  is defined as

$$\operatorname{curl} \mathbf{u} := \frac{\partial u_2}{\partial x_1} - \frac{\partial u_1}{\partial x_2}. \quad (2.9)$$

The determinant of the velocity gradient tensor of a vector field  $\mathbf{u} = (u_1, u_2) \in \mathbb{R}^2$  denoted by  $\det \nabla \mathbf{u}(x)$  is defined as

$$\det \nabla \mathbf{u}(x) := \frac{\partial u_1}{\partial x_1} \frac{\partial u_2}{\partial x_2} - \frac{\partial u_2}{\partial x_1} \frac{\partial u_1}{\partial x_2}. \quad (2.10)$$

Furthermore we define the tensor scalar product denoted by  $\nabla \mathbf{u} : \nabla \mathbf{v}$  by

$$\nabla \mathbf{u} : \nabla \mathbf{v} := \left( \sum_{i,j=1}^d \frac{\partial u_j}{\partial x_i} \frac{\partial v_j}{\partial x_i} \right) \in \mathbb{R}. \quad (2.11)$$

**Note 2.1.1.** Let  $X, Y$  be Hilbert spaces. We denote by  $(\cdot, \cdot)_X$  the inner product in  $X$  and by  $\|\cdot\|_X$  the associated norm.

**Note 2.1.2.** The topological dual of  $X$  is denoted by  $X^*$  and the duality pair is written as  $\langle \cdot, \cdot \rangle_{X^*, X}$ .

**Note 2.1.3.** The set of bounded linear operators from  $X$  to  $Y$  is denoted by  $\mathcal{L}(X, Y)$  or by  $\mathcal{L}(X)$  if  $X = Y$ . The norm of a bounded linear operator  $T : X \mapsto Y$  is given by

$$\|T\|_{\mathcal{L}(X, Y)} := \sup_{v \in X, \|v\|_X=1} \|Tv\|_Y. \quad (2.12)$$

**Definition 2.1.1.** For  $T \in \mathcal{L}(X, Y)$  we can also define an operator  $T^* \in \mathcal{L}(Y^*, X^*)$ , called the adjoint operator of  $T$ , satisfying

$$\langle f, T\phi \rangle_{Y^*, Y} = \langle T^*f, \phi \rangle_{X^*, X} \text{ for all } f \in Y^*, \phi \in X \quad (2.13)$$

and  $\|T\|_{\mathcal{L}(X, Y)} = \|T^*\|_{\mathcal{L}(Y^*, X^*)}$ .

### 2.1.1.2 Function spaces

We summarize the results about functional spaces used in this work. All results of this subsection are detailed in e.g., ([Adams 1975], [Quarteroni 1997, Chap.1] , [Evans 1998, Chap.5]). Therefore the theorems and assertions will be stated without proof.

Let  $\Omega$  be an open set of  $\mathbb{R}^d$ , and  $\bar{\Omega}$  its closure. We denote by  $C(\Omega)$ , the space of continuous real valued functions  $f$  in  $\Omega$ . For any integer  $k \geq 0$ , we denote by  $C^k(\Omega)$ , the space consisting of functions  $f$  which, together with all their partial derivatives  $\partial^\alpha f$  of orders  $0 \leq |\alpha| \leq k$ , are continuous in  $\Omega$ . Note that  $C^0(\Omega) \equiv C(\Omega)$ .

**Note 2.1.4.** Since  $\Omega$  is open, functions in  $C^k(\Omega)$  need not be bounded in  $\Omega$ . If  $f \in C(\Omega)$  is bounded and uniformly continuous in  $\Omega$ , then it possesses a unique, bounded extension to  $\bar{\Omega}$ .

Accordingly, we define the space  $C^k(\bar{\Omega})$  to consist of all those functions  $f \in C^k(\Omega)$  for which  $\partial^\alpha f$  is bounded and uniformly continuous in  $\Omega$  for all  $0 \leq |\alpha| \leq k$ . The space  $C^k(\bar{\Omega})$  is a Banach space endowed with the norm

$$\|f\|_{C^k(\bar{\Omega})} := \max_{0 \leq |\alpha| \leq k} \sup_{x \in \Omega} |\partial^\alpha f(x)|.$$

If moreover the function  $f$  has derivatives of all orders, then it is said to be of class  $C^\infty$  or smooth.

**Definition 2.1.2.** The support of a function  $f$  denoted by  $\text{supp } f$  is defined as

$$\text{supp } f = \overline{\{x \in \Omega \mid f(x) \neq 0\}}, \quad (2.14)$$

where the over line  $\overline{\{\cdot\}}$  indicates the closure of the set.

**Definition 2.1.3.** We denote by  $C_0^\infty(\Omega)$  (or  $\mathcal{D}(\Omega)$ ) the space of functions of class  $C^\infty$  with compact support in  $\Omega$ , i.e.,

$$C_0^\infty(\Omega) = \{f \in C^\infty(\Omega) \mid \text{supp } f \subset \Omega \text{ is compact}\}. \quad (2.15)$$

For  $f \in C_0^\infty(\Omega)$  and  $x_0 \in \partial\Omega$ , there is a neighborhood  $\mathcal{N}(x_0)$  such that all derivatives of  $f$  vanish on  $\mathcal{N}(x_0) \cap \Omega$ .

**Theorem 2.1.1** (Gauss-Theorem-(integration by parts)). Let  $u, v \in C^1(\Omega)$  then

$$\int_{\Omega} v \cdot \frac{\partial u}{\partial x_i} dx = \int_{\partial\Omega} v \cdot u \cdot n_i - \int_{\Omega} u \cdot \frac{\partial v}{\partial x_i} dx, \quad (2.16)$$

where  $\mathbf{n} = (n_1, \dots, n_d)$ .

Note: for  $v \in C_0^\infty(\Omega)$  we have

$$\int_{\Omega} v \cdot \frac{\partial u}{\partial x_i} dx = - \int_{\Omega} u \cdot \frac{\partial v}{\partial x_i} dx.$$

Another important class of functions related to the differentiable class is the class of Hölder continuous functions. If  $0 < \lambda \leq 1$ , we define  $C^{m,\lambda}(\bar{\Omega})$  to be the subspace of  $C^m(\bar{\Omega})$  consisting of

those functions  $f$  for which, for  $0 \leq |\alpha| \leq m$ ,  $\partial^\alpha f$  satisfies in  $\Omega$  a Hölder condition of exponent  $\lambda$ , that is, there exists a constant  $K$  such that

$$|\partial^\alpha f(x) - \partial^\alpha f(y)| < K|x - y|^\lambda, \quad (x, y) \in \Omega.$$

$C^{m,\lambda}(\bar{\Omega})$  is a Banach space with norm given by

$$\|f\|_{C^{m,\lambda}(\bar{\Omega})} = \|f\|_{C^m(\bar{\Omega})} + \max_{0 \leq |\alpha| \leq m} \sup_{\substack{x, y \in \Omega \\ x, y \neq 0}} \frac{|\partial^\alpha f(x) - \partial^\alpha f(y)|}{|x - y|^\lambda}.$$

### 2.1.1.3 The set $\Omega$

Let  $\Omega$  be an open set of  $\mathbb{R}^d$  with boundary  $\partial\Omega$ . In general we shall need some kind of smoothness property for  $\Omega$ , for the solution to have a certain required regularity. The smoothness of  $\Omega$  can be described in the following sense ([Delfour 2001, Chapter 3], [Adams 1975, chapter 4]). Let  $\mathbf{y} = (\mathbf{y}', y_d)$ , where  $\mathbf{y}' = (y_1, \dots, y_{d-1})$ . Denote by  $B$  the open unit ball in  $\mathbb{R}^d$  and define the sets

$$\begin{aligned} B_0 &:= \{\mathbf{y} \in B : y_d = 0\}, \\ B_+ &:= \{\mathbf{y} \in B : y_d > 0\}, \quad B_- := \{\mathbf{y} \in B : y_d < 0\}. \end{aligned}$$

Let  $\Phi$  be a one-to-one transformation of a domain  $U \subset \mathbb{R}^d$  onto a domain  $B \subset \mathbb{R}^d$ , having inverse  $\Psi = \Phi^{-1}$ . We call  $\Phi$ ,  $m$ -smooth if by writing  $y = \Phi(x)$  and

$$\begin{aligned} y_1 &= \Phi_1(x_1, \dots, x_d), & x_1 &= \Psi_1(y_1, \dots, y_d), \\ y_2 &= \Phi_2(x_1, \dots, x_d), & x_2 &= \Psi_2(y_1, \dots, y_d), \\ &\vdots &&\vdots \\ y_n &= \Phi_d(x_1, \dots, x_d), & x_n &= \Psi_d(y_1, \dots, y_d), \end{aligned} \tag{2.17}$$

the functions  $\Phi_1, \dots, \Phi_d$  belong to  $C^m(\bar{U})$  and the functions  $\Psi_1, \dots, \Psi_d$  belong to  $C^m(B)$ .

**Definition 2.1.4.**  $\Omega$  is said to be of class  $C^m$ ,  $0 \leq m \leq \infty$ , if

- a) There exists a locally finite open cover  $\{U_j\}$  of the boundary  $\partial\Omega$ , with  $\partial\Omega \subset \sum_{j=1}^d U_j$  and a corresponding sequence  $\{\Phi_j\}$  of  $m$ -smooth one-to-one transformation functions such that for each  $x \in \partial\Omega$ , there exists a neighborhood  $U_j(x)$  of  $x$  and  $\Phi_j : U_j(x) \mapsto B$ :

$$\begin{aligned} \Phi_j &\in C^m(U_j(x), B), \quad \Psi_j \in C^m(B, U_j(x)), \\ \text{int } \Omega \cap U_j(x) &= \Psi_j(B_+), \\ \partial\Omega \cap U_j(x) &= \Psi_j(B_0). \end{aligned} \tag{2.18}$$

- b)  $\Omega$  is said to be of class  $C^{k,l}$ ,  $0 \leq k$ ,  $0 < l \leq 1$ , if the conditions of (a) are satisfied with a map  $\Phi_j \in C^{k,l}(U_j(x), B)$  and inverse  $\Psi_j \in C^{k,l}(B, U_j(x))$ .

The hypothesis that  $\Omega$  is of class  $C^m$  is too strong for practical situations (such as a flow in a square) and hence for the existence and uniqueness of the solution to the Navier-Stokes equations, a weaker condition namely Lipschitz regularity ( $C^{0,1}$ ) of the boundary is sufficient. On the other hand, the sensitivity equations that we will derive in the following chapter require a higher regularity of the solution of the state equation. A sufficient condition for this regularity is a certain smoothness of the boundary, i.e., ( $C^2$ ) or at least  $C^{1,1}$ . It turns out that in two dimensions, if  $\Omega$  is convex and  $\partial\Omega$  is Lipschitz continuous, the conclusions in Chapter 3, remain valid [Grisvard 1985, Chapter 7].

### Lebesgue and Sobolev Spaces

**Definition 2.1.5** (Integrable functions). *Let  $\Omega$  be an open set of  $\mathbb{R}^d$ . We define by  $L^p(\Omega)$  with  $p \in [0, \infty]$ , the space of measurable functions whose  $p^{\text{th}}$  power is integrable over  $\Omega$ . Equipped with the norm*

$$\|f\|_{L^p(\Omega)} := \left( \int_{\Omega} |f(x)|^p dx \right)^{\frac{1}{p}}, \quad (2.19)$$

$L^p(\Omega)$  is a Banach space.

**Definition 2.1.6.** *For  $p = \infty$ ,  $L^\infty(\Omega)$  is the space the space of measurable functions which are essentially bounded over  $\Omega$ . That is there exists a constant  $K$  such that  $|f(x)| \leq K$  almost everywhere in  $\Omega$ . Equipped with the norm*

$$\|f\|_{L^\infty} = \inf\{K \in \mathbb{R}^+ \text{ such that } |f(x)| \leq K \text{ a.e in } \Omega\}, \quad (2.20)$$

$L^\infty(\Omega)$  is a Banach space.

**Theorem 2.1.2** (Hölder). *Let  $f \in L^p(\Omega)$  and  $g \in L^q(\Omega)$  with  $\frac{1}{p} + \frac{1}{q} = 1$ . Then  $fg \in L^1(\Omega)$  and*

$$\left| \int_{\Omega} fg dx \right| \leq \|f\|_{L^p} \|g\|_{L^q}. \quad (2.21)$$

We obtain the Cauchy Schwarz inequality if we choose  $p = q = 2$  in (2.21). This inequality implies that, for each nonzero, square-integrable  $g$ ,

$$\|f\|_{L^2} \geq \frac{\left| \int_{\Omega} fg dx \right|}{\|g\|_{L^2}}. \quad (2.22)$$

Choosing  $g = f$  yields equality in the above expression. Thus

$$\|f\|_{L^2} = \max_{g \neq 0} \frac{\left| \int_{\Omega} fg \, dx \right|}{\|g\|_{L^2}}. \quad (2.23)$$

The rightmost expression is a “variational characterization” of the  $L^2(\Omega)$  norm, that is, it expresses the norm in terms of something that is optimized.

**Definition 2.1.7.** For  $p = 2$ , the space  $L^2(\Omega)$  equipped with the scalar product

$$(f, g)_{\Omega} = \int_{\Omega} f(x)g(x) \, dx,$$

is a Hilbert space.

**Remark 2.1.1.** If  $\Omega$  is a bounded open set, then  $L^p(\Omega) \subset L^q(\Omega)$  for  $1 \leq q \leq p \leq \infty$ .

We recall the following density result.

**Theorem 2.1.3.** The space  $C_0^\infty$  is dense in  $L^2(\Omega)$ . That is, for all  $f \in L^2(\Omega)$  there exists a sequence  $f_n \in C_0^\infty(\Omega)$  such that

$$\lim_{n \rightarrow \infty} \|f - f_n\|_{L^2(\Omega)} = 0. \quad (2.24)$$

**Definition 2.1.8** (Sobolev space). Let  $\Omega$  be an open set of  $\mathbb{R}^d$ . For  $m \in \mathbb{N}$  and  $p \in [0, \infty]$  we define the Sobolev space

$$W^{m,p}(\Omega) := \{f \in L^p(\Omega) : \partial^\alpha f \in L^p(\Omega) \text{ for all } \alpha \in \mathbb{N}^d, |\alpha| \leq m\}, \quad (2.25)$$

where  $\partial^\alpha$  denotes the weak derivative of order  $|\alpha| := \sum_{i=1}^d \alpha_i$  defined by

$$\partial^\alpha f(x) = \frac{\partial^{|\alpha|} f}{\partial x_1^{\alpha_1} \cdots \partial x_d^{\alpha_d}}(x).$$

The space  $W^{m,p}(\Omega)$  is equipped with the norm

$$\|f\|_{W^{m,p}(\Omega)} := \left( \sum_{|\alpha| \leq m} \int_{\Omega} |\partial^\alpha f(x)|^p \, dx \right)^{\frac{1}{p}}. \quad (2.26)$$

For  $p = 2$ ,  $m = 0$  we obtain the space  $L^2(\Omega)$  with the inner product denoted by  $(\cdot, \cdot)_{\Omega}$

**Comment 2.1.1.** If  $p = 2$ , we denote  $W^{m,2}(\Omega)$  by  $H^m(\Omega)$ , which constitute Hilbert spaces with the scalar product

$$(f, g)_{H^m(\Omega)} := \sum_{|\alpha| \leq m} (\partial^\alpha f(x), \partial^\alpha g(x))_{\Omega}. \quad (2.27)$$

We now define another Sobolev space which is a subspace of  $H^1(\Omega)$  and which will be very useful for problems with Dirichlet boundary conditions.

**Definition 2.1.9.** *The Sobolev space  $H_0^1(\Omega)$  is defined as the closure of  $C_0^\infty(\Omega)$  in  $H^1(\Omega)$ . Equipped with the scalar product of  $H^1(\Omega)$ , the Sobolev space  $H_0^1(\Omega)$  is a Hilbert space, since it is a closed subspace of  $H^1(\Omega)$ .*

For the space  $H_0^1(\Omega)$ , the Poincaré inequality

$$\int_{\Omega} |f(x)|^2 dx \leq C \int_{\Omega} |\nabla f(x)|^2 dx \quad (2.28)$$

holds, where  $C$  is a positive constant dependent on  $\Omega$ . As a consequence of the Poincaré inequality is the following result which gives a simpler equivalent norm in  $H_0^1(\Omega)$ .

**Corollary 2.1.1.** *The seminorm*

$$|f|_{H_0^1(\Omega)} = \left( \int_{\Omega} |\nabla f(x)|^2 dx \right)^{\frac{1}{2}},$$

is a norm over  $H_0^1(\Omega)$  which is equivalent to the usual norm induced by that of  $H^1(\Omega)$ .

**Remark 2.1.2.** For spaces of vector-valued functions, we will use boldface notation. For example,  $\mathbf{H}^m(\Omega) = [H^m(\Omega)]^2$  denotes the space of  $\mathbb{R}^2$ -valued functions such that each component of an element in  $\mathbf{H}^s(\Omega)$  belongs to  $H^s(\Omega)$ . Moreover the norm and scalar products for the vector valued functions will correspond to the sum of norms and scalar products of each vector component for example for  $\mathbf{u} = (u_1, u_2) \in \mathbb{R}^2$ ,  $\|\mathbf{u}\|_{\mathbf{L}^2(\Omega)} = \|u_1\|_{L^2(\Omega)} + \|u_2\|_{L^2(\Omega)}$ . Therefore the above discussion and what follows still remains valid for the vector valued case. In case above notation is not used, then  $\mathbf{H}^m(\Omega) = [H^m(\Omega; \mathbb{R}^2)]$ , equivalently for  $C(\Omega; \mathbb{R}^2)$  etc. for vector valued functions shall often be used in the following chapter.

### Sobolev embeddings

The importance of Sobolev spaces lies in their connections with the spaces of continuous and uniformly continuous functions. This is expressed in embedding theorems that we summarize in the following paragraphs (see e.g., [Girault 1986, Chap.1], [Quarteroni 1997, Chap.1] , [Evans 1998, Chap.5] for more details).

**Definition 2.1.10.** *Let  $X, Y$  be Banach Spaces. We say  $X$  is continuously embedded in  $Y$  and write*

$$X \hookrightarrow Y,$$

*if  $X \subset Y$  and there is a constant  $K$  such that for all  $f \in X$*

$$\|f\|_Y \leq K\|f\|_X.$$

So, in particular definition 2.1.10 says that if  $f^{(j)} \in X$  and  $f^{(j)} \rightarrow f$  as  $j \rightarrow \infty$ , then also  $f^{(j)} \rightarrow f$  as  $j \rightarrow \infty$  in  $Y$ . The next theorem summarizes important results on continuous embedding in Sobolev spaces.

**Theorem 2.1.4** (Sobolev embedding theorem (Case  $m = 1$ )). *Let  $\Omega \subset \mathbb{R}^d$  be an open bounded set of class  $C^1(\Omega)$  and  $1 \leq p \leq \infty$ , then*

$$\begin{cases} \text{if } p < d, W^{1,p}(\Omega) \hookrightarrow L^q \text{ for all } q \in [1, p^*] \text{ with } \frac{1}{p^*} = \frac{1}{p} - \frac{1}{d} \\ \text{if } p = d, W^{1,p}(\Omega) \hookrightarrow L^q \text{ for all } q \in [1, +\infty) \\ \text{if } p > d, W^{1,p}(\Omega) \hookrightarrow C(\overline{\Omega}). \end{cases} \quad (2.29)$$

**Example**(for the case  $m > 1$ ): Let  $\Omega \subset \mathbb{R}^d$  be a bounded set with  $C^1$  boundary and let  $1 \leq p \leq \infty$ . If  $mp > n$  we have

$$W^{m,p} \hookrightarrow C^{m-\lceil \frac{n}{p} \rceil - 1}(\overline{\Omega}).$$

**Definition 2.1.11.** *Let  $X, Y$  be Banach Spaces. We say  $X$  is compactly embedded in  $Y$  and write*

$$X \hookrightarrow \hookrightarrow Y,$$

*if  $X$  is continuously embedded in  $Y$  and every bounded sequence in  $X$  has a subsequence which is convergent in  $Y$ .*

**Theorem 2.1.5** (Rellich-Kondrachov). *Let  $\Omega \subset \mathbb{R}^d$  be an open bounded set of class  $C^1(\Omega)$  and  $1 \leq p \leq \infty$ , then*

$$\begin{cases} \text{if } p < d, W^{1,p}(\Omega) \hookrightarrow \hookrightarrow L^q \text{ for all } q \in [1, p^*) \text{ with } \frac{1}{p^*} = \frac{1}{p} - \frac{1}{d} \\ \text{if } p = d, W^{1,p}(\Omega) \hookrightarrow \hookrightarrow L^q \text{ for all } q \in [1, +\infty) \\ \text{if } p > d, W^{1,p}(\Omega) \hookrightarrow \hookrightarrow C(\overline{\Omega}). \end{cases} \quad (2.30)$$

In particular  $H_0^1(\Omega) \hookrightarrow \hookrightarrow L^4(\Omega)$  for  $d = 2$ .

### Trace

An important property of functions  $v \in H^m(\Omega)$ ,  $m$  an integer  $\geq 1$  is that they have a well-defined restriction to the boundary  $\partial\Omega$ . (This is an issue because functions in  $H^m(\Omega)$  need not be continuous). The theoretical basis for this assertion is the following lemma.

**Theorem 2.1.6.** *Let  $\Omega \subset \mathbb{R}^d$  be an open bounded regular domain of class  $C^m$ ,  $m$  an integer  $\geq 1$ . Then there exists a continuous surjective mapping from  $H^m(\Omega) \mapsto \prod_{j=0}^{m-1} H^{m-j-1/2}(\partial\Omega)$ , which maps  $v \mapsto \{\gamma_j v = \frac{\partial^j v}{\partial n^j}; j = 0, \dots, m-1\}$ .*

**Remark 2.1.3.** The trace theorem 2.1.6 enables us to define the space  $H^{1/2}(\partial\Omega)$  as

$$H^{1/2}(\partial\Omega) := \{\beta \in L^2(\partial\Omega) : \text{there exists } v \in H^1(\Omega), \gamma_0 v = \beta\},$$

with the norm

$$\|\beta\|_{H^{1/2}(\partial\Omega)} = \inf\{\|v\|_{H^1(\Omega)} : \gamma_0(v) = \beta\}.$$

Next we introduce another space, intermediate between  $L^2(\Omega)$  and  $H^1(\Omega)$ , for vector valued functions. This space is very useful in later chapters.

**Definition 2.1.12.** The space  $H_{div}(\Omega)$  is defined by

$$H_{div}(\Omega) = \{\sigma \in (L^2(\Omega))^d : \operatorname{div}\sigma \in L^2(\Omega)\}. \quad (2.31)$$

Equipped with the scalar product  $(\sigma, \zeta)_{H_{div}(\Omega)} = \int_{\Omega} (\sigma(x) : \zeta(x) + \operatorname{div}\sigma(x) \cdot \operatorname{div}\zeta(x)) dx$  and with the norm  $\|\sigma\|_{H_{div}(\Omega)} = \sqrt{(\sigma, \sigma)_{H_{div}(\Omega)}}$ , the space  $H_{div}(\Omega)$  is a Hilbert space.

## 2.1.2 Reference problems

In order to investigate the effect of the three functionals in (1.1-1.3) in minimizing the vortices in a given flow field, 3 reference problems posed on domains shown in Figure 2.1 are considered. In

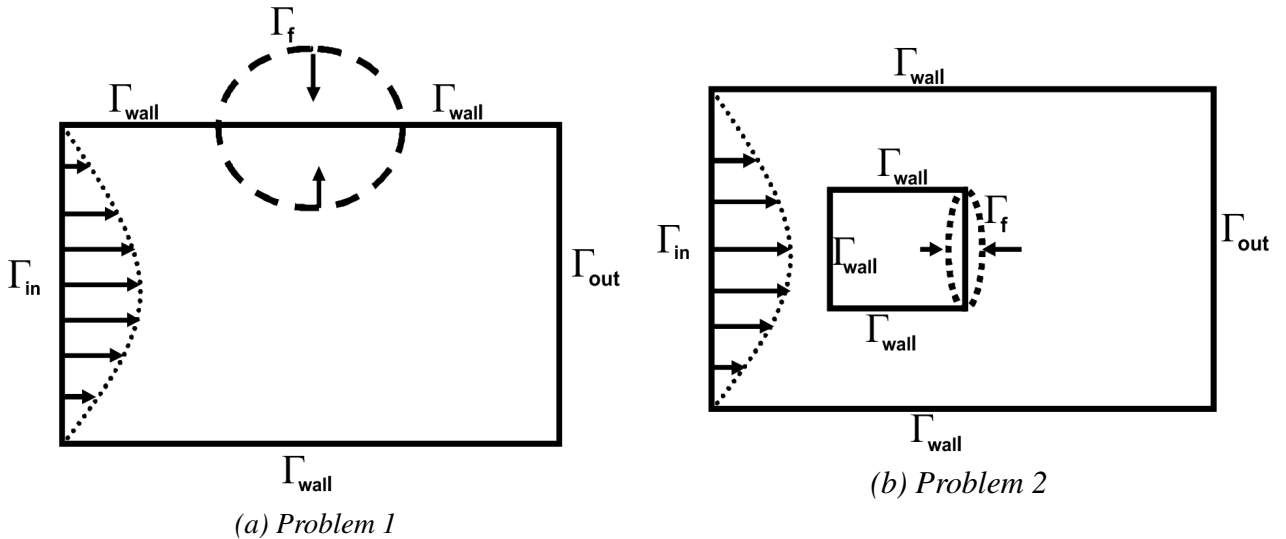


Figure 2.1: Domains for test problems

all cases the reference velocity  $U$  is unity,  $\rho$  is unity, and the reference length  $L$  is of order unity. This means that the Reynolds number of the flow is typically given by  $\frac{1}{\eta}$ , so that a flow problem is convection-dominated whenever  $\eta < 1$ . The forcing term  $\mathbf{f}$  is zero in the two test cases. In all

test cases, the boundary  $\Gamma_f$  is used as a control boundary by means of which the shape of  $\Omega$  will be governed. The boundary conditions for the test problems are given as follows

$$\begin{cases} \mathbf{u} = \mathbf{g} & \text{on } \Gamma_{in}, \\ \mathbf{u} = \mathbf{0} & \text{on } \Gamma_w \cup \Gamma_f, \\ -p\mathbf{n} + \frac{1}{Re} \frac{\partial \mathbf{u}}{\partial \mathbf{n}} = 0 & \text{on } \Gamma_{out}, \end{cases} \quad (2.32)$$

where  $\partial\Omega_D = \Gamma_{in} \cup \Gamma_w \cup \Gamma_f$  and  $\partial\Omega_N = \Gamma_{out}$ , for the first two test problems depicted Figures (2.1 a-b). In the third test problem, we shall consider the following boundary conditions

$$\begin{cases} \mathbf{u} = \mathbf{g} & \text{on } \Gamma_{in} \cup \Gamma_w \cup \Gamma_f \cup \Gamma_{out}, \end{cases} \quad (2.33)$$

given in Figure (2.1 a), where  $\partial\Omega_D = \Gamma_{in} \cup \Gamma_w \cup \Gamma_f \cup \Gamma_{out}$  and  $\partial\Omega_N = \emptyset$ . For the compatibility and regularity for the solutions of the equations (2.1),  $\mathbf{g}$  must satisfy

$$\int_{\partial\Omega} \mathbf{g} \cdot \mathbf{n} \, ds = 0.$$

The test problems consist in solving the stationary incompressible Navier-Stokes equations defined on a parameter-dependent domains as shown in Figures (2.1 a-b) in order to minimize the cost functions introduced earlier in (1.1-1.3), and this gives rise to a shape optimization problem that we introduce in the next subsection.

## 2.2 Optimization problem

In this section, we introduce the optimization problem. We then briefly discuss the concept of convergence of sequences of domains. We further discuss the concept of continuous dependence of solutions of the Navier-Stokes equations on geometry variations. This is a fundamental property ensuring the existence of optimal solutions. An extensive discussion can be found in monographs, see e.g., [Haslinger 2003, Chapt. 2].

Our goal is to find “an optimal”  $\Gamma_f$  by minimizing the cost functionals in (1.1-1.3) which depend on  $(\Omega, \mathbf{u})$ . We let  $\Gamma_f$  be described as a graph represented by the curve  $\alpha : [a, b] \mapsto \mathbb{R}$ . Consequently the problem of finding “an optimal”  $\Gamma_f$  is equivalent to the one of finding an optimal control  $\alpha$  over a set of admissible controls  $\mathcal{U}_{ad}$  to be specified later on. Let  $\mathcal{G}$  be the graph of the control-to-state (generally multi-valued) mapping :

$$\mathcal{G} := \{(\alpha, \mathbf{u}, p); \alpha \in \mathcal{U}_{ad}, (\mathbf{u}, p) \text{ is a weak solution of (2.5)-(2.33)}\}.$$

The optimization problem can be written in the following form:

$$\begin{cases} \text{Find } \{\alpha^*, \mathbf{u}^*, p^*\} \in \mathcal{G} \text{ such that} \\ J(\Omega(\alpha^*), \mathbf{u}(\alpha^*)) \leq J(\Omega(\alpha), \mathbf{u}(\alpha)) \text{ for all } \{\alpha, \mathbf{u}, p\} \in \mathcal{G}. \end{cases} \quad (2.34)$$

To describe  $\mathcal{U}_{ad}$ , we let  $\Gamma_f$  be described as a graph represented by the curve  $\alpha : [a, b] \mapsto \mathbb{R}$  which we assume to be given by

$$\Gamma_f(\alpha) = \{(x_1, x_2) : x_1 \in [a, b], x_2 = \alpha(x_1)\}, \quad (2.35)$$

for problem 1 and

$$\Gamma_f(\alpha) = \{(x_1, x_2) : x_1 = \alpha(x_2), x_2 \in [d, e]\}, \quad (2.36)$$

for problem 2, where  $a, b, d, e$  are given constants. (see Figure 2.2).

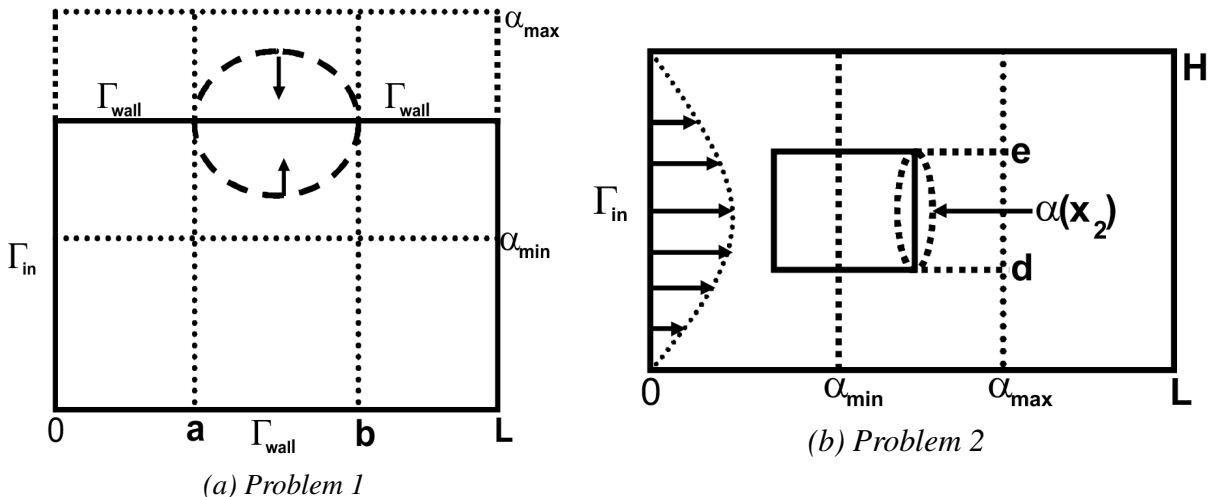


Figure 2.2: Geometric constraints for test problems

Consequently one may define the admissible family of curves defining  $\Gamma_f(\alpha)$  for problem 1 as follows:

$$\begin{aligned} \mathcal{U}_{ad} = \{&\alpha \in C^{0,1}([a, b]) \mid 0 < \alpha_{min} \leq \alpha(x_1) \leq \alpha_{max}, \\ &\alpha(a) = \alpha_0, \alpha(b) = \alpha_1, |\alpha'| \leq L_1, \text{ a.e in } (a, b)\}, \end{aligned}$$

and

$$\begin{aligned} \mathcal{U}_{ad} = \{&\alpha \in C^{0,1}([d, e]) \mid 0 < \alpha_{min} \leq \alpha(x_2) \leq \alpha_{max}, \\ &\alpha(d) = \alpha_0, \alpha(e) = \alpha_1, |\alpha'| \leq L_2, \text{ a.e in } (d, e)\}. \end{aligned}$$

for problem 2, where  $L_1, L_2, a, b, d, e, \alpha_{min}, \alpha_{max}$  are given constants such that  $\mathcal{U}_{ad}$  is non-empty.

## 2.2.1 Existence of solution

In order to establish the existence of a solution to the minimization problem, one needs to examine in the first place whether the PDE constraint equation possesses a solution, and if it does, whether such a solution is unique. It is after a deep understanding of these two concepts that one proceeds to analyze the existence of a solution to the optimization problem. Hence to this end, we shall start our discussion with the existence of solution to the stationary incompressible Navier-Stokes system. Since there exist nice references covering these issues for example, [Temam 1977, Chapter. 2] , [Girault 1986, Chapter. 4] , [Ladyzhenskaya 1969, Chapter. 5] , the proofs will be omitted.

### 2.2.1.1 Existence and uniqueness of solution to state problem

In this subsubsection, we discuss the existence and uniqueness of solutions to the state problem (2.5). We present our analysis based on stationary incompressible Navier-Stokes system with homogeneous Dirichlet boundary conditions, because here one can get a first impression of the importance of a major criterion for stability condition, (the inf-sup-condition), which appears frequently in the analysis and numerical solution of mixed problems. Extension to non-homogeneous Dirichlet boundary conditions is accomplished by standard techniques. Analysis for mixed Dirichlet-Neumann boundary condition is beyond the scope of this work. We refer the reader to [Bach 1998, page. 127] .

### 2.2.1.2 Existence of solution to state problem

We start the discussion with the introduction of the weak formulation of the state system (2.5) with boundary conditions as in (2.33) with  $\mathbf{g} = 0$ . This formulation will form a basis for the finite element approximation of the minimization problem to be introduced in later chapters as well as the general theory of shape sensitivity to be introduced in the next chapter. To begin with, we introduce the following functional spaces

$$\mathbf{H}_0^1 = \{\mathbf{v} \in [H^1(\Omega)]^2 | \mathbf{v} = 0 \text{ on } \partial\Omega_D\}, \quad (2.37)$$

$$L_0^2 = \{q \in L^2(\Omega) | \int_{\Omega} q \, dx = 0\}. \quad (2.38)$$

Then the weak formulation of the state system can be stated as follows:

Given  $\mathbf{f} \in \mathbf{H}^{-1}(\Omega)$ , find  $(\mathbf{u}, p) \in \mathbf{H}_0^1 \times L_0^2(\Omega)$  such that for all  $(\psi, \xi) \in \mathbf{H}_0^1 \times L^2(\Omega)$

$$\begin{cases} \eta \int_{\Omega} \nabla \mathbf{u} : \nabla \psi \, dx + \int_{\Omega} (\mathbf{u} \cdot \nabla) \mathbf{u} \psi \, dx - \int_{\Omega} p \operatorname{div} \psi \, dx = \int_{\Omega} \mathbf{f} \psi \, dx, \\ \int_{\Omega} \operatorname{div} \mathbf{u} \xi \, dx = 0. \end{cases} \quad (2.39)$$

Alternatively to (2.39), we can introduce the divergent free subspace  $\mathcal{H}$  of  $\mathbf{H}_0^1$ , given by

$$\mathcal{H} := \left\{ \psi \in \mathbf{H}_0^1 : \operatorname{div} \psi = 0 \text{ in } \Omega \right\}, \quad (2.40)$$

and formulate the weak formulation of the Navier-Stokes system as follows:

Given  $\mathbf{f} \in \mathbf{H}^{-1}(\Omega)$ , find  $\mathbf{u} \in \mathcal{H} \times L_0^2(\Omega)$  such that for all  $\psi \in \mathcal{H}$

$$\eta \int_{\Omega} \nabla \mathbf{u} : \nabla \psi \, dx + \int_{\Omega} (\mathbf{u} \cdot \nabla) \mathbf{u} \psi \, dx = \int_{\Omega} \mathbf{f} \psi \, dx. \quad (2.41)$$

The existence of  $p$  is discussed below.

**Lemma 2.2.1.** *Let  $\Omega$  be a bounded domain in  $\mathbb{R}^2$  with a Lipschitz continuous boundary, and let  $\mathbf{F}$  be an element of  $(\mathbf{H}_0^1)^*$  (i.e., a linear continuous functional on  $\mathbf{H}_0^1$ ). Then  $\mathbf{F}$  vanishes identically on  $\mathcal{H}$  if and only if there exists a function  $p \in L^2(\Omega)$  such that*

$$\mathbf{F}(\psi) = (p, \operatorname{div} \psi) \text{ for all } \psi \in \mathbf{H}_0^1. \quad (2.42)$$

Further, (2.42) defines a unique function  $p$  up to an additive constant.

*Proof.* The proof of this lemma, that we omit for the sake of brevity, is reported, e.g., in [Girault 1986, page. 22].  $\square$

**Note 2.2.1.** *If  $(\mathbf{u}, p)$  is a solution to (2.39), then  $\mathbf{u}$  is a solution to (2.41). The converse is also true in a sense stated by the following result.*

**Lemma 2.2.2.** *Let  $\mathbf{u}$  be a solution to (2.41). Then there is a unique  $p \in L_0^2(\Omega)$  such that  $(\mathbf{u}, p)$  is a solution to (2.39)*

*Proof.* See, e.g., [Quarteroni 1997, pg. 341], [Temam 1977, page. 164].  $\square$

The challenge here is to establish the existence of weak solution to (2.41) and whether this solution is uniquely defined. The key to establishing the existence of a weak solution to the state equation is the Lax-Milgram theorem [Girault 1986, pg.10]. The other ingredient is a version of Brouwer's fixed point theorem; details are given in [Girault 1986, pg. 284-287] or [Quarteroni 1997, pg. 341-342]. Let us define the bilinear form  $a(\cdot, \cdot) : \mathcal{H} \times \mathcal{H} \mapsto \mathbb{R}$  via

$$a(\mathbf{u}, \psi) = \eta \int_{\Omega} \nabla \mathbf{u} : \nabla \psi \, dx, \quad (2.43)$$

and the trilinear form  $c : \mathbf{H}^1(\Omega) \times \mathbf{H}^1(\Omega) \times \mathbf{H}^1(\Omega) \mapsto \mathbb{R}$  via

$$c(\mathbf{v}; \mathbf{u}, \psi) := \sum_{i,j=1}^2 \int_{\Omega} v_j \frac{\partial u_i}{\partial x_j} \psi_i \, dx = \int_{\Omega} (\mathbf{v} \cdot \nabla) \mathbf{u} \psi \, dx. \quad (2.44)$$

Then (2.41) can be written as

$$a(\mathbf{u}, \psi) + c(\mathbf{u}; \mathbf{u}, \psi) = \langle \mathbf{f}, \psi \rangle. \quad (2.45)$$

Important properties of  $c$  over  $\mathcal{H}$  are listed in the following Lemma.

**Lemma 2.2.3.** *The trilinear form  $c$  has the following properties*

1.  $c(\mathbf{v}; \psi, \psi) = 0$  for all  $\mathbf{v} \in \mathcal{H}$ ,  $\psi \in \mathbf{H}^1(\Omega)$ .
2.  $c(\mathbf{v}; \psi, \mathbf{u}) = -c(\mathbf{v}; \mathbf{u}, \psi)$  for all  $\mathbf{v} \in \mathcal{H}$ ,  $\psi, \mathbf{u} \in \mathbf{H}^1(\Omega)$ .

*Proof.* See e.g., [Temam 1977, page. 163], [Girault 1986, page. 285].  $\square$

**Lemma 2.2.4.** *The trilinear form  $c$  is continuous.*

*Proof.* See e.g., [Girault 1986, page. 284].  $\square$

For  $\mathbf{f} \in \mathbf{H}^{-1}(\Omega)$ , we define

$$\|\mathbf{f}\|_{\mathcal{H}^*} := \sup_{\psi \in \mathcal{H}} \frac{|\langle \mathbf{f}, \psi \rangle|}{\|\nabla \psi\|_{\mathbf{L}^2}}.$$

A well-known (sufficient) condition for existence is stated in the following theorem .

**Theorem 2.2.1.** *For each  $\mathbf{f} \in \mathbf{H}^{-1}(\Omega)$ , there exists a solution  $\mathbf{u}$  to the Navier-stokes problem and a constant  $C > 0$  such that*

$$\|\mathbf{u}\|_{\mathbf{H}^1} \leq \frac{C}{\eta} \|\mathbf{f}\|_{\mathcal{H}^*}. \quad (2.46)$$

*Proof.* The proof is carried out using the Galerkin method. See for example [Girault 1986, pg.284-287] for details.  $\square$

### 2.2.1.3 Uniqueness of weak solutions

A well known condition for uniqueness (see e.g., [Girault 1986, Theorem 2.2]) is that the forcing function is small in the sense that

$$\|\mathbf{f}\|_{\mathcal{H}^*} \leq \frac{\eta^2}{C^*}, \quad (2.47)$$

where

$$C^* = \sup_{\mathbf{u}, \mathbf{v}, \psi \in \mathcal{H}} \frac{|c(\mathbf{v}; \mathbf{u}, \psi)|}{\|\nabla \mathbf{u}\|_{\mathbf{L}^2} \|\nabla \mathbf{v}\|_{\mathbf{L}^2} \|\nabla \psi\|_{\mathbf{L}^2}}.$$

For the more general case of nonhomogeneous Dirichlet boundary condition

$$\mathbf{u} = \mathbf{g} \text{ on } \partial\Omega_D,$$

(that we use for one of our test problem), we need the following technical result to prove the existence and uniqueness (see [Girault 1986, Lemma 2.3]).

**Lemma 2.2.5.** For any  $\varepsilon > 0$ , there exists a function  $\tilde{\mathbf{u}} \in \mathbf{H}^1(\Omega)$  such that  $\operatorname{div} \tilde{\mathbf{u}} = 0$ ,  $\gamma_0 \tilde{\mathbf{u}} = \mathbf{g}$  and

$$|c(\psi; \tilde{\mathbf{u}}, \psi)| \leq \varepsilon \|\nabla \psi\|_{\mathbf{L}^2}^2, \text{ for all } \psi \in \mathcal{H}.$$

*Proof.* A proof can be found in ([Girault 1986, page.287-291]).  $\square$

The following theorem asserts the existence of a solution to the nonhomogeneous Dirichlet problem.

**Theorem 2.2.2.** Let  $\mathbf{f} \in \mathbf{H}^{-1}(\Omega)$  and  $\mathbf{g} \in \mathbf{H}^{\frac{1}{2}}(\partial\Omega_D)$ , then there exists at least one pair  $(\mathbf{u}, p) \in \mathbf{H}^1(\Omega) \times L_0^2(\Omega)$  solution to (2.5),(2.33).

*Proof.* Let  $\tilde{\mathbf{u}} \in \mathbf{H}^1(\Omega)$  be such that

$$\operatorname{div} \tilde{\mathbf{u}} = 0, \quad \gamma_0 \tilde{\mathbf{u}} = \mathbf{g}.$$

For  $\mathbf{w} \in \mathcal{H}$ , we set  $\mathbf{u} = \tilde{\mathbf{u}} + \mathbf{w}$  in problem (2.45) such that it may be equivalently expressed as

$$a(\mathbf{w}, \psi) + c(\mathbf{w}; \mathbf{w}, \psi) + c(\tilde{\mathbf{u}}; \mathbf{w}, \psi) + c(\mathbf{w}; \tilde{\mathbf{u}}, \psi) = (\mathbf{f}, \psi) - a(\tilde{\mathbf{u}}, \psi) - c(\tilde{\mathbf{u}}; \tilde{\mathbf{u}}, \psi). \quad (2.48)$$

Existence of  $\mathbf{w}$  in (2.48) can now be established, using Lemma 2.2.5, and concepts in the proof of Theorem 2.2.1. See [Girault 1986, page 291] for details.  $\square$

Let  $\tilde{\mathbf{u}}$  and  $\mathbf{f}$  be defined as in Lemma 2.2.5 and Theorem 2.2.2. We define the linear form  $l : \mathcal{H} \rightarrow \mathbb{R}$  by

$$\langle l, \psi \rangle = (\mathbf{f}, \psi) - a(\tilde{\mathbf{u}}, \psi) - c(\tilde{\mathbf{u}}; \tilde{\mathbf{u}}, \psi). \quad (2.49)$$

Its  $\mathcal{H}^*$  norm is given by

$$\|l\|_{\mathcal{H}^*} = \sup_{\psi \in \mathcal{H}} \frac{|\langle l, \psi \rangle|}{\|\nabla \psi\|_{\mathbf{L}^2}}. \quad (2.50)$$

Furthermore, we define  $\rho : \mathcal{H} \mapsto \mathbb{R}$  by

$$\rho(\tilde{\mathbf{u}}) = \sup_{\psi \in \mathcal{H}} \frac{c(\psi; \tilde{\mathbf{u}}, \psi)}{\|\nabla \psi\|_{\mathbf{L}^2}^2},$$

and  $\eta_0 := \eta_0(\Omega, ; \mathbf{f}, \mathbf{g})$  by

$$\eta_0 = \inf \left\{ \rho(\tilde{\mathbf{u}}) + (C^* \|l\|_{\mathcal{H}^*})^{1/2} : \tilde{\mathbf{u}} \in \mathbf{H}^1(\Omega) \text{ satisfies conditions of Lemma 2.2.5} \right\}.$$

The basic uniqueness result now follows.

**Theorem 2.2.3.** Assume the hypothesis of Theorem 2.2.2. If  $\eta > \eta_0(\Omega, ; \mathbf{f}, \mathbf{g})$ , then problem (2.5),(2.33) has a unique solution .

*Proof.* See e.g., [Girault 1986, page.292] for the details of the proof.  $\square$

Therefore weak solutions to the PDE constraint equations exist for any Reynolds number, however, uniqueness can be guaranteed only for “large enough ” values of  $\eta$  or for small values of data  $(\mathbf{f}, \mathbf{g})$ .

**Remark 2.2.1.** Despite the mathematical elegance of the velocity formulation (2.41), it is rarely used in practice to approximate the velocity field, see e.g., [Girault 1986, page. 301]. In computations, often the velocity-pressure formulation is used (2.39). Therefore, there is need to ensure that the pressure  $p$  computed can be bounded above by the data. The condition which guarantees that this is the case is the inf-sup condition

$$\inf_{\substack{q \in L_0^2(\Omega) \\ q \neq 0}} \sup_{\substack{\psi \in \mathbf{H}_0^1(\Omega) \\ \psi \neq 0}} \frac{|\int_{\Omega} q \operatorname{div} \psi \, dx|}{\|\psi\|_{\mathbf{H}_0^1} \|q\|_{L_0^2}} \geq \gamma > 0. \quad (2.51)$$

**Remark 2.2.2.** If  $\partial\Omega_N \neq \emptyset$ , then one needs to prescribe the outflow boundary conditions on  $\partial\Omega_N$  to ensure stability of  $\mathbf{u}$  and consequently of  $p$ .

Although the results above provide existence and uniqueness for the basic Navier-Stokes problems, they do not address the continuity of these solutions with respect to the parameter describing the shape of the domain. We address this question in the next subsection.

## 2.2.2 Existence of solution to the optimization problem

To discuss the existence of a solution to the shape optimization problem, one needs to endow the set of admissible solutions  $\mathcal{U}_{ad}$  with a topology (which is a non-trivial task ) and show that with respect to that topology, the set  $\mathcal{U}_{ad}$  is compact. If the cost functional is continuous or at least lower semi-continuous on this set of admissible domains, then we can conclude that there exist at least one minimizer for the optimization problem. It is important to note that the cost functional  $J$  depends on the shape of the domain  $\Omega$  through the solution of the PDE. Hence to discuss continuity of  $J$ , ones needs to show that the solutions of the PDE (which we already know exist and unique under certain conditions discussed above) are continuous with respect to domain changes (which is a non-trivial task) for an appropriate topology of domains. In what follows, we shall briefly discuss how we handle these issues without being exhaustive. An interested reader should visit e.g., [Pironneau 1984, Chapter 3], [Delfour 2001, Chapter 6], and [Haslinger 2003, Chapter 2] for more details.

### 2.2.2.1 Convergence of sequences of domains

The set of domains is not a vector space and has a very rich and complicated structure. Therefore, to deal with the domain optimization problem, we need to define an appropriate convergence criterion with respect to domains. Since domains and corresponding function spaces are changing, we need to embed all domains in a fixed “hold all” domain  $D$  such that  $\cup_{\alpha \in \mathcal{U}_{ad}} \Omega(\alpha) \subset D$  in order to discuss the convergence of domains and corresponding functions . For example in Figure 2.2,  $D = [0, L] \times [0, \alpha_{max}]$ .

#### Topology on the set of domains

There are several important notions of convergence of domains which we discuss briefly in the following paragraphs :

**① Convergence in the sense of the characteristic functions:** A class of domains for which optimal shape design problems has an optimal solution was studied in [Chenais 1975]. It was shown by Chenais that the set of domains with a cone property (see e.g., [Pironneau 1984, page. 35]) is compact for the strong  $L^2(D)$ -topology of characteristic functions of its elements. Let the domain  $\Omega$  be identified with it's characteristic function  $\chi_\Omega$ . The convergence of the sequence  $\{\Omega_n\}$  of domains having the uniform cone property may be defined by

$$\Omega_n \rightarrow \Omega \iff \int_D |\chi_{\Omega_n} - \chi_\Omega|^2 d\Omega \rightarrow 0 \text{ as } n \rightarrow \infty. \quad (2.52)$$

However this topology has some draw backs, for example, it does not preserve the the regularity of domains and it is thus not appropriate for general optimization problems in which the regularity is an issue. In addition,  $\chi_\Omega$  is defined only almost everywhere, whereas the solution of certain partial differential equations may be affected by removing a set of measure zero.

**② Convergence with respect to parametrization:** If the domains  $\Omega$  can be parameterized in a simple way, then it is natural to define convergence in terms of functions  $\alpha$  belonging to  $\mathcal{U}_{ad}$ . For example in our case, the domains  $\{\Omega(\alpha)\}_{\alpha \in \mathcal{U}_{ad}}$  are determined by a variable part  $\Gamma_f(\alpha)$  of the boundary  $\partial\Omega$ . Hence for each  $\alpha_n \in \mathcal{U}_{ad}$ , let  $\Omega_n = \Omega(\alpha_n)$ . Then convergence of  $\Omega_n$  to  $\Omega$  is defined by

$$\begin{aligned} \Omega_n \rightarrow \Omega &\iff \alpha_n \rightrightarrows \alpha \text{ in } [a, b] \text{ for problem 1 and} \\ \Omega_n \rightarrow \Omega &\iff \alpha_n \rightrightarrows \alpha \text{ in } [d, e] \text{ for problem 2,} \end{aligned} \quad (2.53)$$

where  $\alpha_n \rightrightarrows \alpha$  means  $\alpha_n$  converges uniformly to  $\alpha$  in a given interval. However if the

domain can not be parameterized in a simple way, then more stringent topologies need to be introduced.

**③ Convergence in the sense of Hausdorff:** If the inclusion between subdomains of  $\mathbb{R}$  is the main issue, for example in problems of domain identification, the topology induced by the Hausdorff metric is widely used. It is based on the Hausdorff distance between two sets. Let  $A$  and  $B$  be two closed subsets of  $\mathbb{R}$  (see Figure 2.3) and define the Hausdorff metric  $\delta$  by

$$\delta(A, B) = \max\{\rho(A, B), \rho(B, A)\}, \text{ where } \rho(A, B) = \sup_{x \in A} \inf_{y \in B} |x - y|_{\mathbb{R}}.$$

Then, the topology on closed subsets of  $\mathbb{R}$  is defined by

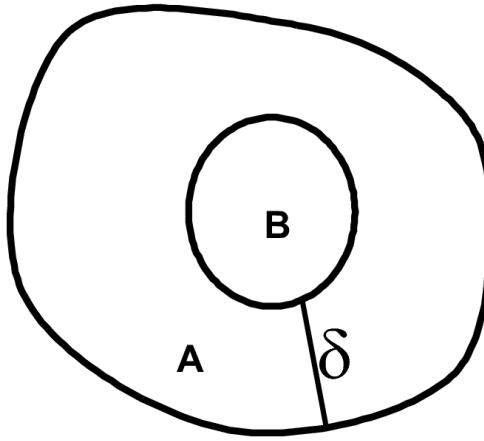


Figure 2.3: The Hausdorff distance  $\delta(A, B)$

$$A_m \rightarrow A \iff \delta(A_m, A) \rightarrow 0.$$

**Remark 2.2.3.** From now onwards, we shall use  $\Omega(\alpha_n) \rightarrow \Omega(\alpha), n \rightarrow \infty$  to mean convergence in the sense of (2.53).

### Compactness

We now turn to the aspect of compactness of the set of admissible domains. From the well known Arzelà-Ascoli theorem it follows that  $\mathcal{U}_{ad}$  is compact with respect to the convergence defined in (2.53) [Haslinger 2003].

### Continuity with respect to the shape

We define the reduced cost functional  $\hat{J}_i : \mathcal{U}_{ad} \mapsto \mathbb{R}, i = 1, 2, 3$  by  $\hat{J}_i(\Omega) = J_i(\mathbf{u}(\Omega), \Omega)$ . In order to obtain the existence of optimal shapes we need the continuity, or at least the lower semi-

continuity of the shape functional  $\hat{J}_i(\Omega)$ . Since our shape functionals depends on the solution  $\mathbf{u}(\Omega)$  of a partial differential equation, we need the continuity of this solution with respect to the shape for an appropriate topology of domains, in particular the topology defined in (2.53). The following lemma will become important in what follows

**Lemma 2.2.6.** *Let  $\Omega(\alpha_n) \rightarrow \Omega(\alpha)$ ,  $n \rightarrow \infty$ , and let  $\chi_n, \chi$  be the characteristic functions of  $\Omega(\alpha_n), \Omega(\alpha)$ , respectively. Then*

$$\chi_n \rightarrow \chi \text{ in } L^p(D) \text{ for all } p \in [1, \infty).$$

*Proof.* See [Chenais 1975] for details of the proof.  $\square$

We begin with the establishment of the continuity of  $\mathbf{u}(\Omega)$  with respect to the shape of the domain  $\Omega$ . A key point to pay attention to, is how to define convergence of functions belonging to  $\Omega(\alpha)$  for different  $\alpha \in \mathcal{U}_{ad}$ . The domains  $\Omega(\alpha)$  are uniformly Lipschitz continuous for each  $\alpha \in \mathcal{U}_{ad}$ , and hence have the uniform extension property, [Chenais 1975]. Let  $D$  be the hold all domain as in the above Lemma and define the extension operator

$$\varepsilon_\Omega : H_0^1(\Omega) \mapsto H_0^1(D)$$

by

$$(\varepsilon_\Omega u)(x) = \begin{cases} u(x), & x \in \Omega \\ 0, & x \in D \setminus \Omega. \end{cases}$$

We shall use the symbol  $\tilde{u}$  to denote the extension of  $u$  from  $H_0^1(\Omega)$  to  $H_0^1(D)$ .

**Definition 2.2.1.** *Let  $\mathbf{u}_n \in \mathbf{H}_0^1(\Omega_n)$ ,  $\mathbf{u} \in \mathbf{H}_0^1(\Omega)$ ,  $\alpha_n, \alpha \in \mathcal{U}_{ad}$ . We say that*

$$\begin{aligned} \mathbf{u}_n \rightarrow \mathbf{u} &\text{ if and only if } \tilde{\mathbf{u}}_n \rightarrow \tilde{\mathbf{u}} \text{ in } \mathbf{H}_0^1(D), \\ \mathbf{u}_n \rightharpoonup \mathbf{u} &\text{ if and only if } \tilde{\mathbf{u}}_n \rightharpoonup \tilde{\mathbf{u}} \text{ in } \mathbf{H}_0^1(D), \quad n \rightarrow \infty. \end{aligned} \tag{2.54}$$

The symbols  $\rightarrow$  and  $\rightharpoonup$  in (2.54) denote strong and weak convergence in  $\mathbf{H}_0^1(\Omega)$  respectively.

**Lemma 2.2.7.** *Let  $\Omega_n, \Omega \in \mathcal{U}_{ad}$ , be such that  $\Omega(\alpha_n) \rightarrow \Omega(\alpha), n \rightarrow \infty$  and let  $\mathbf{u}_n := \mathbf{u}(\alpha_n)$  be the unique solution to the Navier-Stokes equations in  $\Omega_n$ . Then*

$$\tilde{\mathbf{u}}_n \rightarrow \mathbf{u} \text{ in } \mathbf{H}_0^1(D), \quad n \rightarrow \infty.$$

*Proof.* The function  $\mathbf{u}_n$  being a solution of the Navier-Stokes equations satisfies the following

estimate(see previous subsection)

$$\|\tilde{\mathbf{u}}_n\|_{\mathbf{H}^1(D)} = \|\mathbf{u}_n\|_{\mathbf{H}^1(\Omega_n)} \leq \frac{C}{\eta} \|\mathbf{f}\|_{\mathbf{L}^2(D)}, \quad (2.55)$$

with a constant  $C$  independent of  $n$ . From this, one can pass to a subsequence  $\{\tilde{\mathbf{u}}_{n_k}\}$  of  $\{\tilde{\mathbf{u}}_n\}$  such that

$$\tilde{\mathbf{u}}_{n_k} \rightharpoonup \tilde{\mathbf{u}} \text{ in } \mathbf{H}_0^1(D), \quad k \rightarrow \infty. \quad (2.56)$$

We first prove that  $\mathbf{u}|_{D \setminus \bar{\Omega}} = 0$  which implies that  $\mathbf{u}|_{\Omega} \in \mathbf{H}_0^1(\Omega)$ . Since  $\mathbf{H}_0^1(D)$  embeds compactly into  $\mathbf{L}^2(D)$ ,

$$\tilde{\mathbf{u}}_{n_k} \rightarrow \tilde{\mathbf{u}} \text{ in } \mathbf{L}^2(D), \quad k \rightarrow \infty. \quad (2.57)$$

If  $\chi_{\bar{\Omega}^c}$  denotes the characteristic function of the complement of  $\bar{\Omega}$ , then Fatou's Lemma and Theorem 4.3 in Delfour-Zolésio ([Delfour 2001]) imply

$$\begin{aligned} \int_D \chi_{\bar{\Omega}^c} \mathbf{u}^2 dx &\leq \int_D \liminf_{k \rightarrow \infty} \chi_{\bar{\Omega}_{n_k}^c} \mathbf{u}^2 dx \leq \liminf_{k \rightarrow \infty} \int_D \chi_{\bar{\Omega}_{n_k}^c} \mathbf{u}^2 dx \\ &= \liminf_{k \rightarrow \infty} \int_D \chi_{\bar{\Omega}_{n_k}^c} |\mathbf{u} - \tilde{\mathbf{u}}_{n_k}|^2 dx \leq \lim_{k \rightarrow \infty} \int_D |\mathbf{u} - \tilde{\mathbf{u}}_{n_k}|^2 dx = 0. \end{aligned}$$

As a consequence  $\mathbf{u} = 0$  holds almost everywhere on  $\chi_{\bar{\Omega}^c}$  which implies that

$$\mathbf{u}_{\Omega} = \mathbf{u}|_{\Omega} \in \mathbf{H}_0^1(\Omega).$$

We need to show that  $\mathbf{u}|_{\Omega}$  solves

$$\eta \int_{\Omega} \nabla \mathbf{u} : \nabla \psi dx + \int_{\Omega} (\mathbf{u} \cdot \nabla) \mathbf{u} \psi dx = \int_{\Omega} \mathbf{f} \psi dx, \quad \text{for all } \psi \in \mathcal{H}. \quad (2.58)$$

Observe that  $\tilde{\mathbf{u}}_{n_k}$  satisfies

$$\eta \int_D \chi_n \nabla \tilde{\mathbf{u}}_{n_k} : \nabla \tilde{\psi} dx + \int_D \chi_n (\tilde{\mathbf{u}}_{n_k} \cdot \nabla) \tilde{\mathbf{u}}_{n_k} \tilde{\psi} dx = \int_D \chi_n \mathbf{f} \tilde{\psi} dx, \quad \psi \in \mathcal{H}(\Omega_n), \quad (2.59)$$

where  $\chi_n$  is the characteristic function of  $\Omega_n$ . Choose

$$\xi \in \mathbf{V}(\Omega) = \{\phi \in (C_0^\infty(\Omega))^2 \mid \operatorname{div} \phi = 0 \text{ in } \Omega\}.$$

Then there exists  $N_{\xi} \in \mathbb{N}$  such that  $\operatorname{supp}(\xi) \subset \Omega_n$  for  $n \geq N_{\xi}$  [Delfour 2001, page.264]. Consequently we may use  $\tilde{\xi}$  as a test function in (2.59):

$$\eta \int_D \chi_n \nabla \tilde{\mathbf{u}}_{n_k} : \nabla \tilde{\xi} dx + \int_D \chi_n (\tilde{\mathbf{u}}_{n_k} \cdot \nabla) \tilde{\mathbf{u}}_{n_k} \tilde{\xi} dx = \int_D \chi_n \mathbf{f} \tilde{\xi} dx, \quad \xi \in \mathcal{H}(\Omega_n). \quad (2.60)$$

Moreover the extension  $\tilde{\xi}$  belongs to

$$\mathbf{V}(D) = \{\phi \in (C_0^\infty(D))^2 \mid \operatorname{div} \phi = 0 \text{ in } D\}.$$

We examine each term in (2.60) separately. We first note that

$$\begin{aligned} \eta \int_D \chi_n \nabla \tilde{\mathbf{u}}_{n_k} : \nabla \tilde{\xi} \, dx &\xrightarrow{n \rightarrow \infty} \eta \int_D \chi \nabla \tilde{\mathbf{u}} : \nabla \tilde{\xi} \, dx \quad (\text{by equation (2.56)}), \\ &= \eta \int_\Omega \nabla \mathbf{u} : \nabla \tilde{\xi} \, dx. \end{aligned} \tag{2.61}$$

Next, we estimate the nonlinear term. Integrating by parts, one obtains

$$\begin{aligned} \int_D \chi_n (\tilde{\mathbf{u}}_{n_k} \cdot \nabla) \tilde{\mathbf{u}}_{n_k}, \tilde{\xi} \, dx &= \int_{\partial D} \chi_n (\tilde{\mathbf{u}}_{n_k} \cdot \tilde{\xi}) (\tilde{\mathbf{u}}_{n_k} \cdot \mathbf{n}) \, ds - \int_D \chi_n \tilde{\mathbf{u}}_{n_k} \cdot \tilde{\xi} \operatorname{div} \tilde{\mathbf{u}}_{n_k} \, dx \\ &\quad - \int_D \chi_n \tilde{\mathbf{u}}_{n_k} \cdot (\tilde{\mathbf{u}}_{n_k} \cdot \nabla) \tilde{\xi} \, dx. \end{aligned}$$

For the first term  $\int_{\partial D} \chi_n (\tilde{\mathbf{u}}_{n_k} \cdot \tilde{\xi}) (\tilde{\mathbf{u}}_{n_k} \cdot \mathbf{n}) \, ds = 0$ , since  $\tilde{\mathbf{u}}_{n_k}|_{\partial\Omega} = 0$  for every  $n$ . For the second term and third terms, note that  $\tilde{\xi}_i$  and  $(\nabla \tilde{\xi})_{i,j}$  belong to  $L^\infty(\Omega)$ . Since  $\|\operatorname{div} \tilde{\mathbf{u}}_{n_k}\|_{L^2(D)} \leq \|\tilde{\mathbf{u}}_{n_k}\|_{\mathbf{H}^1(D)} < \infty$  for all  $n$ , we may extract a subsequence, again denoted by  $\tilde{\mathbf{u}}_{n_k}$  such that

$$\operatorname{div} \tilde{\mathbf{u}}_{n_k} \rightharpoonup \operatorname{div} \tilde{\mathbf{u}} \text{ in } L^2(D). \tag{2.62}$$

Hence using Lemma 2.2.6, equations (2.56) and (2.62) leads to

$$\begin{aligned} \int_D \chi_n \tilde{\mathbf{u}}_{n_k} \cdot \tilde{\xi} \operatorname{div} \tilde{\mathbf{u}}_{n_k} \, dx - \int_D \tilde{\mathbf{u}} \cdot \tilde{\xi} \operatorname{div} \tilde{\mathbf{u}} \, dx &= \int_D \chi_n \operatorname{div} \tilde{\mathbf{u}}_{n_k} (\tilde{\mathbf{u}}_{n_k} - \tilde{\mathbf{u}}) \tilde{\xi} \, dx \\ &\quad + \int_D \chi_n (\operatorname{div} \tilde{\mathbf{u}}_{n_k} - \operatorname{div} \tilde{\mathbf{u}}) \tilde{\mathbf{u}} \cdot \tilde{\xi} \, dx + \int_D (\chi_n - \chi) \operatorname{div} \tilde{\mathbf{u}} \cdot \tilde{\mathbf{u}} \cdot \tilde{\xi} \, dx \xrightarrow{n \rightarrow \infty} 0. \end{aligned}$$

Thus

$$\int_D \chi_n \tilde{\mathbf{u}}_{n_k} \cdot \tilde{\xi} \operatorname{div} \tilde{\mathbf{u}}_{n_k} \, dx \xrightarrow{n \rightarrow \infty} \int_D \chi \tilde{\mathbf{u}} \cdot \tilde{\xi} \operatorname{div} \tilde{\mathbf{u}} \, dx = \int_\Omega \mathbf{u} \cdot \tilde{\xi} \operatorname{div} \mathbf{u} \, dx.$$

In a similar fashion, we have

$$\int_D \chi_n \tilde{\mathbf{u}}_{n_k} \cdot (\tilde{\mathbf{u}}_{n_k} \cdot \nabla) \tilde{\xi} \, dx \xrightarrow{n \rightarrow \infty} \int_D \chi \tilde{\mathbf{u}} \cdot (\tilde{\mathbf{u}} \cdot \nabla) \tilde{\xi} \, dx = \int_\Omega \mathbf{u} \cdot (\mathbf{u} \cdot \nabla) \tilde{\xi} \, dx.$$

Therefore

$$\int_D \chi_n (\tilde{\mathbf{u}}_{n_k} \cdot \nabla) \tilde{\mathbf{u}}_{n_k} \tilde{\xi} \, dx \xrightarrow{n \rightarrow \infty} \int_D \chi (\tilde{\mathbf{u}} \cdot \nabla) \tilde{\mathbf{u}} \tilde{\xi} \, dx = \int_\Omega (\mathbf{u} \cdot \nabla) \mathbf{u} \tilde{\xi} \, dx.$$

Finally,

$$\int_D \chi_n \mathbf{f} \tilde{\psi} \, dx - \int_D \chi \mathbf{f} \tilde{\psi} \, dx = \int_D (\chi_n - \chi) \mathbf{f} \tilde{\psi} \, dx \xrightarrow{n \rightarrow \infty} 0.$$

Since  $V(\Omega)$  is dense in  $\mathcal{H}$  (see [Girault 1986], page. 26) we can conclude that  $\mathbf{u}|_{\Omega}$  solves (2.58) and moreover  $\mathbf{u}|_{\Omega}$  is divergent free in  $\Omega$  [Haslinger 2003, page.85]. The function  $\mathbf{u}|_{\Omega}$  is the unique solution to (2.41) so that not only a subsequence but the whole sequence tends weakly to  $\mathbf{u}$  in  $\mathbf{H}_0^1(D)$ . To prove strong convergence, from the definition of the problem on  $\Omega_n$  and properties of  $c$  over  $\mathcal{H}$  in Lemma 2.2.3, it follows that

$$\eta \int_D \chi_n |\nabla \tilde{\mathbf{u}}_n|^2 \, dx = \int_D \chi_n \mathbf{f} \tilde{\mathbf{u}}_n \, dx \rightarrow \int_D \chi \mathbf{f} \mathbf{u} \, dx = \eta \int_D \chi |\nabla \mathbf{u}|^2 \, dx. \quad (2.63)$$

□

**Lemma 2.2.8.** *Let  $\Omega_n, \Omega \in \mathcal{U}_{ad}$ , be such that  $\Omega(\alpha_n) \rightarrow \Omega(\alpha), n \rightarrow \infty$  and let  $(\mathbf{u}_n, p_n) := (\mathbf{u}(\alpha_n), p(\alpha_n))$  be the unique solution to the Navier-Stokes equations in  $\Omega_n$ . Then*

$$\tilde{p}_n \rightharpoonup p \text{ in } L_0^2(D), \quad n \rightarrow \infty.$$

*Proof.* Using (2.39), (2.51), and the fact that  $\|\mathbf{u}_n\|_{H^1(\Omega_n)}$  is uniformly bounded, we have that  $\|p\|_{L^2(\Omega_n)}$  is uniformly bounded. Let  $\tilde{p}_n$  be an extension by zero of  $p_n$  to  $D$ . Clearly  $\|\tilde{p}_n\|_{L^2(D)} = \|p_n\|_{L^2(\Omega_n)}$ , so that  $\|\tilde{p}_n\|_{L^2(D)}$  is uniformly bounded. Consequently, one may extract from the sequence  $\{p_n\}$  a subsequence ( again denoted by  $\{p_n\}$  ) in  $L^2(D)$  such that

$$\tilde{p}_n \rightharpoonup \tilde{p} \text{ in } L_0^2(D), \quad n \rightarrow \infty, \quad (2.64)$$

for some  $\tilde{p} \in L^2(D)$ . Now define  $p(\alpha^*) = \tilde{p}|_{\Omega(\alpha^*)}$ . We wish to show that  $(\mathbf{u}, p)$  is a solution to 2.39. Using Lemma 2.2.7 and Lemma 2.2.1, we may conclude that there exists  $\hat{p} \in L^2(D)$  such that

$$\eta \int_D \chi \nabla \tilde{\mathbf{u}} : \nabla \tilde{\xi} \, dx + \int_D \chi (\tilde{\mathbf{u}} \cdot \nabla) \tilde{\mathbf{u}} \tilde{\xi} \, dx - \int_D \chi \hat{p} \operatorname{div} \tilde{\xi} \, dx = \int_D \chi \mathbf{f} \tilde{\xi} \, dx, \quad \tilde{\xi} \in C_0^\infty(\Omega)^2. \quad (2.65)$$

Using (2.64), the density of  $C_0^\infty(\Omega)^2$  in  $(\mathbf{H}_0^1(\Omega))^2$ , and the uniqueness of weak limits, we conclude that  $\hat{p} = \tilde{p}$ , and  $(\mathbf{u}, p)$  is a solution to 2.39. □

**Remark 2.2.4.** *It is important to note that for each  $\alpha \in \mathcal{U}_{ad}$ , the domain  $\Omega(\alpha)$  has the uniform extension property [Chenais 1975]. Using arguments by contradiction from functional analysis, in addition to few elementary techniques from shape optimization, it was shown that for such domains, the Poincaré inequality holds with a constant independent of  $\alpha$  [Boulkhemair 2007].*

Consequently, the uniqueness condition (2.47) holds independent of  $\Omega$ .

The next task is, to prove the continuity of  $\hat{J}_i(\Omega)$ . We need to show that if the domains converge in the sense of (2.53), then  $\hat{J}_i(\Omega_n) \mapsto \hat{J}_i(\Omega)$ ,  $n \rightarrow \infty$ .

**Lemma 2.2.9.** *The cost functional  $\hat{J}_1(\Omega)$  is continuous on  $\mathcal{U}_{ad}$ .*

*Proof.*

$$\begin{aligned}
|J_1(\mathbf{u}_n, \Omega_n) - J_1(\mathbf{u}, \Omega)| &= \left| \int_{\Omega_n} |\mathbf{u}_n - \mathbf{u}_d|^2 dx - \int_{\Omega} |\mathbf{u} - \mathbf{u}_d|^2 dx \right|, \\
&= \left| \int_D |\tilde{\mathbf{u}}_n - \mathbf{u}_d|^2 dx - |\tilde{\mathbf{u}} - \mathbf{u}_d|^2 dx \right|, \\
&= \left| \int_D (\tilde{\mathbf{u}}_n - \tilde{\mathbf{u}})(\tilde{\mathbf{u}}_n + \tilde{\mathbf{u}} - 2\mathbf{u}_d) dx \right|, \\
&\leq \int_D |(\tilde{\mathbf{u}}_n - \tilde{\mathbf{u}})(\tilde{\mathbf{u}}_n + \tilde{\mathbf{u}} - 2\mathbf{u}_d)| dx, \\
&\leq \|(\tilde{\mathbf{u}}_n - \tilde{\mathbf{u}})\|_{L^2(D)} \|(\tilde{\mathbf{u}}_n + \tilde{\mathbf{u}} - 2\mathbf{u}_d)\|_{L^2(D)}. 
\end{aligned} \tag{2.66}$$

Let  $\Omega_n \rightarrow \Omega$ , as  $n \rightarrow \infty$ . Then the term  $\|(\tilde{\mathbf{u}}_n + \tilde{\mathbf{u}} - 2\mathbf{u}_d)\|_{L^2(D)}$  is bounded and since  $\tilde{\mathbf{u}}_n \rightarrow \tilde{\mathbf{u}}$  in  $L^2(D)$ , then  $J_1(\mathbf{u}_n, \Omega_n) \rightarrow J_1(\mathbf{u}, \Omega)$  follows.  $\square$

**Lemma 2.2.10.** *The cost functional  $\hat{J}_2$  is continuous on  $\mathcal{U}_{ad}$ .*

*Proof.* Let us note that, by using the Young's inequality (see [Evans 1998, appendix])

$$\begin{aligned}
\int_{\Omega} |\operatorname{curl} \mathbf{u}|^2 dx &= \int_{\Omega} \left( \frac{\partial u_2}{\partial x_1} \right)^2 + \left( \frac{\partial u_1}{\partial x_2} \right)^2 - 2 \frac{\partial u_2}{\partial x_1} \frac{\partial u_1}{\partial x_2} dx, \\
&\leq \int_{\Omega} \left( \frac{\partial u_2}{\partial x_1} \right)^2 + \left( \frac{\partial u_1}{\partial x_2} \right)^2 + \left( \frac{\partial u_2}{\partial x_1} \right)^2 + \left( \frac{\partial u_1}{\partial x_2} \right)^2 dx, \\
&\leq C \|\nabla \mathbf{u}\|_{L^2(\Omega)} \leq C \|\mathbf{u}\|_{\mathbf{H}^1(\Omega)}, 
\end{aligned} \tag{2.67}$$

for a constant  $C$  independent of  $\mathbf{u}(\alpha)$  and  $\Omega(\alpha)$ , i.e., it is independent of  $\alpha$ . Then we estimate the following

$$\begin{aligned}
|J_2(\mathbf{u}_n, \Omega_n) - J_2(\mathbf{u}, \Omega)| &= \left| \int_{\Omega_n} |\operatorname{curl} \mathbf{u}_n|^2 dx - \int_{\Omega} |\operatorname{curl} \mathbf{u}|^2 dx \right|, \\
&= \left| \int_D |\operatorname{curl} \tilde{\mathbf{u}}_n|^2 dx - |\operatorname{curl} \tilde{\mathbf{u}}|^2 dx \right|, \\
&= \left| \int_D (\operatorname{curl} \tilde{\mathbf{u}}_n - \operatorname{curl} \tilde{\mathbf{u}})(\operatorname{curl} \tilde{\mathbf{u}}_n + \operatorname{curl} \tilde{\mathbf{u}}) dx \right|, \\
&\leq \int_D |(\operatorname{curl} \tilde{\mathbf{u}}_n - \operatorname{curl} \tilde{\mathbf{u}})(\operatorname{curl} \tilde{\mathbf{u}}_n + \operatorname{curl} \tilde{\mathbf{u}})| dx, \\
&\leq \|\operatorname{curl} (\tilde{\mathbf{u}}_n - \tilde{\mathbf{u}})\|_{L^2(D)} \|\operatorname{curl} (\tilde{\mathbf{u}}_n + \tilde{\mathbf{u}})\|_{L^2(D)}, \text{ (by linearity of curl),} \\
&\leq C \|(\tilde{\mathbf{u}}_n - \tilde{\mathbf{u}})\|_{\mathbf{H}^1(D)} \|(\tilde{\mathbf{u}}_n + \tilde{\mathbf{u}})\|_{\mathbf{H}^1(D)}, \text{ (by (2.67)).} 
\end{aligned}$$

Let  $\Omega_n \rightarrow \Omega$ , as  $n \rightarrow \infty$ . Then from Lemma 2.2.7, it follows that  $\mathbf{u}_n \rightarrow \mathbf{u}$  in  $\mathbf{H}_0^1(D)$ . Since  $\|(\tilde{\mathbf{u}}_n + \tilde{\mathbf{u}})\|_{\mathbf{H}^1(D)}$  is bounded by a constant independent  $n$ , then  $J_2(\mathbf{u}_n, \Omega_n) \rightarrow J_2(\mathbf{u}, \Omega)$  follows.  $\square$

**Lemma 2.2.11.** *The cost functional  $J_3$  is continuous on  $\mathcal{U}_{ad}$ .*

*Proof.* Let us first note that  $t^3/(t^2 + 1) \leq t \leq t^2$ , hence it follows that for  $\mathbf{u} \in \mathbf{H}_0^1(\Omega)$ ,

$$\int_{\Omega} g_3(\det \nabla \mathbf{u}) dx \leq \int_{\Omega} |\det \nabla \mathbf{u}| dx.$$

Also note that using the Young's inequality gives

$$\begin{aligned} |\det \nabla \mathbf{u}| &= \left| \frac{\partial u_1}{\partial x_1} \frac{\partial u_2}{\partial x_2} - \frac{\partial u_2}{\partial x_1} \frac{\partial u_1}{\partial x_2} \right| \leq \frac{1}{2} \left[ \left( \frac{\partial u_1}{\partial x_1} \right)^2 + \left( \frac{\partial u_2}{\partial x_1} \right)^2 + \left( \frac{\partial u_1}{\partial x_2} \right)^2 + \left( \frac{\partial u_2}{\partial x_2} \right)^2 \right], \\ &= C(\nabla \mathbf{u} : \nabla \mathbf{u}), \end{aligned} \quad (2.68)$$

where  $C$  is a positive constant independent of  $\mathbf{u}(\alpha)$  and  $\Omega(\alpha)$ , i.e., it's independent of  $\alpha$ . Hence for  $\mathbf{u} \in \mathbf{H}_0^1(\Omega)$ ,

$$\int_{\Omega} g_3(\det \nabla \mathbf{u}) dx \leq C \|\nabla \mathbf{u}\|_{\mathbf{L}^2(\Omega)}^2 \leq C \|\mathbf{u}\|_{\mathbf{H}^1(\Omega)}^2,$$

Let us also note that

$$g'_3(t) = \frac{t^4 + 3t^2}{t^4 + 2t^2 + 1} \leq \frac{t^4 + 3t^2}{t^4 + 2t^2} \leq 3/2.$$

This implies that  $g_3(t)$  is globally Lipschitz with constant  $3/2$ , i.e.,

$$|g_3(t) - g_3(s)| \leq \frac{3}{2} |t - s|, \quad 0 \leq t, s \in \mathbb{R}. \quad (2.69)$$

Now we estimate

$$\begin{aligned} |J_3(\mathbf{u}_n, \Omega_n) - J_3(\mathbf{u}, \Omega)| &= \left| \int_{\Omega_n} g_3(\det \nabla \mathbf{u}_n) dx - \int_{\Omega} g_3(\det \nabla \mathbf{u}) dx \right|, \\ &\leq \int_D \left| g_3(\det(\nabla \tilde{\mathbf{u}}_n)) - g_3(\det(\nabla \tilde{\mathbf{u}})) \right| dx. \end{aligned}$$

Using (2.69) with  $t = \det(\nabla \tilde{\mathbf{u}}_n)$ ,  $s = \det(\nabla \tilde{\mathbf{u}})$ , we find

$$\int_D \left| g_3(\det(\nabla \tilde{\mathbf{u}}_n)) - g_3(\det(\nabla \tilde{\mathbf{u}})) \right| dx \leq \frac{3}{2} \int_D \left| \det(\nabla \tilde{\mathbf{u}}_n) - \det(\nabla \tilde{\mathbf{u}}) \right| dx.$$

Hence

$$\begin{aligned}
|J_3(\mathbf{u}_n, \Omega_n) - J_3(\mathbf{u}, \Omega)| &\leq \frac{3}{2} \int_D \left| \det(\nabla \tilde{\mathbf{u}}_n) - \det(\nabla \tilde{\mathbf{u}}) \right| dx, \\
&= \frac{3}{2} \int_D \left| \frac{\partial \tilde{u}_1^n}{\partial x_1} \frac{\partial \tilde{u}_2^n}{\partial x_2} - \frac{\partial \tilde{u}_2^n}{\partial x_1} \frac{\partial \tilde{u}_1^n}{\partial x_2} - \frac{\partial \tilde{u}_1}{\partial x_1} \frac{\partial \tilde{u}_2}{\partial x_2} + \frac{\partial \tilde{u}_2}{\partial x_1} \frac{\partial \tilde{u}_1}{\partial x_2} \right| dx, \\
&= \frac{3}{2} \int_D \left| \frac{\partial \tilde{u}_1^n}{\partial x_1} \frac{\partial \tilde{u}_2^n}{\partial x_2} - \frac{\partial \tilde{u}_1}{\partial x_1} \frac{\partial \tilde{u}_2}{\partial x_2} + \frac{\partial \tilde{u}_2}{\partial x_1} \frac{\partial \tilde{u}_1}{\partial x_2} - \frac{\partial \tilde{u}_2^n}{\partial x_1} \frac{\partial \tilde{u}_1^n}{\partial x_2} \right| dx, \\
&\leq \frac{3}{2} \int_D \underbrace{\left| \frac{\partial \tilde{u}_1^n}{\partial x_1} \frac{\partial \tilde{u}_2^n}{\partial x_2} - \frac{\partial \tilde{u}_1}{\partial x_1} \frac{\partial \tilde{u}_2}{\partial x_2} \right|}_{A} + \underbrace{\left| \frac{\partial \tilde{u}_2^n}{\partial x_1} \frac{\partial \tilde{u}_1^n}{\partial x_2} - \frac{\partial \tilde{u}_2}{\partial x_1} \frac{\partial \tilde{u}_1}{\partial x_2} \right|}_{B} dx.
\end{aligned}$$

Note that by using the relation  $|a^n b^n - ab| \leq |a^n(b^n - b)| + |(a^n - a)b|$ , and using the Cauchy-Schwarz inequality (2.21), we have that

$$\int_{\Omega} |a^n b^n - ab| dx \leq \|a^n\|_{L^2} \|b^n - b\|_{L^2} + \|b^n\|_{L^2} \|a^n - a\|_{L^2}. \quad (2.70)$$

With  $a = \frac{\partial \tilde{u}_1}{\partial x_1}$ ,  $b = \frac{\partial \tilde{u}_2}{\partial x_2}$ , we find

$$\int_D |A| dx \leq \left\| \frac{\partial \tilde{u}_1^n}{\partial x_1} \right\|_{L^2} \left\| \frac{\partial \tilde{u}_2^n}{\partial x_2} - \frac{\partial \tilde{u}_2}{\partial x_2} \right\|_{L^2} + \left\| \frac{\partial \tilde{u}_2^n}{\partial x_2} \right\|_{L^2} \left\| \frac{\partial \tilde{u}_1^n}{\partial x_1} - \frac{\partial \tilde{u}_1}{\partial x_1} \right\|_{L^2}. \quad (2.71)$$

Similarly, with  $a = \frac{\partial \tilde{u}_2}{\partial x_1}$ ,  $b = \frac{\partial \tilde{u}_1}{\partial x_2}$ , we find

$$\int_D |B| dx \leq \left\| \frac{\partial \tilde{u}_2^n}{\partial x_1} \right\|_{L^2} \left\| \frac{\partial \tilde{u}_1^n}{\partial x_2} - \frac{\partial \tilde{u}_1}{\partial x_2} \right\|_{L^2} + \left\| \frac{\partial \tilde{u}_1^n}{\partial x_2} \right\|_{L^2} \left\| \frac{\partial \tilde{u}_2^n}{\partial x_1} - \frac{\partial \tilde{u}_2}{\partial x_1} \right\|_{L^2}. \quad (2.72)$$

Let  $\Omega_n \rightarrow \Omega$ , as  $n \rightarrow \infty$ . Then from Lemma 2.2.7, it follows that  $\mathbf{u}_n \rightarrow \mathbf{u}$  in  $\mathbf{H}_0^1(D)$ . Since by (2.68) the terms  $\left\| \frac{\partial \tilde{u}_1^n}{\partial x_1} \right\|_{L^2}$ ,  $\left\| \frac{\partial \tilde{u}_2^n}{\partial x_2} \right\|_{L^2}$ ,  $\left\| \frac{\partial \tilde{u}_2^n}{\partial x_1} \right\|_{L^2}$  and  $\left\| \frac{\partial \tilde{u}_1^n}{\partial x_2} \right\|_{L^2}$  are bounded for all  $n$ , then  $J_3(\mathbf{u}_n, \Omega_n) \rightarrow J_3(\mathbf{u}, \Omega)$  follows.  $\square$

**Lemma 2.2.12.** *The optimization problem has a solution.*

*Proof.* Since  $J_1$ ,  $J_2$  and  $J_3$  are continuous and  $\mathcal{U}_{ad}$  is compact, the classical Bolzano-Weierstrass theorem asserts that  $J_1$ ,  $J_2$  and  $J_3$  attain their minima on  $\mathcal{U}_{ad}$ .  $\square$

**Remark 2.2.5.** As noted in Haslinger and Mäkinen [Haslinger 2003, Chapter 3], continuity of solution to the optimization problem is important but not enough. One often needs other properties to better understand the problem at hand. One of these important aspects is differentiability. The need to deal with such information gave rise to a special discipline in optimization called sensitivity analysis. Sensitivity analysis develops appropriate tools and concepts enabling us to analyze the differentiability of various objects, such as solutions to state problems, cost and con-

straint functionals, etc., with respect to control variables, and in particular with respect to design variables in shape optimization.

Therefore in the spirit of remark 2.2.5, the next chapter is devoted to the discussion on how to obtain derivative information of the criteria functions with respect to the domain. This derivative information is important in order solve the optimization problem (2.34) using a gradient type algorithm.

# 3

## SOLVING SHAPE OPTIMIZATION PROBLEMS

There are several approaches to solve shape optimization problems once we know how to compute derivatives. If a computer program is used to yield the numerical solution of a PDE describing an optimal shape design problem, an optimization algorithm will have to be written (usually a gradient type algorithm is used). Such algorithms require derivative information and so, the first section provides the basic techniques for computing the derivatives of the criteria functions with respect to the domain. The second section will be devoted to providing several alternatives for constructing the optimization algorithm once we have the derivative information.

### 3.1 Sensitivity analysis

The goal now is to furnish the first order optimality conditions associated to the optimization problem (2.34). These conditions are essential since they are the basis in order to build both a rigorous mathematical analysis and gradient based optimization algorithms. We remark here that the space of shapes is not a linear space and the associated differential calculus becomes more tricky. To realize this, one of three distinct techniques can be used: J. Hadarmard's normal variational method [Hadamard], the perturbation of the identity method by J. Simon [Simon 1980] and the velocity method ( Cea and J. P. Zolesio [Sokolowski 1992] ). Here we follow the approach of Murat and Simon .

#### 3.1.1 Generalized problem

To make the exposition more general, we shall instead of (2.34), consider the following optimization problem

$$\min_{\Omega \in \mathcal{U}_{ad}} J(u, \Omega) \equiv \int_{\Omega} j_1(C_{\gamma} u) dx, \quad (3.1)$$

subject to the constraint

$$E(u, \Omega) = 0, \quad u \in X \quad (3.2)$$

and carry out its sensitivity analysis. Here  $E(u, \Omega) = 0$  represents a partial differential equation posed on a domain  $\Omega$  with a boundary  $\partial\Omega$ ,  $X \subset L^2(\Omega)^l$ ,  $l \in \mathbb{N}$ , a Hilbert space with a dual  $X^*$  and  $\mathcal{U}_{ad}$  is a class of admissible domains to be specified later. A formal derivation of the shape derivative of  $J$  can be found in literature (see e.g., [Sokolowski 1992], [Delfour 2001]). Here we present a computation of the shape derivative of  $J$  under minimal regularity assumptions. The technique we employ was first suggested in [Ito 2006] and then used in [Haslinger 2009] and allows to compute the shape derivative of the mapping  $\Omega \mapsto J(\Omega)$  without using the chain rule. In [Ito 2006], a cost functional of the form  $J(u, \Omega) = \int_{\Omega} j_1(u)$  was considered. In this note, we consider a generalized cost functional of the form  $J(u, \Omega) = \int_{\Omega} j_1(C_{\gamma}u)$  where  $C_{\gamma}$  is an affine operator

$$C_{\gamma} : u(\cdot) \mapsto Cu(\cdot) + \gamma(\cdot) \quad \gamma \in L^2(\Omega),$$

$\gamma$  is assumed to be independent of  $\Omega$ , and  $C \in \mathcal{L}(X, L^2(\Omega))$  is a linear differential operator.

### 3.1.2 Admissible class of domains

To describe the class of admissible domains  $\mathcal{U}_{ad}$ , let  $D \in \mathbb{R}^d$ ,  $d = 2, 3$  be a fixed bounded domain with a  $C^{1,1}$  boundary  $\partial D$  and let  $S$  be a domain with a  $C^{1,1}$  boundary  $\Gamma := \partial S$  satisfying  $\bar{S} \subset D$  (see Figure (3.1)).

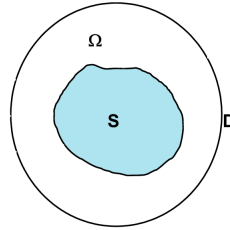


Figure 3.1: Domain

For the reference domain, either of the following three cases is admitted

- (i)  $\Omega = S$ ,
- (ii)  $\Omega = D$ ,
- (iii)  $\Omega = D \setminus \bar{S}$ .

Then the boundary  $\partial\Omega$  for the three cases is given by

- (i)  $\partial\Omega = \Gamma$ ,
- (ii)  $\partial\Omega = \partial D$ ,
- (iii)  $\partial\Omega = \Gamma \cup \partial D$ .

### 3.1.3 Method of mappings

To introduce the admissible class of perturbations, a common technique is to introduce a family of perturbations  $\Omega_t$  of a given admissible bounded domain  $\Omega$  which depend on a parameter  $t$ . It can be constructed, for instance, by perturbation of the identity. Let  $\Omega \subset \bar{D}$  be open and let

$$\mathcal{H} = \{\mathbf{h} \in C^{1,1}(\bar{D}) : \mathbf{h}|_{\partial D} = 0\} \quad (3.3)$$

be the space of deformation fields which define for  $t > 0$  a perturbation of  $\Omega$  by

$$T_t : D \mapsto \mathbb{R}^d, \quad (3.4)$$

$$x \mapsto T_t(x) = x + t\mathbf{h}(x). \quad (3.5)$$

Then for each  $h \in \mathcal{H}$ , there exists  $\tau > 0$  such that  $T_t(D) = D$  and  $\{T_t\}$  is a family of  $C^{1,1}$ -diffeomorphisms for  $|t| < \tau$ . For each  $t \in \mathbb{R}$  with  $|t| < \tau$ , we set

$$\Omega_t = T_t(\Omega), \quad \Gamma_t = T_t(\Gamma).$$

Thus  $\Omega_0 = \Omega, \Gamma_0 = \Gamma, \Omega_t \subset D$ . Methods for computing shape gradients, which involve  $T_t$  are referred to as the methods of mapping.

#### 3.1.3.1 Notation

In what follows, the following notation will be used:

$$I_t = \det DT_t \quad A(t) = I_t(DT_t)^{-1}(DT_t)^{-T}, \quad (3.6)$$

and  $\nabla u$  shall stand for  $(Du)^T$  where  $u$  is either a scalar or vector valued function (if  $u$  is bold faced, i.e.,  $\mathbf{u}$ ). In (3.6),  $(DT_t)^{-T}$  takes the meaning of transpose of the inverse matrix  $(DT_t)^{-1}$ . Furthermore, two symbols for the inner product in  $\mathbb{R}^d$  shall be used, namely  $(x, y)$  respectively  $x \cdot y$ . The latter shall be used in case of nested inner products. In addition, throughout this work, unless specified, the following parenthesis  $(\cdot, \cdot)_\Omega, (\cdot, \cdot)_{\partial\Omega}$  shall denote the  $L^2(\Omega)$ ,  $L^2(\partial\Omega)$  inner products respectively. In some cases, the subscript  $\Omega$  may be omitted, but the

meaning will remain clear in the given context. The scalar product and the norm in the Hilbert space  $X$  will be denoted by  $(\cdot, \cdot)_X$  and  $\|\cdot\|_X$  respectively, and the duality pairing between  $X^*$  and  $X$  is denoted by  $\langle \cdot, \cdot \rangle_{X^* \times X}$ .

### Properties of $T_t$

Let  $\mathcal{J} = [0, \tau_0]$  with  $\tau_0$  sufficiently small. Then the following regularity properties of the transformation  $T_t$  can be shown, see for example ([Ito 2006], [Sokolowski 1992, Chapter 2], [Delfour 2001, Chapter 7]):

$$\begin{aligned}
 T_0 &= id & t \mapsto T_t &\in C^1(\mathcal{J}, C^{1,1}(\bar{D}; \mathbb{R}^d)) \\
 t \mapsto T_t^{-1} &\in C^1(\mathcal{J}, C^{1,1}(\bar{D}; \mathbb{R}^d)) & t \mapsto I_t &\in C^1(\mathcal{J}, C(\bar{D})) \\
 t \mapsto (DT_t)^{-T} &\in C(\mathcal{J}, C^{1,1}(\bar{D}; \mathbb{R}^{d \times d})) & \frac{d}{dt} T_t|_{t=0} &= \mathbf{h} \\
 \frac{d}{dt} T_t^{-1}|_{t=0} &= -\mathbf{h} & \frac{d}{dt} DT_t|_{t=0} &= D\mathbf{h} \\
 \frac{d}{dt} DT_t^{-1}|_{t=0} &= -D\mathbf{h} & \frac{d}{dt} I_t|_{t=0} &= \operatorname{div} \mathbf{h} \\
 I_t|_{t=0} &= 1 & I_t^{-1}|_{t=0} &= 1.
 \end{aligned} \tag{3.7}$$

The limits defining the derivatives at  $t = 0$  exist uniformly in  $x \in \bar{D}$ .

**Remark 3.1.1.** The properties in (3.7) imply that  $\Omega_t$  and  $\Omega$  have the same topological structure, i.e., the same connectivity components, and regularity.

**Remark 3.1.2.** The notations

$$t \mapsto T_t \in C^1(\mathcal{J}, C^{1,1}(\bar{D}; \mathbb{R}^d)), t \mapsto I_t \in C^1(\mathcal{J}, C(\bar{D})), t \mapsto (DT_t)^{-T} \in C(\mathcal{J}, C^{1,1}(\bar{D}; \mathbb{R}^{d \times d}))$$

in (3.7) simply mean that,

$$\|T_t\|_{C^{1,1}(\bar{D}; \mathbb{R}^d)} \in C^1(\mathcal{J}), \|I_t\|_{C(\bar{D})} \in C^1(\mathcal{J}), \|(DT_t)^{-T}\|_{C^{1,1}(\bar{D}; \mathbb{R}^{d \times d})} \in C(\mathcal{J}),$$

with respective norms defined in the previous chapter.

The surface divergence  $\operatorname{div}_\Gamma$  is defined for  $\phi \in C^1(\bar{D}, \mathbb{R}^d)$  by

$$\operatorname{div}_\Gamma \phi := \operatorname{div} \phi|_\Gamma - (D\phi \cdot \mathbf{n}) \cdot \mathbf{n}, \tag{3.8}$$

and tangential gradient is defined as

$$\nabla_\Gamma \phi := \nabla \phi|_\Gamma - (D\phi \cdot \mathbf{n}) \cdot \mathbf{n}. \tag{3.9}$$

## 3.2 The Eulerian derivative

**Definition 3.2.1.** *The Eulerian derivative of  $J$  at  $\Omega$  in the direction of the deformation field  $h$  is defined as*

$$dJ(u, \Omega)h = \lim_{t \rightarrow 0} \frac{J(u_t, \Omega_t) - J(u, \Omega)}{t}, \quad (3.10)$$

where  $u_t$  satisfies

$$E(u_t, \Omega_t) = 0. \quad (3.11)$$

The functional  $J$  is called shape differentiable at  $\Omega$  if  $dJ(\Omega, h)$  exists for all  $h \in C^{1,1}(\bar{D}, \mathbb{R}^d)$  and  $h \mapsto dJ(\Omega, h)$  defines a continuous linear functional on  $C^{1,1}(\bar{D}, \mathbb{R}^d)$ .

### 3.2.1 The derivative of the state equation with respect to t

For computing the Eulerian derivative of  $J$ , we will need the derivative of (3.11) with respect to  $t$  at  $t = 0$ . To this end, let  $\{X_t\}_{t \geq 0}$  be a family of functional spaces on  $\Omega_t$  and we introduce the variational form of (3.11) given by :

Find  $u_t \in X_t$  such that

$$\langle E(u_t, \Omega_t), \psi_t \rangle_{X_t^* \times X_t} = 0, \quad (3.12)$$

holds for all  $\psi_t \in X_t$ . Throughout we choose  $X_t = T_t(X)$  and we assume that equation (3.12) has a unique solution,  $u_t$ , for all  $t$  sufficiently small.

For  $t = 0$ , equation (3.12) represents the weak form of the reference problem (3.2) given by

$$\langle E(u, \Omega), \psi \rangle_{X^* \times X} = 0, \quad \text{for all } \psi \in X \quad (3.13)$$

whose adjoint state  $p \in X$  is defined as the solution to

$$\langle E_u(u, \Omega) \psi, p \rangle_{X^* \times X} = (C^* j'_1(C_\gamma u), \psi). \quad (3.14)$$

Any function  $u_t : \Omega_t \mapsto \mathbb{R}^l$ , for  $l \in \mathbb{N}$ , can be mapped back to the reference domain by

$$u^t = u_t \circ T_t : \Omega \mapsto \mathbb{R}^l. \quad (3.15)$$

From the chain rule it follows that the gradients of  $u_t$  and  $u^t$  are related by

$$\nabla u_t \circ T_t = (DT_t)^{-T} \nabla u^t, \quad (3.16)$$

(see [Sokolowski 1992] Prop: 2.29). Moreover  $u^t : \Omega \mapsto \mathbb{R}^l$  satisfies the equation on the reference domain which we express as

$$\tilde{E}(u^t, t) = 0, \quad |t| < \tau. \quad (3.17)$$

Because  $T_0 = id$ , one obtains  $u^0 = u$  and

$$\tilde{E}(u^0, 0) = E(u, \Omega). \quad (3.18)$$

In IKP [Ito 2006], the following assumptions (H1-H4) were imposed on  $\tilde{E}$ , respectively  $E$ :

(H1) There is a  $C^1$ -function  $\tilde{E} : X \times (-\tau, \tau) \mapsto X^*$  such that  $E(u_t, \Omega_t) = 0$  is equivalent to

$$\tilde{E}(u^t, t) = 0 \text{ in } X^*,$$

with  $\tilde{E}(u, 0) = E(u, \Omega)$  for all  $u \in X$ .

(H2) There exists  $0 < \tau_0 \leq \tau$  such that for  $|t| < \tau_0$ , there exists a unique solution  $u^t \in X$  to

$\tilde{E}(u^t, t) = 0$  and

$$\lim_{t \rightarrow 0} \frac{\|u^t - u^0\|_X}{|t|^{\frac{1}{2}}} = 0.$$

(H3)  $E_u(u, \Omega) \in \mathcal{L}(X, X^*)$  satisfies

$$\langle E(v, \Omega) - E(u, \Omega) - E_u(u, \Omega)(v - u), \psi \rangle_{X^* \times X} = \mathcal{O}(|v - u|_X^2).$$

(H4)  $\tilde{E}$  and  $E$  satisfy

$$\lim_{t \rightarrow 0} \frac{1}{t} \langle \tilde{E}(u^t, t) - \tilde{E}(u, t) - E(u^t, \Omega) + E(u, \Omega), \psi \rangle_{X^* \times X} = 0.$$

With regards to the cost functional  $J$ , we require:

(H5)  $j_1 \in C^{1,1}(\mathbb{R}^l, \mathbb{R})$

Condition (H5) implies that  $j_1(C_\gamma u) \in L^2(\Omega, \mathbb{R})$  and  $j'_1(C_\gamma u) \in L^2(\Omega, \mathbb{R}^l)$  for  $u \in L^2(\Omega, \mathbb{R}^l)$ . In particular  $J(u, \Omega)$  is well defined for every  $u \in X$ . To compute the Eulerian derivative of  $J(u, \Omega)$  in (3.10), we need to transform the value of  $J(u_t, \Omega_t) = \int_{\Omega_t} j_1(C_\gamma u_t) dx_t$  back to  $\Omega$ . This is done by using the relation

$$J(u_t, \Omega_t) = \int_{\Omega_t} j_1(C_\gamma u_t) dx_t = \int_{\Omega} j_1(C_\gamma u_t \circ T_t) I_t dx.$$

The transformation of  $C_\gamma u_t \circ T_t$  back to  $\Omega$  induces some matrix  $A_t$  that we shall require to satisfy the following additional assumption:

$$(H6) \quad \left\{ \begin{array}{l} \text{There exists a matrix } A_t \text{ such that } t \mapsto A_t \in C(\mathcal{J}, C(\bar{D}, \mathbb{R}^{d \times d})) \text{ and} \\ C_\gamma u_t \circ T_t = A_t C u^t + \gamma, \\ C_\gamma(u \circ T_t^{-1}) = A_t C u \circ T_t^{-1} + \gamma, \\ \lim_{t \rightarrow 0} \frac{A_t - I}{t} \text{ exists, } A_t|_{t=0} = I. \end{array} \right.$$

Using (H1), the transformation of (3.12) back to  $\Omega$  becomes,

$$\langle \tilde{E}(u^t, t), \psi \rangle_{X^* \times X} = 0 \text{ for all } \psi \in X. \quad (3.19)$$

Some examples of (H6),  $E$ , and  $\tilde{E}$  and are given next. Let

$$C_\gamma = C = \nabla, \text{ i.e., } \gamma = 0.$$

Then (3.16) gives the first relation in (H6) with

$$A_t = D T_t^{-T}.$$

Again by applying chain rule on  $D(u \circ T_t^{-1})$ , we have

$$D(u \circ T_t^{-1}) = D u \circ T_t^{-1} D T_t^{-1}. \quad (3.20)$$

Transposing equation (3.21) gives

$$\nabla(u \circ T_t^{-1}) = D T_t^{-T} \nabla u \circ T_t^{-1}, \quad (3.21)$$

a second relation in (H6), with  $A_t = D T_t^{-T}$ . The third relation in (H6) is satisfied by  $A_t$  since  $\lim_{t \rightarrow 0} \frac{D T_t^{-T} - I}{t} = -D h^T$ , and  $\lim_{t \rightarrow 0} D T_t^{-T} = I$ .

To construct an example for  $E$ , and  $\tilde{E}$ , let us consider for simplicity the following PDE,

$$\begin{aligned} -\Delta u &= f, \text{ in } \Omega \subset \mathbb{R}^2, \\ u &= 0, \text{ on } \partial\Omega = \Gamma, \end{aligned} \quad (3.22)$$

where  $\Omega = D$ ,  $\Gamma = \partial\Omega$ . Let  $X = H_0^1(\Omega)$ ,  $f \in L^2(\Omega)$ , then  $E(u, \Omega) : X \mapsto X^*$  is given by

$$\langle E(u, \Omega), \varphi \rangle_{X^* \times X} = (\nabla u, \nabla \varphi)_\Omega - (f, \varphi)_\Omega = 0.$$

The equation on the perturbed domain  $\Omega_t$  is given by

$$\langle E(u_t, \Omega_t), \varphi_t \rangle_{X_t^* \times X_t} = (\nabla u_t, \nabla \varphi_t)_{\Omega_t} - (f_t, \varphi_t)_{\Omega_t} = 0. \quad (3.23)$$

Making use of (3.15),(3.16), the equation (3.23) is mapped back onto  $\Omega$ . This gives rise to an expression for  $\tilde{E} : X^* \times X \mapsto \mathbb{R}$  that reads as follows

$$\begin{aligned} \langle \tilde{E}(u^t, t), \varphi \rangle_{X^* \times X} &= (I_t(DT_t)^{-T} \nabla u^t, (DT_t)^{-T} \nabla \varphi^t)_{\Omega} - (f^t, \varphi^t I_t)_{\Omega} \\ &= (A(t) \nabla u^t, \nabla \varphi^t)_{\Omega} - (f^t, \varphi^t I_t)_{\Omega} = 0, \end{aligned} \quad (3.24)$$

where  $A(t)$  and  $I_t$  are defined in (3.6).

### 3.2.2 The Eulerian derivative of the generalized cost functional $J$

For computing the Eulerian derivative of  $J$ , we will need the derivative of (3.19) with respect to  $t$  at  $t = 0$ . To compute this derivative, we transform the expressions  $\tilde{E}(u, t)$  and  $p$  to  $E(u \circ T_t^{-1}, \Omega_t)$  and  $p \circ T_t^{-1}$  which are defined on  $\Omega_t$  and utilize the following two lemmas from, e.g., [Ito 2006].

**Lemma 3.2.1.** (1) Let  $f \in C(\mathcal{J}, W^{1,1}(D))$ , and assume that  $f_t(0)$  exists in  $L^1(D)$ . Then

$$\frac{d}{dt} \int_{\Omega_t} f(t, x) dx|_{t=0} = \int_{\Omega} f_t(0, x) dx + \int_{\Gamma} f(0, x) \mathbf{h} \cdot \mathbf{n} ds. \quad (3.25)$$

(2) Let  $f \in C(\mathcal{J}, W^{2,1}(D))$ , and assume that  $f_t(0)$  exists in  $W^{1,1}(D)$ . Then

$$\frac{d}{dt} \int_{\Gamma_t} f(t, x) dx|_{t=0} = \int_{\Gamma} f_t(0, x) ds + \int_{\Gamma} \left( \frac{\partial f(0, x)}{\partial \mathbf{n}} + \kappa f(0, x) \right) \mathbf{h} \cdot \mathbf{n} ds, \quad (3.26)$$

where  $\kappa$  stands for the mean curvature of  $\Gamma$ .

As noted in [Ito 2006], the first part of the Lemma 3.2.1 above holds also for domains with Lipschitz continuous boundary while the additional  $C^{1,1}$  regularity is used as a sufficient condition for the second part of Lemma 3.2.1 in [Delfour 2001]. Moreover, domains with a  $C^{1,1}$  boundary are said to have a boundary with bounded curvature [Grisvard 1985, page 134], which makes the boundary term in (3.26) well defined. The assumptions of Lemma 3.2.1 can be verified using the following Lemma

**Lemma 3.2.2.** (1) If  $u \in L^p(D)$ , then  $t \mapsto u \circ T_t^{-1} \in C(\mathcal{J}, L^p(D))$ ,  $1 \leq p < \infty$ .

(2) If  $u \in H^2(D)$ , then  $t \mapsto u \circ T_t^{-1} \in C(\mathcal{J}, H^2(D))$ .

(3) If  $u \in H^2(D)$ , then  $\frac{d}{dt}(u \circ T_t^{-1})|_{t=0}$  exists in  $H^1(D)$  and is given by

$$\frac{d}{dt}(u \circ T_t^{-1})|_{t=0} = -(Du)\mathbf{h}.$$

*Proof.* see [Sokolowski 1992, Chapter.2].  $\square$

**Note 3.2.1.** As a consequence of Lemma 3.2.2, it is important to note that  $\frac{d}{dt}\nabla(u \circ T_t^{-1})|_{t=0}$  exists in  $L^2(D)$  and is given by

$$\frac{d}{dt}\nabla(u \circ T_t^{-1})|_{t=0} = -\nabla(Du\mathbf{h}). \quad (3.27)$$

Furthermore, we will need the following modified lemma extracted from [Ito 2006].

**Lemma 3.2.3.** There is a constant  $c > 0$ , such that

$$|j_1(C_\gamma v) - j_1(C_\gamma u) - (j'_1(C_\gamma u), C(v-u))|_{L^1} \leq c\|C_\gamma(v-u)\|_X \quad (3.28)$$

hold for all  $v, u \in X$ .

*Proof.* Note that

$$\begin{aligned} & \int_{\Omega} \left| j_1(C_\gamma v) - j_1(C_\gamma u) - (j'_1(C_\gamma u), C(v-u)) \right| dx \\ & \leq \int_{\Omega} \int_0^1 \left| \left[ j_1(C_\gamma v) - j_1(C_\gamma u) - (j'_1(C_\gamma u), C(v-u)) \right] \right| ds dx, \\ & \leq \int_{\Omega} \int_0^1 \left| \left[ j'_1(C_\gamma(u+s(v-u))) - j'_1(C_\gamma u) \right] \right| ds \|C_\gamma(v-u)\| dx, \\ & \leq \frac{M}{2} \|C_\gamma(v-u)\|_{L^2(\Omega)} \leq c\|C_\gamma(v-u)\|_X, \end{aligned}$$

where  $M$  is a Lipschitz constant for  $j'_1$ , as a mapping from  $L^2(\Omega, \mathbb{R}^l)$  to  $L^2(\Omega, \mathbb{R}^l)$ .  $\square$

For the transformation of domain integrals, the following well known fact will be used repeatedly.

**Lemma 3.2.4.** Let  $\phi_t \in L^1(\Omega_t)$ , then  $\phi_t \circ T_t \in L^1(\Omega)$  and

$$\int_{\Omega_t} \phi_t dx_t = \int_{\Omega} \phi_t \circ T_t I_t dx. \quad (3.29)$$

**Theorem 3.2.1.** If (H1-H6) hold,  $j_1(u) = |u|^2$ , and  $j_1(C_\gamma u) \in W^{1,1}(\Omega)$ , then the Eulerian derivative of  $J$  in the direction  $\mathbf{h} \in C^{1,1}(\bar{D}, \mathbb{R}^d)$  exists and is given by the expression

$$dJ(u, \Omega)\mathbf{h} = -\frac{d}{dt} \langle \tilde{E}(u, t), p \rangle_{X^* \times X}|_{t=0} + \int_{\partial\Omega} j_1(C_\gamma u) \mathbf{h} \cdot \mathbf{n} ds - (j'_1(C_\gamma u), C_\gamma(\nabla u^T \cdot \mathbf{h}))_{\Omega}. \quad (3.30)$$

*Proof.* The Eulerian derivative of a cost functional  $J(u, \Omega)$  is defined by

$$dJ(u, \Omega)\mathbf{h} = \lim_{t \rightarrow 0} \frac{J(u_t, \Omega_t) - J(u, \Omega)}{t}.$$

Using Lemma 3.2.4 we obtain

$$J(u_t, \Omega_t) - J(u, \Omega) = \int_{\Omega} j_1(C_\gamma u_t \circ T_t) I_t - j_1(C_\gamma u) dx. \quad (3.31)$$

and by (H6)

$$\begin{aligned} J(u_t, \Omega_t) - J(u, \Omega) &= \int_{\Omega} \left( I_t j_1(A_t C_\gamma u^t) - I_t j_1(C_\gamma u^t) + I_t j_1(C_\gamma u^t) - j_1(C_\gamma u) \right) dx, \\ &= \int_{\Omega} \left( I_t j_1(C_\gamma u^t) - j_1(C_\gamma u) \right) dx + \int_{\Omega} I_t \left( j_1(A_t C_\gamma u^t) - j_1(C_\gamma u^t) \right) dx. \end{aligned} \quad (3.32)$$

The following estimate is obtained along the lines of [Ito 2006]. We set

$$\begin{aligned} R(t) &= \int_{\Omega} \left( I_t j_1(C_\gamma u^t) - j_1(C_\gamma u) \right) dx, \\ S(t) &= \int_{\Omega} I_t \left( j_1(A_t C_\gamma u^t) - j_1(C_\gamma u^t) \right) dx. \end{aligned} \quad (3.33)$$

Since  $C$  is a linear differential operator, we have

$$\begin{aligned} R(t) &= \int_{\Omega} I_t \left[ j_1(C_\gamma u^t) - j_1(C_\gamma u) - (j'_1(C_\gamma u), C(u^t - u)) \right] dx + \\ &\quad \int_{\Omega} (I_t - 1) (j'_1(C_\gamma u), C(u^t - u)) + (j'_1(C_\gamma u), C(u^t - u)) dx \\ &\quad + \int_{\Omega} (I_t - 1) j_1(C_\gamma u) dx. \end{aligned} \quad (3.34)$$

We express  $R(t) = R_1(t) + R_2(t) + R_3(t) + R_4(t)$ . Using (3.7), Lemma 3.2.3, and (H2), we have that

$$\lim_{t \rightarrow 0} \frac{1}{t} R_i(t) = 0 \text{ for } i = 1, 2.$$

Next observe that using (3.14) with  $\psi = u^t - u \in X$ , we have that

$$\begin{aligned} R_3(t) &= (J'(C_\gamma u), C(u^t - u)) = (C^* J'(C_\gamma u), (u^t - u)) \\ &= \langle E_u(u, \Omega)(u^t - u), p \rangle_{X^* \times X}. \end{aligned} \quad (3.35)$$

We arrange terms on the right hand side of (3.35) in an efficient manner so as to avoid the com-

putation of the shape derivative of  $u$  and utilize (H1) to obtain

$$\begin{aligned} \langle E_u(u, \Omega)(u^t - u), p \rangle_{X^* \times X} &= -\langle E(u^t, \Omega) - E(u, \Omega) - E_u(u, \Omega)(u^t - u), p \rangle_{X^* \times X} \\ &\quad - \langle \tilde{E}(u^t, t) - \tilde{E}(u, t) - E(u^t, \Omega) + E(u, \Omega), p \rangle_{X^* \times X} \\ &\quad - \langle \tilde{E}(u, t) - \tilde{E}(u, 0), p \rangle_{X^* \times X}. \end{aligned} \quad (3.36)$$

By using assumptions (H3) and (H4), we have that

$$-\lim_{t \rightarrow 0} \frac{1}{t} \langle E(u^t, \Omega) - E(u, \Omega) - E_u(u, \Omega)(u^t - u), p \rangle_{X^* \times X} = 0, \quad (3.37)$$

and

$$-\lim_{t \rightarrow 0} \frac{1}{t} \langle \tilde{E}(u^t, t) - \tilde{E}(u, t) - E(u^t, \Omega) + E(u, \Omega), p \rangle_{X^* \times X} = 0, \quad (3.38)$$

such that

$$\lim_{t \rightarrow 0} \frac{R_3(t)}{t} = -\frac{d}{dt} \langle \tilde{E}(u, t), p \rangle_{X^* \times X}|_{t=0}. \quad (3.39)$$

We shall turn our attention to  $R_4(t)$  later. Now let us focus on

$$S(t) = \int_{\Omega} I_t(j_1(A_t C_{\gamma} u^t) - j_1(C_{\gamma} u^t)) dx,$$

and consider the expression

$$j_1(A_t C_{\gamma} u^t) - j_1(C_{\gamma} u^t).$$

This can be written as

$$j_1(A_t C_{\gamma} (u^t - u) + A_t C_{\gamma} u) - j_1(C_{\gamma} (u^t - u) + C_{\gamma} u).$$

Since  $j_1$  takes the form  $j_1(u) = |u|^2$ , we can write the first term as

$$j_1(A_t C_{\gamma} (u^t - u) + A_t C_{\gamma} u) = |(A_t C_{\gamma} (u^t - u) + A_t C_{\gamma} u)|^2. \quad (3.40)$$

Developing the right hand side of (3.40) we obtain

$$\begin{aligned} |(A_t C_{\gamma} (u^t - u) + A_t C_{\gamma} u)|^2 &= (A_t C_{\gamma} (u^t - u), A_t C_{\gamma} (u^t - u)) \\ &\quad + 2(A_t C_{\gamma} (u^t - u), A_t C_{\gamma} u) + (A_t C_{\gamma} u, A_t C_{\gamma} u). \end{aligned} \quad (3.41)$$

Similarly, the second term can be expressed as

$$\begin{aligned} |C_\gamma(u^t - u) + C_\gamma u|^2 &= (C_\gamma(u^t - u), C_\gamma(u^t - u)) + 2(C_\gamma(u^t - u), C_\gamma u) \\ &\quad + (C_\gamma u, C_\gamma u). \end{aligned} \quad (3.42)$$

Subtracting (3.42) from (3.41), we obtain

$$\begin{aligned} &\left( (A_t C_\gamma(u^t - u), A_t C_\gamma(u^t - u)) - (C_\gamma(u^t - u), C_\gamma(u^t - u)) \right) + \\ &2 \left( (A_t C_\gamma(u^t - u), A_t C_\gamma u) - (C_\gamma(u^t - u), C_\gamma u) \right) \\ &+ \left( (A_t C_\gamma u, A_t C_\gamma u) - (C_\gamma u, C_\gamma u) \right). \end{aligned} \quad (3.43)$$

Using  $(a^2 - b^2) = (a + b)(a - b)$  on the first term, and upon adding and subtracting the term  $(C_\gamma(u^t - u), A_t C_\gamma u)$  on the second term in (3.43), we obtain

$$\begin{aligned} &\left( (A_t - I) C_\gamma(u^t - u), (A_t + I) C_\gamma(u^t - u) \right) + 2 \left( (A_t - I) C_\gamma(u^t - u), A_t C_\gamma u \right) + \\ &2 \left( C_\gamma(u^t - u), (A_t - I) C_\gamma u \right) + \left( (A_t C_\gamma u, A_t C_\gamma u) - (C_\gamma u, C_\gamma u) \right). \end{aligned} \quad (3.44)$$

Therefore

$$\begin{aligned} S(t) &= \int_{\Omega} I_t \left( ((A_t - I) C_\gamma(u^t - u), (A_t + I) C_\gamma(u^t - u)) \right) dx \\ &\quad + 2 \int_{\Omega} I_t \left( ((A_t - I) C_\gamma(u^t - u), A_t C_\gamma u) \right) dx \\ &\quad + 2 \int_{\Omega} I_t \left( (C_\gamma(u^t - u), (A_t - I) C_\gamma u) \right) dx \\ &\quad + \int_{\Omega} I_t \left( (A_t C_\gamma u, A_t C_\gamma u) - (C_\gamma u, C_\gamma u) \right) dx. \end{aligned} \quad (3.45)$$

Expressing  $S(t) = S_1(t) + S_2(t) + S_3(t) + S_4(t)$ , where  $S_i(t)$  is the i-th term in (3.45). Using (H2) and (H6), we have that  $\lim_{t \rightarrow 0} \frac{S_i(t)}{t}$ ,  $i = 1, 2, 3 \rightarrow 0$ . Therefore collecting the remaining terms, i.e.,  $R_4(t)$  and  $S_4(t)$  into  $S_5(t) := R_4(t) + S_4(t)$ , and recalling that  $(C_\gamma u, C_\gamma u) = j_1(C_\gamma u)$ , and  $(A_t C_\gamma u, A_t C_\gamma u) = j_1(A_t C_\gamma u)$ , we have that

$$S_5(t) = \int_{\Omega} I_t j_1(A_t C_\gamma u) - j_1(C_\gamma u) dx. \quad (3.46)$$

Since  $j_1(C_\gamma u) \in W^{1,1}(\Omega)$ ,  $\frac{d}{dt} \left[ j_1(C_\gamma(u \circ T_t^{-1})) \right]_{t=0}$  exists in  $L^1(\Omega)$ . Therefore, using Lemma

3.2.4, Lemma (3.2.2) and Lemma 3.2.1, we have that

$$\begin{aligned}
\lim_{t \rightarrow 0} \frac{S_5(t)}{t} &= \lim_{t \rightarrow 0} \frac{\int_{\Omega} I_t j_1(A_t C_\gamma u) - j_1(C_\gamma u) dx}{t} \\
&= \frac{d}{dt} \int_{\Omega_t} j_1(C_\gamma(u \circ T_t^{-1})) dx \Big|_{t=0} \\
&= \int_{\Omega} \frac{d}{dt} [j_1(C_\gamma(u \circ T_t^{-1}))]_{t=0} dx + \int_{\partial\Omega} j_1(C_\gamma u) \mathbf{h} \cdot \mathbf{n} ds \\
&= \int_{\partial\Omega} j_1(C_\gamma u) \mathbf{h} \cdot \mathbf{n} ds - (j'_1(C_\gamma u), C_\gamma(\nabla u^T \cdot \mathbf{h}))_{\Omega}.
\end{aligned} \tag{3.47}$$

Hence

$$\begin{aligned}
dJ(u, \Omega) \mathbf{h} &= \lim_{t \rightarrow 0} \frac{R(t) + S(t)}{t} \\
&= -\frac{d}{dt} \langle \tilde{E}(u, t), p \rangle_{X^* \times X} |_{t=0} + \int_{\partial\Omega} j_1(C_\gamma u) \mathbf{h} \cdot \mathbf{n} ds - (j'_1(C_\gamma u), C_\gamma(\nabla u^T \cdot \mathbf{h}))_{\Omega}.
\end{aligned} \tag{3.48}$$

□

### 3.3 The Eulerian derivative of the 3 cost functionals

In the previous section we derived the Eulerian derivative of a generalized cost functional of the form  $J(u, \Omega) = \int_{\Omega} j_1(C_\gamma u)$  where  $C_\gamma$  is an affine operator. It was found to be

$$dJ(u, \Omega) \mathbf{h} = -\frac{d}{dt} \langle \tilde{E}(u, t), p \rangle_{X^* \times X} |_{t=0} + \int_{\partial\Omega} j_1(C_\gamma u) \mathbf{h} \cdot \mathbf{n} ds - (j'_1(C_\gamma u), C_\gamma(\nabla u^T \cdot \mathbf{h}))_{\Omega},$$

for  $j_1(u) = |u|^2$ . In the following subsections, we shall derive the Eulerian derivative of the 3 cost functionals.

#### 3.3.1 The Eulerian derivative of the curl type cost

In the this subsection we derive the Eulerian derivative of the curl type cost functional. We shall for simplicity consider the following shape optimization problem:

$$\min_{\Omega \in \mathcal{U}_{ad}} J(\mathbf{u}, \Omega) = \frac{1}{2} \int_{\Omega} |\operatorname{curl} \mathbf{u}|^2 dx \tag{3.49}$$

where

$$\operatorname{curl} \mathbf{u} = \frac{\partial u_2}{\partial x_1} - \frac{\partial u_1}{\partial x_2}, \tag{3.50}$$

subject to the Navier-Stokes equations

$$\begin{cases} -\eta \Delta \mathbf{u} + \mathbf{u} \cdot \nabla \mathbf{u} + \nabla p = \mathbf{f} & \text{in } \Omega, \\ \operatorname{div} \mathbf{u} = 0 & \text{in } \Omega, \\ \mathbf{u} = 0 & \text{on } \partial\Omega, \end{cases} \quad (3.51)$$

with  $\eta > 0$ ,  $\Omega$  is a bounded domain in  $\mathbb{R}^2$  which is assumed to be sufficiently smooth, i.e., with a  $C^2$  boundary  $\partial\Omega$  and  $\mathbf{f} \in \mathbf{L}^2(\Omega)$ .

**Note 3.3.1.** *The space  $\mathbf{L}^2(\Omega)$  is equivalent to  $L^2(\Omega, \mathbb{R}^2)$ ,  $\mathbf{H}^1(\Omega)$  is equivalent to  $H^1(\Omega)^2$  and hence the two notations will be used interchangeably throughout this subsection.*

In this example,  $E(u, \Omega) = 0$  is given by system (3.51). The operator

$$C_\gamma = C = \operatorname{curl}$$

and  $C_\gamma^* = \operatorname{curl}$  with  $\gamma = 0$ . Moreover it is easy to check that  $C \in \mathcal{L}(X, L^2)$  where  $X \equiv \mathbf{H}_0^1(\Omega) \times L_0^2(\Omega)$ . Further more, since  $\mathbf{u} \in \mathbf{H}_0^1(\Omega)$  we have that  $\operatorname{curl} \mathbf{u} \in L^2(\Omega, \mathbb{R})$ , i.e.,

$$\mathbf{u} \in H(\operatorname{curl}, \Omega) := \{\mathbf{u} \in L^2(\Omega, \mathbb{R}^2) : \operatorname{curl} \mathbf{u} \in L^2(\Omega, \mathbb{R})\}.$$

Hence the cost functional (3.49) is well defined. The variational formulation of (3.51) is:

Find  $(\mathbf{u}, p) \in X$  such that

$$\begin{aligned} \langle E((\mathbf{u}, p), \Omega), (\psi, \xi) \rangle_{X^* \times X} &\equiv \eta(\nabla \mathbf{u}, \nabla \psi)_\Omega + ((\mathbf{u} \cdot \nabla) \mathbf{u}, \psi)_\Omega - (p, \operatorname{div} \psi)_\Omega \\ &\quad - (\mathbf{f}, \psi)_\Omega + (\operatorname{div} \mathbf{u}, \xi)_\Omega = 0, \end{aligned} \quad (3.52)$$

holds for all  $(\psi, \xi) \in X$ , whose specific adjoint state  $(\lambda, q) \in X$  is given as a solution to

$$\langle E'((\mathbf{u}, p), \Omega)(\psi, \xi), (\lambda, q) \rangle_{X^* \times X} = \langle \operatorname{curl} \operatorname{curl} \mathbf{u}, \psi \rangle, \quad (3.53)$$

with right hand side  $\operatorname{curl} \operatorname{curl} \mathbf{u} = -\Delta \mathbf{u}$ , which amounts to

$$-\eta(\nabla \psi, \nabla \lambda)_\Omega + ((\psi \cdot \nabla) \mathbf{u} + (\mathbf{u} \cdot \nabla) \psi, \lambda)_\Omega - (\xi, \operatorname{div} \lambda)_\Omega + (\operatorname{div} \psi, q) = \langle -\Delta \mathbf{u}, \psi \rangle_\Omega. \quad (3.54)$$

Integrating by parts, one obtains

$$(\mathbf{u} \cdot \nabla) \psi, \lambda)_\Omega = \int_{\partial\Omega} (\psi \cdot \lambda) (\mathbf{u} \cdot \mathbf{n}) - \int_\Omega \psi \cdot \lambda \operatorname{div} \mathbf{u} - \int_\Omega \psi \cdot (\mathbf{u} \cdot \nabla) \lambda \, dx.$$

Since  $\mathbf{u} \in \mathbf{H}_0^1(\Omega)$  and  $\operatorname{div} \mathbf{u} = 0$ , we have

$$((\psi \cdot \nabla) \mathbf{u} + (\mathbf{u} \cdot \nabla) \psi, \lambda)_\Omega = (\psi, (\nabla \mathbf{u})^T \lambda - (\mathbf{u} \cdot \nabla) \lambda)_\Omega$$

holds for all  $\psi \in \mathbf{H}^1(\Omega)$ . As a consequence the adjoint equation in (3.54) can be written in strong form as

$$\begin{cases} -\alpha \Delta \lambda + (\nabla \mathbf{u})^T \cdot \lambda - (\mathbf{u} \cdot \nabla) \lambda + \nabla q = -\Delta \mathbf{u} & \text{in } \Omega, \\ \operatorname{div} \lambda = 0 & \text{in } \Omega, \\ \lambda = 0 & \text{on } \partial\Omega, \end{cases} \quad (3.55)$$

where the first equation hold in  $\mathbf{L}^2(\Omega)$  and the second one in  $L^2(\Omega)$ .

It is well known that equation (3.52) and (3.54) have unique solutions  $(\mathbf{u}, p), (\lambda, q) \in X$  respectively (see for example [Ito 2006], [Temam 1977] Chap.2 ), and since  $\partial\Omega \in C^2$ ,

$$(\mathbf{u}, p), (\lambda, q) \in H^2(\Omega)^2 \cap H_0^1(\Omega)^2 \times H^1(\Omega), \quad (3.56)$$

(see e.g [Ito 2006] and references there in). On  $\Omega_t$  the perturbed weak formulation of (3.51) reads:

Find  $(\mathbf{u}_t, p_t) \in X_t \equiv H_0^1(\Omega_t) \times L_0^2(\Omega_t)$  such that

$$\begin{aligned} \langle E((\mathbf{u}_t, p_t), \Omega_t), (\psi_t, \xi_t) \rangle_{X_t^* \times X_t} &\equiv \eta (\nabla \mathbf{u}_t, \nabla \psi_t)_{\Omega_t} + ((\mathbf{u}_t \cdot \nabla) \mathbf{u}_t, \psi_t)_{\Omega_t} \\ &\quad - (p_t, \operatorname{div} \psi_t)_{\Omega_t} - (\mathbf{f}_t, \psi_t)_{\Omega_t} + (\operatorname{div} \mathbf{u}_t, \xi_t)_{\Omega_t} = 0, \end{aligned} \quad (3.57)$$

holds for all  $(\psi_t, \xi_t) \in X_t$ .

Using the summation convention, the transformation of the divergence [Ito 2006] is given by

$$\operatorname{div} \psi_t \circ T_t = (D\psi_t^i A_t^T e_i) = ((A_t)_i \nabla \psi_t^i), \quad (3.58)$$

where  $e_i$  stands for the i-th canonical basis vector in  $\mathbb{R}^d$  and  $(A_t)_i$  denotes the i-th row of  $A_t = (DT_t)^{-T}$ . Thus the transformation of (3.57) back to  $\Omega$  becomes,

$$\begin{aligned} \langle \tilde{E}((\mathbf{u}^t, p^t), t), (\psi, \xi) \rangle_{X^* \times X} &\equiv \eta (I_t A_t \nabla \mathbf{u}^t, A_t \nabla \psi)_{\Omega} + ((\mathbf{u}^t \cdot A_t \nabla) \mathbf{u}^t, I_t \psi)_{\Omega} \\ &\quad - (p^t, I_t (A_t)_k \nabla \psi_k^t)_{\Omega} - (\mathbf{f}^t I_t, \psi)_{\Omega} + (I_t (A_t)_k \nabla u_k^t, \xi)_{\Omega} = 0 \quad \text{for all } (\psi, \xi) \in X. \end{aligned} \quad (3.59)$$

For computing the Eulerian derivative of  $J$ , we will need the derivative of (3.59) with respect to  $t$

at  $t = 0$ . To compute this derivative, we transform this expression back to  $\Omega_t$  to obtain

$$\begin{aligned} \langle \tilde{E}((\mathbf{u}, p), t), (\lambda, q) \rangle_{X^* \times X} &\equiv \eta(\nabla \mathbf{u} \circ T_t^{-1}, \nabla \lambda \circ T_t^{-1})_{\Omega_t} + ((\mathbf{u} \circ T_t^{-1} \cdot \nabla) \mathbf{u} \circ T_t^{-1}, \lambda \circ T_t^{-1})_{\Omega_t} \\ &\quad - (p \circ T_t^{-1}, \operatorname{div} \lambda \circ T_t^{-1})_{\Omega_t} - (\mathbf{f}, \lambda \circ T_t^{-1})_{\Omega_t} + (\operatorname{div} \mathbf{u} \circ T_t^{-1}, q \circ T_t^{-1})_{\Omega_t} = 0, \end{aligned} \quad (3.60)$$

where  $(\mathbf{u}, p), (\lambda, q) \in X$  are solutions of (3.52), respectively (3.54).

We compute the derivative of (3.60) term by term with respect to  $t$  at  $t = 0$  with the help of Lemma (3.2.1), Lemma (3.2.2) and (3.56). The derivative of the first term  $\alpha(\nabla \mathbf{u} \circ T_t^{-1}, \nabla \lambda \circ T_t^{-1})_{\Omega_t}$  with respect to  $t$  at  $t = 0$  is given by,

$$\begin{aligned} \frac{d}{dt} \eta(\nabla \mathbf{u} \circ T_t^{-1}, \nabla \lambda \circ T_t^{-1})_{\Omega_t} |_{t=0} &= \eta\left(\nabla(-\nabla \mathbf{u}^T \cdot \mathbf{h}), \nabla \lambda\right)_\Omega \\ &\quad + \eta\left(\nabla \mathbf{u}, \nabla(-\nabla \lambda^T \cdot \mathbf{h})\right) + \eta \int_{\partial \Omega} (\nabla \mathbf{u}, \nabla \lambda) \mathbf{h} \cdot \mathbf{n} \, ds. \end{aligned} \quad (3.61)$$

Similarly of the derivative of the second term  $((\mathbf{u} \circ T_t^{-1} \cdot \nabla) \mathbf{u} \circ T_t^{-1}, \lambda \circ T_t^{-1})_{\Omega_t}$  with respect to  $t$  at  $t = 0$  results in,

$$\begin{aligned} \frac{d}{dt} ((\mathbf{u} \circ T_t^{-1} \cdot \nabla) \mathbf{u} \circ T_t^{-1}, \lambda \circ T_t^{-1})_{\Omega_t} |_{t=0} &= \left( ((-\nabla \mathbf{u}^T \cdot \mathbf{h}) \cdot \nabla) \mathbf{u}, \lambda \right) + \\ &\quad \left( (\mathbf{u} \cdot \nabla)(-\nabla \mathbf{u}^T \cdot \mathbf{h}), \lambda \right) + \left( (\mathbf{u} \cdot \nabla) \mathbf{u}, -\nabla \lambda^T \cdot \mathbf{h} \right) + \int_{\partial \Omega} \left( (\mathbf{u} \cdot \nabla) \mathbf{u}, \lambda \right) \mathbf{h} \cdot \mathbf{n} \, ds, \end{aligned} \quad (3.62)$$

the third term gives

$$\begin{aligned} -\frac{d}{dt} (p \circ T_t^{-1}, \operatorname{div} \lambda \circ T_t^{-1})_{\Omega_t} |_{t=0} &= -\left(-\nabla p^T \cdot \mathbf{h}, \operatorname{div} \lambda\right) - \left(p, \operatorname{div}(-\nabla \lambda^T \cdot \mathbf{h})\right) \\ &\quad + \int_{\partial \Omega} \left(p, \operatorname{div} \lambda\right) \mathbf{h} \cdot \mathbf{n} \, ds, \end{aligned} \quad (3.63)$$

the fourth term gives

$$-\frac{d}{dt} (\mathbf{f}, \lambda \circ T_t^{-1})_{\Omega_t} |_{t=0} = -\left(\mathbf{f}, -\nabla \lambda^T \cdot \mathbf{h}\right) - \int_{\partial \Omega} \mathbf{f} \lambda \mathbf{h} \cdot \mathbf{n} \, ds, \quad (3.64)$$

and fifth term gives

$$\begin{aligned} \frac{d}{dt} (\operatorname{div} \mathbf{u} \circ T_t^{-1}, q \circ T_t^{-1})_{\Omega_t} |_{t=0} &= \left(\operatorname{div}(-\nabla \mathbf{u}^T \cdot \mathbf{h}), q\right) + \left(\operatorname{div} \mathbf{u}, -\nabla q^T \cdot \mathbf{h}\right) \\ &\quad + \int_{\partial \Omega} \operatorname{div} \mathbf{u} q \cdot \mathbf{n} \, ds. \end{aligned} \quad (3.65)$$

Thus collecting all results above, we obtain

$$\begin{aligned} \frac{d}{dt} \langle \tilde{E}((\mathbf{u}, p), t), (\lambda, q) \rangle_{X^* \times X} |_{t=0} &= \eta \left( \nabla(-\nabla \mathbf{u}^T \cdot \mathbf{h}), \nabla \lambda \right)_\Omega + \eta \left( \nabla \mathbf{u}, \nabla(-\nabla \lambda^T \cdot \mathbf{h}) \right)_\Omega \\ &\quad + \eta \int_{\partial\Omega} (\nabla \mathbf{u}, \nabla \lambda) \mathbf{h} \cdot \mathbf{n} \, ds + \left( ((-\nabla \mathbf{u}^T \cdot \mathbf{h}) \cdot \nabla) \mathbf{u}, \lambda \right) \\ &\quad + \left( (\mathbf{u} \cdot \nabla)(-\nabla \mathbf{u}^T \cdot \mathbf{h}), \lambda \right) + \left( (\mathbf{u} \cdot \nabla) \mathbf{u}, -\nabla \lambda^T \cdot \mathbf{h} \right) \\ &\quad + \eta \int_{\partial\Omega} \left( (\mathbf{u} \cdot \nabla) \mathbf{u}, \lambda \right) \mathbf{h} \cdot \mathbf{n} \, ds - \left( -\nabla p^T \cdot \mathbf{h}, \operatorname{div} \lambda \right) \\ &\quad - \left( p, \operatorname{div} (-\nabla \lambda^T \cdot \mathbf{h}) \right) + \int_{\partial\Omega} \left( p, \operatorname{div} \lambda \right) \mathbf{h} \cdot \mathbf{n} \, ds \\ &\quad - \left( \mathbf{f}, -\nabla \lambda^T \cdot \mathbf{h} \right) - \int_{\partial\Omega} \mathbf{f} \lambda \mathbf{h} \cdot \mathbf{n} \, ds + \left( \operatorname{div} (-\nabla \mathbf{u}^T \cdot \mathbf{h}), q \right) \\ &\quad + \left( \operatorname{div} \mathbf{u}, -\nabla q^T \cdot \mathbf{h} \right) + \int_{\partial\Omega} \operatorname{div} \mathbf{u} q \cdot \mathbf{n} \, ds. \end{aligned}$$

Since  $\operatorname{div} \mathbf{u} = \operatorname{div} \lambda = 0$  in  $\Omega$ , and  $\mathbf{u}, \lambda \in H_0^1(\Omega)^d$ , this expression simplifies to

$$\begin{aligned} \frac{d}{dt} \langle \tilde{E}((\mathbf{u}, p), t), (\lambda, q) \rangle_{X^* \times X} |_{t=0} &= \eta \left( \nabla \psi_u, \nabla \lambda \right)_\Omega + \eta \left( \nabla \mathbf{u}, \nabla \psi_\lambda \right)_\Omega + \\ &\quad \eta \int_{\partial\Omega} (\nabla \mathbf{u}, \nabla \lambda) \mathbf{h} \cdot \mathbf{n} \, ds + \left( (\psi_u \cdot \nabla) \mathbf{u}, \lambda \right)_\Omega + \left( (\mathbf{u} \cdot \nabla) \psi_u, \lambda \right)_\Omega + \left( (\mathbf{u} \cdot \nabla) \mathbf{u}, \psi_\lambda \right)_\Omega \\ &\quad - \left( p, \operatorname{div} \psi_\lambda \right)_\Omega - \left( \mathbf{f}, \psi_\lambda \right)_\Omega + \left( \operatorname{div} \psi_u, q \right)_\Omega, \end{aligned} \tag{3.66}$$

where

$$\psi_u = -\nabla \mathbf{u}^T \cdot \mathbf{h}, \quad \psi_\lambda = -\nabla \lambda^T \cdot \mathbf{h}.$$

Note  $\psi_u, \psi_\lambda \in \mathbf{H}^1(\Omega)$  but not  $\mathbf{H}_0^1(\Omega)$ . Applying Greens theorem to each term in (3.66) results for the first term in

$$\eta \left( \nabla \psi_u, \nabla \lambda \right)_\Omega = \eta \left( \psi_u, \nabla \lambda \cdot \mathbf{n} \right)_{\partial\Omega} - \eta \left( \psi_u, \Delta \lambda \right)_\Omega, \tag{3.67}$$

the second gives

$$\eta \left( \nabla \mathbf{u}, \nabla \psi_\lambda \right)_\Omega = \eta \left( \psi_\lambda, \nabla \mathbf{u} \cdot \mathbf{n} \right)_{\partial\Omega} - \eta \left( \psi_\lambda, \Delta \mathbf{u} \right)_\Omega, \tag{3.68}$$

and others

$$\left( (\psi_u \cdot \nabla) \mathbf{u}, \lambda \right)_\Omega = \left( \psi_u, (\nabla \mathbf{u}) \cdot \lambda \right)_\Omega, \quad (3.69)$$

$$\left( (\mathbf{u} \cdot \nabla) \psi_u, \lambda \right)_\Omega = \int_{\partial\Omega} (\psi_u \cdot \lambda) (\mathbf{u} \cdot \mathbf{n}) \, ds - \left( (\mathbf{u} \cdot \nabla) \lambda, \psi_u \right)_\Omega, \quad (3.70)$$

$$- \left( p, \operatorname{div} \psi_\lambda \right)_\Omega = \left( -p \cdot \mathbf{n}, \psi_\lambda \right)_{\partial\Omega} + \left( \nabla p, \psi_\lambda \right)_\Omega, \quad (3.71)$$

$$\left( \operatorname{div} \psi_u, q \right)_\Omega = \left( \psi_u, q \cdot \mathbf{n} \right)_{\partial\Omega} - \left( \nabla q, \psi_u \right)_\Omega. \quad (3.72)$$

Collecting terms from (3.67-3.72), we obtain

$$\begin{aligned} \frac{d}{dt} \langle \tilde{E}((\mathbf{u}, p), t), (\lambda, q) \rangle_{X^* \times X} |_{t=0} &= (-\eta \Delta \mathbf{u} + (\mathbf{u} \cdot \nabla \mathbf{u} + \nabla p - \mathbf{f}, \psi_\lambda)_\Omega + \\ &\quad \eta (\nabla \mathbf{u} \cdot \mathbf{n}, \psi_\lambda)_{\partial\Omega} - (p \psi_\lambda, \mathbf{n})_{\partial\Omega} + (-\eta \Delta \lambda + (\nabla \mathbf{u}) \lambda - (\mathbf{u} \cdot \nabla) \lambda - \nabla q, \psi_u)_\Omega \\ &\quad + \eta (\psi_u, \nabla \lambda \cdot \mathbf{n})_{\partial\Omega} + (q \cdot \mathbf{n}, \psi_u)_{\partial\Omega} + \eta \int_{\partial\Omega} (\nabla \mathbf{u}, \nabla \lambda) \mathbf{h} \cdot \mathbf{n} \, ds). \end{aligned} \quad (3.73)$$

For the curvilinear integrals in (3.73), we find

$$(\eta \nabla \mathbf{u} \nabla \lambda, \mathbf{h} \cdot \mathbf{n})_{\partial\Omega} = \left( \eta \frac{\partial \mathbf{u}}{\partial \mathbf{n}} \frac{\partial \lambda}{\partial \mathbf{n}} + \eta \frac{\partial \mathbf{u}}{\partial \mathbf{s}} \frac{\partial \lambda}{\partial \mathbf{s}}, \mathbf{h} \cdot \mathbf{n} \right)_{\partial\Omega} = \int_{\partial\Omega} \eta \left[ \frac{\partial \mathbf{u}}{\partial \mathbf{n}} \frac{\partial \lambda}{\partial \mathbf{n}} \right] (\mathbf{h} \cdot \mathbf{n}) \, ds, \quad (3.74)$$

$$\begin{aligned} \eta (\nabla \mathbf{u} \cdot \mathbf{n}, \psi_\lambda)_{\partial\Omega} &= \eta (\nabla \mathbf{u} \cdot \mathbf{n}, -\nabla \lambda^T \cdot \mathbf{h})_{\partial\Omega} = -\eta \left( \frac{\partial \mathbf{u}}{\partial \mathbf{n}}, \frac{\partial \lambda}{\partial \mathbf{n}} (\mathbf{h} \cdot \mathbf{n}) + \frac{\partial \lambda}{\partial \mathbf{s}} (\mathbf{h} \cdot \mathbf{s}) \right)_{\partial\Omega} \\ &= - \int_{\partial\Omega} \eta \left[ \frac{\partial \mathbf{u}}{\partial \mathbf{n}} \frac{\partial \lambda}{\partial \mathbf{n}} \right] (\mathbf{h} \cdot \mathbf{n}) \, ds, \end{aligned} \quad (3.75)$$

$$(p \psi_\lambda, n)_{\partial\Omega} = - \int_{\partial\Omega} (p \nabla \lambda^T \cdot \mathbf{h}, \mathbf{n}) \, ds = - \int_{\partial\Omega} p \left( \frac{\partial \lambda}{\partial \mathbf{n}}, \mathbf{n} \right) \mathbf{h} \cdot \mathbf{n} \, ds, \quad (3.76)$$

$$(q \cdot \mathbf{n}, \psi_u)_{\partial\Omega} = - \int_{\partial\Omega} (q \cdot \mathbf{n}, \nabla \mathbf{u}^T \cdot \mathbf{h}) \, ds = - \int_{\partial\Omega} q \left( \frac{\partial \mathbf{u}}{\partial \mathbf{n}}, \mathbf{n} \right) \mathbf{h} \cdot \mathbf{n} \, ds, \quad (3.77)$$

since  $\mathbf{u}, \lambda \in \mathbf{H}_0^1(\Omega)$ , yielding  $\frac{\partial \lambda}{\partial \mathbf{s}} = \frac{\partial \mathbf{u}}{\partial \mathbf{s}} = 0$ , where  $\frac{\partial}{\partial \mathbf{s}}$  stands for the derivative along  $\partial\Omega$ . Furthermore the first term on the right hand side of (3.73) vanishes since it satisfies the strong formulation of (3.52), while the fourth term satisfies the adjoint equation (3.54) with test function  $\psi_u$ . Thus rearranging all terms we obtain

$$\begin{aligned} \frac{d}{dt} \langle \tilde{E}((\mathbf{u}, p), t), (\lambda, q) \rangle_{X^* \times X} |_{t=0} &= - \int_{\partial\Omega} \left[ \eta \frac{\partial \mathbf{u}}{\partial \mathbf{n}} \frac{\partial \lambda}{\partial \mathbf{n}} - p \left( \frac{\partial \lambda}{\partial \mathbf{n}}, \mathbf{n} \right) + q \left( \frac{\partial \mathbf{u}}{\partial \mathbf{n}}, \mathbf{n} \right) \right] \mathbf{h} \cdot \mathbf{n} \, ds \\ &\quad + (\Delta \mathbf{u}, \nabla \mathbf{u}^T \cdot \mathbf{h})_\Omega. \end{aligned} \quad (3.78)$$

Using the definition of tangential divergence (3.8), we have that:

$$p\left(\frac{\partial \lambda}{\partial \mathbf{n}}, \mathbf{n}\right) = p(\nabla \lambda \cdot \mathbf{n}) \cdot \mathbf{n} = p \operatorname{div} \lambda|_{\partial \Omega} - p \operatorname{div}_{\partial \Omega} \lambda. \quad (3.79)$$

Since  $\lambda = 0$  on  $\partial \Omega$ , the last term in (3.79) vanishes (see [Sokolowski 1992] Page 82 for details). Furthermore  $\operatorname{div} \lambda = 0$  which renders this expression to be zero. Analogously,  $q\left(\frac{\partial \mathbf{u}}{\partial \mathbf{n}}, \mathbf{n}\right) = 0$ . Thus

$$\frac{d}{dt} \langle \tilde{E}((\mathbf{u}, p), t), (\lambda, q) \rangle_{X^* \times X}|_{t=0} = - \int_{\partial \Omega} \left[ \eta \frac{\partial \mathbf{u}}{\partial \mathbf{n}} \frac{\partial \lambda}{\partial \mathbf{n}} \right] \mathbf{h} \cdot \mathbf{n} ds + (\Delta \mathbf{u}, \nabla \mathbf{u}^T \cdot \mathbf{h})_{\Omega}. \quad (3.80)$$

### Shape derivative

To apply Theorem 3.2.1 to compute the Eulerian derivative of  $J$  in this example, we need to show that all the assumptions (H1-H6) stated in the previous section hold. Furthermore, we need to show that  $|\operatorname{curl} \mathbf{u}|^2 \in W^{1,1}(\Omega)$ .

Indeed for this particular example, assumptions (H1-H4) were verified in [Ito 2006]. Moreover for this particular choice of cost functional  $J$ , its easy to see that (H5) also holds. Furthermore, since (3.56) holds, it follows that  $\nabla \operatorname{curl} \mathbf{u} \in \mathbf{L}^2(\Omega)$ . Therefore, we infer that  $\nabla |\operatorname{curl} \mathbf{u}|^2 = 2 \operatorname{curl} \mathbf{u} \nabla \operatorname{curl} \mathbf{u} \in \mathbf{L}^2(\Omega) \hookrightarrow \mathbf{L}^1(\Omega)$ . This leads to the conclusion that  $|\operatorname{curl} \mathbf{u}|^2 \in W^{1,1}(\Omega)$ . It now remains to check whether (H6) holds. To this end, we state the following lemma whose proof can be found in [Monk 2003] (Lemma 3.57, Corollary 3.58).

**Lemma 3.3.1.** *Let  $T_t : \Omega \mapsto \Omega_t$  be a continuously differentiable, invertible and surjective map, and  $\mathbf{u}^t \in H(\operatorname{curl}, \Omega)$ . Then the transformation*

$$\mathbf{u}_t \circ T_t = D T_t^{-T} \mathbf{u}^t, \quad (3.81a)$$

implies  $\mathbf{u}_t \in H(\operatorname{curl}, \Omega_t)$  with

$$\operatorname{curl} \mathbf{u}_t \circ T_t = I_t^{-1} D T_t \operatorname{curl} \mathbf{u}^t \quad (3.81b)$$

for  $\Omega_t \subset \mathbb{R}^3$ . In two dimensions, we obtain instead

$$\operatorname{curl} \mathbf{u}_t \circ T_t = I_t^{-1} \operatorname{curl} \mathbf{u}^t, \quad (3.81c)$$

where  $I_t = \det(D T_t)$ .

Thus from the above transformation of the curl, since  $\Omega \subset \mathbb{R}^2$ , we have that  $A_t = I_t^{-1} I$  and by

(3.7), we have  $\lim_{t \rightarrow 0} A_t - I = 0$ . Moreover

$$\lim_{t \rightarrow 0} \frac{A_t - I}{t} = -\operatorname{div} \mathbf{h}.$$

Since all assumptions of Theorem 3.2.1 are satisfied, using (3.30), we can express the Eulerian derivative of (3.49) as

$$\begin{aligned} dJ(\mathbf{u}, \Omega) \mathbf{h} &= \int_{\partial\Omega} \left[ \eta \frac{\partial \mathbf{u}}{\partial \mathbf{n}} \frac{\partial \lambda}{\partial \mathbf{n}} \right] ds - (\Delta \mathbf{u}, \nabla \mathbf{u}^T \cdot \mathbf{h})_\Omega + \frac{1}{2} \int_{\Omega} |\operatorname{curl} \mathbf{u}|^2 \mathbf{h} \cdot \mathbf{n} ds \\ &\quad - (\operatorname{curl} \mathbf{u}, \operatorname{curl} (\nabla \mathbf{u}^T \cdot \mathbf{h}))_\Omega. \end{aligned} \quad (3.82)$$

Using the Greens formula [Monk 2003]

$$\int_{\Omega} \operatorname{curl} \mathbf{u} \cdot \operatorname{curl} (\nabla \mathbf{u}^T \cdot \mathbf{h}) dx = -(\Delta \mathbf{u}, \nabla \mathbf{u}^T \cdot \mathbf{h})_\Omega + \int_{\partial\Omega} ((\operatorname{curl} \mathbf{u} \times \mathbf{n}) \cdot \nabla \mathbf{u}^T \cdot \mathbf{h}) ds, \quad (3.83)$$

we obtain

$$dJ(\mathbf{u}, \Omega) \mathbf{h} = \int_{\partial\Omega} \left[ \eta \frac{\partial \mathbf{u}}{\partial \mathbf{n}} \frac{\partial \lambda}{\partial \mathbf{n}} + \frac{1}{2} |(\operatorname{curl} \mathbf{u})|^2 \right] \mathbf{h} \cdot \mathbf{n} ds - \int_{\partial\Omega} ((\operatorname{curl} \mathbf{u} \times \mathbf{n}) \cdot \nabla \mathbf{u}^T \cdot \mathbf{h}) ds. \quad (3.84)$$

Using similar arguments as before (see equation 3.75), since  $\mathbf{u} \in \mathbf{H}_0^1(\Omega)$ , we have that

$$(\nabla \mathbf{u}, \mathbf{h}) = \frac{\partial \mathbf{u}}{\partial \mathbf{n}}(\mathbf{h}, \mathbf{n}),$$

and thus we further simplify (3.84) to

$$dJ(\mathbf{u}, \Omega) \mathbf{h} = \int_{\partial\Omega} \left[ \eta \frac{\partial \mathbf{u}}{\partial \mathbf{n}} \frac{\partial \lambda}{\partial \mathbf{n}} + \frac{1}{2} |\operatorname{curl} \mathbf{u}|^2 - (\operatorname{curl} \mathbf{u} \times \mathbf{n}) \frac{\partial \mathbf{u}}{\partial \mathbf{n}} \right] \mathbf{h} \cdot \mathbf{n} ds. \quad (3.85)$$

**Remark 3.3.1.** We remark here that for some reference problems we presented earlier, instead of (3.51) a general flow problem is considered:

$$\left\{ \begin{array}{l} -\eta \Delta \mathbf{u} + \mathbf{u} \cdot \nabla \mathbf{u} + \nabla p = \mathbf{f} \text{ in } \Omega, \\ \operatorname{div} \mathbf{u} = 0 \text{ in } \Omega, \\ \mathbf{u} = 0 \text{ on } \Gamma_w, \\ -p \cdot \mathbf{n} + \eta \frac{\partial \mathbf{u}}{\partial \mathbf{n}} = 0, \text{ on } \Gamma_{\text{out}} \\ \mathbf{u} = \mathbf{u}_{\text{in}} \text{ on } \Gamma_{\text{in}}, \\ \mathbf{u} = \mathbf{g} \text{ on } \Gamma_f, \end{array} \right. \quad (3.86)$$

where the boundary  $\partial\Omega$  consist of the inflow boundary  $\Gamma_{\text{in}}$ , the outflow boundary  $\Gamma_{\text{out}}$ , the bound-

ary  $\Gamma_f$  to be optimized, and other fixed boundaries  $\Gamma_w$  where we prescribe no-slip boundary conditions. It is important to note that the deformation field  $\mathbf{h}$  is zero on all fixed boundaries except on  $\Gamma_f$ . This means that if  $\mathbf{g}$  is zero, then formulae (3.85) still holds for the general problem (3.86) but with support on  $\Gamma_f$ . If  $\mathbf{g}$  is not equal to zero, we can find an extension ( $\tilde{\mathbf{g}} \in \mathbf{H}^1(\Omega)$ ) of  $\mathbf{g}$  such that  $\tilde{\mathbf{g}}|_{\Gamma_f} = \mathbf{g}$ . The difference  $\mathbf{u} - \tilde{\mathbf{g}} \in \mathbf{H}_0^1(\Omega)$ , satisfies the results of the previous discussions, and consequently (3.85) becomes

$$dJ(\mathbf{u}, \Omega)\mathbf{h} = \int_{\Gamma_f} \left[ \eta \frac{\partial(\mathbf{u} - \mathbf{g})}{\partial \mathbf{n}} \frac{\partial \lambda}{\partial \mathbf{n}} + \frac{1}{2} |\operatorname{curl} \mathbf{u}|^2 - (\operatorname{curl} \mathbf{u} \times \mathbf{n}) \frac{\partial(\mathbf{u} - \mathbf{g})}{\partial \mathbf{n}} \right] \mathbf{h} \cdot \mathbf{n} \, ds. \quad (3.87)$$

where  $\lambda$  solves (instead of (3.55)) the following system

$$\begin{cases} -\eta \Delta \lambda + (\nabla \mathbf{u})^T \cdot \lambda - (\mathbf{u} \cdot \nabla) \lambda + \nabla q = -\Delta \mathbf{u} & \text{in } \Omega, \\ \operatorname{div} \lambda = 0 & \text{in } \Omega, \\ \lambda = 0 & \text{on } \Gamma_w \cup \Gamma_f \cup \Gamma_{in}, \\ q \cdot \mathbf{n} - \eta \nabla \lambda \cdot \mathbf{n} - (\mathbf{u} \cdot \mathbf{n}) \lambda = 0 & \text{on } \Gamma_{out}. \end{cases} \quad (3.88)$$

**Remark 3.3.2.** Formula (3.87) makes sense because by regularity of  $\mathbf{u}$  and  $\lambda$ , i.e.,  $(\mathbf{u}, p), (\lambda, q) \in H^2(\Omega)^2 \cap H_0^1(\Omega)^2 \times H^1(\Omega)$  and therefore  $\frac{\partial(\mathbf{u} - \mathbf{g})}{\partial \mathbf{n}}$  and  $\frac{\partial \lambda}{\partial \mathbf{n}}$  belong to  $\mathbf{L}^2(\Gamma_f)$  by the trace theorem 2.1.6.

### 3.3.2 The Eulerian derivative of a tracking type cost

In this subsection we derive the shape derivative of a general tracking type cost functional

$$J(\mathbf{u}, \Omega) = \frac{1}{2} \int_{\Omega} (A\mathbf{u} - \mathbf{u}_d)^2 \, dx, \quad A \in \mathbb{R}^{2 \times 2}. \quad (3.89)$$

using the general theory developed in the last subsection, that is we need to show that all the assumptions (H1-H6) stated in the previous subsection hold so that we can apply Theorem 3.2.1 to compute the Eulerian derivative of  $J$ . We consider the following constrained shape optimization problem

$$\min_{\Omega \in \mathcal{U}_{ad}} J(\mathbf{u}, \Omega) = \frac{1}{2} \int_{\Omega} (A\mathbf{u} - \mathbf{u}_d)^2 \, dx, \quad A \in \mathbb{R}^{2 \times 2} \quad (3.90)$$

subject to the Navier-Stokes equations (3.51).

**Theorem 3.3.1.** *Let  $\Omega$  be of class  $C^{1,1}$ ,  $\mathbf{h}$  a vector field, the shape derivative of the cost functional  $J$  can be expressed as*

$$dJ(\mathbf{u}, \Omega)\mathbf{h} = \int_{\partial\Omega} \left[ \eta \frac{\partial \mathbf{u}}{\partial \mathbf{n}} \frac{\partial \lambda}{\partial \mathbf{n}} + \frac{1}{2} (A\mathbf{u} - \mathbf{u}_d)^2 \right] \mathbf{h} \cdot \mathbf{n} \, ds. \quad (3.91)$$

where  $(\lambda, q) \in X$  is given as a solution to adjoint state

$$\langle E'((\mathbf{u}, p), \Omega)(\psi, \xi), (\lambda, q) \rangle_{X^* \times X} = \langle A\mathbf{u} - \mathbf{u}_d, \psi \rangle, \quad (3.92)$$

which amounts to

$$-\eta(\nabla\psi, \nabla\lambda)_\Omega + ((\psi \cdot \nabla)\mathbf{u} + (\mathbf{u} \cdot \nabla)\psi, \lambda)_\Omega - (\xi, \operatorname{div} \lambda)_\Omega + (\operatorname{div} \psi, q) = \langle A\mathbf{u} - \mathbf{u}_d, \psi \rangle_\Omega. \quad (3.93)$$

Integrating by parts of  $(\mathbf{u} \cdot \nabla)\psi, \lambda)_\Omega$  in (3.93), results in the strong form

$$\begin{cases} -\alpha\Delta\lambda + (\nabla\mathbf{u})^T \cdot \lambda - (\mathbf{u} \cdot \nabla)\lambda + \nabla q = (A\mathbf{u} - \mathbf{u}_d), & \text{in } \Omega, \\ \operatorname{div} \lambda = 0 \text{ in } \Omega, \\ \lambda = 0 \text{ on } \partial\Omega, \end{cases} \quad (3.94)$$

where the first equation in (3.94) hold in  $\mathbf{L}^2(\Omega)$  and the second one in  $L^2(\Omega)$ .

*Proof.* In this case,  $C_\gamma : \mathbf{u}(x) \mapsto A\mathbf{u} - \mathbf{u}_d \in \mathbf{L}^2(\Omega)$  with  $\gamma = -\mathbf{u}_d \in \mathbf{L}^2(\Omega)$ . The linear differential operator  $C \in \mathcal{L}(X, \mathbf{L}^2(\Omega))$  is such that

$$C : \mathbf{u}(\cdot) \mapsto A\mathbf{u}(\cdot),$$

and moreover

$$C_\gamma \mathbf{u}_t \circ T_t = C\mathbf{u}^t - \mathbf{u}_d. \quad (3.95)$$

Consequently  $A_t$  from (H6) is given by  $A_t = I$  and

$$\lim_{t \rightarrow 0} \frac{A_t - I}{t} = 0.$$

As observed in the previous example, we have that

$$\frac{d}{dt} \langle \tilde{E}((\mathbf{u}, p), t), (\lambda, q) \rangle_{X^* \times X} |_{t=0} = - \int_{\partial\Omega} \left[ \eta \frac{\partial \mathbf{u}}{\partial \mathbf{n}} \frac{\partial \lambda}{\partial \mathbf{n}} \right] ds - (A\mathbf{u} - \mathbf{u}_d, A(\nabla \mathbf{u}^T) \mathbf{h})_\Omega, \quad (3.96)$$

where  $(\lambda, q)$  solves (3.93) and

$$\langle J'(C\mathbf{u}), C\nabla \mathbf{u}^T \mathbf{h} \rangle = (A\mathbf{u} - \mathbf{u}_d, A(\nabla \mathbf{u}^T) \mathbf{h})_\Omega. \quad (3.97)$$

It is also clear by the Sobolev embedding (Theorem (2.1.4)) that since  $\mathbf{u} \in \mathbf{H}^2(\Omega)$ , then  $|A\mathbf{u} -$

$|\mathbf{u}_d|^2 \in W^{1,1}$ . Furthermore, since all assumptions (H1-H6) are satisfied, we use (3.30) to obtain

$$dJ(\mathbf{u}, \Omega)\mathbf{h} = \int_{\partial\Omega} \left[ \eta \frac{\partial \mathbf{u}}{\partial \mathbf{n}} \frac{\partial \lambda}{\partial \mathbf{n}} + \frac{1}{2} (\mathbf{A}\mathbf{u} - \mathbf{u}_d)^2 \right] \mathbf{h} \cdot \mathbf{n} \, ds. \quad (3.98)$$

□

**Note 3.3.2.** If  $A = I$  we obtain

$$dJ(\mathbf{u}, \Omega)\mathbf{h} = \int_{\partial\Omega} \left[ \eta \frac{\partial \mathbf{u}}{\partial \mathbf{n}} \frac{\partial \lambda}{\partial \mathbf{n}} + \frac{1}{2} (\mathbf{u} - \mathbf{u}_d)^2 \right] \mathbf{h} \cdot \mathbf{n} \, ds, \quad (3.99)$$

which is the shape derivative of a tracking type cost functional.

**Remark 3.3.3.** As noted in Remark 3.3.1, for a general flow problem (3.86), formulae (3.98) becomes

$$dJ(\mathbf{u}, \Omega)\mathbf{h} = \int_{\Gamma_f} \left[ \eta \frac{\partial(\mathbf{u} - \mathbf{g})}{\partial \mathbf{n}} \frac{\partial \lambda}{\partial \mathbf{n}} + \frac{1}{2} |\mathbf{A}\mathbf{u} - \mathbf{u}_d|^2 \right] \mathbf{h} \cdot \mathbf{n} \, ds. \quad (3.100)$$

where  $\lambda$  solves instead of (3.94) the following system

$$\begin{cases} -\eta \Delta \lambda + (\nabla \mathbf{u})^T \cdot \lambda - (\mathbf{u} \cdot \nabla) \lambda + \nabla q = (\mathbf{A}\mathbf{u} - \mathbf{u}_d) & \text{in } \Omega, \\ \operatorname{div} \lambda = 0 & \text{in } \Omega, \\ \lambda = 0 & \text{on } \Gamma_w \cup \Gamma_f \cup \Gamma_{in}, \\ q \cdot \mathbf{n} - \eta \nabla \lambda \cdot \mathbf{n} - (\mathbf{u} \cdot \mathbf{n}) \lambda = 0 & \text{on } \Gamma_{out}. \end{cases} \quad (3.101)$$

**Remark 3.3.4.** Again Formula (3.100) makes sense by remark 3.3.2.

### 3.3.3 The Eulerian derivative of cost functional $J_3$

In this subsection we derive the shape derivative of the cost functional

$$J_3(\Omega, \mathbf{u}) = \int_{\Omega} g_3(\det \nabla \mathbf{u}) \, dx,$$

where

$$g_3 = \begin{cases} 0 & t \leq 0 \\ l(t) & t > 0 \end{cases} \quad \text{with } l(t) = \frac{t^3}{t^2 + 1}.$$

The functional  $J_3$  is continuous and moreover for  $\mathbf{u} \in \mathbf{H}_0^1(\Omega)$  and  $\delta \mathbf{u} \in \mathbf{H}_0^1(\Omega)$  there exists a directional derivative  $J'_3(\Omega, \mathbf{u})(\delta \mathbf{u})$  given by

$$J'_3(\Omega, \mathbf{u})(\delta \mathbf{u}) = \int_{\Omega} g'_3(\det(\nabla \mathbf{u})) \cdot (u_{x_1}^1 \delta u_{x_2}^2 + \delta u_{x_1}^1 u_{x_2}^2 - u_{x_1}^2 \delta u_{x_2}^1 - u_{x_2}^1 \delta u_{x_1}^2) \, dx. \quad (3.102)$$

Here we cannot use the general theory developed in the last subsection, that is, assumption H6 stated in the previous subsection is not satisfied and thus we cannot apply Theorem 3.2.1 to compute the Eulerian derivative of  $J_3$ . Therefore we shall use here the classical results of shape derivative as in [Sokolowski 1992]. We shall need to first compute the derivative of the state equation. The shape derivative of the state variables  $(\mathbf{u}, p)$  is the solution of the following linear system [Henrot 2009]:

$$\begin{cases} -\eta \Delta \mathbf{u}' + D\mathbf{u} \cdot \mathbf{u}' + D\mathbf{u}' \cdot \mathbf{u} + \nabla p' = 0 & \text{in } \Omega, \\ \operatorname{div} \mathbf{u}' = 0 & \text{in } \Omega, \\ \mathbf{u}' = -D\mathbf{u} \cdot \mathbf{n}(\mathbf{h}, \mathbf{n}) & \text{on } \partial\Omega. \end{cases} \quad (3.103)$$

Now, we have (see Lemma (3.2.1))

$$dJ_3(\Omega; \mathbf{u})\mathbf{h} = \int_{\Omega} g'_3(\det(\nabla \mathbf{u})) \cdot \left( u_{x_1}^1 (u'_2)_{x_2} + (u'_1)_{x_1} u_{x_2}^2 - u_{x_1}^2 (u'_1)_{x_2} - u_{x_2}^1 (u'_2)_{x_1} \right) dx + \int_{\partial\Omega} g_3(\det \nabla \mathbf{u}) \mathbf{h} \cdot \mathbf{n} ds. \quad (3.104)$$

It is more convenient to work with another expression of the shape derivative. For that purpose, we need to introduce an adjoint state.

**Proposition 3.3.1.** *Let us consider  $(\lambda, q) \in X$ , solution of the following adjoint problem*

$$\begin{cases} -\eta \Delta \lambda + (\nabla \mathbf{u})^T \cdot \lambda - (\mathbf{u} \cdot \nabla) \lambda + \nabla q = R(\mathbf{u}) & \text{in } \Omega, \\ \operatorname{div} \lambda = 0 & \text{in } \Omega, \\ \lambda = 0 & \text{on } \partial\Omega, \end{cases} \quad (3.105)$$

where

$$R(\mathbf{u}) = \begin{pmatrix} -\operatorname{curl}(g'_3(\det \nabla \mathbf{u})) \nabla u_2 \\ \operatorname{curl}(g'_3(\det \nabla \mathbf{u})) \nabla u_1 \end{pmatrix}, \quad (3.106)$$

If the viscosity  $\eta$  is large enough, then the problem (3.105) has a unique solution  $(\lambda, q)$ .

*Proof.* The proof follows ideas in [Henrot 2009] but with a right hand side as  $R(u)$ .  $\square$

**Theorem 3.3.2.** *Let  $\Omega$  be of class  $C^2$ ,  $\mathbf{h}$  a vector field, the shape gradient  $\nabla J_3$  of the cost functional  $J_3$  can be expressed as*

$$\nabla J_3 = [g_3(\det \nabla \mathbf{u}) + (D(\mathbf{u} - \mathbf{g}) \cdot \mathbf{n}) \cdot (\eta(D\lambda \cdot \mathbf{n}) - P(\mathbf{u}))] \mathbf{n}, \quad (3.107)$$

where the adjoint state  $\lambda$  satisfies (3.105) and

$$P(\mathbf{u}) = \begin{pmatrix} g'_3(\det \nabla \mathbf{u}) \left( \frac{\partial u_2}{\partial x_2} - \frac{\partial u_2}{\partial x_1} \right) \\ g'_3(\det \nabla \mathbf{u}) \left( \frac{\partial u_1}{\partial x_1} - \frac{\partial u_1}{\partial x_2} \right) \end{pmatrix}.$$

*Proof.* Since  $J_3(\Omega)$  is differentiable with respect to  $\mathbf{u}$ , and the state  $\mathbf{u}$  is differentiable with respect to  $t$ , we obtain the Eulerian derivative of  $J_3(\Omega)$  with respect to  $t$ ,

$$\begin{aligned} dJ_3(\Omega; \mathbf{h}) &= \int_{\Omega} g'_3(\det(\nabla \mathbf{u})) \cdot \left( u_{x_1}^1 (u'_2)_{x_2} + (u'_1)_{x_1} u_{x_2}^2 - u_{x_1}^2 (u'_1)_{x_2} - u_{x_2}^1 (u'_2)_{x_1} \right) dx + \\ &\quad \int_{\partial\Omega} g_3(\det \nabla \mathbf{u}) \mathbf{h} \cdot \mathbf{n} ds, \end{aligned} \quad (3.108)$$

where  $u'_1 := \frac{\partial u^1}{\partial t}$ ,  $u'_2 := \frac{\partial u^2}{\partial t}$  and  $\mathbf{u}' = (u'_1, u'_2)$ .

Using integration by parts, the first term in (3.108) can be written as

$$\begin{aligned} \int_{\Omega} g'_3(\det(\nabla \mathbf{u})) \cdot \left( u_{x_1}^1 (u'_2)_{x_2} + (u'_1)_{x_1} u_{x_2}^2 - u_{x_1}^2 (u'_1)_{x_2} - u_{x_2}^1 (u'_2)_{x_1} \right) dx &= \int_{\Omega} R(\mathbf{u}) \mathbf{u}' dx \\ &\quad + \int_{\partial\Omega} P(\mathbf{u}) \mathbf{u}' ds. \end{aligned} \quad (3.109)$$

From system (6.60), and using greens formula , we have for any

$(\mathbf{w}, \pi) \in \mathbf{H}_0^1(\Omega) \times L_0^2(\Omega)$  that

$$\begin{aligned} 0 &= \int_{\Omega} (-\eta \Delta \mathbf{u}' + D\mathbf{u} \cdot \mathbf{u}' + D\mathbf{u}' \cdot \mathbf{u} + \nabla p') \cdot \mathbf{w} - (\operatorname{div} \mathbf{u}') \cdot \pi dx \\ &= \int_{\Omega} (-\eta \Delta \mathbf{w} - D\mathbf{w} \cdot \mathbf{u} + *D\mathbf{u} \cdot \mathbf{w} + \nabla \pi) \cdot \mathbf{u}' - (\operatorname{div} \mathbf{w}) \cdot p' dx \\ &\quad + \int_{\partial\Omega} \eta \mathbf{u}' D\mathbf{w} \cdot \mathbf{n} - \eta \mathbf{w} D\mathbf{u}' \cdot \mathbf{n} ds \\ &\quad + \int_{\partial\Omega} (\mathbf{u}' \cdot \mathbf{w})(\mathbf{u} \cdot \mathbf{n}) + \mathbf{w} p' \cdot \mathbf{n} - \mathbf{u}' \pi \cdot \mathbf{n} ds. \end{aligned} \quad (3.110)$$

We define  $(\lambda, q)$  to be the solution of the adjoint equation (3.105) and set  $(\mathbf{w}, \pi) = (\lambda, q)$  in (3.110) to obtain

$$\begin{aligned} 0 &= \int_{\Omega} R(\mathbf{u}) \cdot \mathbf{u}' dx + \int_{\partial\Omega} \eta \mathbf{u}' D\lambda \cdot \mathbf{n} - \mathbf{u}' q \cdot \mathbf{n} ds \\ \int_{\Omega} R(\mathbf{u}) \cdot \mathbf{u}' dx &= - \int_{\partial\Omega} (\eta D\lambda \cdot \mathbf{n} - q \cdot \mathbf{n}) \mathbf{u}' ds. \end{aligned}$$

Since  $\mathbf{u}' = -D\mathbf{u} \cdot \mathbf{n}(\mathbf{h}, \mathbf{n})$  on  $\partial\Omega$  and  $\operatorname{div} \mathbf{u}' = 0$  in  $\Omega$ , we obtain the Eulerian derivative from (3.108):

$$dJ_3(\Omega; \mathbf{h}) = \int_{\partial\Omega} \left( g_3(\det \nabla \mathbf{u}) + D\mathbf{u} \cdot \mathbf{n} \cdot (\eta D\lambda \cdot \mathbf{n} - P(\mathbf{u})) \right) \mathbf{h} \cdot \mathbf{n} ds. \quad (3.111)$$

Since the mapping  $\mathbf{h} \mapsto dJ_3(\Omega; \mathbf{u})\mathbf{h}$  is linear and continuous, we get the expression for the shape gradient (4.2).  $\square$

**Remark 3.3.5.** Again as noted in Remark 3.3.1, for a general flow problem (3.86), formulae (3.111) becomes

$$dJ_3(\mathbf{u}, \Omega)\mathbf{h} = \int_{\Gamma_f} \left[ g_3(\det \nabla \mathbf{u}) + D(\mathbf{u} - \mathbf{g}) \cdot \mathbf{n} \cdot (\eta D\lambda \cdot \mathbf{n} - P(\mathbf{u})) \right] \mathbf{h} \cdot \mathbf{n} \, ds. \quad (3.112)$$

where  $\lambda$  solves instead of (3.105) the following system

$$\begin{cases} -\eta \Delta \lambda + (\nabla \mathbf{u})^T \cdot \lambda - (\mathbf{u} \cdot \nabla) \lambda + \nabla q = R(\mathbf{u}) \text{ in } \Omega, \\ \operatorname{div} \lambda = 0 \text{ in } \Omega, \\ \lambda = 0 \text{ on } \Gamma_w \cup \Gamma_f \cup \Gamma_{in}, \\ q \cdot \mathbf{n} - \eta \nabla \lambda \cdot \mathbf{n} - (\mathbf{u} \cdot \mathbf{n}) \lambda = 0 \text{ on } \Gamma_{out}. \end{cases} \quad (3.113)$$

**Remark 3.3.6.** Again Formula (3.112) makes sense by remark 3.3.2.

**Remark 3.3.7.** As a consequence of the preceding discussion, we find,

$$dJ(\mathbf{u}, \Omega)\mathbf{h} = \int_{\Gamma_f} G \mathbf{h} \cdot \mathbf{n} \, ds, \quad (3.114)$$

where  $\mathbf{n}$  denotes the unit outer normal on the free-boundary ( $\Gamma_f$ ) to be optimized and  $G$  is the shape gradient for example in (3.99)

$$G = \left[ \eta \frac{\partial \mathbf{u}}{\partial \mathbf{n}} \frac{\partial \lambda}{\partial \mathbf{n}} + \frac{1}{2} (\mathbf{u} - \mathbf{u}_d)^2 \right] \mathbf{n}.$$

Thus the shape sensitivity is a linear functional of  $\mathbf{h}$  concentrated on  $(\partial\Omega)$ .

**Remark 3.3.8.** Another key observation is that the shape sensitivity  $dJ(\mathbf{u}, \Omega)\mathbf{h}$  depends on  $\mathbf{h} \cdot \mathbf{n}|_{\partial\Omega}$  only while it is completely independent of the values for  $\mathbf{h}$  inside  $\Omega$ , and of its tangential component. Consequently, we may directly consider variations of  $\partial\Omega$  with a velocity  $\mathbf{h} = h_n \mathbf{n}$  where  $h_n$  is a scalar speed function. The shape sensitivity then becomes

$$dJ(\mathbf{u}, \Omega)h_n = \int_{\partial\Omega} Gh_n \, ds. \quad (3.115)$$

The statement that the shape sensitivity is a linear functional of  $\mathbf{h} \cdot \mathbf{n}$  holds for very general classes of objective functionals, it is usually known as the "Hadamard-Zolésio Structure Theorem". The independence of the shape sensitivity on tangential components is clear from geometric intuition, since those components correspond to a change of parametrization only. The independence on

values of  $\mathbf{h}$  in the interior of  $\Omega$  seems obvious, too, since they do not change the domain of integration in the objective functional.

## 3.4 Solution approaches

In this section we discuss several approaches for solving shape problems in general without claiming to be complete. The goal is to give the reader sufficient background on possible choices as well as to highlight which choice is taken in the present study.

Shape optimization problems are usually solved numerically, by using iterative methods. That is, one starts with an initial guess for a shape, and then gradually evolves it, until it morphs into the optimal shape. This means one needs to find a way to represent a shape in the computer memory, and follow its evolution. Below we shall briefly describe several approaches that are usually used with special emphasis on the boundary variation method that we use in this work.

### 3.4.1 Level set method

One approach is to consider a function defined on a rectangular box around the shape, which is positive inside of the shape, zero on the boundary of the shape, and negative outside of the shape. One can then evolve this function instead of the shape itself. One can consider a rectangular grid on the box and sample the function at the grid points. As the shape evolves, the grid points do not change; only the function values at the grid points change. This approach, of using a fixed grid, is called the **Eulerian approach**. The idea of using a function to represent the shape is at the basis of the **level set method**. This method was introduced in [Osher 1988] to track moving interfaces. In this method, a domain and its boundary are represented as level sets of a continuous function  $\psi$ . We refer to [Sethian 1999] for a complete description of this method. We give a brief description of the level set formulation for the evolution of a domain  $\Omega \subset D \subset \mathbb{R}^2$  under a given velocity field  $\mathbf{h}$ . Let us consider the domain

$$\Omega_t = (I + t\mathbf{h})(\Omega), \quad t \in \mathbb{R}^+, \quad (3.116)$$

with a smooth vector field  $\mathbf{h}$  compactly supported in  $D$ . For  $t \in [0, T]$ , the domain  $\Omega_t$  and its boundary are defined by a function  $\psi = \psi(x, y, t) \in \mathbb{R}$ ,  $(x, y) \in D$  such that for  $t \in [0, T]$

$$\Omega_t = \{(x, y) \in D, \psi(x, y, t) < 0\}, \quad (3.117)$$

$$\partial\Omega_t = \{(x, y) \in D, \psi(x, y, t) = 0\}. \quad (3.118)$$

We consider the position  $(x(t), y(t))$  of a particle on a (given) level curve of  $\psi(\cdot, t)$  moving with velocity  $\mathbf{h} = (x'(t), y'(t))$ . Then we have

$$\psi(x(t), y(t), t) = \text{constant for all } t \in [0, T]. \quad (3.119)$$

Differentiating (3.119) with respect to  $t$ , we obtain the following transport equation

$$\psi_t + \mathbf{h} \cdot \nabla \psi = 0, \quad (3.120)$$

$$\psi(\cdot, 0) = \psi_0, \quad (3.121)$$

where  $\psi_0$  is any function such that  $\Omega_0 = \{(x, y) \in D, \psi_0(x, y) < 0\}$ . The unit normal vectors  $\mathbf{n}$  to the level sets of  $\psi$  are given by  $\mathbf{n} = \nabla \psi / |\nabla \psi|$ . Substituting this in (3.119) leads to the Hamilton-Jacobi equation

$$\psi_t + h_n |\nabla \psi| = 0 \quad \text{in } D \times [0, T], \quad (3.122)$$

$$\psi(\cdot, 0) = \psi_0, \quad (3.123)$$

where  $h_n = (\mathbf{h} \cdot \mathbf{n})$  is the normal component of velocity. The initial data  $\psi_0(x, y)$  to this equation is chosen as a signed distance function to the initial boundary  $\partial\Omega_0 = \partial\Omega$ , i.e.,

$$\psi_0(x, y) = \pm \text{dist}((x, y), \partial\Omega_0) \quad \text{for } (x, y) \in D, \quad (3.124)$$

with the minus sign (resp. plus sign) if the point  $x$  is inside the initial domain  $\Omega_0 = \Omega$ . A homogenous Neumann boundary condition on the boundary  $\partial D$  is chosen for the whole domain  $D$ , (see e.g., [Fulmanski 2008],[Ameur 2004]).

### 3.4.1.1 Normal velocity for level set method

Recall that the Eulerian derivative of the cost  $J$  associated to a velocity field  $h$  can be expressed as

$$dJ(u, \Omega)\mathbf{h} = \int_{\partial\Omega} G(\mathbf{h} \cdot \mathbf{n}) d\Omega, \quad (3.125)$$

where the kernel  $G$  is the shape derivative. We locally (i.e., under small perturbations of the domain) require that  $dJ(u, \Omega)\mathbf{h} < 0$ . This leads to the following choice for the normal component  $h_n = \mathbf{h} \cdot \mathbf{n}$  of the velocity :

$$h_n = -G \text{ on } \Gamma \quad (3.126)$$

where  $\partial\Omega = \Gamma \cup \partial D$ .

According to (3.126), the normal component of velocity is only imposed along the boundary  $\Gamma$ .

But in order to solve the Hamilton-Jacobi equation (3.122), we need a velocity field defined on the whole domain  $D$ . This then suggests the extension of the normal velocity part  $h_n$  to the whole domain  $D$ . If  $h_{\text{next}} = -G_{\text{ext}}$  denotes the extension of the normal component of the velocity field, then the Hamilton-Jacobi equation (3.122) becomes

$$\psi_t + h_{\text{next}} |\nabla \psi| = 0 \quad \text{in } D \times [0, T], \quad (3.127)$$

$$\psi(\cdot, 0) = \psi_0. \quad (3.128)$$

Summarizing, the level set method described to the following algorithm 1:

---

**Algorithm 1** Level set algorithm

---

- (1) Solve the state and adjoint equations on the current domain  $\Omega_0$ ,
  - (2) Compute the kernel  $G$  and an extension  $G_{\text{ext}}$ ,
  - (3) Solve the Hamilton-Jacobi equation (3.122) for  $\psi$ ,
  - (4) Update  $\Omega_0$  by  $\Omega_T = \{(x, y) \in D : \psi(x, y, t) < 0\}$ .
- 

Algorithm 1 requires some details such as choosing  $T$ , computations of  $G_{\text{ext}}$  which can be found in, e.g., [Ito 2006].

### 3.4.2 The method of mappings

A second approach is to think of the shape evolution as a flow problem. That is, one can imagine that the shape is made of a plastic material gradually deforming such that any point inside or on the boundary of the shape can be always traced back to a point of the original shape in a one-to-one fashion. Mathematically, if  $\Omega_0$  is the initial shape, and  $\Omega_t$  is the shape at time  $t$ , one considers the diffeomorphisms

$$T_t : \Omega_0 \mapsto \Omega_t \text{ for } 0 \leq t \leq t_0. \quad (3.129)$$

Using  $T_t$ , one transforms the variable (unknown) domain to a fixed region and this gives rise to the **method of mappings**. The given problem then turns into a parameter estimation problem to determine the coefficients of the PDE on a fixed domain, where the unknowns now are expressed in terms of the transformation  $T_t$ . This method leads naturally to numerical algorithms using finite difference method and is discussed in detail in ([Pironneau 1984], Ch.8). This method has the advantage that the theory also covers a class of optimal control problems, where the coefficients of the variational equation are influenced by the control. However, from a computational standpoint, the transformation can be a complex process for partial differential equations with spatial domains in  $\mathbb{R}^2$  or  $\mathbb{R}^3$ . In addition, there is loss of accuracy by transformations that produce co-

ordinate systems that are not orthogonal at boundaries.( see [Pironneau 1984], pg.132). Usually this method is used in the context of shape optimization for domains that can be described by a graph [Laumen 1999], however for problems involving complex geometries, determining the mappings can be a complicated process.

### 3.4.3 Embedding domain technique

The classical boundary variation technique has several draw backs if the finite element method is used to solve the state equation namely,

- for every new shape, one has to remesh the corresponding domain,
- assemble the new stiffness matrix and the load vector of the system,
- solve the new system of algebraic equations.

All these steps have to be repeated until convergence of the optimization problem to the optimal domain is achieved. To avoid the remeshing, and partially the second step, we work on a new larger fixed domain  $\hat{\Omega}$  (called fictitious) with the property that  $\Omega \subset \hat{\Omega}$  for all  $\Omega \in \mathcal{U}_{ad}$ , where  $\mathcal{U}_{ad}$  is the set of admissible domains. The **original PDE** is replaced by a **new PDE** defined on a larger fixed domain  $\hat{\Omega}$ . There must be a natural link between solutions  $\mathbf{u}(\Omega)$  of the **original PDE** and  $\hat{\mathbf{u}}$  of the **new PDE**: namely  $\mathbf{u}(\Omega) \equiv \hat{\mathbf{u}}|_{\Omega}$ . This link is established through introduction of new additional variables (Lagrange multipliers ). These Lagrange multipliers are of two types namely, **boundary Lagrange(BL)** or a **distributed Lagrange (DL)** multipliers and are discussed in detail in [Haslinger 2003, Chap.6]. This method allows use of uniform or almost uniform meshes for constructing finite element spaces yielding a special structure of the finite element matrices that can be solved by a fast algorithm. Examples of such meshes include the so called body fitted meshes. However as noted in [Haslinger 2003, Chap.6], the sensitivity analysis of the fictitious domain problem with non-fitted meshes reduce the smoothness of the respective control-to-state mapping and consequently may lead to non-differentiable optimization problems.

### 3.4.4 Boundary variation technique

Another approach which is implemented in this work is to follow the boundary of the shape explicitly. For this purpose, one must sample the shape of the boundary in a relatively dense and uniform manner, that is, to consider enough points to get a sufficiently accurate outline of the shape. Then, one can evolve the shape by gradually moving the boundary points. This is called the **Lagrangian approach**.

When using the finite element method, the boundary mesh nodes are used as design variables [Liu 2007] and this is better known in literature as Computer Aided Design (CAD) free parametrization. During the optimization procedure, mesh nodal position need to be updated on the structural boundary and inside the design domain. This procedure is elucidated in the following algorithm below.

#### 3.4.4.1 The descent direction

As was seen in the previous section, the analytical expression of the gradient of the cost with respect to the domain can be expressed as

$$dJ(\Omega, \mathbf{u})\mathbf{h} = \int_{\partial\Omega} G(\Omega, \mathbf{u}, \mathbf{v})\mathbf{h} \cdot \mathbf{n} \, ds, \quad (3.130)$$

where  $G(\Omega, \mathbf{u}, \mathbf{v})$  is a function (which depends on the state  $\mathbf{u}$  and adjoint state  $\mathbf{v}$ ). To numerically minimize the cost functional  $J(\Omega, \mathbf{u})$  by a gradient method, we need to choose a descent direction  $\mathbf{h}$  such that  $dJ(\Omega, \mathbf{u})\mathbf{h} < 0$ . Ignoring smoothness considerations, a descent direction is found by defining a vector field

$$\mathbf{h} = -G\mathbf{n}. \quad (3.131)$$

The domain is subsequently updated by means of

$$\Omega_t = (I_d + t\mathbf{h})\Omega, \quad (3.132)$$

where  $t > 0$  is a proper step size. Formally we obtain

$$J(\Omega_t, \mathbf{u}_t) = J(\Omega, \mathbf{u}) - t \int_{\partial\Omega} G^2 \, ds + \mathcal{O}(t^2)$$

which guarantees a decrease in the objective function.

In the equation (3.131) there remain an ambiguity to the definition of  $\mathbf{h}$ . Indeed in (3.132),  $\mathbf{h}$  must be defined on the whole domain  $\Omega$  while  $G(\Omega)\mathbf{n}$  is a priori defined on the boundary  $\partial\Omega$ . Therefore, we must extend this trace to  $\Omega$  to get the vector field  $\mathbf{h}$ . We revisit this issue in the next subsubsection.

There are other difficulties of theoretical and practical nature with (3.131). Indeed, it was always assumed that  $\mathbf{h} \in C^{1,1}(\bar{D})$ , but the integrand  $G(\Omega)$  and the normal  $\mathbf{n}$  may be less regular. If this is the case, we should perhaps regularize these terms (we discuss this later on in subsubsection 3.4.4.3).

### 3.4.4.2 Extension of the displacement field

In the previous subsubsection, we noted the ambiguity in definition of  $\mathbf{h}$  in (3.131). In this regard, there are two possibilities to resolve this matter. First we can instead say that the only interesting information is the position of the boundary  $\partial\Omega_{k+1}$  which depends only on the normal trace  $\mathbf{h}_k \cdot \mathbf{n}_k$  on the boundary (in the case of small deformations of the domain). In other words, the values of  $\mathbf{h}_k$  within  $\Omega_k$  are not important for determining the boundary  $\partial\Omega_{k+1}$  and just use (3.131) on the boundary (or more precisely movement of the nodes on the boundary of the mesh).

However, this approach has a practical disadvantage since it will be necessary to re-mesh the new domain  $\Omega_{k+1}$  and this is expensive (especially in 3D).

A second approach, which is sometimes preferable is to extend the trace of  $\mathbf{h}_k$  on  $\partial\Omega_k$  in  $\Omega_k$ . For example, such an extension is obtained by solving the following problem

$$\begin{aligned} -\Delta\mathbf{h}_k + \mathbf{h}_k &= 0 \quad \text{in } \Omega_k, \\ \mathbf{h}_k &= -G(\Omega_k)\mathbf{n}_k \quad \text{on } \Gamma_f, \\ \mathbf{h}_k &= 0 \quad \text{on } \Gamma_{fixed}. \end{aligned} \tag{3.133}$$

Once one knows  $\mathbf{h}_k$  everywhere in the current domain  $\Omega_k$ , one can then deform the whole of the mesh of  $\Omega_k$  and directly obtain a new mesh of the domain  $\Omega_{k+1}$ .

**Remark 3.4.1.** In most cases only one part of the boundary  $\partial\Omega$  is optimized, we call this part  $\Gamma_f$  in (3.133).

### 3.4.4.3 Regularization of the displacement field

Another shortcoming of the vector field  $\mathbf{h}_k$  defined by (3.133) is its possible low regularity. This may result in possible oscillations of the boundary that is avoided through regularization of  $\mathbf{h}_k$ . Combined with the extension procedure that we just described, this regularization can be obtained by solving instead of (3.133) the following problem

$$\begin{aligned} -\Delta\mathbf{h}_k + \mathbf{h}_k &= 0 \quad \text{in } \Omega_k, \\ \frac{\partial\mathbf{h}_k}{\partial\mathbf{n}} &= -G(\Omega_k)\mathbf{n}_k \quad \text{on } \Gamma_f, \\ \mathbf{h}_k &= 0 \quad \text{on } \Gamma_{fixed}. \end{aligned} \tag{3.134}$$

By integrating by parts the above system (3.134), we observe that  $\mathbf{h}_k$  computed from (3.134) gives a descent direction for the cost since

$$dJ(\Omega, \mathbf{u})\mathbf{h}_k = \int_{\Gamma_f} G(\Omega_k)\mathbf{h}_k \cdot \mathbf{n} \, ds = - \int_{\Omega_k} |\nabla\mathbf{h}_k|^2 + |\mathbf{h}_k|^2 \, dx \leq 0. \tag{3.135}$$

On the other hand, the solution of (3.134) has more regularity than that of (3.133) since the solution of (3.134) can be interpreted as application the Neumann-to-Dirichlet map to  $-G\mathbf{n}$  which has the effect of increasing the regularity of  $\mathbf{h}_k$  on  $\Gamma_f$  (with respect to that of  $-G\mathbf{n}$ ). It is the method which we used for the numerical examples presented in Chapter 5.

#### 3.4.4.4 The boundary variation algorithm

Summarizing we obtain algorithm 2. In algorithm 2,  $\Omega_{k+1}$  represents a new domain as a result of

---

##### **Algorithm 2** Boundary variation algorithm

---

1. Choose initial shape  $\Omega_0$
  2. Iteration until convergence for  $k \geq 0$ ,
    - (a) Compute  $\mathbf{h}_k$  from (3.134) with  $\Omega = \Omega_k$ .
    - (b) Set  $\Omega_{k+1} = (Id + t\mathbf{h}_k)$  where  $t$  is a small positive real.
- 

movement of mesh points in the domain  $\Omega_k$  in the direction of velocity field  $\mathbf{h}_k$  with step size  $t$ . Each  $\Omega_{k+1}$  is obtained from a  $\Omega_k$  as  $\Omega_t$  is obtained from  $\Omega_0$ . In other words, at each iteration  $k$  using  $\Omega_k$  as a reference domain to calculate the derivative with respect to the domain (we do not go back each time to the initial domain  $\Omega_0$ ).

#### 3.4.4.5 Algorithmic details of the method

To ensure that the above method is efficient and effective, several key aspects need to be added to it. Some of these aspects are reported in e.g., ([Allaire 2006]).

##### **Regularization of the mesh.**

In the discussion of extension problem we have just made, the displacement field  $\mathbf{h}_k$ , the state, and the adjoint variables are defined on the same grid. Therefore the same grid can be used for these variables. However, in applications many times it is preferred to utilize two grids, where the state and adjoint variables are defined on a fine grid and the displacement variables are defined on a coarse grid. There are at least two reasons for this choice.

First of all the issue of numerical stability: there is a risk of oscillation of the boundary during optimization that would be caused by a resonance of numerical errors on the same grid for  $\mathbf{h}_k$ , the state, and the adjoint variables. (This is more of an experimental finding than that of a rigorous analysis).

Then a reason of convenience of representation or parameterization of domains: Domains of "industrial" problems are generally not characterized by the mesh but by the parameters of CAD.

Typically, these parameters are splines, curves of Bézier or any other form of representation used in approximation of surfaces.

Therefore, we project the displacement field  $\mathbf{h}_k$  from the fine grid onto the coarse grid that uses typically much less control nodes on the boundary of the shape. This is a very natural link between geometric optimization and parametric optimization.

In the numerical examples presented in Chapter 5, we indeed use two grids: one (relatively) coarse to represent the deformation, i.e.,  $\mathbf{h}_k$ , and another the finer to calculate with accuracy the state and adjoint variables. The coarse grid is deformed with each iteration of optimization and the fine grid follows it by simple interpolation.

### Regularization of the shape gradient.

The numerical solution of the displacement usually presents singularities at the corners of the structural boundaries or at the changes of boundary conditions type (see e.g., [Liu 2007]). As a consequence, the sensitivity is not accurate anymore. This leads to strong oscillations of the shape near its corners and produces unresolved meshing errors. To circumvent this problem, the shape gradient is set to zero on the corner of the shape and the point of intersection of the (Dirichlet-Neumann) boundary conditions.

### Stopping criterion.

A typical convergence criterion for stopping the optimization loop would be to check that the shape sensitivity is small enough in some appropriate form. In [Liu 2007], two criteria are used to stop the optimization algorithm, one is the square norm of the sensitivity vector and the other is the maximum value of the mesh displacement on the boundary. We use the later in a combination with visual inspection in case we come to a halt.

### Remeshing

To avoid the influence of the numerical discretization error caused by the distorted mesh, the design domain is re-meshed with high quality mesh and then the shape optimization is re-started. The quality of the mesh is measured by using the minimum area

$$A_{min}|_{\Omega_k} = \frac{1}{2} \begin{vmatrix} 1 & 1 & 1 \\ x_j^1 & x_j^2 & x_j^3 \\ y_j^1 & y_j^2 & y_j^3 \end{vmatrix}$$

of triangular elements in the domain  $\Omega_k$ . Here  $(x_j^1, y_j^1)$ ,  $(x_j^2, y_j^2)$ ,  $(x_j^3, y_j^3)$  denote the coordinates of element  $j$  belonging to a mesh of domain  $\Omega^k$ . If the minimum area of triangular elements in the mesh of domain  $\Omega_{k+1} < \frac{A_{min}|_{\Omega_k}}{10}$ . Then we remesh the domain  $\Omega_{k+1}$  with a new mesh of good quality. Otherwise, we keep the mesh in  $\Omega_{k+1}$ . The whole procedure is stopped only if the movement of the boundary nodes is still small enough after mesh regeneration.

### Line search algorithm

The choice of the step size  $t$  is tricky. Too big, the algorithm is unstable, too small the rate of convergence is insignificant. We follow the approach in [Allaire 2006], which we state here for completeness.

The current decent direction  $\mathbf{h}_k$  is compared with the previous one  $\mathbf{h}_{k-1}$ . If the scalar product  $(\mathbf{h}_k, \mathbf{h}_{k-1})_{H^1(\Omega)^2}$  is negative, the step is reduced and the algorithm returns to the previous shape  $\Omega_{k-1}$ . The next iteration is initialized with the previous shape  $\Omega_{k-1}$ . If  $\mathbf{h}_k$  and  $\mathbf{h}_{k-1}$  are very close, i.e., if either  $(\mathbf{h}_k, \mathbf{h}_{k-1})_{H^1(\Omega)^2} \leq \frac{1}{2}||h_k||_{H^1(\Omega)}$ , and  $(\mathbf{h}_k, \mathbf{h}_{k-1})_{H^1(\Omega)^2}$  is positive, or  $(\mathbf{h}_k, \mathbf{h}_{k-1})_{H^1(\Omega)^2} \geq \frac{1}{4}||h_k||_{H^1(\Omega)}$ , and  $(\mathbf{h}_k, \mathbf{h}_{k-1})_{H^1(\Omega)^2} > 0$ , then the step  $t$  is increased. Before we finally update the mesh, we must check if the minimum area of elements in a mesh corresponding to the domain  $\Omega_{k+1} = \Omega_k + t\mathbf{h}_k$ , is negative. If that is the case, then it means that some triangle(s) are reversed in the domain  $\Omega_{k+1}$  and hence the step  $t$  must be reduced until no reversed triangles occur.

### Domain variation restriction

In applications, the domain variation is sometimes restricted in certain design spaces for manufacturing and/or construction reasons. In other words, the design domain is allowed to vary but limited to a certain range. Therefore restriction of the domain variation is important in shape optimization. Moreover, from the theoretical point of view, such constraints lead to the compactness of the set of admissible domains for an appropriate topology, hence leading to existence of optimal shapes.

Typical constraints that are handled by the method we use, are for example, volume and perimeter constraints [Allaire 2006]. Here we need to find a way to introduce constraints on the mesh nodal movements while maintaining the smoothness of the domains.

We consider the constrained optimization problem

$$\min_{\Omega} J(\Omega) = \int_{\Omega} j_1(C_{\gamma} u_{\Omega}) dx, \text{ subject to } \mathcal{E}(\Omega) = 0. \quad (3.136)$$

Here  $\mathcal{E}(\Omega) : \mathbb{R}^2 \rightarrow \mathbb{R}^1$  describes constraints on admissible shapes  $\Omega$ . If  $\mathcal{E}$  and  $J$  are shape differentiable, then there exist shape gradients  $\nabla \mathcal{E}$  and  $\nabla J$  of  $\mathcal{E}(\Omega)$  and  $J(\Omega)$  respectively. One of the methods for solving (3.136) is the penalty method [Nocedal 1999, Chapter 17]. By combining the cost functional  $J(\Omega)$  and constraints  $\mathcal{E}(\Omega)$  into a penalized functional, we can solve problem (3.136) by solving a sequence of unconstrained problems. Let  $\mathfrak{F}$  denote a penalized functional, and  $\mu$  a positive penalty constant:

$$\mathfrak{F}(\Omega, \mu) = J(\Omega) + \mu \mathcal{E}(\Omega).$$

The Eulerian derivative of  $\mathfrak{F}$  with respect  $\Omega$  in the direction  $\mathbf{h}$  reads

$$d\mathfrak{F}(\Omega, \mu)\mathbf{h} = dJ(\Omega)\mathbf{h} + \mu d\mathcal{E}(\Omega)\mathbf{h}.$$

In our case, we have lower and upper point wise constraints. If  $\mathcal{E}_u(x, y)$  and  $\mathcal{E}_l(x, y)$  denoted the upper and lower constraints on the shape respectively, then  $\mathcal{E}(\Omega)$  can be expressed as

$$\mathcal{E}(\Omega) = \int_{\Omega} \left[ \max(\mathcal{E}_u(x, y), 0) + \min(\mathcal{E}_l(x, y), 0) \right] dx.$$

We remark that the shape derivative of the objective functional  $\mathcal{E}(\Omega)$  is independent of the  $x, y$  nodal positions of the mesh, but only depends on deformation fields along the normal. Hence using Lemma 3.2.1, the Eulerian derivative of the functional  $\mathcal{E}(\Omega)$  can be expressed as

$$d\mathcal{E}(\Omega)\mathbf{h} = \int_{\Gamma_f} \left[ \max(\mathcal{E}_u(x, y), 0) + \min(\mathcal{E}_l(x, y), 0) \right] \mathbf{h} \cdot \mathbf{n} ds,$$

whose  $L^2$  gradient reads

$$\nabla \mathcal{E}(\Omega) = \left[ \max(\mathcal{E}_u(x, y), 0) + \min(\mathcal{E}_l(x, y), 0) \right] \mathbf{n}.$$

Similarly, the  $L^2$  gradient of  $J(\Omega)$  can be expressed

$$\nabla J(\Omega) = G(\Omega)\mathbf{n},$$

where  $G$  is the shape derivative kernel of  $J$  which depends on the state and adjoint variable. Therefore, the optimality condition reads

$$G(\Omega)\mathbf{n} + \mu \left[ \max(\mathcal{E}_u(x, y), 0) + \min(\mathcal{E}_l(x, y), 0) \right] \mathbf{n} = 0. \quad (3.137)$$

The computational step 2(a) in algorithm 2 is thus replaced by

$$\begin{aligned} -\Delta \mathbf{h}_k + \mathbf{h}_k &= 0 \text{ in } \Omega_k, \\ \frac{\partial \mathbf{h}_k}{\partial \mathbf{n}} &= - \left[ G(\Omega)\mathbf{n} + \mu \left[ \max(\mathcal{E}_u(x, y), 0) + \min(\mathcal{E}_l(x, y), 0) \right] \mathbf{n} \right] \text{ on } \Gamma_f, \\ \mathbf{h}_k &= 0 \text{ on } \Gamma_{fixed}. \end{aligned} \quad (3.138)$$

As an illustrative example, let us take  $G = (x^2 - y^2)$ , and  $\Omega$  be a unit circle, and  $\Gamma_f = \partial\Omega$ . Then, this choice of  $G$  will constitute a perturbation of a unit circle with a velocity field

$$\mathbf{h} = (x^2 - y^2)\mathbf{n},$$

(see Figures 3.2,3.3 (a)) where  $\mathbf{n}$  is the unit outward normal vector to the perturbed boundary. If  $\Omega$  is constrained to lie between two concentric circles of radii 2 and 0.8 respectively, then by (3.137),  $\mathbf{h}$  is redefined such that

$$\mathbf{h}_c = \mathbf{h} + \mu [\max(x^2 + y^2 - 4, 0)\mathbf{n} + \min(x^2 + y^2 - 0.64, 0)\mathbf{n}],$$

where  $\mathbf{h}_c$  is the constrained velocity field and  $\mu$  is chosen large enough to ensure that constraints are satisfied.

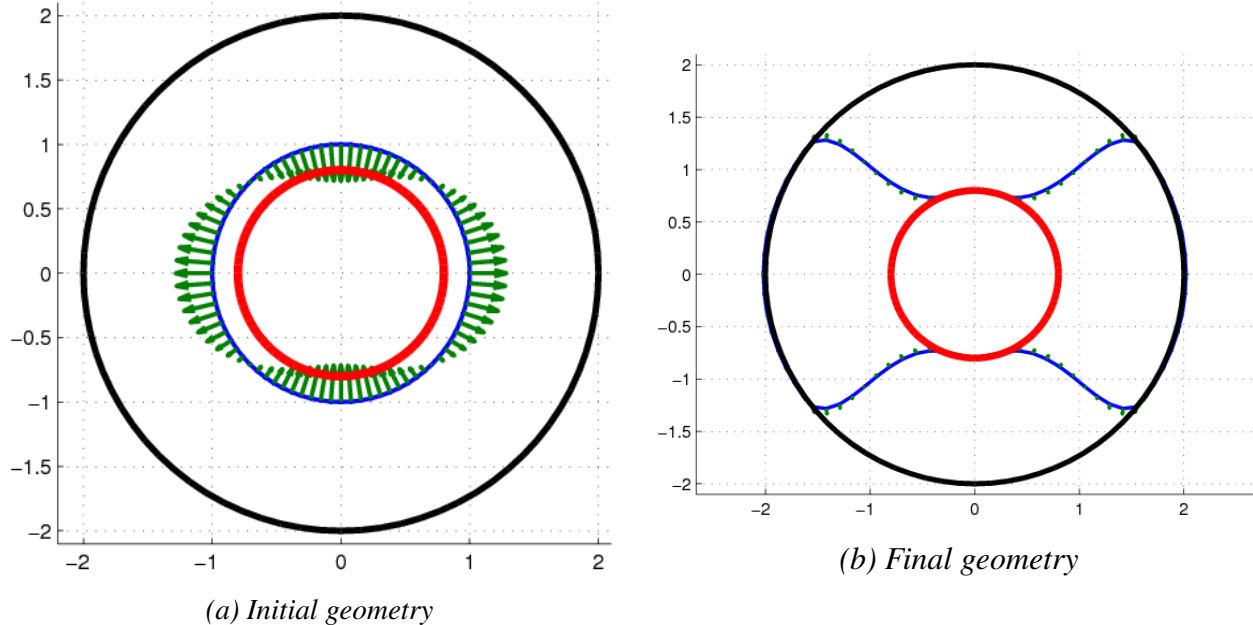


Figure 3.2: Constrained perturbation of a circle

At the optimal domain,  $\mathbf{h}_c = 0$  (see Figures 3.2, 3.3(b)).

**Comment 3.4.1.** *The disadvantage of the boundary variation technique is that if the shape is deformed too much, then it is necessary to remesh which can be very costly especially in 3d. Secondly different parts of the boundary may want to merge or split, but as well known, topological changes are very difficult to handle with such Lagrangian or front-tracking methods.*

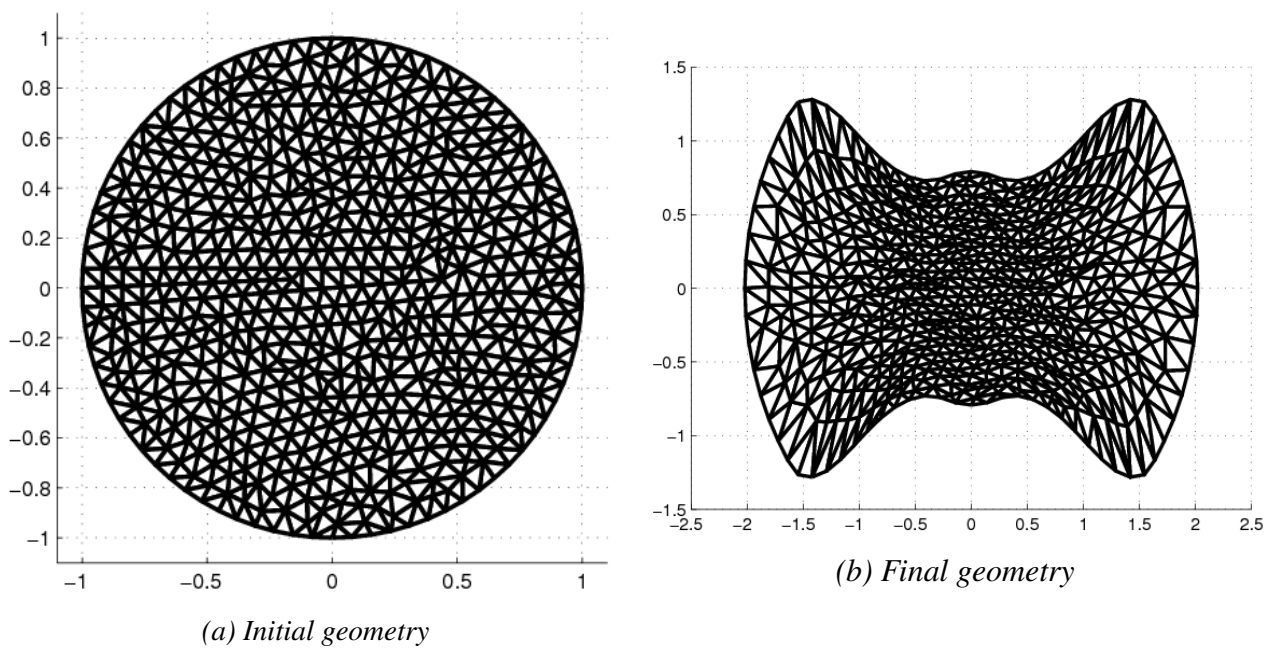


Figure 3.3: Constrained perturbation of a circle (domain mesh)

# 4

## FINITE ELEMENT APPROXIMATION AND DISCRETIZATION

During past four decades, the finite element method has dramatically been developed, and many engineering applications have been solved using this method. In this chapter, a finite element approximation of the state, adjoint as well as continuous sensitivity equations is developed. The fact that the incompressibility constraint does not involve the pressure variable in the Navier-Stokes equations, makes the construction of finite element approximations problematic. In particular, the discrete spaces used to approximate the velocity and pressure fields cannot be chosen independently of one another—there is a compatibility condition that needs to be satisfied if the resulting mixed approximation is to be effective. Unfortunately, as we will see, the simplest and most natural mixed approximation methods are unsuitable. The basic aim in this chapter is to identify the finite element spaces that are compatible, so as to define candidate approximation methods for the Navier-Stokes equations. Furthermore, since the design variation is taken at the continuum domain and then followed by discretization, this is called the continuum discrete method. A first step towards constructing a finite element approximation to the state and adjoint equations is the derivation of weak formulation of the state and adjoint equations. We have done this already in the previous two chapters but we shall repeat it here for the sake of clarity of the presentation. We consider the approximation for a particular reference problem described by

$$\begin{cases} -\eta \Delta \mathbf{u} + \mathbf{u} \cdot \nabla \mathbf{u} + \nabla p = \mathbf{f} & \text{in } \Omega, \quad \eta = \frac{1}{Re}, \\ \operatorname{div} \mathbf{u} = 0 & \text{in } \Omega, \end{cases} \quad (4.1)$$

together with boundary conditions

$$\begin{cases} \mathbf{u} = \mathbf{g} \text{ on } \Gamma_{in}, \\ \mathbf{u} = \mathbf{0} \text{ on } \Gamma_w \cup \Gamma_f, \\ -p\mathbf{n} + \frac{1}{Re} \frac{\partial \mathbf{u}}{\partial \mathbf{n}} = 0 \text{ on } \Gamma_{out}. \end{cases} \quad (4.2)$$

The adjoint system system of (4.1-4.2) reads as follows

$$\begin{cases} -\eta \Delta \lambda + (\nabla \mathbf{u})^T \cdot \lambda - (\mathbf{u} \cdot \nabla) \lambda + \nabla q = J'_i(\mathbf{u}) \text{ in } \Omega, i = 1, 2, 3. \\ \operatorname{div} \lambda = 0 \text{ in } \Omega, \\ \lambda = 0 \text{ on } \Gamma_w \cup \Gamma_f \cup \Gamma_{in}, \\ q \cdot \mathbf{n} - \eta \nabla \lambda \cdot \mathbf{n} - (\mathbf{u} \cdot \mathbf{n}) \lambda = 0 \text{ on } \Gamma_{out}. \end{cases} \quad (4.3)$$

where  $J'_1(\mathbf{u}) = (\mathbf{u} - \mathbf{u}_d)$ ,  $J'_2(\mathbf{u}) = -\Delta \mathbf{u}$  and  $J'_3(\mathbf{u}) = R(\mathbf{u})$ , with  $R(\mathbf{u})$  is defined in (3.106).

## 4.1 Weak formulation

In this subsection, we derive the weak formulation of the state and adjoint equations. To begin with, we introduce the following functional spaces

$$\mathbf{H}_g^1(\Omega) = \{\mathbf{v} \in [H^1(\Omega)]^2 \mid \mathbf{v} = \mathbf{g} \text{ on } \Gamma_{in}, \mathbf{v} = 0 \text{ on } \Gamma_w \cup \Gamma_f\}, \quad (4.4)$$

$$\mathbf{H}_0^1(\Omega) = \{\mathbf{v} \in [H^1(\Omega)]^2 \mid \mathbf{v} = \mathbf{0} \text{ on } \Gamma_{in} \cup \Gamma_w \cup \Gamma_f\}. \quad (4.5)$$

Then the weak formulation of the state system reads:

Find  $(\mathbf{u}, p) \in \mathbf{H}_g^1(\Omega) \times L^2(\Omega)$  such that for all  $(\psi, \xi) \in \mathbf{H}_0^1(\Omega) \times L^2(\Omega)$

$$\begin{cases} \int_{\Omega} \eta \nabla \mathbf{u} : \nabla \psi \, dx + \int_{\Omega} (\mathbf{u} \cdot \nabla) \mathbf{u} \psi \, dx - \int_{\Omega} p \operatorname{div} \psi \, dx = \int_{\Omega} \mathbf{f} \psi \, dx, \\ \int_{\Omega} \operatorname{div} \mathbf{u} \xi \, dx = 0, \end{cases} \quad (4.6)$$

and that of the adjoint system reads:

Find  $(\lambda, q) \in \mathbf{H}_0^1(\Omega) \times L^2(\Omega)$  such that for all  $(\psi, \xi) \in \mathbf{H}_0^1(\Omega) \times L^2(\Omega)$

$$\begin{cases} \int_{\Omega} \eta \nabla \lambda : \nabla \psi + (\psi \cdot \nabla) \mathbf{u} \lambda + (\mathbf{u} \cdot \nabla) \psi \lambda - q \operatorname{div} \psi \, dx = \int_{\Omega} J'_i(\mathbf{u}) \psi \, dx, \\ \int_{\Omega} \operatorname{div} \lambda \xi \, dx = 0. \end{cases} \quad (4.7)$$

Here  $\nabla \mathbf{u} : \nabla \psi$  represents the componentwise scalar product, for example, in two dimensions  $\nabla u_1 \cdot \nabla \psi_1 + \nabla u_2 \cdot \nabla \psi_2$ .

**Remark 4.1.1.** *The fact that there are no derivatives for the state and adjoint pressures in the*

weak formulations above means that  $L^2(\Omega)$  is an appropriate space for  $p$  and  $q$ .

The variational problems (4.6-4.7) are of mixed type, i.e., two different spaces  $\mathbf{H}_g^1$  and  $L^2$  are involved. The essential boundary conditions are explicitly assigned through the definition of functional spaces. The natural boundary conditions; i.e., boundary conditions on the outflow boundary are implicitly specified through the variational form.

The existence and uniqueness as well as stability of weak solution to (4.6) has been discussed in Chapter 2, while that of (4.7) in Chapter 3. We now proceed to the approximation of these formulations.

## 4.2 Approximation using mixed finite elements

Since equations (4.6-4.7) are in infinite dimensional spaces, we project the spaces  $\mathbf{H}_g^1(\Omega)$ ,  $\mathbf{H}_0^1(\Omega)$  and  $L^2(\Omega)$  into finite dimensional subspaces  $\mathbf{V}_{gh}$ ,  $\mathbf{V}_{0h}$  and  $Q_h$ . This is accomplished by spatial discretization of the domain  $\Omega$ . We thus obtain the following two families of finite dimensional subspaces

$$\mathbf{X}_h \subset H^1(\Omega)^2 \text{ and } S_h \subset L^2(\Omega)$$

depending on the discretization parameter  $h$  which tends to zero. We then consider the following discrete spaces

$$\begin{aligned} \mathbf{V}_{gh} &:= \{\mathbf{u}_h \in \mathbf{X}_h : \mathbf{u}_h = 0 \text{ on } \Gamma_w \cup \Gamma_f, \mathbf{u}_h = \mathbf{g}_h \text{ on } \Gamma_{in}\}, \\ \mathbf{V}_{0h} &:= \{\mathbf{u}_h \in \mathbf{X}_h : \mathbf{u}_h = 0 \text{ on } \Gamma_w \cup \Gamma_f \cup \Gamma_{in}\}. \\ Q_h &:= \begin{cases} p_h \in S_h : \int_{\Omega} p_h \, dx = 0, & \text{if } \text{meas}(\Gamma_{out}) = 0, \\ S_h & \text{otherwise.} \end{cases} \end{aligned} \tag{4.8}$$

The fact that these spaces are approximated independently leads to the nomenclature mixed approximation. Implementation entails defining appropriate bases for the chosen finite element spaces and construction of the associated finite element coefficient matrix. Specifically, given a velocity solution space  $\mathbf{V}_{gh}$ , the discrete weak formulation of the state problem is :

Find  $(\mathbf{u}_h, p_h) \in \mathbf{V}_{gh} \times Q_h$  such that for all  $(\psi_h, \xi_h) \in \mathbf{V}_{0h} \times Q_h$

$$\begin{cases} \int_{\Omega} \eta \nabla \mathbf{u}_h : \nabla \psi_h + (\mathbf{u}_h \cdot \nabla) \mathbf{u}_h \psi_h - p_h \operatorname{div} \psi_h \, dx = \int_{\Omega} \mathbf{f} \psi_h \, dx, \\ \int_{\Omega} \operatorname{div} \mathbf{u}_h \xi_h \, dx = 0, \end{cases} \tag{4.9}$$

and the discrete weak formulation of the adjoint problem:

Find  $(\lambda_h, q_h) \in \mathbf{V}_{0h} \times Q_h$  such that for all  $(\psi_h, \xi_h) \in \mathbf{V}_{0h} \times Q_h$

$$\begin{cases} \int_{\Omega} \eta \nabla \lambda_h : \nabla \psi_h + (\psi_h \cdot \nabla) \mathbf{u}_h \lambda_h + (\mathbf{u}_h \cdot \nabla) \psi_h \lambda_h - q_h \operatorname{div} \psi_h dx = \int_{\Omega} J'_i(\mathbf{u}_h) \psi_h dx, \\ \int_{\Omega} \operatorname{div} \lambda_h \xi dx = 0. \end{cases} \quad (4.10)$$

Further more, we need to discretize both the cost and shape gradients of the three cost functionals  $J_1, J_2$  and  $J_3$ . We obtain the following discrete expressions

$$\begin{aligned} J_{1h}(\mathbf{u}_h, \Omega) &= \frac{1}{2} \int_{\Omega} |\mathbf{u}_h - \mathbf{u}_{dh}|^2 dx, \quad J_{2h}(\mathbf{u}_h, \Omega) = \frac{1}{2} \int_{\Omega} |\operatorname{curl} \mathbf{u}_h|^2 dx, \\ \text{and } J_{3h}(\mathbf{u}_h, \Omega) &= \int_{\Omega} g_3(\det \nabla \mathbf{u}_h) dx, \end{aligned} \quad (4.11)$$

where  $\operatorname{curl} \mathbf{u}_h$  and  $g_3(t)$  have the meaning described in the previous chapter. The integrals in (4.11) are evaluated using the Gauss quadrature rule and in particular a 7 point rule. This rule is exact on polynomial of degree 5 on triangles or edges. The details and references are summarized in the Appendix (7.4). The discrete shape gradients read as follows

$$\begin{aligned} \nabla J_{1h} &= \left[ \frac{1}{2} |\mathbf{u}_h - \mathbf{u}_{dh}|^2 + \eta \frac{\partial(\mathbf{u}_h - \mathbf{g}_h)}{\partial \mathbf{n}} \cdot \frac{\partial \lambda_h}{\partial \mathbf{n}} \right] \mathbf{n}, \\ \nabla J_{2h} &= \left[ \eta \frac{\partial(\mathbf{u}_h - \mathbf{g}_h)}{\partial \mathbf{n}} \cdot \frac{\partial \lambda_h}{\partial \mathbf{n}} + \frac{1}{2} |\operatorname{curl} \mathbf{u}_h|^2 - (\operatorname{curl} \mathbf{u}_h \times \mathbf{n}) \cdot \frac{\partial(\mathbf{u}_h - \mathbf{g}_h)}{\partial \mathbf{n}} \right] \mathbf{n}, \\ \nabla J_{3h} &= \left[ g_3(\det \nabla \mathbf{u}_h) + \frac{\partial(\mathbf{u}_h - \mathbf{g}_h)}{\partial \mathbf{n}} \cdot \left( \eta \frac{\partial \lambda_h}{\partial \mathbf{n}} - P(\mathbf{u}_h) \right) \right] \mathbf{n}, \end{aligned}$$

where  $\mathbf{n} = (n_x, n_y)$  with  $n_x$  the outward  $x$ -component of the normal vector on the boundary and  $n_y$ , the outward  $y$  component of the normal vector on the boundary and  $P(\mathbf{u})$  is defined in the previous chapter. The details on computing the derivative of the discrete state and adjoint solutions are summarized in the Appendix (7.3). Concerning the existence and uniqueness of the solution to the discrete system (4.9-4.10), we refer the reader to [Girault 1986, Chapter 4].

## 4.2.1 Approximation error

We have shown how the discrete state and adjoint problems are derived from the continuous problems. We would like, therefore, to determine in what sense the solutions of the discrete problems are a good approximation to the solutions of the continuous problems. It is shown by, for instance, Boland and Nicolaides [Boland 1983], that as long as the solution of the continuous problem  $(\mathbf{u}, p)$  has a particular smoothness, then the error in the approximation can be bounded in terms of the mesh parameter  $h$ . Specifically for the Taylor-Hood element pair (see subsection

4.2.3), their approximation theorem is paraphrased as follows

**Theorem 4.2.1.** *For  $m = 2$  or  $3$ , if the solutions  $\mathbf{u}$  and  $p$  to the continuous Navier Stokes problem satisfy:*

$$\begin{aligned}\mathbf{u} &\in \mathbf{H}^m(\Omega) \cap \mathbf{H}_0^1(\Omega), \\ p &\in H^{m-1}(\Omega) \cap L_0^2(\Omega),\end{aligned}$$

*then the following error estimates, which compare the solutions of the continuous problem to the solutions  $\mathbf{u}^h$  and  $p^h$  of the discretized problem, hold uniformly in  $h$ :*

$$\|\nabla(\mathbf{u} - \mathbf{u}_h)\|_{\mathbf{L}^2} = O(h^{m-1}), \quad (4.12)$$

$$\|\mathbf{u} - \mathbf{u}_h\|_{\mathbf{L}^2} = O(h^m), \quad (4.13)$$

$$\|p - p_h\|_{L^2} = O(h^{m-1}). \quad (4.14)$$

Similarly, as a consequence of the above theorem, the following also holds

**Theorem 4.2.2.** *For  $m = 2$  or  $3$ , if the solutions  $\lambda$  and  $q$  to the continuous adjoint to the Navier-Stokes problem satisfy:*

$$\begin{aligned}\lambda &\in \mathbf{H}^m(\Omega) \cap \mathbf{H}_0^1(\Omega), \\ q &\in H^{m-1}(\Omega) \cap L_0^2(\Omega),\end{aligned}$$

*then the following error estimates, holds*

$$\|\nabla(\lambda - \lambda_h)\|_{\mathbf{L}^2} = O(h^{m-1}), \quad (4.15)$$

$$\|\lambda - \lambda_h\|_{\mathbf{L}^2} = O(h^m), \quad (4.16)$$

$$\|q - q_h\|_{L^2} = O(h^{m-1}). \quad (4.17)$$

**Remark 4.2.1.** *The results in Theorems (4.2.1)-(4.2.2) hold if  $\Omega$  is a polygonal domain in  $\mathbb{R}^2$  or polyhedral domain in  $\mathbb{R}^3$ . Moreover, through the use of, e.g., isoparametric elements, they also remain valid for domains with curved boundaries provided the latter satisfy appropriate smoothness criteria [Gunzburger 1989, Pg. 25].*

Theorems (4.2.1-4.2.2) requires that the state and adjoint problems are smooth enough for a better accuracy. The actual smoothness of the solutions depends strongly on the amount of deviation from convexity in case  $\Omega$  is polygonal. For the class of problems we have chosen, we can expect that the exact velocities will be elements of  $\mathbf{H}^2(\Omega)$ . This means that, we can expect  $O(h^2)$  accurate approximation of velocities  $(\mathbf{u}, \lambda)$ , and  $O(h)$  accurate approximation of pressures  $(p, q)$ .

The error estimates given in Theorems (4.2.1) and (4.2.2) for the homogeneous boundary condition still holds if a non-homogeneous condition is given. See, e.g., [Gunzburger 1989, Chapter 2] for a complete discussion.

These results suggest that the solution to the finite element problems are indeed close to the solutions to the original continuous problems, and that the error of approximation goes to zero with  $h$ .

## 4.2.2 The algebraic problem

We now consider the algebraic system associated with (4.9). We introduce a set of vector valued (velocity) basis functions  $\{\vec{\phi}_j\}$  such that

$$\mathbf{u}_h(x) = \sum_{j=1}^{n_u} u_j \vec{\phi}_j(x) + \sum_{j=n_u+1}^{n_u+n_\partial} u_j \vec{\phi}_j(x) \quad (4.18)$$

with  $\sum_{j=1}^{n_u} u_j \vec{\phi}_j(x) \in \mathbf{V}_{0h}$ . Here  $\vec{\phi}_1, \dots, \vec{\phi}_{n_u}$  is assumed to be a convenient basis for the finite  $n_u$ -dimensional vector space  $\mathbf{V}_{0h}$ . The specific choice of the basis that we choose in our computations is specified later in subsection (4.2.3). In order to ensure that the Dirichlet boundary condition is satisfied, we extend this basis set by defining additional functions  $\vec{\phi}_{n_u+1}, \dots, \vec{\phi}_{n_u+n_\partial}$  and selecting fixed coefficients  $u_j : j = n_u + 1, \dots, n_u + n_\partial$  so that the second term in (4.18) interpolates the boundary data on  $\partial\Omega_D$ . Here  $n_\partial$  is the number of degrees of freedom for the boundary nodes and  $n_u$  is the number of degrees of freedom of interior nodes of the finite element mesh. The finite element approximation  $\mathbf{u}_h \in \mathbf{V}_{gh}$  is then uniquely associated with the vector  $\mathbf{u} = (u_1, u_2, \dots, u_{n_u})^T$  of real coefficients in the expansion (4.18). Similarly, we introduce a set of scalar (pressure) basis functions  $\{w_k\}$ , and set

$$p_h(x) = \sum_{k=1}^{n_p} p_k w_k(x). \quad (4.19)$$

Inserting the expansions (4.18-4.19) into (4.9) and choosing  $\psi_h = \vec{\phi}_i, \xi_h = w_k$  yields

$$\begin{aligned} & \eta \sum_{j=1}^{n_u} u_j \int_{\Omega} \nabla \vec{\phi}_i : \nabla \vec{\phi}_j dx + \sum_{j=1}^{n_u} u_j \int_{\Omega} \vec{\phi}_i \cdot (\mathbf{u}_h \cdot \nabla) \vec{\phi}_j dx - \sum_{k=1}^{n_p} p_k \int_{\Omega} w_k \nabla \cdot \vec{\phi}_i dx \\ &= \int_{\Omega} \vec{\phi}_i \cdot \mathbf{f} dx - \eta \sum_{j=n_u+1}^{n_u+n_\partial} u_j \int_{\Omega} \nabla \vec{\phi}_i : \nabla \vec{\phi}_j dx - \sum_{j=n_u+1}^{n_u+n_\partial} u_j \int_{\Omega} \vec{\phi}_i \cdot (\mathbf{u}_h \cdot \nabla) \vec{\phi}_j dx \end{aligned} \quad (4.20)$$

$$- \sum_{j=1}^{n_u} u_j \int_{\Omega} w_k \nabla \cdot \vec{\phi}_j dx = \sum_{j=n_u+1}^{n_u+n_\partial} u_j \int_{\Omega} w_k \nabla \cdot \vec{\phi}_j dx. \quad (4.21)$$

We find that (4.20-4.21) can be expressed as a system of non-linear equations

$$\begin{aligned} \eta \mathbf{A}\mathbf{u} + \mathbf{C}(\mathbf{u})\mathbf{u} + \mathbf{B}^T \mathbf{p} &= \mathbf{f}, \\ \mathbf{B}\mathbf{u} &= \mathbf{s}, \end{aligned} \quad (4.22)$$

or equivalently

$$\begin{pmatrix} \eta \mathbf{A} + \mathbf{C}(\mathbf{u}) & \mathbf{B}^T \\ \mathbf{B} & 0 \end{pmatrix} \begin{pmatrix} \mathbf{u} \\ \mathbf{p} \end{pmatrix} = \begin{pmatrix} \mathbf{f} \\ \mathbf{s} \end{pmatrix}. \quad (4.23)$$

The matrix  $\mathbf{A}$  is called the vector-Laplacian matrix ,  $\mathbf{B}$  is the divergence matrix and the matrix  $\mathbf{C}(\mathbf{u})$  the vector-convection matrix. The entries are given by

$$\begin{aligned} \mathbf{A} &= [a_{ij}], \quad a_{i,j} = \int_{\Omega} \nabla \vec{\phi}_i : \nabla \vec{\phi}_j \, dx, \\ \mathbf{B} &= [b_{k,j}], \quad b_{k,j} = - \int_{\Omega} w_k \nabla \cdot \vec{\phi}_j \, dx, \\ \mathbf{C}(\mathbf{u}) &= [\mathbf{c}(\mathbf{u})_{i,j}], \quad \mathbf{c}(\mathbf{u})_{i,j} = \int_{\Omega} \vec{\phi}_i \cdot (\mathbf{u}_h \cdot \nabla) \vec{\phi}_j \, dx, \end{aligned}$$

for  $i$  and  $j = 1, \dots, n_u$  and  $k = 1, \dots, n_p$ . The entries of the righthand side vector are

$$\begin{aligned} \mathbf{f} &= [f_i], \quad f_i = \int_{\Omega} \vec{\phi}_i \cdot \mathbf{f} \, dx - \eta \sum_{j=n_u+1}^{n_u+n_{\partial}} u_j \int_{\Omega} \nabla \vec{\phi}_i : \nabla \vec{\phi}_j \, dx - \sum_{j=n_u+1}^{n_u+n_{\partial}} u_j \int_{\Omega} \vec{\phi}_i \cdot (\mathbf{u}_h \cdot \nabla) \vec{\phi}_j \, dx, \\ \mathbf{s} &= [s_k], \quad s_k = - \sum_{j=n_u+1}^{n_u+n_{\partial}} \int_{\Omega} w_k \nabla \cdot \vec{\phi}_j \, dx, \end{aligned}$$

and the function pair  $(\mathbf{u}_h, p_h)$  obtained by substituting the solution vectors  $\mathbf{u} \in \mathbb{R}^{n_u}$  and  $\mathbf{p} \in \mathbb{R}^{n_p}$  into (4.18) and (4.19) is the mixed finite element solution of the state system.

Similarly if we let

$$\begin{aligned} q_h(x) &= \sum_{k=1}^{n_q} q_k w_k(x), \\ \lambda_h(x) &= \sum_{j=1}^{n_{\lambda}} \lambda_j \vec{\phi}_j(x) + \sum_{j=n_{\lambda}+1}^{n_{\lambda}+n_{\partial}} \lambda_j \vec{\phi}_j(x). \end{aligned}$$

We can write the discrete adjoint system in the following form

$$\begin{pmatrix} \eta \mathbf{A} + \mathbf{M}(\mathbf{u}) + \mathbf{E}(\mathbf{u}) & \mathbf{B}^T \\ \mathbf{B} & 0 \end{pmatrix} \begin{pmatrix} \lambda \\ \mathbf{q} \end{pmatrix} = \begin{pmatrix} \tilde{\mathbf{f}} \\ \tilde{\mathbf{s}} \end{pmatrix}, \quad (4.24)$$

where the entries of the new matrices are given by

$$\begin{aligned}\mathbf{M}(\mathbf{u}) &= [m_{i,j}], \quad m_{i,j} = \int_{\Omega} (\vec{\phi}_i \cdot \nabla) \mathbf{u}_h \vec{\phi}_j \, dx, \\ \mathbf{E}(\mathbf{u}) &= [e_{i,j}], \quad e_{i,j} = \int_{\Omega} (\mathbf{u}_h \cdot \nabla) \vec{\phi}_i \vec{\phi}_j \, dx,\end{aligned}$$

for  $i$  and  $j = 1, \dots, n_u$  and  $k = 1, \dots, n_p$ . The entries of the righthand side vector for the adjoint system are

$$\begin{aligned}\tilde{\mathbf{f}} &= [\tilde{f}_i], \quad \tilde{f}_i = \int_{\Omega} J'_i(\mathbf{u}_h) \vec{\phi}_i \, dx - \eta \sum_{j=1}^{n_u+n_\partial} u_j \int_{\Omega} \nabla \vec{\phi}_i : \nabla \vec{\phi}_j \, dx - \sum_{j=1}^{n_u+n_\partial} u_j \int_{\Omega} \vec{\phi}_i \cdot (u_h \cdot \nabla) \vec{\phi}_j \, dx, \\ \tilde{\mathbf{s}} &= \mathbf{s}.\end{aligned}$$

**Remark 4.2.2.** In practice, the 2 components of velocity are always approximated using a single finite element space. Given scalar finite element basis functions  $\{\varphi_i\}_{i=1}^n$ , we set  $n_u = 2n$  where  $n_u = \dim(\mathbf{V}_{0h})$  and define the basis set

$$\{\vec{\phi}_1, \dots, \vec{\phi}_{2n}\} := \{(\varphi_1, 0)^T, \dots, (\varphi_n, 0)^T, (0, \varphi_1)^T, \dots, (0, \varphi_n)^T\}. \quad (4.25)$$

This componentwise splitting induces a natural block partitioning for (4.23). Specifically, with  $\mathbf{u} := (\vec{\mathbf{u}}_1, \vec{\mathbf{u}}_2)^T$ , where  $\vec{\mathbf{u}}_1 = ([u_1]_1, \dots, [u_1]_n)^T$ ,  $\vec{\mathbf{u}}_2 = ([u_2]_1, \dots, [u_2]_n)^T$ , (4.23) can be rewritten as

$$\begin{pmatrix} \eta A + C_{1,1}(\mathbf{u}) & 0 & B_x^T \\ 0 & \eta A + C_{2,2}(\mathbf{u}) & B_y^T \\ B_x & B_y & 0 \end{pmatrix} \begin{pmatrix} \vec{\mathbf{u}}_1 \\ \vec{\mathbf{u}}_2 \\ \mathbf{p} \end{pmatrix} = \begin{pmatrix} \mathbf{f}_1 \\ \mathbf{f}_2 \\ \mathbf{s} \end{pmatrix}, \quad (4.26)$$

where the  $n \times n$  matrix  $A$  is the scalar Laplacian matrix:

$$A = [a_{ij}], \quad a_{ij} = \int_{\Omega} \nabla \varphi_i \cdot \nabla \varphi_j \, dx,$$

and the  $n_p \times n$  matrices  $B_x$  and  $B_y$  are defined as

$$\begin{aligned}B_x &= [b_{x,ki}], \quad b_{x,ki} = - \int_{\Omega} w_k \frac{\partial \varphi_i}{\partial x} \, dx, \\ B_y &= [b_{y,ki}], \quad b_{y,ki} = - \int_{\Omega} w_k \frac{\partial \varphi_i}{\partial y} \, dx.\end{aligned}$$

The two block  $n \times n$  matrices arising from the linearization of the convective terms read as follows

$$\begin{aligned} C_{1,1}(\mathbf{u}) &= [c(\mathbf{u})_{i,j}], \quad c_{1,1}(\mathbf{u})_{i,j} = \int_{\Omega} \frac{\partial \varphi_i}{\partial x} u_1 \varphi_j + \frac{\partial \varphi_i}{\partial y} u_2 \varphi_j \, dx, \text{ for } (i, j) = 1 \dots n, \\ C_{2,2}(\mathbf{u}) &= [c(\mathbf{u})_{i,j}], \quad c_{2,2}(\mathbf{u})_{i,j} = \int_{\Omega} \frac{\partial \varphi_i}{\partial x} u_1 \varphi_j + \frac{\partial \varphi_i}{\partial y} u_2 \varphi_j \, dx, \text{ for } (i, j) = n \dots 2n. \end{aligned}$$

A partitioning for system (4.24) results in.

$$\begin{pmatrix} \eta A + E_{1,1} + M_{1,1} & M_{1,2} & B_x^T \\ M_{2,1} & \eta A + E_{2,2} + M_{2,2} & B_y^T \\ B_x & B_y & 0 \end{pmatrix} \begin{pmatrix} \vec{\lambda}_1 \\ \vec{\lambda}_2 \\ \mathbf{q} \end{pmatrix} = \begin{pmatrix} \tilde{\mathbf{f}}_1 \\ \tilde{\mathbf{f}}_2 \\ \tilde{\mathbf{s}} \end{pmatrix}, \quad (4.27)$$

where the  $n \times n$  matrix  $A$  is the scalar Laplacian matrix and the  $n_p \times n$  matrices  $B_x$  and  $B_y$  are as defined above. The  $n \times n$  block matrices

$$\begin{aligned} M(\mathbf{u})_{1,1} &= [m_{i,j}], \quad m_{1,1}(\mathbf{u})_{i,j} = \int_{\Omega} \frac{\partial w_1}{\partial x} \varphi_i \varphi_j \, dx, \text{ for } (i, j) = 1 \dots n, \\ M(\mathbf{u})_{1,2} &= [m_{i,j}], \quad m_{1,2}(\mathbf{u})_{i,j} = \int_{\Omega} \frac{\partial w_2}{\partial x} \varphi_i \varphi_j \, dx, \text{ for } i = 1 \dots n, j = n+1, \dots, 2n, \\ M(\mathbf{u})_{2,1} &= [m_{i,j}], \quad m_{2,1}(\mathbf{u})_{i,j} = \int_{\Omega} \frac{\partial w_1}{\partial y} \varphi_i \varphi_j \, dx, \text{ for } i = n \dots 2n, j = 1, \dots, n, \\ M(\mathbf{u})_{2,2} &= [m_{i,j}], \quad m_{2,2}(\mathbf{u})_{i,j} = \int_{\Omega} \frac{\partial w_2}{\partial y} \varphi_i \varphi_j \, dx, \text{ for } i = n \dots 2n, j = n, \dots, 2n, \end{aligned}$$

and

$$\begin{aligned} E_{1,1}(\mathbf{u}) &= [e(\mathbf{u})_{i,j}], \quad e_{1,1}(\mathbf{u})_{i,j} = \int_{\Omega} \frac{\partial \varphi_i}{\partial x} u_1 \varphi_j + \frac{\partial \varphi_i}{\partial y} u_2 \varphi_j \, dx, \text{ for } (i, j) = 1 \dots n, \\ E_{2,2}(\mathbf{u}) &= [e(\mathbf{u})_{i,j}], \quad e_{2,2}(\mathbf{u})_{i,j} = \int_{\Omega} \frac{\partial \varphi_i}{\partial x} u_1 \varphi_j + \frac{\partial \varphi_i}{\partial y} u_2 \varphi_j \, dx, \text{ for } (i, j) = n \dots 2n. \end{aligned}$$

See section (7.1) of the appendix for more details.

### 4.2.3 Choice of the finite element spaces $\mathbf{V}_{0h}$ and $Q_h$

The weak forms of the state and adjoint equations do not require the pressure to be continuous. Thus, we may choose spaces of continuous or discontinuous functions for the pressure, while for the velocity we will always consider continuous basis functions. We remark here that since the state and adjoint equations are of second order in  $\mathbf{u}$  and  $\lambda$ , and first order in  $p$  and  $q$  respectively, it makes sense to use polynomials of degree  $k+1$ ,  $k \geq 1$  for the space  $\mathbf{V}_{0h}$  and of degree  $k$  for the space  $Q_h$ . Several other choices of the finite element spaces are possible, see for example [Girault 1986, Chapter 2] for details. In our case, we choose polynomials of degree 2 for velocity

space and polynomials of degree 1 for the pressure space. The resulting mixed method is called  $P_2 - P_1$  approximation, but is often referred to in the literature as the Taylor-Hood method, (see e.g, [Girault 1986, Pg.176] ). This choice leads to a well posed discrete system as discussed later on in the following paragraphs.

#### 4.2.4 Solving the discrete algebraic problems

We now study possible methods for solving the discrete state and adjoint systems.

##### 4.2.4.1 Solving the discrete state system

The discrete state equation (4.23) is a non-linear, typically very large system. Iterative methods must be used for non-linear problems. The nonlinear problem is turned into a succession of linear problems, and this is the basis of the so called Picard iteration [Cuvier 1986, Pg.255]. This is a simple fixed point strategy where the velocity computed from the preceding iteration is substituted into the convective term. This results into a linearized discrete state system after the  $n^{th}$  iteration and the fixed point algorithm can thus be written as shown in algorithm 3.

A commonly used initial guess in algorithm 3 is the solution of the linear Stokes equations. No

---

##### Algorithm 3 Picard algorithm

---

###### 1. Initialization:

- Read the simulation parameters and the mesh
- Initialize the velocity and the pressure :  $(\mathbf{u}_h, p_h)$

###### 2. Loop (Picard iteration). For $n = 0, 1, \dots$ ,

- Solve the linearized problem:

$$\begin{pmatrix} \eta \mathbf{A} + \mathbf{C}(\mathbf{u}_h^n) & \mathbf{B}^T \\ \mathbf{B} & 0 \end{pmatrix} \begin{pmatrix} \mathbf{u}_h^{n+1} \\ p_h^{n+1} \end{pmatrix} = \begin{pmatrix} \mathbf{f}_h \\ \mathbf{s}_h \end{pmatrix}.$$

- update the velocity and pressure  $\mathbf{u}_h^{n+1} = \mathbf{u}_h^n, p_h^{n+1} = p_h$  until

$$\frac{\|\mathbf{u}_h^{n+1} - \mathbf{u}_h^n\|_{H^1}}{\|\mathbf{u}_h^0\|_{H^1}} + \frac{\|p_h^{n+1} - p_h^n\|_{L^2}}{\|p_h^0\|_{L^2}} \leq tol,$$

where  $tol$  is some given tolerance.

###### 3. End Loop

---

initial pressure needs to be specified. Under certain conditions on  $\eta$  (which should not be too small) and  $\mathbf{f}$  (which should not be too large in an appropriate norm), the steady Navier-Stokes

equations have a unique solution  $(\mathbf{u}_h, p_h)$  and the iterates  $(\mathbf{u}_h^n, p_h^n)$  converge to it as  $n \rightarrow \infty$  for any choice of the initial velocity  $\mathbf{u}_h^0$ . We refer to Chapter 2 for existence and uniqueness results and to [Karakashian 1982] for a proof of the global convergence of Picard's iteration.

**Remark 4.2.3.** Alternatively a quadratically convergent Newton method could be used for solving (4.23). For the initial guess one can again use the solution of the Stokes system. However the main drawback of Newton's method is that the radius of the ball of convergence is typically proportional to the viscosity parameter  $\eta$ . Thus, as the Reynolds number is increased, better and better initial guesses are needed in order for the Newton iteration to converge. The advantage of the Picard iteration is that, compared to the Newton iteration, it has a larger radius of convergence.

#### 4.2.4.2 Solvability and well posedness of the discrete linearized state and adjoint systems

We note that the finite-dimensional system arising from a finite element discretization of the equations has the same structure as the continuous problem, but now posed on discrete function spaces. The inf-sup condition ([Girault 1986] Pg. 58) for the discrete spaces is equivalent to the solvability of the finite dimensional systems (4.26-4.24). The validity of the inf-sup condition, i.e.,

$$\inf_{q_h \in Q_h} \sup_{\mathbf{v}_h \in \mathbf{V}_{gh}} \frac{(q_h, \nabla \cdot \mathbf{v}_h)}{\|\mathbf{v}_h\|_1 \|q_h\|_0} \geq \beta_h \quad (4.28)$$

for some  $\beta_h > 0$  has to be checked for each pair  $(\mathbf{V}_{gh}, Q_h)$  of discrete spaces that is used to approximate velocity and pressure, respectively. To this end, one has to choose a stable discretization for the spaces  $\mathbf{V}_{gh}$ ,  $\mathbf{V}_{0h}$  and  $Q_h$  so as to satisfy (4.28), e.g., in our case we choose the Taylor-Hood pair (see e.g [Girault 1986] Pg.176), i.e.,

$$\mathbf{V}^h = \{\mathbf{v} \in \mathbf{V} : \mathbf{v}|_K = (P^2(K))^2\}$$

and

$$Q^h = \{q \in Q : q|_K = P^1(K)\},$$

which satisfies the inf-sup condition ([Girault 1986] Pg.58). Therefore the systems(4.26-4.24) are well posed and solvable. It now remains to find a method for solving these systems. Since these systems are large and sparse, iterative techniques for solving saddle point problems such as Uzawa's method (see e.g [Elman 1994], [Benzi ] and references there in) or Direct sparse solves can be used. We choose to use the latter, since we have to solve the inner most loop several times on changing domains. That means that, at each step of the Picard loop, the linearized discrete problem is solved using a multi-frontal Gauss LU factorization(cf. [Davis 1999]) implemented in

the package UMFPACK<sup>1</sup> [Davis 2004]).

---

<sup>1</sup><http://www.netlib.org/linalg>

# 5

## NUMERICAL SOLUTIONS OF REFERENCE PROBLEMS

In this section we present numerical results for the implementation of shape design sensitivity formulas that have been derived in the previous chapters. The optimization is carried out by the boundary variation algorithm to optimize the shapes of the given reference domains in Chapter 2, to obtain a vortex reduction using cost functionals  $J_1$ ,  $J_2$  and  $J_3$ . Numerical tests and simulations have been carried out using Bamg [[Hecht a](#)], a Bi-dimensional Anisotropic Mesh Generator and FreeFem++ [[Hecht b](#)], a finite element Library developed at INRIA, the French National Institute for Research in Computer Science and Control, with the development of algorithms based on control theory and shape optimization. In order to investigate the performance of the 3 cost functions, three test cases are considered. The first involving a parallel flow in a channel with a bump which is discussed in section [5.1](#). The second test case involving an irrotational flow field in a channel with a bump is discussed in section [5.2](#). For these first two test cases, a priori knowledge of the nature of optimal shape is known. The goal therefore, is to test the performance of the algorithms as well as the objectivity of the 3 cost functionals. The third test case is carried out on the flow in a channel with an obstacle in section [5.3](#). The goal is to reduce the vortex shedding behind an obstacle placed in a parallel channel by changing the shape of one of its boundaries. The knowledge of the location of the optimal shape corresponding to each of the 3 cost functions for this case is not known. Therefore the problem becomes more interesting and moreover since the cost functionals are non-convex, we might get stuck into a local minima if our initialization is not good enough. Therefore we shall investigate, how to initialize the algorithms.

## 5.1 Shape optimization of flow in a channel with a bump

In this example, we study the optimization of flow in a channel with a bump. We consider steady, incompressible, viscous flow in a channel  $-1 < x_1 < 1$  and  $-1 < x_2 < 1$  having a bump on the upper wall extending from  $x_1 = -0.5$  to  $x_1 = 0.5$  (see Figure 5.1). That is, we set  $a = -0.5$ ,

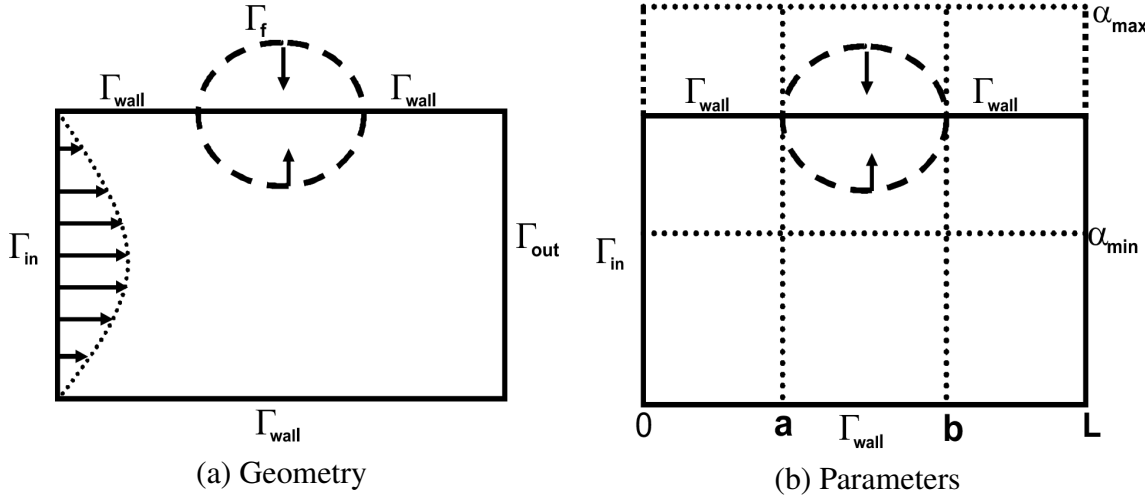


Figure 5.1: Domain for test problem 1

$b = 0.5$ ,  $L = 1$ ,  $\alpha_{min}(x_1) = 0.5$ , and  $\alpha_{max}(x_1) = 1.5$  as parameters in Figure (5.1 b). The flow is described by the solution of the stationary Navier-Stokes system

$$-\frac{1}{Re} \Delta \mathbf{u} + \mathbf{u} \cdot \nabla \mathbf{u} + \nabla p = 0 \quad \text{and} \quad \operatorname{div} \mathbf{u} = 0 \quad \text{in the channel}, \quad (5.1)$$

along with boundary conditions

$$\mathbf{u} = 0 \quad \text{on } \Gamma_1, \Gamma_3 \text{ and } \Gamma_f, \quad (5.2)$$

$$\mathbf{u} = \begin{pmatrix} u_1 \\ u_2 \end{pmatrix} = \begin{pmatrix} \beta(x_2 + 1)(1 - x_2) \\ 0 \end{pmatrix} \quad \text{at the inflow } x_1 = -1 \quad (\Gamma_4), \quad (5.3)$$

and the natural "do-nothing" boundary conditions ( proposed in [Heywood 1996])

$$p \cdot \mathbf{n} - \frac{1}{Re} \frac{\partial \mathbf{u}}{\partial \mathbf{n}} = 0 \quad \text{on } \Gamma_2, \quad (5.4)$$

where  $\mathbf{n}$  is the normal field to the outflow boundary,  $\Gamma_1 \cup \Gamma_3 \equiv \Gamma_{wall}$ , and  $\Gamma_4 \equiv \Gamma_{in}$ . In this case,  $\Gamma_1, \Gamma_2, \Gamma_3$  and  $\Gamma_4$  are fixed parts of the boundary and  $\Gamma_f$  the moving part of the boundary.

In (5.1-5.4),  $\mathbf{u}$  and  $p$  denote the velocity and pressure fields respectively,  $Re$  is the Reynolds number, and  $\beta$  is a parameter that determines that mass flow rate at the inflow. The geometry is constructed by analytic description of the boundaries piece by piece. For instance, the bump,

which is the free boundary in this case, is constructed using a sum of 3 pieces of Bézier polynomials of degree three so that the bump continuously meets the straight channel wall on either side of it. In Figure (5.2) we isolate two possible locations to the bump, each drawn to scale. Each of the computational domains in Figure 5.2 is discretized by triangular elements generated by the bi-dimensional anisotropic mesh generator (BAMG)[Hecht a], to obtain discretized domains shown in Figure (5.3). The control points for the optimization are the nodes of the finite element mesh on the bump. We solve the Navier-Stokes equations first on the geometry in Figure(5.3 (a)) where we set the parameter  $\beta$  to 2.5, the Reynolds number  $Re$  to 50, and the following Figures (5.4-5.5) for the velocity distributions and field respectively, are obtained.

**Note 5.1.1.** The colors for the arrows in the velocity field plots indicate the magnitude of the velocity field.

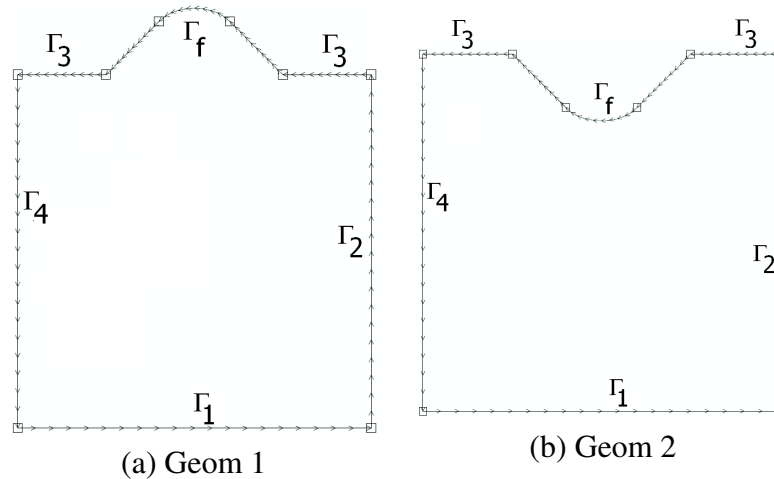


Figure 5.2: Test case geometries

The flow field pattern (Figure (5.5)) posses a vortex in the bump of the computational domain. This is what we want to reduce/minimize by using the freely moving boundary part of the domain ( $\Gamma_f$ ) as the control. In order to reduce the vortex, we choose one of the three criteria that were analyzed in the previous chapters.

### 5.1.0.3 Choice of boundary conditions

The choice of boundary condition for this example ensures that the solution of (5.1-5.4) has a parabolic profile if  $\Omega$  is a square. More precisely, if  $\Omega$  is a square  $[-1, 1] \times [-1, 1]$ , the solution of (5.1-5.4) is given by:

$$\begin{cases} \mathbf{u}(x_1, x_2) = (2.5(x_2 + 1)(1 - x_2), 0), \\ p(x_1, x_2) = \frac{5}{Re}(1 - x_1). \end{cases} \quad (5.5)$$

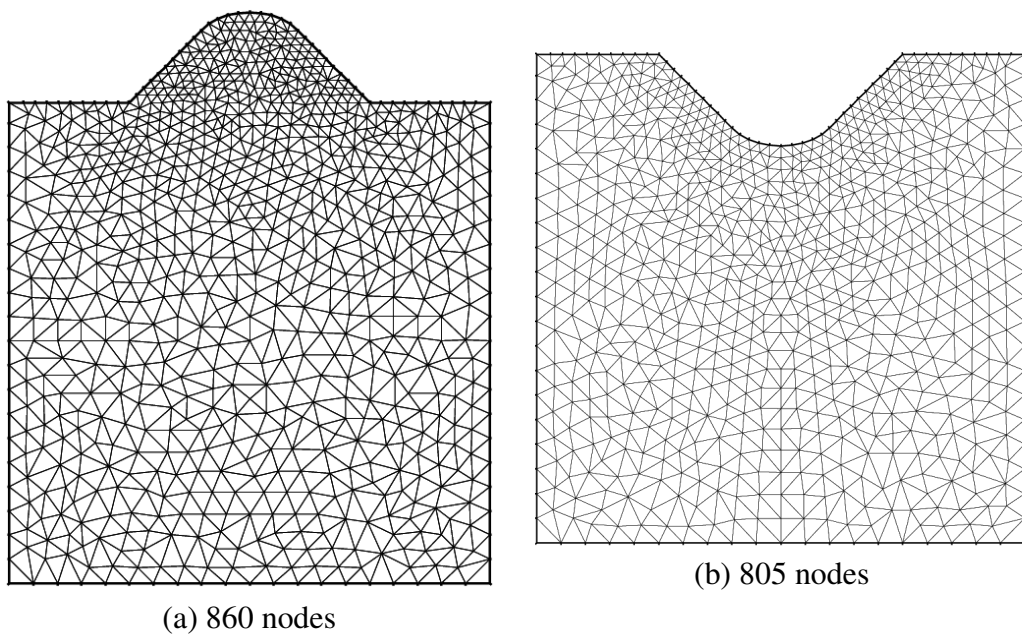


Figure 5.3: Discretized computational geometries

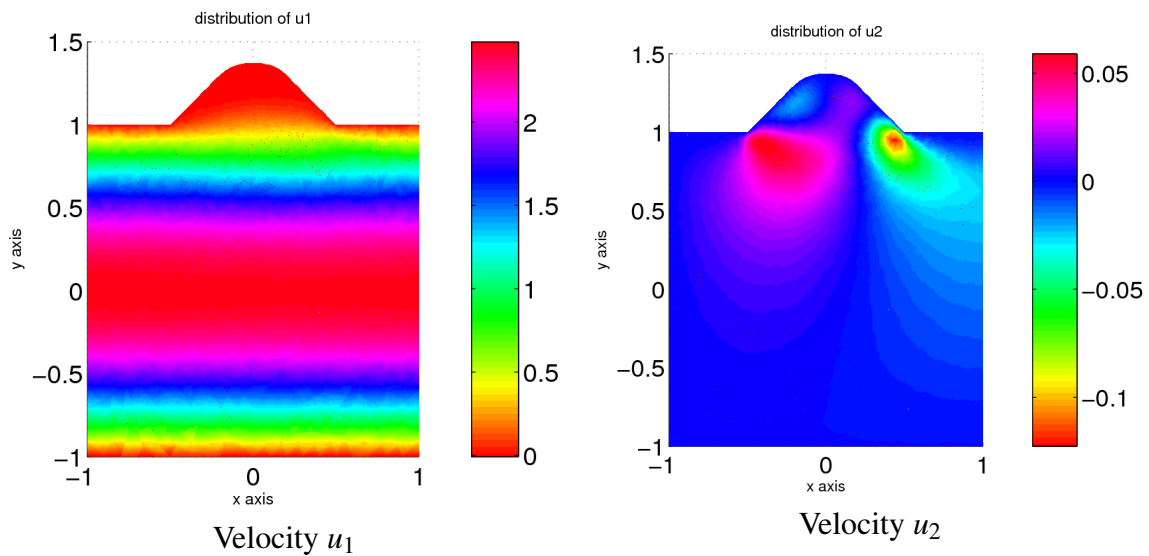
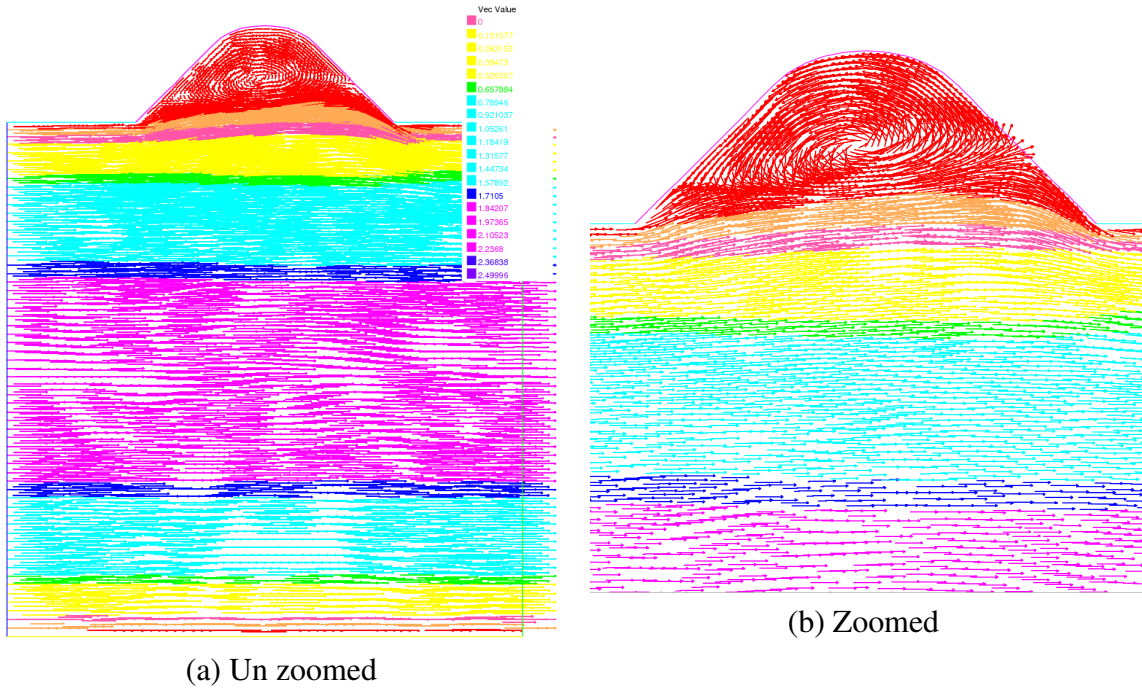


Figure 5.4: Plot of distribution of vertical and horizontal components of velocity

Figure 5.5: Vector plot of velocity vectors  $u_1$  and  $u_2$ 

### 5.1.1 Shape optimization with cost $J_1$

In this subsection, we want to suppress the vortex by forcing the flow field to be as close as possible to the parabolic inflow profile. This leads to the following tracking type cost functional

$$\min_{\Omega} J_1(\mathbf{u}, \Omega) = \frac{1}{2} \int_{\Omega} |\mathbf{u} - \mathbf{u}_d|^2 dx,$$

where the desired state is chosen as  $\mathbf{u}_d = (2.5(x_2 + 1)(1 - x_2), 0)$ . With this choice of target flow, the functional  $J_1$  vanishes at the optimal domain, which in this case is known to be a square.

As discussed in the previous subsections, we move the control boundary in the direction of the negative deformation velocity field  $\mathbf{h}$ .

We start the algorithm with initial geometry and mesh as in Figure (5.2 (a)) and Figure (5.3 (a)). We set some fixed number of iterations, in this case 15 as the stopping criterion. If it is too small, we restart the algorithm, with the last shape as the initial shape until our algorithm stagnates, then we stop. Stagnation is determined by a combination of the values of  $dJ(\Omega, \mathbf{u})\mathbf{h}$  and visual inspection.

#### 5.1.1.1 Results

In Figure (5.6) we display the results that we obtain when we implement the boundary variational algorithm.

In Figure (5.6 (a)) we see the triangulation of  $\Omega_0$ . In Figure (5.6 (b)), we see the final

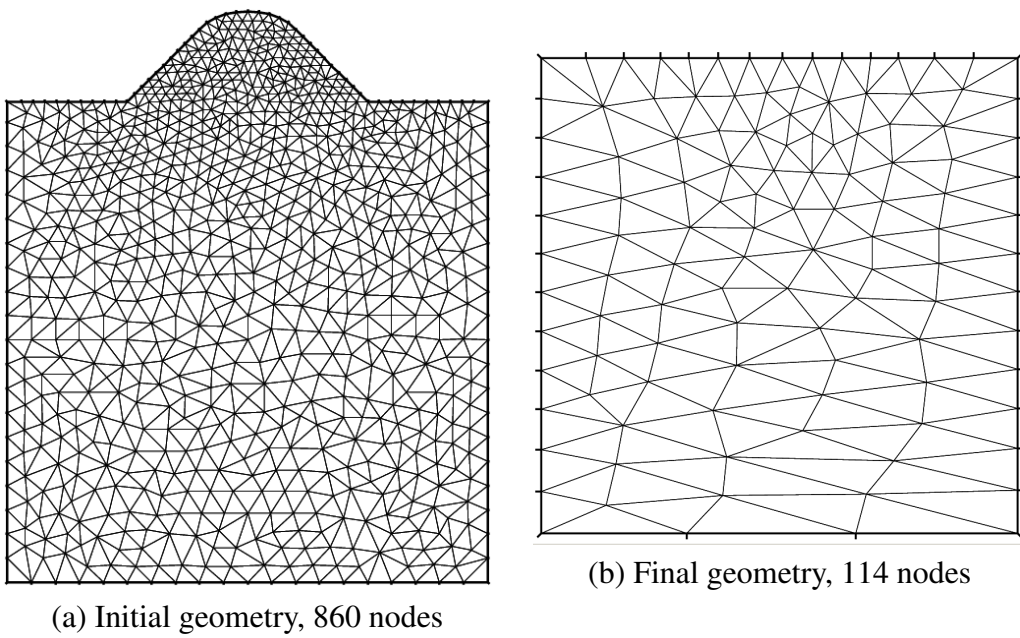


Figure 5.6: Initial and final domain

geometry which is also optimal. The final geometry is obtained after 14 iterations. The value of the cost  $J_1$  on the initial geometry is 0.118577 while that on the final geometry is found to be  $1.97727e^{-11}$ . As expected, the flow field on the optimal geometry has a parabolic profile with no vortices as shown in Figure (5.7) (c)). The mesh topology on the final geometry is different from that of the initial geometry because during the minimization routine, a regularization procedure which explicitly smoothes the shape at each iteration is used (see Chapter 3 for details).

A plot of the history of the three cost functions during the minimization process according to

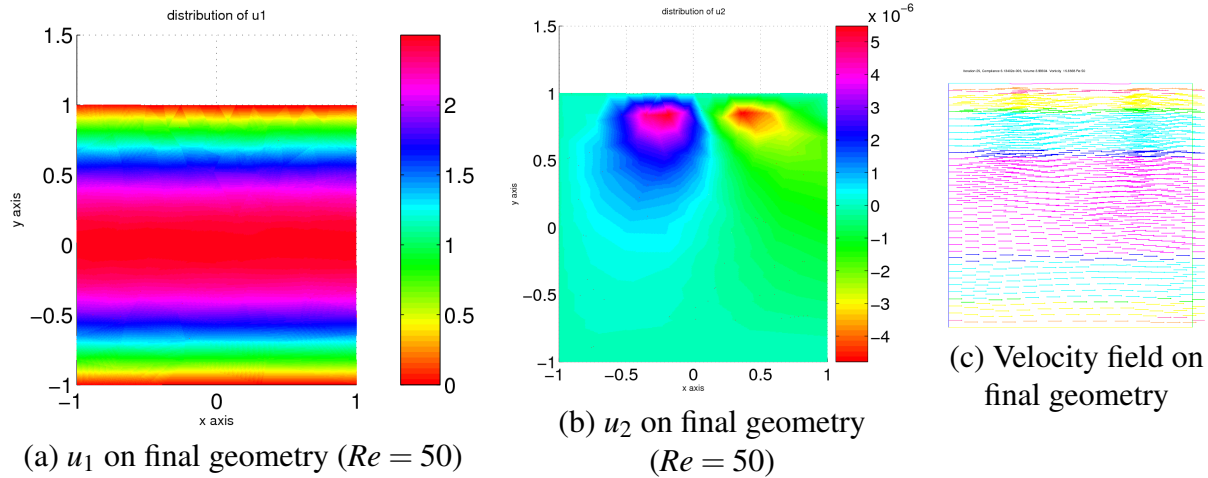


Figure 5.7: Velocity on final geometry

$J_1$  results in Figures (5.8). From these figures, we see that as the number of iterations increases, both cost  $J_1$  and  $J_3$  decrease while  $J_2$  increases. This means that the optimal geometry which

minimizes both  $J_1$  and  $J_3$  is not the optimal one for  $J_2$ .

In the next subsection, we shall investigate further the optimal geometry which minimizes cost

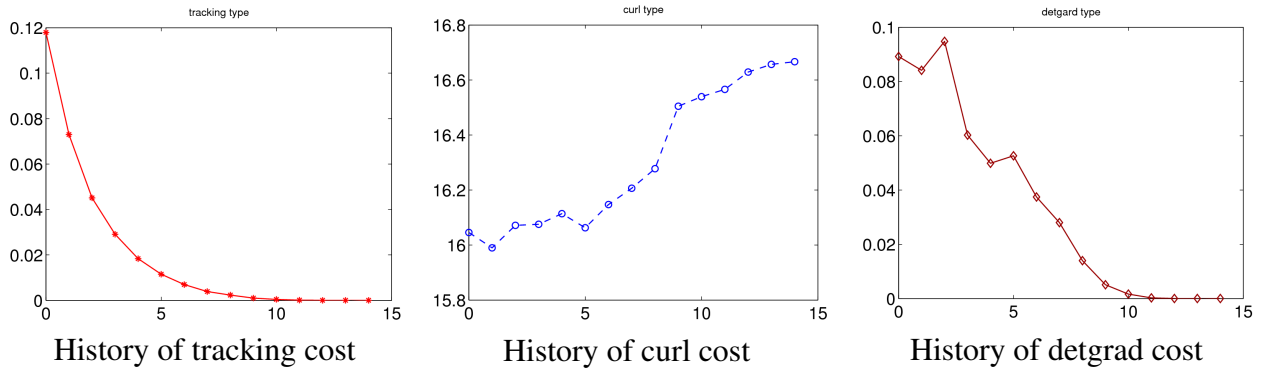


Figure 5.8: History of three cost functionals during minimization of tracking type cost

$J_2$ .

### 5.1.2 Shape optimization with cost $J_2$

In this subsection, we want to suppress the vortex by minimizing the cost functional  $J_2(\Omega)$ . Results from the previous subsection indicate that the optimal geometry which minimizes  $J_2$  is not a square. In this case, the initial guess  $\Omega_0$  is set to be the domain shown in Figure 5.2 (b). In Figure 5.9 (a) we see the triangulation of  $\Omega_0$ . In Figure 5.9 (b), we see the final geometry which is also optimal. The value of the cost on  $\Omega_0$  is 32.69 and for the final design 16.0, which gives a relative

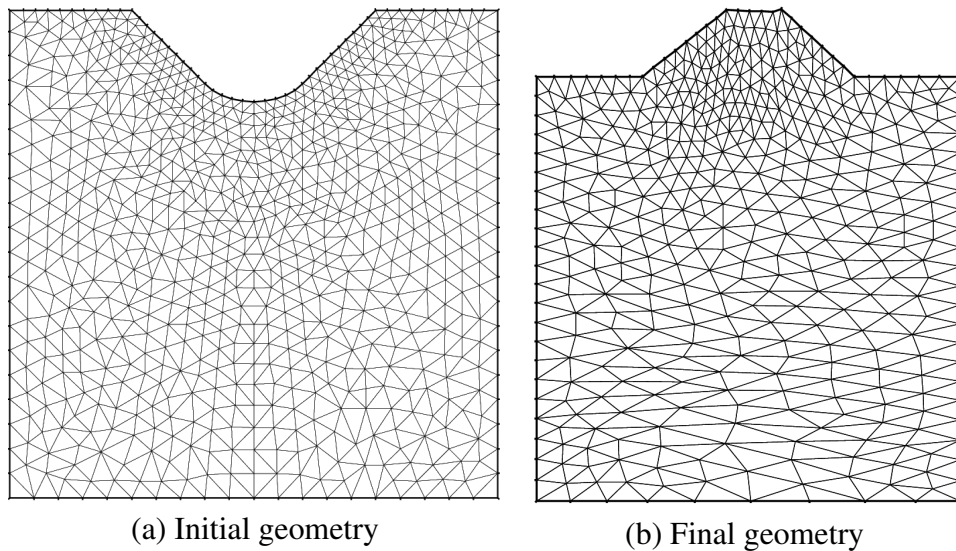


Figure 5.9: Initial and final design

reduction of 50.87% of the initial cost. During the minimization for the curl type cost, we record the value for each of the three cost functionals  $J_1$ ,  $J_2$  and  $J_3$ . In Figure 5.10, we display the history

of the three cost functions. Cost functionals  $J_1$  and  $J_3$  reduce with the number of iterations during

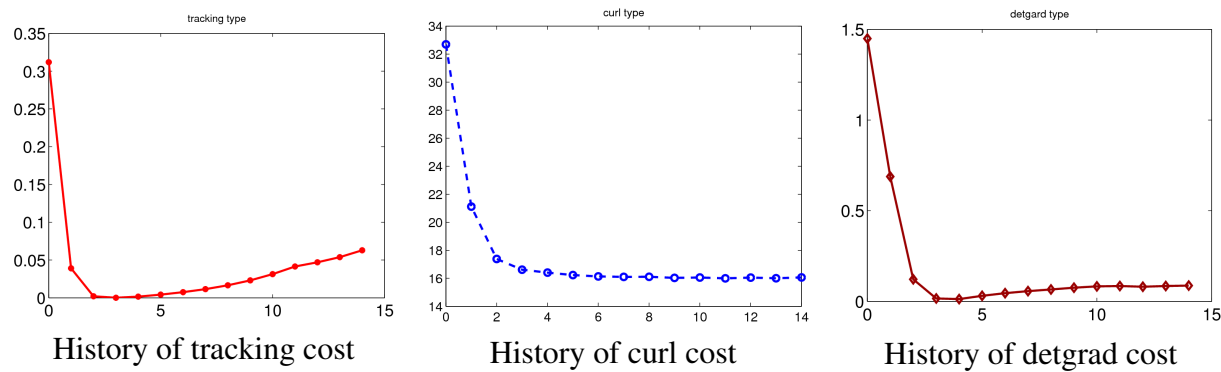


Figure 5.10: History of three cost functionals during minimization of curl type cost

the approximately first 4 iterations where they attain their minima and there after start to increase. The minimal cost  $J_2$  does not coincide with that of  $J_1$  and  $J_3$  and this leads to different optimal geometries. When we plot the velocity field on the initial and optimal domains, Figures(5.11a) and (5.11b) are obtained. From these figures, we see that although we have reduced the value

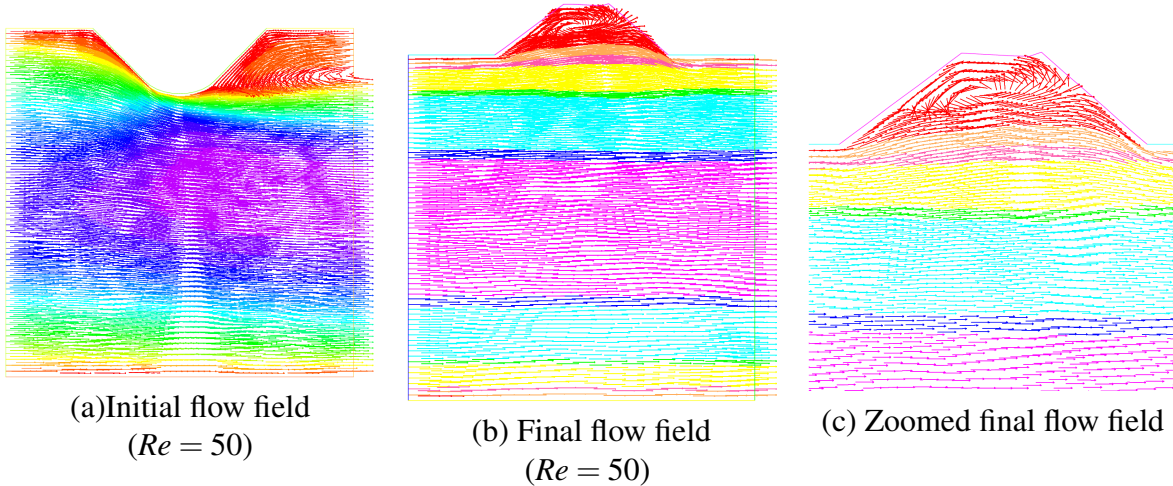


Figure 5.11: Initial geometry, flow field and final flow field with  $J_2$

of the cost functional  $J_2$  in a mathematical point of view, we have created a vortex. A physical explanation of these results is the following: For the flow in a geometrical configuration as in

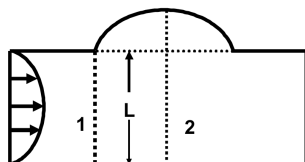


Figure 5.12: Illustration figure

Figure (5.12),  $|\frac{\partial u_2}{\partial x_1}|$  is smaller in magnitude than  $|\frac{\partial u_1}{\partial x_2}|$ , and hence

$$|\operatorname{curl} \mathbf{u}| \approx \left| \frac{\partial u_1}{\partial x_2} \right|. \quad (5.6)$$

The mass flow rate  $\dot{m}$  of the incoming fluid is given by

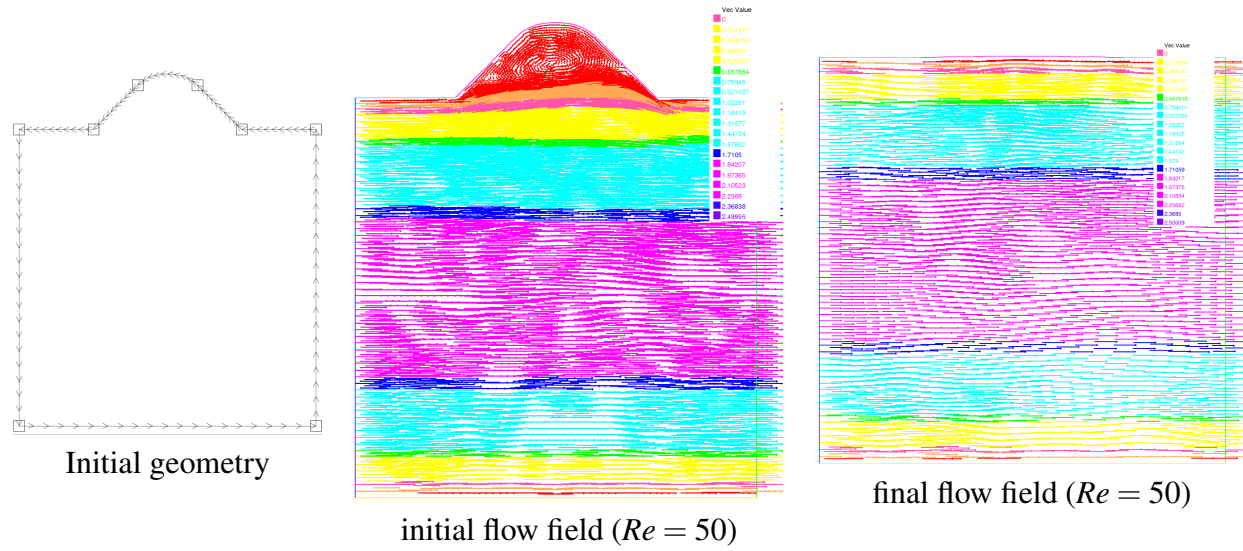
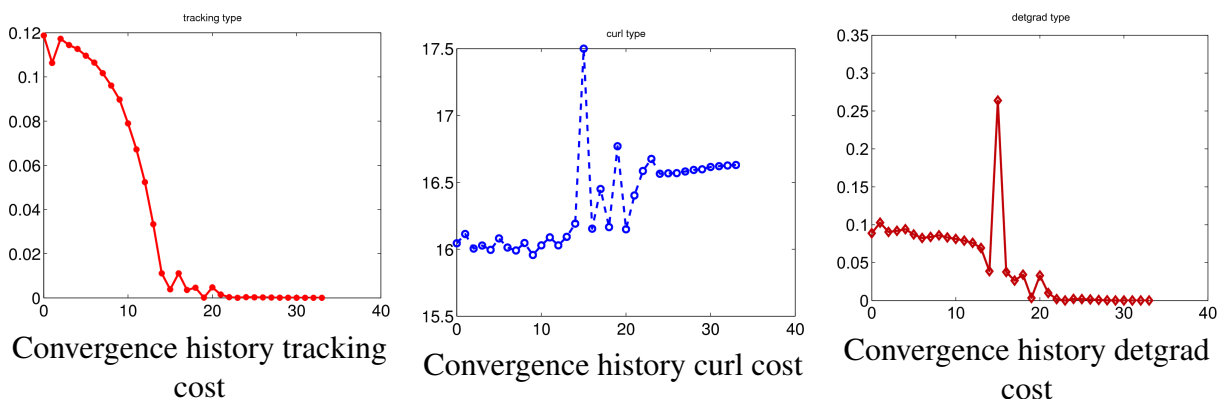
$$\dot{m} = \rho A \mathbf{u},$$

where  $A$  is the cross section area of the tube. Since the mass flow rate is fixed during optimization, then in order to minimize  $|\operatorname{curl} \mathbf{u}|$  in (5.6) over the same length scale  $L$  at different position  $x_1$ , the fluid must decelerate from position 1 to position 2, (see Figure 5.12). Furthermore, Bernoulli's principle suggests that a decrease in velocity from 1 to 2, leads to an increase in pressure in position 2 relative to position 1 [Kundu 1990, Chapter 5]. The change in pressure  $\Delta p = p_2 - p_1 > 0$  is known as adverse pressure gradient, since it opposes the flow field. From our optimization algorithm, we observed an increase in the cross section between the two ends of the bump with number of iterations. The preceding discussion then implies that the fluid decelerates with iteration count, and this consequently leads to an increase in the adverse pressure gradient. A point is then reached when the adverse pressure gradient is so much that it leads to the reversal in direction of the flow field. Consequently this leads to the recirculation of the flow field in the bump region that is observed in our final flow field shown in Figure (5.11 b-c ). An alternative but equivalent explanation in terms of pressure loss and energy can be found in [Lehnhäuser 2005]. This particular example shows cost functional  $J_2$  seems not to be a good candidate for vortex reduction in this shape optimization problem. In the next subsection, we shall investigate the effect of using the cost functional  $J_3$  for vortex reduction.

### 5.1.3 Shape optimization with cost $J_3$

In this subsection, we perform the optimization using cost functional  $J_3$ . In Figure (5.13(a)) we see the initial computational geometry  $\Omega_0$ . In Figure (5.13(b)), the initial flow field, and in Figure (5.13(c)) the flow field on the final geometry which is also optimal. The value of the cost on the initial geometry is 0.0914646 and its value on the final geometry is  $5.35e^{-7}$ . Again we see here that the value of the cost functional is reduced by almost 100% and moreover the resultant geometry yields a flow without vortices. During the minimization of cost  $J_3$ , again we record the value of each of the three cost functionals  $J_1$ ,  $J_2$  and  $J_3$  which we plot in Figure 5.14. This further indicates the conclusion we made about cost  $J_2$ .

**Remark 5.1.1.** We remark here that the optimal geometry obtained when using the tracking type cost functional depends on how we define the desired flow  $\mathbf{u}_d$ . A different choice other than the

Figure 5.13: Initial geometry, flow field and final flow field with  $J_3$ Figure 5.14: History of three cost functionals during minimization of cost  $J_3$

parabolic flow profile will yield a different optimal geometry.

### 5.1.4 Conclusion

We come to the conclusion that the cost functional  $J_3$  seems a better choice than  $J_1$  and  $J_2$  at least in this particular example of minimizing the vortex in the channel flow with a bump on one of the boundaries.

## 5.2 Shape optimization of an irrotational flow in a channel with a bump

In this example we consider steady, incompressible, viscous irrotational flow in a channel  $-1 < x_1 < 1$  and  $-1 < x_2 < 1$  having a bump on the upper wall extending from  $x_1 = -0.5$  to  $x_1 = 0.5$  (see Figure 5.2(a) in the previous section). The flow is again described by solution of the stationary Navier-Stokes system

$$-\frac{1}{Re} \Delta \mathbf{u} + \mathbf{u} \cdot \nabla \mathbf{u} + \nabla p = \mathbf{f} \quad \text{and} \quad \operatorname{div} \mathbf{u} = 0 \quad \text{in the channel.} \quad (5.7)$$

Since the flow under consideration is assumed to be irrotational flow, then

$$\operatorname{curl} \mathbf{u} = 0. \quad (5.8)$$

This guarantees existence of a scalar function  $\Phi$ , called the velocity potential, which is related to the velocity components by

$$u_1 = \frac{\partial \Phi}{\partial x_1} \quad \text{and} \quad u_2 = \frac{\partial \Phi}{\partial x_2}. \quad (5.9)$$

In order to construct an exact irrotational velocity field that solves (5.7), we choose  $\Phi = -2x_1x_2$  such that

$$\mathbf{u} = (-2x_2, -2x_1). \quad (5.10)$$

This results in the following boundary conditions

$$\left\{ \begin{array}{l} \mathbf{u} = (2, -2x_1) \text{ on } \Gamma_1, \\ \mathbf{u} = (-2x_2, -2) \text{ on } \Gamma_2, \\ \mathbf{u} = (-2, -2x_1) \text{ on } \Gamma_3 \cup \Gamma_f, \\ \mathbf{u} = (-2x_2, 2) \text{ on } \Gamma_4. \end{array} \right. \quad (5.11)$$

The body forces  $\mathbf{f}$  are chosen in such a way that if  $\Omega$  is a square  $(-1, 1) \times (-1, 1)$ , then the exact solution of (5.7), (5.11) is given by (5.10). Consequently, by substituting (5.10) in (5.7), we construct  $\mathbf{f}$  such that

$$\mathbf{f} = (4x_1, 4x_2). \quad (5.12)$$

The goal is again is to find the domain  $\Omega$  that minimizes each of the three cost functionals stated in the previous section by using part of the boundary  $\Gamma_f$  as a control. In Figure (5.15), we display the

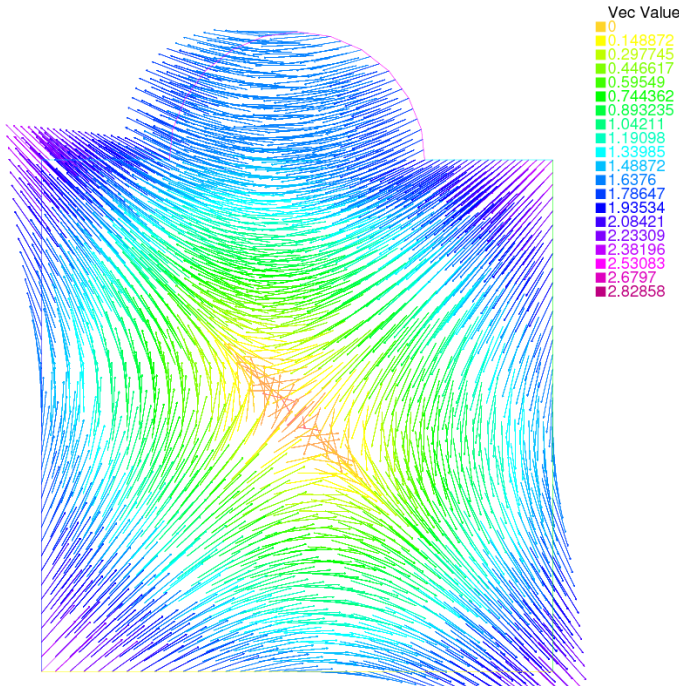


Figure 5.15: Flow on initial geometry

flow field on the initial domain computed with the value of Reynolds number set to 50. Since we prescribe only Dirichlet boundary conditions, pressure can only be determined up to a constant. Thus to ensure its unique solvability, we prescribe it's value at the point  $(-1, -1)$  to be zero.

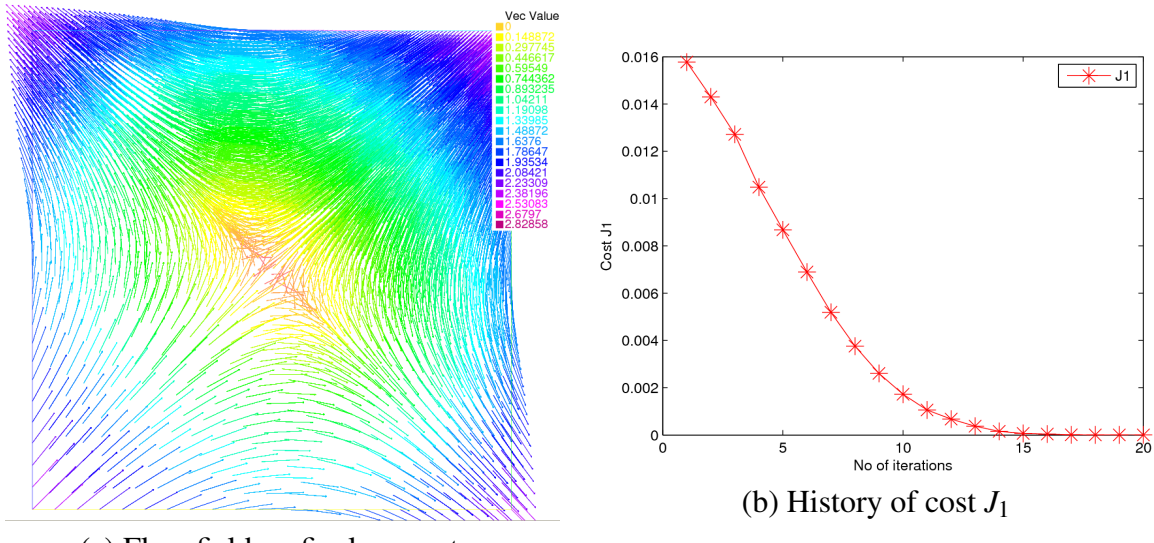
**Remark 5.2.1.** This example is chosen to further highlight the different behavior of the three cost functionals. For this irrotational flow, a proper choice of cost functional for vortex reduction should have the property that it is insensitive with respect to changes of the domain. In particular, an iterative algorithm is expected to stop after the first iteration from any initial choice  $\Omega_0$ . However as we shall see below, this is not the case. There is still a clear distinction between the optimal domains corresponding to the 3 cost functionals.

### 5.2.1 Shape optimization with cost $J_1$

We choose the desired flow field  $\mathbf{u}_d = (-2x_2, -2x_1)$  and we minimize cost functional  $J_1$  (see previous section). We start the algorithm with initial geometry as in Figure (5.15). A particular number of iterations (in this case 25) is set as the stopping criterion. If it is too small, we restart the algorithm, with the previous shape as the initial shape until our algorithm stagnates, then we stop. Stagnation is determined by a combination of the values of  $dJ(\Omega, \mathbf{u})\mathbf{h}$  and visual inspection.

#### Results

In Figure (5.16) we display the results that we obtain when we implement the boundary variational algorithm. In Figure (5.16 (a)) we see the flow field on  $\Omega_f$ . In Figure (5.16 (b)), we see



(a) Flow field on final geometry

Figure 5.16: Final geometry and history of cost  $J_1$

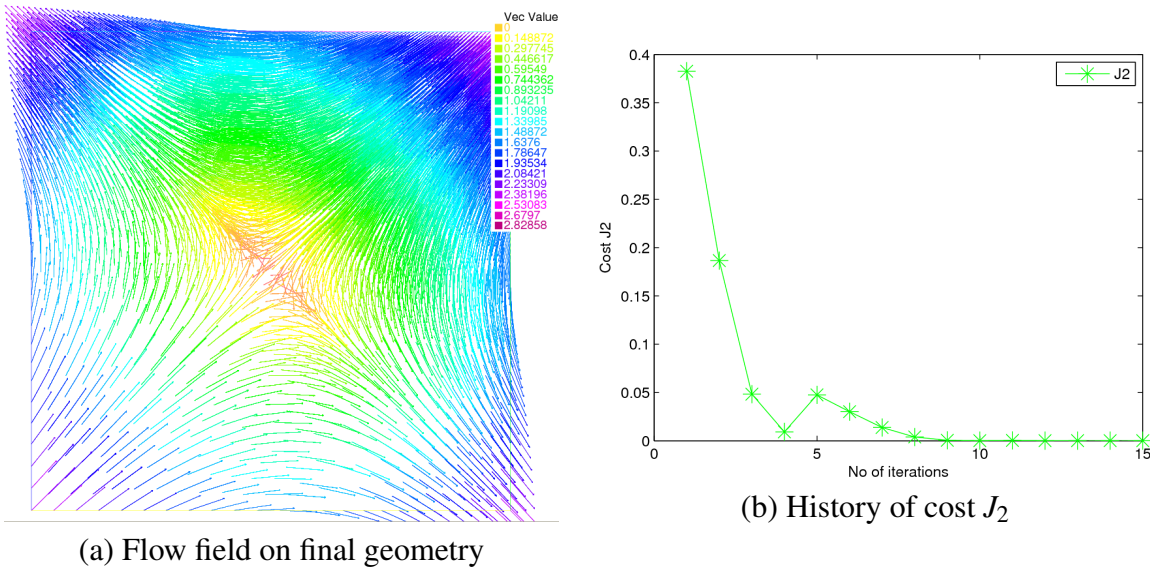
the history of cost  $J_1$ . The final geometry is obtained after 20 iterations. The value of the cost  $J_1$  on the initial geometry is 0.01577 while that on the final geometry is found to be  $3.731e^{-9}$ . As expected, the final geometry is a square with an irrotational flow field.

### 5.2.2 Shape optimization with cost $J_2$

In this subsection, we minimize the cost functional  $J_2$ . We start the algorithm with initial geometry and stopping criterion as in the previous subsection.

#### Results

The cost  $J_2$  is found to be sensitive with respect to changes of the domain, and in Figure (5.17) we display the results obtained after optimization. In Figure (5.17 (a)), we depict the flow field

Figure 5.17: Final geometry and history of cost  $J_2$ 

on  $\Omega_f$ , and in (5.17 (b)), the history of cost  $J_2$ . The final geometry is obtained after 15 iterations. The value of the cost  $J_2$  on the initial geometry is 0.3827 while that on the final geometry is found to be  $3.21e^{-6}$ . Again as expected, the final geometry is a square with an irrotational flow field.

### 5.2.3 Shape optimization with cost $J_3$

In this subsection, we minimize the cost functional  $J_3$ . We start the algorithm with initial geometry and stopping criterion as in the previous subsection.

#### Results

The cost  $J_3$  is found to be insensitive with respect to domain changes, i.e., we observe stagnation after 1 iterations and we stop the algorithm. This is the case since the cost as well as the shape gradient are already zero for the given flow field. Thus the deformation field required to change the geometry is zero just after the first iteration, and the returned geometry is the same as the initial geometry with the value of the cost of order  $10^{-8}$ .

### 5.2.4 Conclusions

This particular academic example shows a clear distinction between the three cost functionals. Cost functional  $J_3$  is again observed to be effective in the sense of identifying a vortex in a given flow field than the tracking type cost functional as well as the curl type cost functional. Furthermore the minimizers for the 3 cost functions do not coincide with exception of  $J_1$  and  $J_2$  because of the way we chose the desired flow field. A different choice of the desired flow field

will yield a different geometry. In the next section we shall study an example where the optimal shape which minimizes either of the three cost functionals is not known a priori.

## 5.3 Flow in a channel with an obstacle

In this section, we want to reduce the vortex shedding behind an obstacle placed in a channel by changing the shape of one of the boundaries of the obstacle (see Figure 5.18). The flow is again

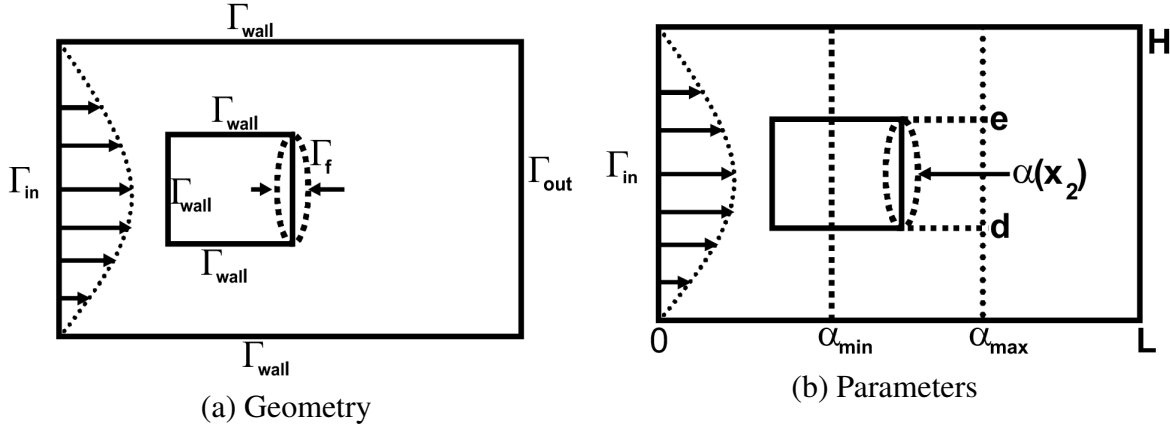


Figure 5.18: Domain for test problem 2

assumed to be steady, incompressible and viscous. The dimensions of the channel are as follows,  $L = 2$ ,  $H = 1$ ,  $d = 0.3$ ,  $e = 0.7$ ,  $\alpha_{min}(x_2) = 0.54$  and  $\alpha_{max}(x_2) = 0.95$ . The cost criteria are again the three cost functionals introduced in the previous sections. In this example, the exact solution to this flow problem is not known, which means that the optimal shape which minimizes either of the three cost functionals is not known a priori. Due to the fact that the cost functionals are non-convex, the initialization of the algorithm can be important. We perform a direct numerical simulation for different geometries and we compute the value of each of the three cost functionals on these geometries. The geometry which gives the least cost will be used as the initial guess for the boundary variation algorithm.

### 5.3.1 Computational geometries and direct numerical simulation

We isolate three possible locations of the variable boundary  $\Gamma_f$ , each drawn to scale as shown in Figure 5.19. Each of the computational domains in Figure 5.19 is then discretized by triangular elements generated by the bi-dimensional anisotropic mesh generator ([Hecht a]), to obtain discretized domains shown in Figure (5.20).

We chose no slip boundary conditions on fixed walls ( $\Gamma_{wall}$ ) and the free boundary  $\Gamma_f$ , i.e.,  $\mathbf{u} = (0, 0)$ . On the inflow boundary  $\Gamma_{in}$ , we chose  $\mathbf{u} = \left( \frac{4U_m}{H^2} (0.5 - x_2)(x_2 + 0.5), 0 \right)$ , and on the

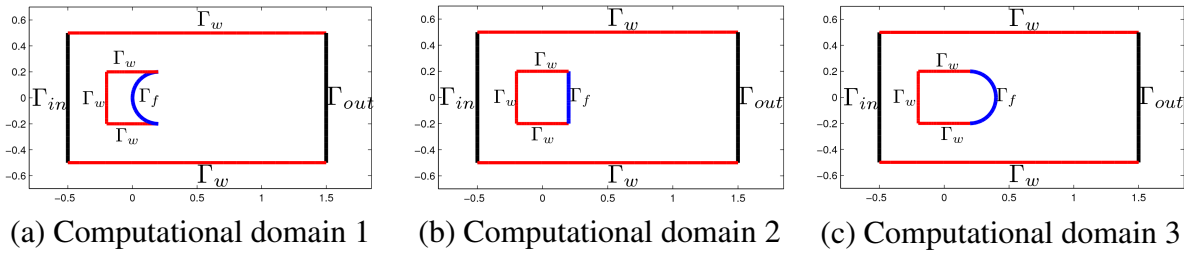


Figure 5.19: Direct numerical simulation geometries

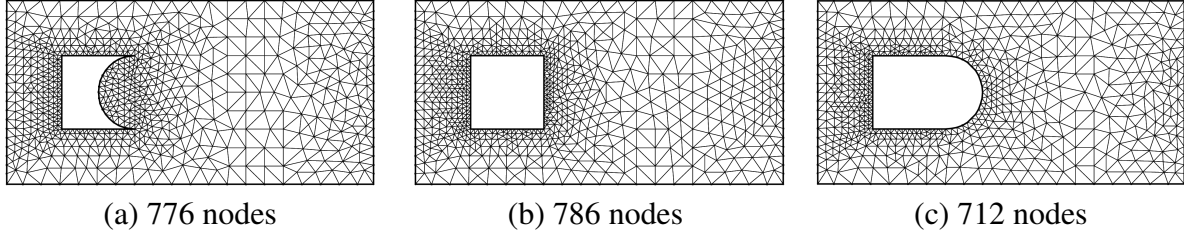


Figure 5.20: Discretized computational geometries

outflow boundary  $\Gamma_{out}$ , we impose the free outlet condition, i.e.,  $p \cdot \mathbf{n} - \frac{1}{Re} \frac{\partial \mathbf{u}}{\partial \mathbf{n}} = 0$ . The parameters  $H$  is set to 1,  $Re$  to 120 and  $U_m$  to 0.3. For each of the three computational domains, we solve the discrete linearized stationary Navier-Stokes system (4.23) subject to the above boundary conditions and evaluate each of the three discretized cost functionals in (4.11).

### 5.3.2 Results from direct numerical simulation

The following flow field patterns (5.21 (a), (b) and (c)) are obtained on each of the three computational geometries in Figure (5.20). After computation of the numerical solution in each of

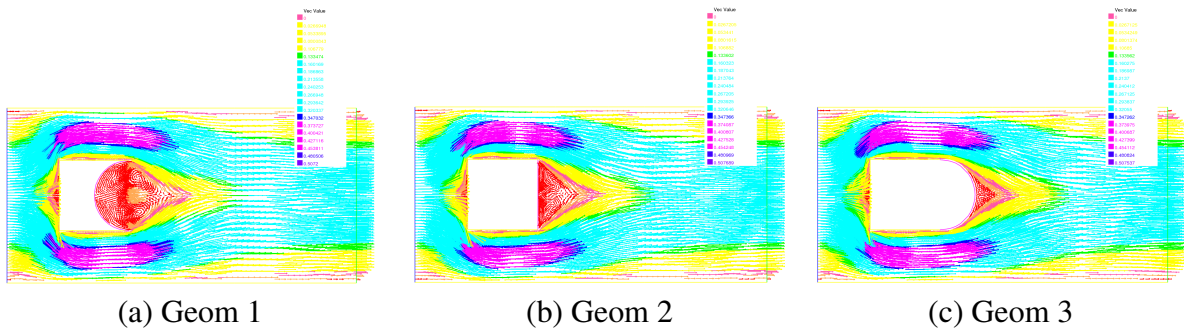


Figure 5.21: Vector plots of flow field patterns

the three cases, we evaluate the values of each of the three cost functionals. In Table 5.1, we report the results obtained. In each column, we mark with bold font the least value of the cost obtained after evaluation on each of the three geometries, e.g, for the tracking type cost, the second geometry gives the least value of this cost functional and so on. Now that we have some idea of where the optimal geometry of each of the three cost functional lie, the task is to use a

Geom	Cost $J_1$ (Tracking)	Cost $J_2$ (Curl)	Detgrad cost $J_3$
1	0.0567474	3.96193	0.329811
2	<b>0.0565549</b>	<b>3.95435</b>	0.327914
3	0.0577802	4.25205	<b>0.310867</b>

Table 5.1: The values of the cost functions on the three geometries

numerical optimization procedure to find the optimal shapes that minimize each of the three cost functionals.

### 5.3.3 Optimization with tracking cost $J_1$

In this subsection, we find an optimal shape that minimizes the tracking type cost functional

$$\min_{\Omega \in \mathcal{U}_{ad}} J(\mathbf{u}, \Omega) = \frac{1}{2} \int_{\Omega} |\mathbf{u} - \mathbf{u}_d|^2 dx, \quad (5.13)$$

subject to the Navier-Stokes system, with the desired state chosen as

$\mathbf{u}_d = (0.07(0.5 - x_2)(x_2 + 0.5), 0)$ . Our choice of the desired state is motivated by the fact that we want to suppress the vortex in the flow around the obstacle. We start the optimization from the geometry that gives a minimum cost after direct numerical simulation. (c.f. Table 5.1). In this case we start with discretized geometry (Figure 5.20 b) and we use the boundary variation algorithm already explained in the previous section. The following results are obtained.

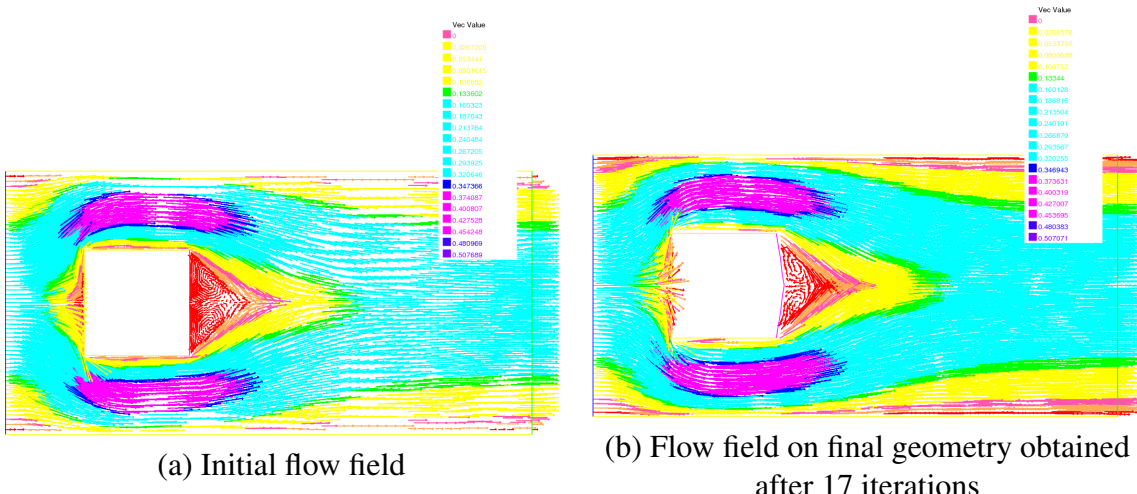


Figure 5.22: Vector plot of velocity field on initial and optimal geometry

In Figure (5.22 a) we show the flow field on the initial geometry and in Figure (5.22b) the flow field on the final geometry. The value of the cost on the initial geometry is found to be 0.0577918 while that on the final geometry is found to be 0.0564491. Although the cost has been reduced relatively by 2.3%, a zoomed flow field in Figure (5.23(b)) clearly shows that the flow field on the

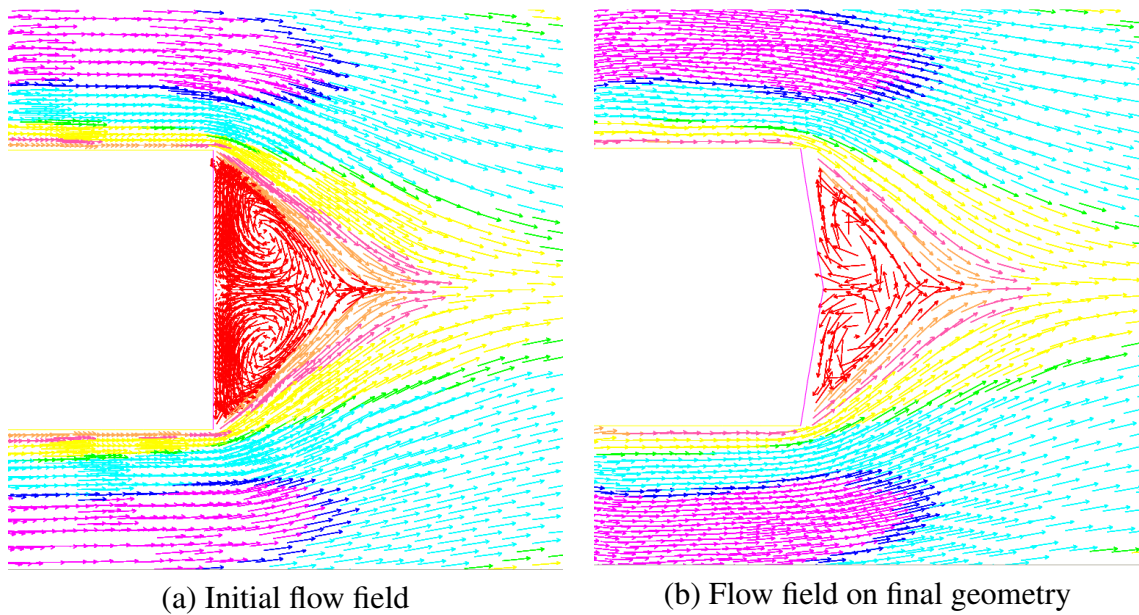


Figure 5.23: Zoomed velocity field on initial and optimal geometry

final geometry still possess a vortex that we intended to reduce/minimize. Again we remark that the optimization using this cost depends upon the definition of the desired state, i.e., different desired state values  $\mathbf{u}_d$  yield different optimal shapes.

### 5.3.4 Optimization with curl type cost $J_2$

In this subsection, we find an optimal shape that minimizes the curl type cost functional subject to the Navier-Stokes system. We start the optimization from the geometry that gives a minimum value of the cost after direct numerical simulation. (c.f. Table 5.1). In this case we start with discretized geometry (Figure (5.20) b) and we use the boundary variation algorithm already explained in the previous section. The following results in Figure (5.24) are obtained.

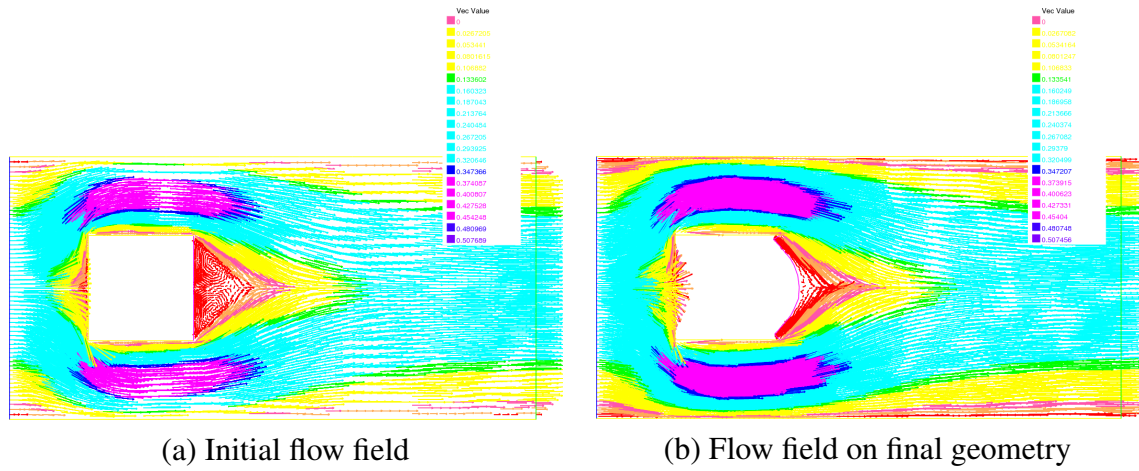


Figure 5.24: Vector plot of velocity field on initial and optimal geometry

In Figure ((5.24) a) we show the flow field on the initial geometry and in Figure (5.24b) the flow field on the final geometry. The value of the cost on the initial geometry is 3.95709 while that on the final geometry is found to be 3.91294. The gives a relative reduction of 1.1137% in the value of the cost. However, when we zoom in the final flow field in ((5.24) b), the region marked

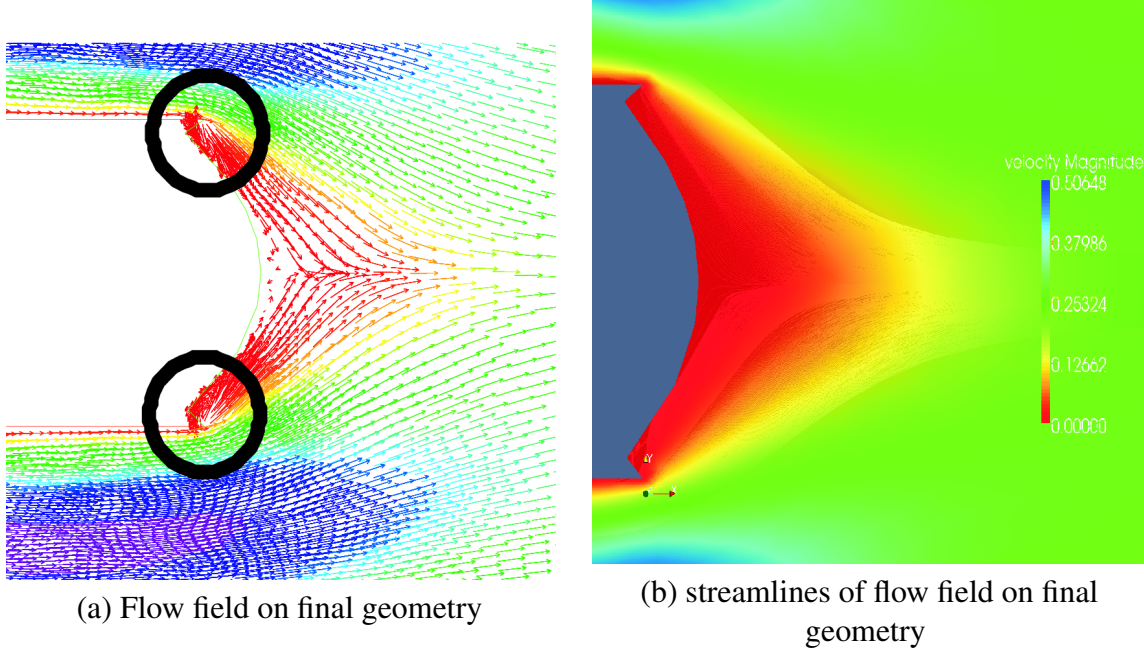
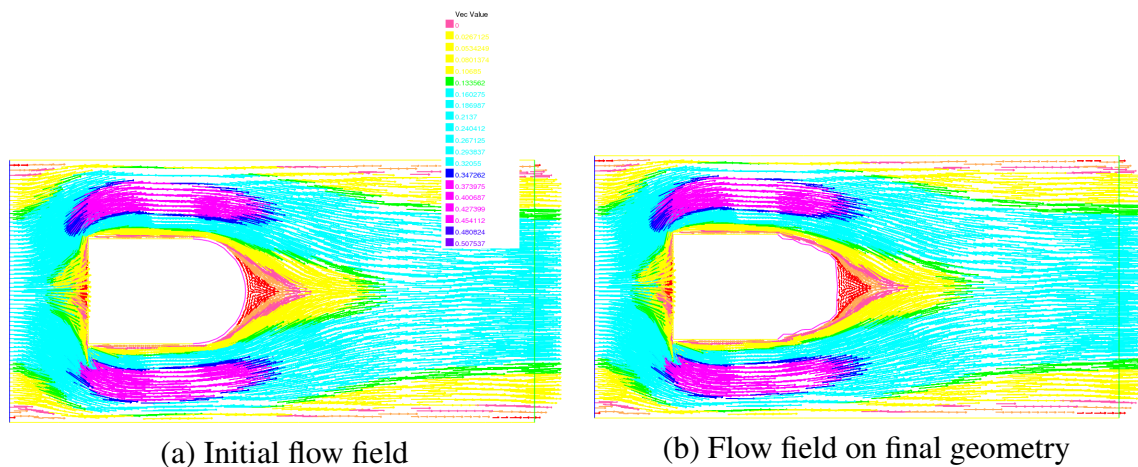


Figure 5.25: Zoomed velocity field and streamlines on the optimal geometry

by bold circles in (Figure 5.25 (a)) still possess small vortices. Moreover, this observation is further confirmed when we plot the streamlines for the zoomed final flow field which is depicted in (Figure 5.25 (b)).

### 5.3.5 Optimization with cost $J_3$

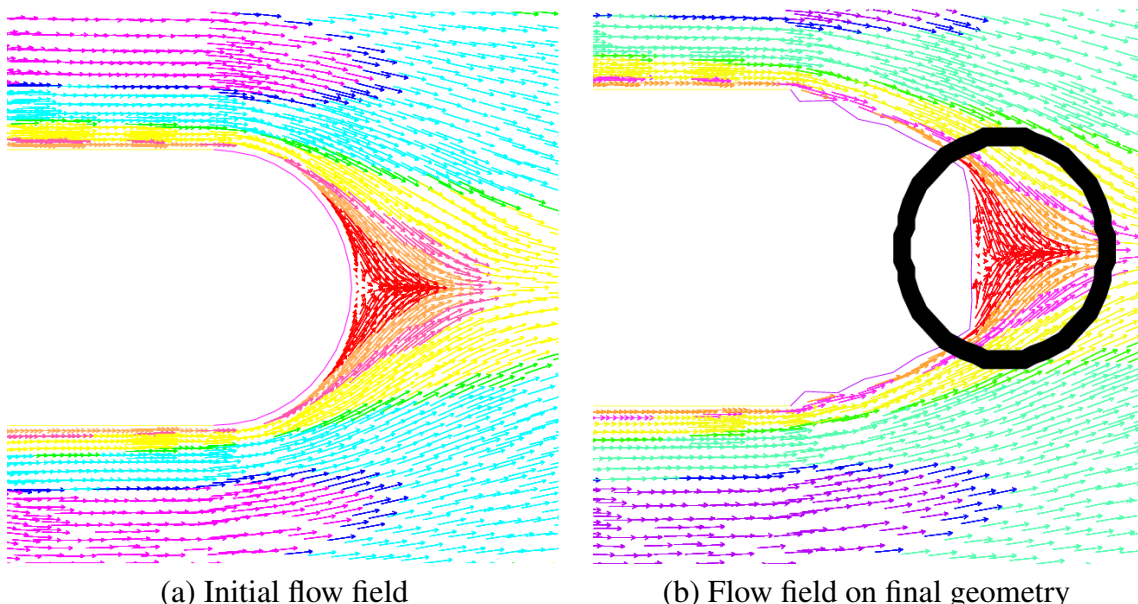
In this subsection, we minimize cost functional  $J_3(\Omega, \mathbf{u})$ , subject to the Navier-Stokes system. We start the computation with the initial geometry  $\Omega_0$  as shown in Figure (5.20 (c)). The flow field on this geometry is as shown in Figure (5.26(a)). The value of the cost  $J_3$  on  $\Omega_0$  is found to be 0.311156 (c.f table 5.1) while that on  $\Omega_{\text{opt}}$  (Figure 5.26(b)) is found to be 0.2994 and this gives a relative reduction of 3.7782% in the value of the cost after 17 iterations. A further zoom of the final flow field in a region marked with a circle in Figure 5.27 indicated no visual presence of vortices in the flow field. These results from minimization of  $J_3$  suggest that cost  $J_3$  performs better than to  $J_1$  (see Figure 5.23(b)) and  $J_2$  (see Figure 5.25) in reducing the vortex in the region behind the obstacle.



(a) Initial flow field

(b) Flow field on final geometry

Figure 5.26: Vector plot of velocity field on initial and optimal geometry



(a) Initial flow field

(b) Flow field on final geometry

Figure 5.27: Zoomed velocity field on initial and optimal geometry

### 5.3.6 Conclusion

In a nutshell, our results confirm that the choice of cost functional is important for vortex reduction in fluid dynamics. Cost functional  $J_3$  should be preferred over functionals  $J_1$  and  $J_2$ .



# 6

## FREE SURFACE PDE CONSTRAINED SHAPE OPTIMIZATION

In this chapter, we consider a PDE constrained shape optimization problem, where the PDE takes the form of stationary incompressible Navier-Stokes equations with over determined boundary conditions on one of the boundaries of the computational domain. The boundary where this phenomena occurs is referred to as the free surface. Our goal is to minimize the cost functionals introduced in Chapter 1, by using parameters describing some part(s) of the boundary of the computational domain as the control for the optimization. We shall assume that the control boundary is different from the free surface boundary, which will significantly help in overcoming technical issues that can arise especially where the free surface might intersect the optimization/ control boundary. The problem of identifying the boundary where the over determined boundary conditions hold, gives rise to a free surface problem. As we shall see later on in this chapter, a free surface problem itself can be treated as a shape optimization problem. Therefore, one can say that we have one shape optimization problem embedded into another shape optimization problem. This makes this problem more complicated in all aspects, than the one discussed in the previous chapters. Therefore the shape sensitivity analysis and the numerical solution for this problem, which we treat later on in this chapter, are novel.

### 6.1 The free surface problem

In this section, a free surface problem is introduced. Several techniques for solving this problem are introduced, and a method that we follow in this work is then discussed in detail.

### 6.1.1 Introduction

Flows often encountered in nature and engineering practice involve a separation of the fluid with air. The separation surface is called the free surface. Free surface flows are flows in which the computational domain is partially bounded by a free surface. The boundary of the free surface is not known a priori and its part of the problem. Often only liquid flow is of interest but sometimes the interaction of gas and liquid flow is essential. The main factors affecting free-surface flows are gravity (and other body forces) and surface tension.

### 6.1.2 Setting of the state problem

We consider an incompressible fluid flow in a domain  $\Omega \subset \mathbb{R}^2$  with a free surface boundaries  $\Gamma_2$  and  $\Gamma_7$  (see Figure 6.1), governed by the following system of equations:

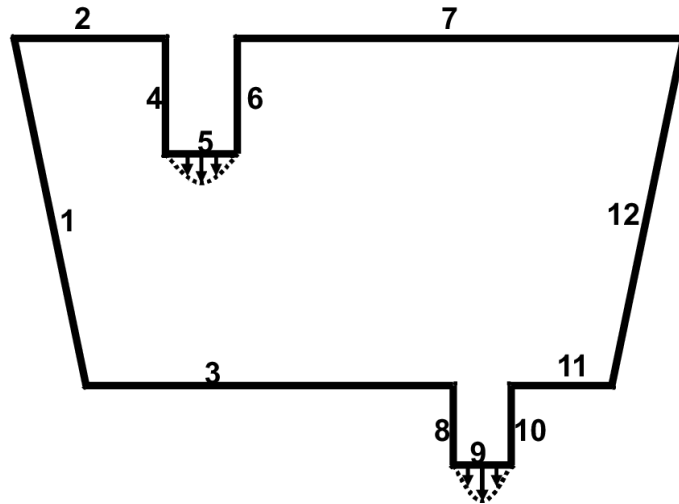


Figure 6.1: Model domain

$$\begin{cases} -\frac{1}{Re} \Delta \mathbf{u} + \mathbf{u} \cdot \nabla \mathbf{u} + \nabla p = \mathbf{f}, & \text{in } \Omega, \\ \operatorname{div} \mathbf{u} = 0, & \text{in } \Omega, \end{cases} \quad (6.1)$$

in non-dimensionless form. In equation (6.1),  $\mathbf{u}$  denotes the scaled velocity of the flow,  $p$  the scaled pressure,  $\mathbf{f}$  the scaled external body forces, and  $Re$  the Reynolds number of the flow. We refer the reader to Chapter 2 for details. In order to make (6.1) well-posed, we have to impose appropriate boundary conditions.

### 6.1.3 Boundary conditions

At the inflow boundary ( $\Gamma_5$ ), the flow is not allowed to move in the tangential direction, but only in the normal direction and hence we set

$$\mathbf{u} \cdot \mathbf{n} = u_n \text{ and } \mathbf{u} \cdot \mathbf{t} = 0, \quad (6.2)$$

where here and in what follows,  $\mathbf{n}$  denotes the outer unit normal to the boundary and  $\mathbf{t}$  denotes the unit tangent vector to the boundary.

At the outflow ( $\Gamma_9$ ), we set the natural "do-nothing" boundary conditions proposed in [Heywood 1996] written in component wise form as :

$$\begin{aligned} \left( -p\mathbf{n} + \frac{1}{Re} \mathbf{n} \cdot \nabla \mathbf{u} \right) \cdot \mathbf{n} &= 0, \\ \left( -p\mathbf{n} + \frac{1}{Re} \mathbf{n} \cdot \nabla \mathbf{u} \right) \cdot \mathbf{t} &= 0. \end{aligned} \quad (6.3)$$

On boundaries  $\Gamma_1, \Gamma_3, \Gamma_8, \Gamma_{10}, \Gamma_{11}, \Gamma_{12}, \Gamma_6$  and  $\Gamma_4$  we set

$$\begin{aligned} \mathbf{u} \cdot \mathbf{n} &= 0, \\ \left( -p\mathbf{n} + \frac{1}{Re} \mathbf{n} \cdot \nabla \mathbf{u} \right) \cdot \mathbf{t} &= 0. \end{aligned} \quad (6.4)$$

Conditions (6.4) describe that there is no flow out of these boundaries, and the tangential stress at these boundaries is zero [Tropea 2007, Chapter 19]. Hence the fluid can slip freely on these boundaries. The boundary conditions on the free boundaries  $\Gamma_2$  and  $\Gamma_7$  require special attention and discussion.

#### 6.1.3.1 Discussion of free-surface boundary conditions

Free surfaces occur at the interface between two fluids which require two conditions to be applied namely:

- (i) The dynamic condition, describing the balance of forces, and
- (ii) the kinematic condition, which relates the motion of the free interface with the fluid velocities at the free surface.

#### The dynamic boundary condition

The dynamic boundary condition for a free surface involve the balance of forces in the directions of the normal and tangent to the surface. Neglecting drag effects from the surrounding medium,

these conditions are given by (see for example [Cuvelier 1990])

$$\begin{aligned} \left( -p\mathbf{n} + \frac{1}{Re} \mathbf{n} \cdot \nabla \mathbf{u} \right) \cdot \mathbf{n} &= \gamma \left( \frac{1}{R} \right) - p_a, \\ \left( -p\mathbf{n} + \frac{1}{Re} \mathbf{n} \cdot \nabla \mathbf{u} \right) \cdot \mathbf{t} &= 0, \end{aligned} \quad (6.5)$$

where  $\gamma$  is the surface tension,  $R$  is the principal radius of curvature of the surface,  $p_a$  is the ambient pressure .

### The kinematic boundary condition

In addition to dynamic boundary conditions (6.5), a kinematic condition on the surface is required. The position of the free surface can always be given in implicit form as  $F(x_j, t) = 0$ . For instance in Fig.(6.2), the height of the free surface above the  $x_1$ -axis is specified as  $x_2 = h(x_1, t)$  and an appropriate function  $F(x_1, x_2, t)$  would be given by  $F(x_1, x_2, t) = h(x_1, t) - x_2$ . Fluid parti-

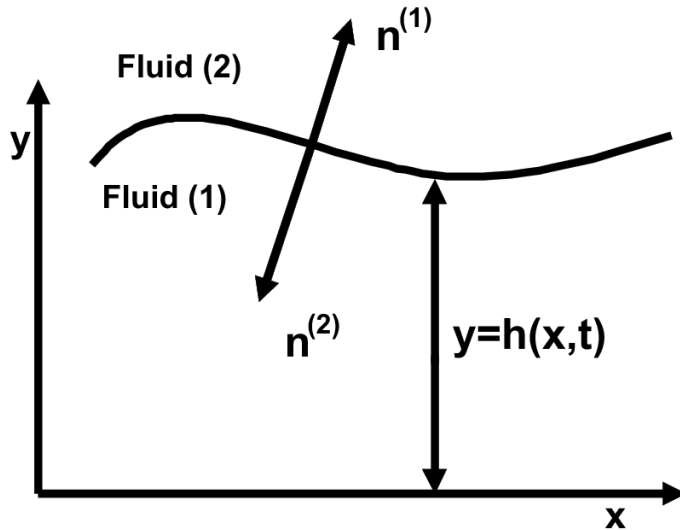


Figure 6.2: Conditions at a free surface formed by an interface between two fluids

cles on the surface always remain part of the free surface, therefore we must have

$$\frac{DF}{Dt} = \frac{\partial F}{\partial t} + u_j \frac{\partial F}{\partial x_j} = 0, \quad (6.6)$$

and this is the kinematic boundary condition. For time dependent problems, such as filling of the cavity or mold with a viscous fluid, equation (6.6) provides an evolution equation for the free surface location. In case of time-independent problems (steady flows),  $\frac{\partial F}{\partial t} = 0$  and the kinematic boundary condition can be written as

$$u_j n_j = 0, \quad \text{or symbolically} \quad \mathbf{u} \cdot \mathbf{n} = 0, \quad (6.7)$$

where  $\mathbf{n}$  is the outward normal [Gartling 1994, pages. 276-279]. This condition implies that there is no flow through the free surface (but there can be flow tangential to it), in other words the free surface is a stream surface.

### 6.1.3.2 Simplification and assumptions

For many applications surface tension effects are negligible. Also, without loss of generality the ambient pressure may be set to zero. Thus, the appropriate boundary conditions in many cases correspond to a vanishing of the normal and tangential stresses on the free surface which read

$$\begin{aligned} \left( -p\mathbf{n} + \frac{1}{Re}\mathbf{n} \cdot \nabla \mathbf{u} \right) \cdot \mathbf{n} &= 0, \\ \left( -p\mathbf{n} + \frac{1}{Re}\mathbf{n} \cdot \nabla \mathbf{u} \right) \cdot \mathbf{t} &= 0. \end{aligned} \quad (6.8)$$

Both conditions in (6.8) together imply the dynamic boundary condition

$$-p\mathbf{n} + \frac{1}{Re}\mathbf{n} \cdot \nabla \mathbf{u} = 0, \quad (6.9)$$

to be imposed on  $\Gamma_2 \cup \Gamma_7$ .

### 6.1.3.3 The free surface problem

To sum up, the free surface problem can be formally stated as follows: If  $Re$  denotes the Reynolds number of the flow, given the body forces  $\mathbf{f}$ , and the function  $u_n$ . Find a domain  $\Omega$ , the fluid velocity  $\mathbf{u}$ , and pressure  $p$  such that:

$$\left\{ \begin{array}{l} -\frac{1}{Re}\Delta \mathbf{u} + \mathbf{u} \cdot \nabla \mathbf{u} + \nabla p = \mathbf{f} \text{ in } \Omega, \alpha = \frac{1}{Re} > 0, \\ \operatorname{div} \mathbf{u} = 0 \text{ in } \Omega, \\ \mathbf{u} \cdot \mathbf{n} = u_n \text{ and } \mathbf{u} \cdot \mathbf{t} = 0 \text{ on } \Gamma_5, \\ -p + \frac{1}{Re}\mathbf{n} \cdot \nabla \mathbf{u} \cdot \mathbf{n} = 0, \frac{1}{Re}\mathbf{n} \cdot \nabla \mathbf{u} \cdot \mathbf{t} = 0 \text{ on } (\Gamma_9), \\ \mathbf{u} \cdot \mathbf{n} = 0, \frac{1}{Re}\mathbf{n} \cdot \nabla \mathbf{u} \cdot \mathbf{t} = 0 \text{ on } \Gamma_1, \Gamma_3, \Gamma_8, \Gamma_{10}, \Gamma_{11}, \Gamma_{12}, \Gamma_6 \text{ and } \Gamma_4, \\ \mathbf{u} \cdot \mathbf{n} = 0, (-p\mathbf{n} + \frac{1}{Re}\mathbf{n} \cdot \nabla \mathbf{u}) = 0, \text{ on } \Gamma_2, \Gamma_7. \end{array} \right. \quad (6.10)$$

### 6.1.4 Solving the free surface problem

Free surface problems have in common the difficulty that the geometry (here the domain  $\Omega$ ) has to be determined simultaneously with the solution  $\mathbf{u}, p$  of the state problem, which implies that a numerical solution has to be done iteratively [Kärkkäinen 1999]. Several techniques have been developed for the solution of free surface flow problems. These techniques are roughly classified

by [Wei 1996, et al] as Eulerian, Lagrangian or mixed Eulerian-Lagrangian.

In Eulerian-like (volume-tracking) approaches, the mesh remains stationary or moves in a predetermined manner, the free surface is not explicitly tracked, so it is reconstructed from other field properties such as the fluid fractions, as the fluid moves in/out of the computational flow domain. It can handle large displacements without loss of accuracy, but it is rather difficult to impose the free boundary conditions, since a sharp definition is lacking, e.g., see [Kawahara 1984]. Methods that fall in this category include, the level set method and volume of fluid method (see e.g., [Losasso 2006] and the references there in).

In Lagrangian-like (surface-tracking) approaches, the mesh is configured to conform to the shape of the free surface and, thus, it adapts continually to it. The free surface is a discontinuity and we explicitly track its evolution as an  $(n - 1)$  dimensional entity in an  $n$ -dimensional space. No modelling is necessary to define the free surface or its effects on the flow field. The grid points move with the local fluid particles, so the free surface is sharply defined. However, mesh refinement or remeshing is usually necessary for large deformations, e.g., see [Kawahara 1987].

Solution strategies that fall into the second category described above are of particular interest in this work, since we solve the optimization problem for which system (6.10) takes the role of the PDE constraint in a similar way. These strategies include trial methods, total linearization methods (continuous or discrete)[Cuvelier 1990], and shape optimization methods [Haslinger 2003].

The trial method assigns a shape to the free boundary and the PDE is solved for this shape after one of the boundary conditions on the free boundary is disregarded. Next, a new free boundary-shape is computed that satisfies as closely as possible the boundary condition that was relaxed. This procedure is repeated until convergence is attained. We decided to use the pseudo-transient approach, which is a trial method. The main advantage of this approach is that there is no explicit parametrization of the shape of the free boundary using, e.g., splines, but instead the boundary nodes can move freely. Moreover, this method converges linearly [Cuvelier 1990](equivalent to the rate of convergence of a shape optimization method, which requires calculation of shape derivatives which is really only feasible for fairly simple systems).

### 6.1.5 Pseudo-transient approach

The zero stress conditions (6.9) encountered for the zero surface tension case are precisely the conditions that are enforced by the “natural” boundary conditions arising from the Galerkin finite element form of the momentum equations. With these conditions automatically enforced, it remains to find a method for locating the position of the free surface.

In two dimensions examples include ([VanLohuizen 1996], [Jenny ], [Peterson 1999]) which make use of a kinematic boundary condition to drive the motion of the free surface. This ef-

fectively says that the instantaneous normal velocity of the free surface is equal to the normal component of the fluid velocity at the free surface at all times, i.e., if the free surface is represented by a curve  $x(s)$  parameterized by arc length  $s$ , the kinematic boundary condition can be expressed as

$$\mathbf{n} \cdot \left( \frac{d\mathbf{x}}{dt} - \mathbf{u} \right) = 0, \text{ on free surface,} \quad (6.11)$$

where  $\mathbf{x}$  and  $\mathbf{u}$  denote the position of the free/moving boundary and the velocity at this boundary respectively, and  $t$  denotes the pseudo time. For a converged solution of the free surface,  $\frac{d\mathbf{x}}{dt} = 0$  and (6.11) reduces to (6.7). To set the method described above into context, algorithm 4 is included illustrating the scheme employed in this work.

---

**Algorithm 4** Free surface flow solution algorithm

---

1. Set the initial grid  $\Omega_0$  and free surface position  $\Gamma_0$ .
2. Solve the Navier-Stokes equations

$$\begin{cases} -\frac{1}{Re}\Delta\mathbf{u}^k + \mathbf{u}^k \cdot \nabla \mathbf{u}^k + \nabla p^k = \mathbf{f} & \text{in } \Omega_k, \alpha = \frac{1}{Re} > 0 \\ \operatorname{div} \mathbf{u}^k = 0 & \text{in } \Omega_k, \\ \mathbf{u}^k \cdot \mathbf{n} = u_n \text{ and } \mathbf{u}^k \cdot \mathbf{t} = 0 & \text{on } \Gamma_5^k, \\ -p^k + \frac{1}{Re}\mathbf{n} \cdot \nabla \mathbf{u}^k \cdot \mathbf{n} = 0, \quad \frac{1}{Re}\mathbf{n} \cdot \nabla \mathbf{u}^k \cdot \mathbf{t} = 0 & \text{on } \Gamma_9^k, \\ \mathbf{u}^k \cdot \mathbf{n} = 0, \quad \frac{1}{Re}\mathbf{n} \cdot \nabla \mathbf{u}^k \cdot \mathbf{t} = 0 & \text{on } \Gamma_1^k, \Gamma_3^k, \Gamma_8^k, \Gamma_{10}^k, \Gamma_{11}^k, \Gamma_{12}^k, \Gamma_6^k \text{ and } \Gamma_4^k, \\ (-p^k\mathbf{n} + \frac{1}{Re}\mathbf{n} \cdot \nabla \mathbf{u}^k) = 0, & \text{on } \Gamma_2^k, \Gamma_7^k, \end{cases} \quad (6.12)$$

for the current geometry to compute the velocity field  $(u^k, v^k)$  and pressure  $p^k$  on this geometry.

3. Compute the new geometry  $(\Omega_{k+1})$  by updating the coordinates at the free surface with aid of (6.11) using  $(u^k, v^k)$ , and regenerating the mesh such that

$$(x_1^{k+1}, x_2^{k+1}) = (x_1^k, x_2^k) + \Delta t(\mathbf{u}^k \cdot \mathbf{n})(n_{x_1}, n_{x_2}), \text{ where } \Delta t \text{ is the step size.} \quad (6.13)$$

4. If free surface is moving, go to 2.
- 

If we reach a steady state in algorithm 4, then the free surface will stop moving and we can halt, i.e., we are converged. This algorithm is called the kinematic update scheme because of its use of the kinematic condition for updating the surface geometry. Since we are using the forward Euler time stepping algorithm, we must use a small step size  $\Delta t$  to ensure stability of the algorithm [VanLohuizen 1996]. For step 3, we need to define a local normal direction for a free surface node to move along. This should work, even in the absence of surface tension. But it may be more unstable since the surface tension tends to suppress oscillations. In equation (6.13), the coordinates  $(x_1, x_2)$  are defined on the free surface, thus we need to cater for the interior node

movements to avoid mesh distortions.

### 6.1.5.1 The interior and boundary mesh updates

The interior mesh can be updated by solving a Poisson problem in the interior of the domain using boundary vertex displacements as boundary conditions. The choice of the boundary conditions for the displacement field  $\Theta$  is dictated by the physics of the problem. In Figure 1.1, we need the fluid to slip freely on walls  $\Gamma_1, \Gamma_{12}, \Gamma_4$ , and  $\Gamma_6$ . In fact, if we are to impose the no-slip boundary conditions on  $\Gamma_4$  and  $\Gamma_6$ , then a singularity would result at contact points where the boundaries  $\Gamma_2$  and  $\Gamma_7$ , meet the boundaries  $\Gamma_4$  and  $\Gamma_6$  respectively. The same reasoning holds at intersection points where  $\Gamma_2$  and  $\Gamma_7$ , meet the boundaries  $\Gamma_1$  and  $\Gamma_{12}$  respectively. Therefore the choice of the free-slip boundary condition on  $\Gamma_1, \Gamma_{12}, \Gamma_4$ , and  $\Gamma_6$  supports itself. On boundaries,  $\Gamma_3, \Gamma_8, \Gamma_9, \Gamma_{10}$ , and  $\Gamma_{11}$ , we don't want the mesh to move, and hence these boundaries are fixed. Likewise on  $\Gamma_2$  and  $\Gamma_7$ , the mesh moves with the normal component of the fluid velocity, in the direction of the unit outward normal vector to these boundaries. This translates into solving the following PDE for the interior and boundary mesh updates:

$$\Delta\Theta = 0, \text{ in } \Omega, \quad (6.14)$$

$$\Theta \cdot \mathbf{n} = 0, \text{ and } \left( \frac{\partial \Theta}{\partial \mathbf{n}} \right) \cdot \mathbf{t} = 0, \text{ on } \Gamma_1, \Gamma_4, \Gamma_6, \Gamma_{12}, \quad (6.15)$$

$$\Theta = 0, \text{ on } \Gamma_3, \Gamma_5, \Gamma_8, \Gamma_9, \Gamma_{10}, \Gamma_{11}, \quad (6.16)$$

$$\Theta = (\mathbf{u} \cdot \mathbf{n})\mathbf{n}, \text{ on } \Gamma_2, \Gamma_7, \quad (6.17)$$

where  $\Theta$  is a globally defined deformation vector field. The mesh update at the  $k^{th}$  time step is now given by

$$(x_1^{k+1}, x_2^{k+1}) = (x_1^k, x_2^k) + \Delta t \Theta^k, \quad (6.18)$$

where  $(x_1, x_2)$  in (6.18) are global node locations. This approach can be interpreted as an Arbitrary -Lagrangian-Eulerian method [Li ]. This is the case since on the free boundary, we have a Lagrangian-type description, on fixed boundaries, an Eulerian type description and in the interior of the domain, an arbitrary description of the motion. The governing equations (6.12) and (6.14-6.17) are solved using the fast development environment Freefem++ [Hecht b]. This means that the code uses a finite element method based on the weak formulation of the problem. The numerical formulation of the equations governing the flow and the motion of the interface will be presented in the following subsection.

### 6.1.6 Numerical solution of the free surface problem

In order to obtain the numerical solution to the free surface problem (6.10), it suffices to explain how systems (6.12) and (6.14-6.17) for the mesh updates can be solved. The numerical treatment of system of the form (6.12) has been covered in Chapter 4. Therefore the explanation will not be exhaustive, and where necessary we shall refer to that chapter to avoid repetition. The numerical treatment proceeds by translating the strong formulations of the governing equations (6.12) and (6.14 - 6.17) into their respective weak formulations, which we discuss in subsubsection 6.1.6.1. Then, the discrete approximation to the continuous spaces is introduced, giving rise to the finite element method which is discussed in subsubsection 6.1.6.3.

#### 6.1.6.1 Weak formulation

To begin with, we introduce the following solution spaces

$$\begin{aligned}\mathbf{H}_g^1(\Omega) &= \{\mathbf{v} \in [H^1(\Omega)]^2 \mid \mathbf{v} = \mathbf{g} \text{ on } \Gamma_5, \mathbf{v} \cdot \mathbf{n} = 0 \text{ on } \Gamma^*\}, \\ \mathbf{W}_g(\Omega) &= \{\mathbf{v} \in [H^1(\Omega)]^2 \mid \mathbf{v} = \mathbf{g} \text{ on } \Gamma \setminus \Gamma^{**}, \mathbf{v} \cdot \mathbf{n} = \mathbf{0} \text{ on } \Gamma^{**}\},\end{aligned}\quad (6.19)$$

and test spaces:

$$\begin{aligned}\mathbf{H}_0^1(\Omega) &= \{\mathbf{v} \in [H^1(\Omega)]^2 \mid \mathbf{v} = \mathbf{0} \text{ on } \Gamma_5, \mathbf{v} \cdot \mathbf{n} = \mathbf{0} \text{ on } \Gamma^*\}, \\ \mathbf{W}_0(\Omega) &= \{\mathbf{v} \in [H^1(\Omega)]^2 \mid \mathbf{v} = \mathbf{0} \text{ on } \Gamma \setminus \Gamma^{**}, \mathbf{v} \cdot \mathbf{n} = \mathbf{0} \text{ on } \Gamma^{**}\},\end{aligned}\quad (6.20)$$

where

$$\Gamma^* = \Gamma_1 \cup \Gamma_3 \cup \Gamma_8 \cup \Gamma_{10} \cup \Gamma_{11} \cup \Gamma_{12} \cup \Gamma_6 \cup \Gamma_4,$$

$$\Gamma^{**} = \Gamma_1 \cup \Gamma_4 \cup \Gamma_6 \cup \Gamma_{12}.$$

The weak formulation of equation (6.12) then reads:

Given  $\mathbf{f} \in \mathbf{L}^2(\Omega)$ ,  $\mathbf{g} \in \mathbf{H}^{\frac{1}{2}}(\Gamma_5)$ , find  $(\mathbf{u}, p) \in \mathbf{H}_g^1(\Omega)(\Omega) \times L^2(\Omega)$  such that for all  $(\psi, \xi) \in \mathbf{H}_0^1(\Omega) \times L^2(\Omega)$

$$\begin{cases} \frac{1}{Re} \int_{\Omega} \nabla \mathbf{u} : \nabla \psi \, dx + \int_{\Omega} (\mathbf{u} \cdot \nabla) \mathbf{u} \psi \, dx - \int_{\Omega} p \operatorname{div} \psi \, dx = \int_{\Omega} \mathbf{f} \psi \, dx, \\ \int_{\Omega} \operatorname{div} \mathbf{u} \xi \, dx = 0, \end{cases} \quad (6.21)$$

and that of (6.14 - 6.17) reads:

Given  $\mathbf{g} \in \mathbf{H}^{\frac{1}{2}}(\Gamma \setminus \Gamma^{**})$ , find  $\Theta \in \mathbf{W}_g(\Omega)$  such that for all  $\psi \in \mathbf{W}_0(\Omega)$

$$\begin{cases} \int_{\Omega} \nabla \Theta \nabla \psi \, dx = 0, \end{cases} \quad (6.22)$$

where  $\psi, \xi$  are test functions.

### 6.1.6.2 Regularization

It is not easy to numerically construct test functions from the function spaces  $\mathbf{H}_0^1(\Omega)$  and  $\mathbf{W}_0(\Omega)$  above because of the constraints  $\mathbf{v} \cdot \mathbf{n} = 0$  on  $\Gamma^*$ , and  $\mathbf{v} \cdot \mathbf{n} = \mathbf{0}$  on  $\Gamma^{**}$  respectively. If the boundaries  $\Gamma_1$  and  $\Gamma_{12}$  were vertical, then implementation would entail fixing the horizontal component of velocity to zero on vertical boundaries, e.g.,  $\Gamma^{**}$ , and the vertical component of velocity to zero on horizontal boundaries, e.g.,  $\Gamma_3$  and  $\Gamma_{11}$ . However, since the boundaries  $\Gamma_1$  and  $\Gamma_{12}$  are slanting, the approach just explained does not work, and therefore one needs to find another alternative. Imposing the constraint  $\mathbf{v} \cdot \mathbf{n}$  in a strong form seems not to be very practical, since this involves both local co-ordinate transformations, and approximation of the normal at the corners. One possible way to overcome this difficulty is to relax the conditions  $\mathbf{u} \cdot \mathbf{n} = 0$ , on  $\Gamma^*$ , and  $\Theta \cdot \mathbf{n} = 0$ , on  $\Gamma^{**}$ , to the Robin type conditions:

$$\begin{aligned} \varepsilon \left( p\mathbf{n} - \frac{1}{Re} \mathbf{n} \cdot \nabla \mathbf{u} \right) \cdot \mathbf{n} + \mathbf{u} \cdot \mathbf{n} &= 0 \text{ on } \Gamma^*, \\ -\varepsilon \left( \frac{\partial \Theta}{\partial \mathbf{n}} \right) \cdot \mathbf{n} + \Theta \cdot \mathbf{n} &= 0 \text{ on } \Gamma^{**}, \end{aligned} \quad (6.23)$$

where  $\varepsilon$  is a small parameter to be chosen. Under this development, we now seek functions from the functional spaces

$$\begin{aligned} \bar{\mathbf{H}}_0^1(\Omega) &= \{ \mathbf{v} \in [H^1(\Omega)]^2 \mid \mathbf{v} = \mathbf{0} \text{ on } \Gamma_5 \}, \\ \bar{\mathbf{W}}_0(\Omega) &= \{ \mathbf{v} \in [H^1(\Omega)]^2 \mid \mathbf{v} = \mathbf{0} \text{ on } \Gamma \setminus \Gamma^{**} \}. \end{aligned} \quad (6.24)$$

The new weak formulation of (6.21) then reads as follows:

Find  $(\mathbf{u}, p) \in \mathbf{H}_g^1(\Omega) \times L^2(\Omega)$  such that for all  $(\psi, \xi) \in \bar{\mathbf{H}}_0^1(\Omega) \times L^2(\Omega)$

$$\begin{cases} \int_{\Omega} \left( \frac{1}{Re} \nabla \mathbf{u} : \nabla \psi + (\mathbf{u} \cdot \nabla) \mathbf{u} \psi - p \operatorname{div} \psi \right) dx - \int_{\Gamma^*} \frac{1}{\varepsilon} (\mathbf{u} \cdot \mathbf{n}) (\psi \cdot \mathbf{n}) ds = \int_{\Omega} \mathbf{f} \psi dx, \\ \int_{\Omega} \operatorname{div} \mathbf{u} \xi dx = 0. \end{cases} \quad (6.25)$$

Similarly that of (6.22) reads:

Find  $\Theta \in \mathbf{W}_g(\Omega)$  such that for all  $\psi \in \bar{\mathbf{W}}_0(\Omega)$

$$\int_{\Omega} \nabla \Theta \nabla \psi dx - \int_{\Gamma^{**}} \frac{1}{\varepsilon} (\Theta \cdot \mathbf{n}) (\psi \cdot \mathbf{n}) ds = 0. \quad (6.26)$$

The above approach is known as the penalty method for weak implementation of Dirichlet boundary conditions. Here  $\varepsilon$  takes the meaning of a regularizing parameter to be chosen appropriately. Other approaches such as the Nitsche method [Juntunen 2009], can as well be used.

**Remark 6.1.1.** For the existence and uniqueness of weak solutions to the free surface problem, an interested reader can consult [*Cuvelier 1986*] and the references given there in.

### 6.1.6.3 Finite element formulation

The velocities  $\mathbf{u}$  and  $\Theta$  are written in a  $P_2$  finite element space  $X_h$  with basis functions  $\{\phi_j, j = 1, \dots, N_{dof}\}$ , where  $N_{dof}$  is the degree of freedom. To avoid numerical instability, the pressure is described in a  $P_1$  finite element space  $M_h$  using basis functions  $\{w_k, k = 1, \dots, K_{dof}\}$  where  $K_{dof}$  is the degree of freedom (see the definition of  $P_1$  and  $P_2$  elements space in previous chapter, and also in the appendix.). The fields  $u_i$  (resp.  $\Theta_i$ ) and  $p$  are then defined in the finite element domain  $X_h$  and  $M_h$  by:

$$\begin{aligned} u_i &= \sum_{j=1}^{N_{dof}} u_i[j] \phi_j, \\ p &= \sum_{k=1}^{K_{dof}} p_k w_k. \end{aligned} \tag{6.27}$$

where  $u_i[j]$  and  $p_k$  are respectively, the value of  $u_i$  and  $p$  at the nodes  $j$  and  $k$ . Using an array representation such as

$$\begin{aligned} \mathbf{u} &= \begin{bmatrix} u_1[j = \{1, \dots, N_{dof}\}] \\ u_2[j = \{1, \dots, N_{dof}\}] \end{bmatrix}, \quad p = p[k = \{1, \dots, K_{dof}\}], \\ \Theta &= \begin{bmatrix} \theta_1[j = \{1, \dots, N_{dof}\}] \\ \theta_2[j = \{1, \dots, N_{dof}\}] \end{bmatrix}, \end{aligned} \tag{6.28}$$

we can write equations (6.25-6.26) as :

$$\begin{pmatrix} A + C(\mathbf{u}) & -B^T \\ B & 0 \end{pmatrix} \begin{pmatrix} \mathbf{u} \\ p \end{pmatrix} = \begin{pmatrix} \mathbf{f} \\ 0 \end{pmatrix}, \tag{6.29}$$

$$L\Theta = \mathbf{g}. \tag{6.30}$$

The matrices  $A, C, B, L$  stand for the linear operators defined in (6.25-6.26). See the appendix 7.1 for details on component wise splitting of the system in (6.29). As already noted in Chapter 4, the algebraic system (6.29) is nonlinear and typically very large. Therefore iterative techniques must be used. We chose to use the Picard iteration, where the velocity computed from the preceding iteration is substituted into the convective term, (see algorithm 3 in Chapter 4). Due to the choice of the approximation basis, the discrete linearized system is well posed and solvable, (see subsubsection 4.2.4.2). Finally the discrete linearized form of algebraic system (6.29), and the

system (6.30) can be solved either using iterative techniques such as Krylov-subspace methods for example, the GMRES method or using a sparse direct solvers. We chose to use the later because of the robustness of the code (Freefem++) in solving large sparse linear systems. We used in particular, a multi-frontal Gauss LU factorization [Davis 1999] implemented in the package UMFPACK.

#### 6.1.6.4 Numerical result

The equations are solved using FreeFem++, a free-liscence software developed at INRIA. This is a two-dimensional finite element solver, coupled to an anisotropic unstructured mesh generator that can automatically refine the mesh where solutions have large gradients. We set the body force  $\mathbf{f} = (-1, 0)$ , the inflow speed to  $u_{in} = (-0.56, 0)$ , the penalty  $\varepsilon$  to  $10^3$ , and Reynolds number  $Re = 50$ . In Figure (6.3 (a)), a geometry drawn to scale is shown and in Figure (6.3 (b)), a

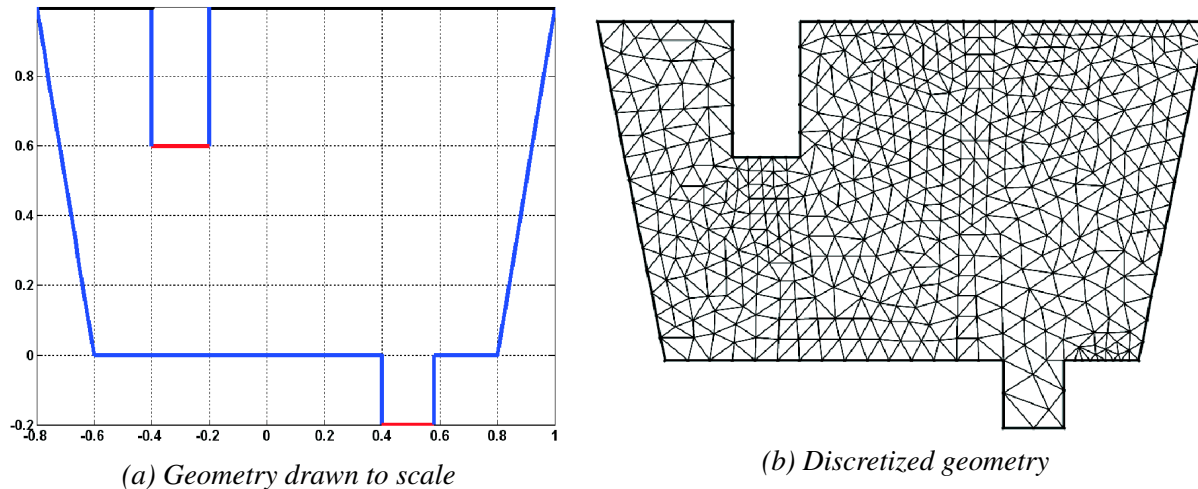


Figure 6.3: Computational geometry

discretized geometry is displayed. The triangular elements are generated by the bi-dimensional anisotropic mesh generator. The flow equations are solved on this discretized geometry and the resulting flow field patterns obtained at subsequent steps until convergence are displayed in Figures (6.4-6.5). We observe that initially the flow field does not satisfy the kinematic boundary conditions. One can quickly see this by looking at the direction of the velocity field on  $\Gamma_2 \cup \Gamma_7$ . We continue to run the algorithm until the  $L^2$  norm of the displacement field  $\Theta$  is less than  $10^{-3}$  and we stop. This stopping criterion is met after 17 iterations. The corresponding geometry and flow solving the free surface problem are depicted in Figure 6.5 (d).

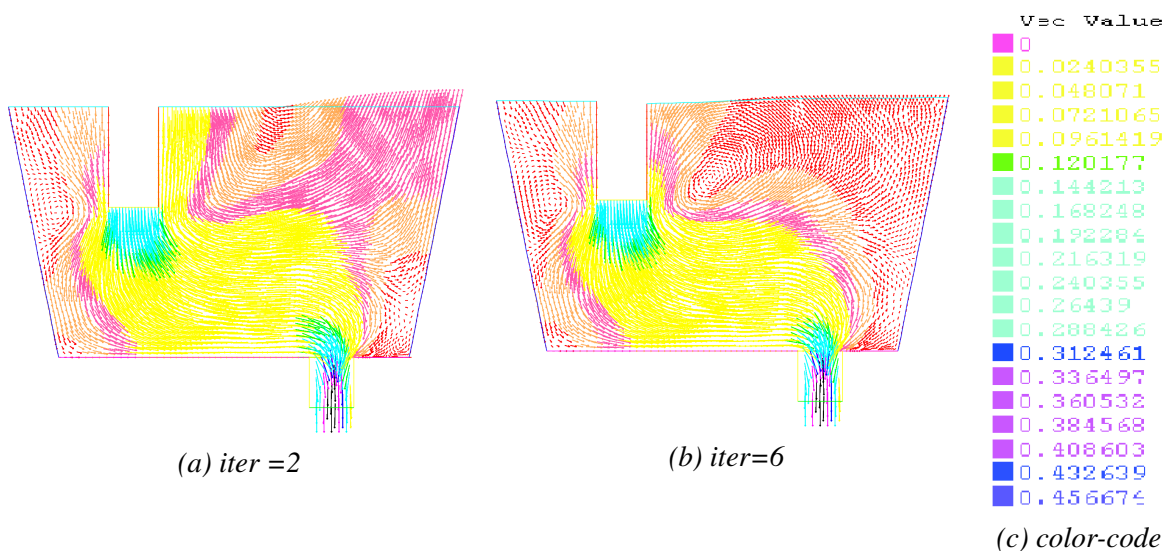


Figure 6.4: Snapshots of velocity field at different iteration numbers

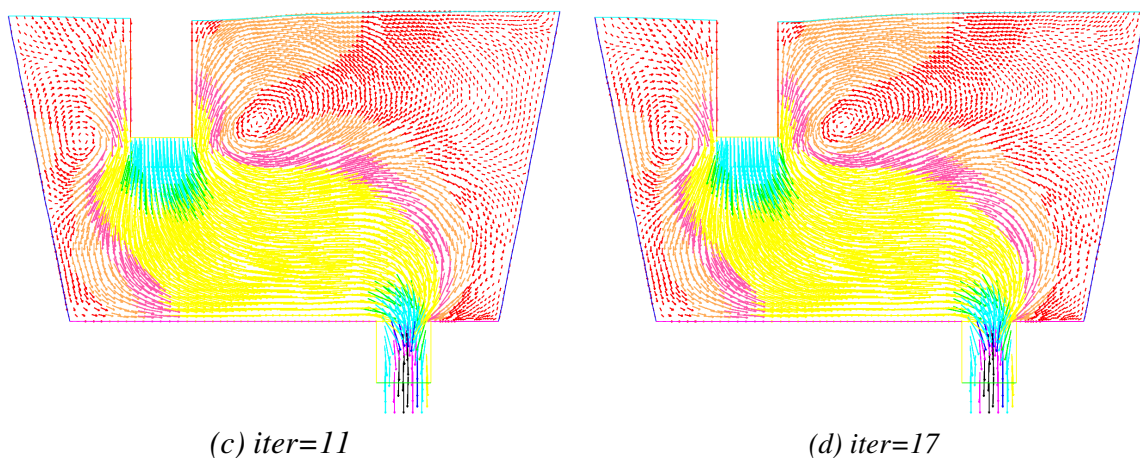


Figure 6.5: Snapshots of velocity field at different iteration numbers

### 6.1.6.5 Conclusion

A pseudo-transient approach for the free surface flow has been presented. For given data, and boundary conditions, we obtained the numerical solution of the free surface problem.

## 6.2 Optimization problem

In this section, our objective is to find a domain that solves the free surface problem (6.10) and at the same time minimizes the 3 cost functionals introduced in Chapter 1. A subset of the boundary of the domain  $\Omega$ , which we denote by  $\Gamma_{opt}$  is taken as the control boundary. Therefore, we have a class of optimal control problems in which (6.10) represents a PDE constraint with  $\Gamma_{opt}$  as the control variable. Such an optimization problem has been treated for the Bernoulli problem in [Toivanen 2008] and has not been considered previously for the free surface flows governed by the Navier-Stokes equations. Furthermore in [Toivanen 2008], a sensitivity analysis was performed on a discretized Bernoulli problem using an automatic differentiation technique. However, as the name of the technique reads, it is like a black box to the user and therefore does not aid to the better understanding of the problem at hand. In this section, we carry out the sensitivity analysis on the continuous formulation (6.10) using the techniques introduced in Chapter 3. The optimization problem can formally be stated as follows:

Find the shape of  $\Gamma_{opt}$  which minimizes the cost functionals

$$\min_{\Omega \in \mathcal{U}_{ad}} J_i(\mathbf{u}, \Omega), \quad i = 1, \dots, 3 \quad (6.31)$$

over a class of admissible domains  $\mathcal{U}_{ad}$  (to be specified later) while satisfying the free surface problem (6.10) which we rewrite below:

$$\left\{ \begin{array}{l} -\alpha \Delta \mathbf{u} + (\mathbf{u} \cdot \nabla) \mathbf{u} + \nabla p = \mathbf{f} \text{ in } \Omega, \quad \alpha = \frac{1}{Re} > 0, \\ \operatorname{div} \mathbf{u} = 0 \text{ in } \Omega, \\ \mathbf{u} \cdot \mathbf{n} = u_n \text{ and } \mathbf{u} \cdot \mathbf{t} = 0 \text{ on } \Gamma_5, \\ -p + \alpha \mathbf{n} \cdot \nabla \mathbf{u} \cdot \mathbf{n} = 0, \quad \frac{1}{Re} \mathbf{n} \cdot \nabla \mathbf{u} \cdot \mathbf{t} = 0 \text{ on } (\Gamma_9), \\ \mathbf{u} \cdot \mathbf{n} = 0, \quad \alpha \mathbf{n} \cdot \nabla \mathbf{u} \cdot \mathbf{t} = 0 \text{ on } \Gamma_1, \Gamma_3, \Gamma_8, \Gamma_{10}, \Gamma_{11}, \Gamma_{12}, \Gamma_6 \text{ and } \Gamma_4, \\ \mathbf{u} \cdot \mathbf{n} = 0, \quad (-p \mathbf{n} + \alpha \mathbf{n} \cdot \nabla \mathbf{u}) = 0, \text{ on } \Gamma_2, \Gamma_7. \end{array} \right. \quad (6.32)$$

A possibility to realize numerically the optimization problem (6.31-6.32) is to discard one of the boundary conditions on  $\Gamma_2 \cup \Gamma_7$  and to append it to the cost functional by using a penalty or augmented Lagrangian approach. Using this strategy, the state relation now becomes a classical boundary value problem with well-posed boundary data. Unfortunately, as noted in [Toivanen 2008],

this approach may lead to serious convergence problems. A further disadvantage with this approach is that, depending on the formulation, a locally optimal triplet  $(\Gamma_{opt}, \mathbf{u}, \Omega)$  might not represent a physical solution to (6.32)[Toivanen 2008]. For this reason we solve the optimization problem in its original setting, i.e., to find a solution to (6.32) first, and then proceed to the upper level represented by the minimization of the cost functional. The first part has been treated in the previous subsubsection (6.1.6.4), therefore we now proceed to the upper level.

### 6.2.1 Sensitivity analysis

Our goal in this subsection is to build gradient type methods in order to solve the shape optimization problem (6.31-6.32). Due to the the regularity requirements, the sensitivity analysis of the problem under consideration is not treated by the general theory presented in Chapter 3. In the following, we shall implicitly assume that the underlying functions are regular enough to ensure well posedness of all the operations. Furthermore, we shall adopt the notations, basic definitions and lemmas used in Chapter 3, in this subsection.

#### 6.2.1.1 The formal Lagrangian approach

In order to set up the optimality system for the optimization problem, the Lagrangian functional  $\mathcal{L}$  is set up as follows:

$$\begin{aligned} \mathcal{L}(\mathbf{u}, p, \mathbf{v}, q, \mu_1, \mu_2, \eta, \gamma, \Omega) = & \int_{\Omega} J_i(\mathbf{u}) dx - \int_{\Omega} \mathbf{v} \left( -\alpha \Delta \mathbf{u} + (\mathbf{u} \cdot \nabla) \mathbf{u} + \nabla p - \mathbf{f} \right) dx + \\ & \int_{\Omega} q \operatorname{div} \mathbf{u} dx - \int_{\Gamma_5} (\mathbf{u} - \mathbf{g}) \eta ds - \int_{\Gamma_9} (-p \mathbf{n} + \alpha \mathbf{n} \cdot \nabla \mathbf{u}) \gamma ds - \int_{\Gamma_*} (\mathbf{u} \cdot \mathbf{n}) \mu_1 ds \\ & - \int_{\Gamma_*} \alpha \frac{\partial \mathbf{u}}{\partial \mathbf{n}} \cdot \mathbf{t} \mu_2 ds, \end{aligned} \quad (6.33)$$

where  $\mathbf{v}, q, \eta, \gamma, \mu_1$  and  $\mu_2$  are Lagrange multipliers to enforce the momentum equation, the incompressibility condition, as well as the boundary conditions. Note that  $\mu_1$  and  $\mu_2$  are bounded scalar valued Lagrange multipliers.

The boundary conditions

$$\begin{cases} -p \mathbf{n} + \alpha \frac{\partial \mathbf{u}}{\partial \mathbf{n}} = 0, & \text{on free surface, } \Gamma_2 \cup \Gamma_7, \\ \mathbf{u} \cdot \mathbf{n} = 0, & \text{on free surface, } \Gamma_2 \cup \Gamma_7, \end{cases} \quad (6.34)$$

have not been enforced through the Lagrange functional. Therefore any variations  $\tilde{\mathbf{u}}$  and  $\tilde{p}$  in the states  $\mathbf{u}$  and  $p$  must be such that

$$\begin{cases} -\tilde{p}\mathbf{n} + \alpha \frac{\partial \tilde{\mathbf{u}}}{\partial \mathbf{n}} = 0, & \text{on free surface, } \Gamma_2 \cup \Gamma_7, \\ \tilde{\mathbf{u}} \cdot \mathbf{n} = 0, & \text{on free surface, } \Gamma_2 \cup \Gamma_7. \end{cases} \quad (6.35)$$

To obtain the optimality system for the optimization problem (6.31-6.32), we take the first variation of  $\mathcal{L}$  with respect to Lagrange multipliers, state variables  $\mathbf{u}, p$ , the domain  $\Omega$ , in directions  $(\tilde{\mathbf{v}}, \tilde{q}, \tilde{\eta}, \tilde{\gamma}, \tilde{\mu}_1, \tilde{\mu}_2)$ ,  $(\tilde{\mathbf{u}}, \tilde{p})$ , and  $\mathbf{h}$ , respectively to zero, i.e.,

$$\mathcal{L}_{\mathbf{v}, q, \eta, \gamma, \mu_1, \mu_2} \tilde{\mathbf{v}}, \tilde{q}, \tilde{\eta}, \tilde{\gamma}, \tilde{\mu}_1, \tilde{\mu}_2 = 0, \quad (6.36)$$

$$\mathcal{L}_{\mathbf{u}, p} \tilde{\mathbf{u}}, \tilde{p} = 0, \quad (6.37)$$

$$\mathcal{L}_\Omega \mathbf{h} = 0. \quad (6.38)$$

Equation (6.36) leads to the state problem (6.32), (6.37) to the adjoint problem that we derive in Theorem 6.2.1, and (6.38) leads to the optimality conditions, whose derivation is discussed in subsubsection 6.2.1.2.

**Theorem 6.2.1.** *Formally the adjoint equations associated to (6.32) are given by*

$$\begin{cases} -\alpha \Delta \mathbf{v} - \nabla \mathbf{v} \cdot \mathbf{u} + [\nabla \mathbf{u}]^t \cdot \mathbf{v} + \nabla q = J'_i(\mathbf{u}) & \text{in } \Omega, \\ \operatorname{div} \mathbf{v} = 0, & \text{in } \Omega, \\ \mathbf{v} \cdot \mathbf{n} = 0, \quad \mathbf{t} \cdot [q \cdot \mathbf{n} - (\mathbf{u} \cdot \mathbf{n})\mathbf{v} - \alpha \nabla \mathbf{v} \cdot \mathbf{n}] = 0 & \text{on } \Gamma_*, \\ \mathbf{v} = 0, & \text{on } \Gamma_5, \\ \mathbf{v} \cdot \mathbf{n} = 0, \quad [q \cdot \mathbf{n} - (\mathbf{u} \cdot \mathbf{n})\mathbf{v} - \alpha \nabla \mathbf{v} \cdot \mathbf{n}] = 0, & \text{on } \Gamma_f, \\ q \cdot \mathbf{n} - (\mathbf{u} \cdot \mathbf{n})\mathbf{v} - \alpha \nabla \mathbf{v} \cdot \mathbf{n} = 0, & \text{on } \Gamma_9. \end{cases} \quad (6.39)$$

*Proof.* (a) Setting the first variation of  $\mathcal{L}$  with respect to  $p$  in direction  $\tilde{p}$  to zero, i.e.,  $\mathcal{L}_p \tilde{p} = 0$ , leads to

$$\mathcal{L}_p \tilde{p} = - \int_{\Omega} \mathbf{v} \nabla \tilde{p} \, dx - \int_{\Gamma_9} (-\tilde{p} \cdot n) \gamma \, ds = 0.$$

Integrating by parts to remove where possible, derivatives from  $\tilde{p}$ , one obtains

$$\int_{\Omega} \operatorname{div} \mathbf{v} \tilde{p} \, dx - \int_{\Gamma} \mathbf{v} \tilde{p} \cdot \mathbf{n} \, ds - \int_{\Gamma_9} (-\tilde{p} \cdot n) \gamma \, ds = 0,$$

where  $\Gamma = \Gamma_2 \cup \Gamma_7 \cup \Gamma_* \cup \Gamma_9 \cup \Gamma_5$ . Choosing  $\tilde{p} \in C_0^\infty(\Omega)$ , we obtain

$$\int_{\Omega} \operatorname{div} \mathbf{v} \tilde{p} dx = 0. \quad (6.40)$$

Since  $C_0^\infty(\Omega)$  is dense in  $L^2(\Omega)$ , the relation (6.40) holds almost every where in  $\Omega$ . Hence

$$\operatorname{div} \mathbf{v} = 0, \text{ in } \Omega.$$

By similar arguments, we can show that

$$\begin{aligned} \mathbf{v} \cdot \mathbf{n} &= 0 \text{ on } \Gamma_* \cup \Gamma_5 \cup \Gamma_2 \cup \Gamma_7, \\ \gamma \cdot \mathbf{n} &= \mathbf{v} \cdot \mathbf{n} \text{ on } \Gamma_9. \end{aligned} \quad (6.41)$$

- (b) Setting the variation of  $\mathcal{L}$  with respect to the state  $\mathbf{u}$  in the direction  $\tilde{\mathbf{u}}$  equal to zero results in

$$\begin{aligned} \mathcal{L}_{\mathbf{u}} \tilde{\mathbf{u}} &= \int_{\Omega} J'_i(\mathbf{u}) \tilde{\mathbf{u}} dx - \int_{\Omega} \mathbf{v} \left( -\alpha \Delta \tilde{\mathbf{u}} + \nabla \mathbf{u} \cdot \tilde{\mathbf{u}} + \nabla \tilde{\mathbf{u}} \cdot \mathbf{u} \right) dx + \int_{\Omega} q \operatorname{div} \tilde{\mathbf{u}} dx \\ &\quad - \int_{\Gamma_5} \tilde{\mathbf{u}} \eta ds - \int_{\Gamma_9} \alpha \mathbf{n} \cdot \nabla \tilde{\mathbf{u}} \gamma ds - \int_{\Gamma_*} (\tilde{\mathbf{u}} \cdot \mathbf{n}) \mu_1 ds - \int_{\Gamma_*} (\alpha \mathbf{n} \cdot \nabla \tilde{\mathbf{u}} \cdot t) \mu_2 ds = 0, \end{aligned}$$

where  $\tilde{\mathbf{u}}$  denotes an arbitrary variation in the state variable  $\mathbf{u}$  satisfying (6.35). Integrating by parts to remove where possible, derivatives from  $\tilde{\mathbf{u}}$ , one obtains

$$\begin{aligned} &\int_{\Omega} \left( J'_i(\mathbf{u}) + \alpha \Delta \mathbf{v} + \nabla \mathbf{v} \cdot \mathbf{u} - [\nabla \mathbf{u}]^t \cdot \mathbf{v} - \nabla q \right) \tilde{\mathbf{u}} dx + \int_{\Gamma} (\alpha \nabla \tilde{\mathbf{u}} \cdot \mathbf{n} \mathbf{v} - \alpha \nabla \mathbf{v} \cdot \mathbf{n} \tilde{\mathbf{u}}) ds \\ &\quad + \int_{\Gamma} [\tilde{\mathbf{u}} q \cdot \mathbf{n} - (\mathbf{u} \cdot \mathbf{n})(\mathbf{v} \cdot \tilde{\mathbf{u}})] ds - \int_{\Gamma_5} \tilde{\mathbf{u}} \eta ds - \int_{\Gamma_9} \alpha \mathbf{n} \cdot \nabla \tilde{\mathbf{u}} \gamma ds - \int_{\Gamma_*} (\tilde{\mathbf{u}} \cdot \mathbf{n}) \mu_1 ds \\ &\quad - \int_{\Gamma_*} \alpha \frac{\partial \tilde{\mathbf{u}}}{\partial \mathbf{n}} \cdot \mathbf{t} \mu_2 ds = 0. \end{aligned}$$

- (i) Choosing  $\tilde{\mathbf{u}} \in C_0^\infty(\Omega)$ , and using density arguments as before leads to

$$-\alpha \Delta \mathbf{v} - \nabla \mathbf{v} \cdot \mathbf{u} + [\nabla \mathbf{u}]^t \cdot \mathbf{v} + \nabla q = J'_i(\mathbf{u}), \text{ in } \Omega. \quad (6.42)$$

Thus we remain with the expression,

$$\begin{aligned} &\int_{\Gamma} (\alpha \nabla \tilde{\mathbf{u}} \cdot \mathbf{n} \mathbf{v} - \alpha \nabla \mathbf{v} \cdot \mathbf{n} \tilde{\mathbf{u}}) ds + \int_{\Gamma} [\tilde{\mathbf{u}} q \cdot \mathbf{n} - (\mathbf{u} \cdot \mathbf{n})(\mathbf{v} \cdot \tilde{\mathbf{u}})] ds - \int_{\Gamma_5} \tilde{\mathbf{u}} \eta ds \\ &\quad - \int_{\Gamma_9} \alpha \mathbf{n} \cdot \nabla \tilde{\mathbf{u}} \gamma ds - \int_{\Gamma_*} (\tilde{\mathbf{u}} \cdot \mathbf{n}) \mu_1 ds - \int_{\Gamma_*} \alpha \frac{\partial \tilde{\mathbf{u}}}{\partial \mathbf{n}} \cdot \mathbf{t} \mu_2 ds = 0. \end{aligned} \quad (6.43)$$

- (ii) Choosing  $\tilde{\mathbf{u}} \in C^\infty(\Gamma)$ , we can find an extension  $\tilde{\mathbf{u}} \in C^\infty(\Omega)$  such that  $\tilde{\mathbf{u}}|_\Gamma = \tilde{\mathbf{u}}$ ,  $\tilde{\mathbf{u}}|_{\Gamma \setminus \Gamma_5} = 0$ , then we have that

$$\int_{\Gamma_5} (\alpha \nabla \tilde{\mathbf{u}} \cdot \mathbf{n} \mathbf{v} - \alpha \nabla \mathbf{v} \cdot \mathbf{n} \tilde{\mathbf{u}}) ds + \int_{\Gamma_5} [\tilde{\mathbf{u}} q \cdot \mathbf{n} - (\mathbf{u} \cdot \mathbf{n})(\mathbf{v} \cdot \tilde{\mathbf{u}})] ds - \int_{\Gamma_5} \tilde{\mathbf{u}} \eta ds = 0,$$

from which we obtain

$$\begin{aligned} \mathbf{v} &= 0, \quad \text{on } \Gamma_5, \\ \eta &= q \cdot \mathbf{n} - (\mathbf{u} \cdot \mathbf{n})\mathbf{v} - \alpha \nabla \mathbf{v} \cdot \mathbf{n} \quad \text{on } \Gamma_5. \end{aligned} \tag{6.44}$$

- (iii) Similarly choosing  $\tilde{\mathbf{u}} \in C^\infty(\Gamma)$ , we can find an extension  $\tilde{\mathbf{u}} \in C^\infty(\Omega)$  such that  $\tilde{\mathbf{u}}|_\Gamma = \tilde{\mathbf{u}}$ ,  $\tilde{\mathbf{u}}|_{\Gamma \setminus \Gamma_*} = 0$ , we have that

$$\begin{aligned} \int_{\Gamma_*} (\alpha \nabla \tilde{\mathbf{u}} \cdot \mathbf{n} \mathbf{v} - \alpha \nabla \mathbf{v} \cdot \mathbf{n} \tilde{\mathbf{u}}) ds + \int_{\Gamma_*} [\tilde{\mathbf{u}} q \cdot \mathbf{n} - (\mathbf{u} \cdot \mathbf{n})(\mathbf{v} \cdot \tilde{\mathbf{u}})] ds \\ - \int_{\Gamma_*} (\tilde{\mathbf{u}} \cdot \mathbf{n}) \mu_1 ds - \int_{\Gamma_*} \alpha \frac{\partial \tilde{\mathbf{u}}}{\partial \mathbf{n}} \cdot \mathbf{t} \mu_2 ds = 0. \end{aligned} \tag{6.45}$$

Re-arranging terms in (6.45) we obtain,

$$\begin{aligned} \int_{\Gamma_*} (\alpha \nabla \tilde{\mathbf{u}} \cdot \mathbf{n} \mathbf{v}) ds + \int_{\Gamma_*} [q \cdot \mathbf{n} - (\mathbf{u} \cdot \mathbf{n})\mathbf{v} - \alpha \nabla \mathbf{v} \cdot \mathbf{n}] \tilde{\mathbf{u}} ds \\ - \int_{\Gamma_*} \alpha \frac{\partial \tilde{\mathbf{u}}}{\partial \mathbf{n}} \cdot \mathbf{t} \mu_2 ds - \int_{\Gamma_*} (\tilde{\mathbf{u}} \cdot \mathbf{n}) \mu_1 ds = 0. \end{aligned} \tag{6.46}$$

Since  $\mu_1, \mu_2$  are scalar valued lagrange multipliers, we can again re-write the first and second terms in (6.46) in component form to obtain,

$$\begin{aligned} \int_{\Gamma_*} \left( \alpha \frac{\partial \tilde{\mathbf{u}}}{\partial \mathbf{n}} \cdot \mathbf{n} \right) \mathbf{v} \cdot \mathbf{n} + \left( \alpha \frac{\partial \tilde{\mathbf{u}}}{\partial \mathbf{n}} \cdot \mathbf{t} \right) \mathbf{v} \cdot \mathbf{t} ds + \int_{\Gamma_*} \mathbf{n} \cdot [q \cdot \mathbf{n} - (\mathbf{u} \cdot \mathbf{n})\mathbf{v} - \alpha \nabla \mathbf{v} \cdot \mathbf{n}] \tilde{\mathbf{u}} \cdot \mathbf{n} ds \\ + \int_{\Gamma_*} \mathbf{t} \cdot [q \cdot \mathbf{n} - (\mathbf{u} \cdot \mathbf{n})\mathbf{v} - \alpha \nabla \mathbf{v} \cdot \mathbf{n}] \tilde{\mathbf{u}} \cdot \mathbf{t} ds - \int_{\Gamma_*} \alpha \frac{\partial \tilde{\mathbf{u}}}{\partial \mathbf{n}} \cdot \mathbf{t} \mu_2 ds - \int_{\Gamma_*} (\tilde{\mathbf{u}} \cdot \mathbf{n}) \mu_1 ds = 0. \end{aligned}$$

- (iv) Now choosing variations  $\tilde{\mathbf{u}}$  on  $\Gamma_*$  such that  $\tilde{\mathbf{u}} \cdot \mathbf{n} = \tilde{\mathbf{u}} \cdot \mathbf{t} = 0$ ,  $\mathbf{t} \cdot \nabla \tilde{\mathbf{u}} \cdot \mathbf{n} = \mathbf{n} \cdot \nabla \tilde{\mathbf{u}} \cdot \mathbf{t} = 0$ ,  $\mathbf{n} \cdot \nabla \tilde{\mathbf{u}} \cdot \mathbf{n}$  arbitrary, we obtain

$$\mathbf{v} \cdot \mathbf{n} = 0, \quad \text{on } \Gamma_*.$$

Similarly, the following can be independently shown

$$\begin{aligned}\mu_2 &= \mathbf{v} \cdot \mathbf{t} \text{ on } \Gamma_*, \\ \mu_1 &= \mathbf{n} \cdot [q \cdot \mathbf{n} - (\mathbf{u} \cdot \mathbf{n})\mathbf{v} - \alpha \nabla \mathbf{v} \cdot \mathbf{n}] \text{ on } \Gamma_*, \\ \mathbf{t} \cdot [q \cdot \mathbf{n} - (\mathbf{u} \cdot \mathbf{n})\mathbf{v} - \alpha \nabla \mathbf{v} \cdot \mathbf{n}] &= 0 \text{ on } \Gamma_*.\end{aligned}\quad (6.47)$$

- (v) Choosing  $\tilde{\mathbf{u}} \in C^\infty(\Gamma)$ , we can find an extension  $\tilde{\mathbf{u}} \in C^\infty(\Omega)$  such that  $\tilde{\mathbf{u}}|_\Gamma = \tilde{\mathbf{u}}$ ,  $\tilde{\mathbf{u}}|_{\Gamma \setminus \Gamma_9} = 0$ , then we have that

$$\begin{aligned}\int_{\Gamma_9} (\alpha \nabla \tilde{\mathbf{u}} \cdot \mathbf{n} \mathbf{v} - \alpha \nabla \mathbf{v} \cdot \mathbf{n} \tilde{\mathbf{u}}) ds + \int_{\Gamma_9} [\tilde{\mathbf{u}} q \cdot \mathbf{n} - (\mathbf{u} \cdot \mathbf{n})(\mathbf{v} \cdot \tilde{\mathbf{u}})] ds \\ - \int_{\Gamma_9} \alpha \mathbf{n} \cdot \nabla \tilde{\mathbf{u}} \gamma ds = 0,\end{aligned}$$

from which we obtain

$$\begin{aligned}[q \cdot \mathbf{n} - (\mathbf{u} \cdot \mathbf{n})\mathbf{v} - \alpha \nabla \mathbf{v} \cdot \mathbf{n}] &= 0 \text{ on } \Gamma_9, \\ \mathbf{v} &= \gamma \text{ on } \Gamma_9.\end{aligned}\quad (6.48)$$

- (vi) Finally setting variations  $\tilde{\mathbf{u}}$  such that  $\tilde{\mathbf{u}} = 0$  on  $\Gamma \setminus \Gamma_f$ , where  $\Gamma_f \equiv \Gamma_2 \cup \Gamma_7$ , we obtain

$$\int_{\Gamma_f} \alpha \nabla \tilde{\mathbf{u}} \cdot \mathbf{n} \mathbf{v} ds - \int_{\Gamma_f} \tilde{\mathbf{u}} (-q \cdot \mathbf{n} + \alpha \nabla \mathbf{v} \cdot \mathbf{n}) ds = 0. \quad (6.49)$$

Using (6.35) and (6.41), the first integral in (6.49) vanishes and we obtain for any arbitrary variations satisfying (6.35) that

$$-q \cdot \mathbf{n} + \alpha \frac{\partial \mathbf{v}}{\partial \mathbf{n}} = 0, \text{ on } \Gamma_f. \quad (6.50)$$

Collecting all the assertions, we arrive at the adjoint system (6.39) where we note that  $(\mathbf{u} \cdot \mathbf{n}) = 0$  on  $\Gamma_f$ .  $\square$

**Note 6.2.1.** It is important to note that (6.31-6.32) is equivalent to the min-max problem [Pironneau 2001, pg.22].

$$\min_{\Omega \in \mathcal{U}_{ad}, \mathbf{u}, p} \left\{ \max_{\mathbf{v}, q, \eta, \gamma, \mu_1, \mu_2} \mathcal{L}(\mathbf{u}, p, \mathbf{v}, q, \mu_1, \mu_2, \eta, \gamma, \Omega) \right\}. \quad (6.51)$$

Further more, from the theory of min-max, the Eulerian derivative of  $\mathcal{L}$  in the direction of the deformation field  $\mathbf{h}$ , is equivalent to the Eulerian derivative of  $J_i(\mathbf{u}, \Omega)$  with respect to  $\Omega$  in the

direction  $\mathbf{h}$ , i.e.,

$$dJ_i(\Omega, \mathbf{u})\mathbf{h} = d\mathcal{L}(\mathbf{u}, p, \mathbf{v}, q, \mu_1, \mu_2, \eta, \gamma, \Omega)\mathbf{h}, \quad (6.52)$$

at the solution of the min-max problem (6.51).

Relation (6.52) constitute the optimality condition for the optimization problem. Its derivation is the major focus of what follows. Let us assume for now that  $\Gamma_{opt} \equiv \Gamma_5$ , where  $\mathbf{u} = \mathbf{g} = (0, u_n)$  on  $\Gamma_{opt}$ . In order to take into account the non-homogenous Dirichlet boundary conditions on  $\Gamma_{opt}$ , we use the change of variable  $\hat{\mathbf{u}} = \mathbf{u} - \hat{\mathbf{g}}$ , where the vectorial function  $\hat{\mathbf{g}}$  satisfies

$$\begin{cases} \operatorname{div} \hat{\mathbf{g}} = 0 & \text{in } \Omega, \\ \hat{\mathbf{g}} = \mathbf{g} & \text{on } \Gamma_5, \\ \hat{\mathbf{g}} = \mathbf{0} & \text{on } \Gamma \setminus \Gamma_5. \end{cases} \quad (6.53)$$

It is shown in [Girault 1986, Pg. 24] that such a  $\hat{\mathbf{g}}$  in (6.53) exists and is unique. Moreover in what follows, we shall assume that  $\hat{\mathbf{g}}$  is independent of the shape  $\Omega$ . Substituting  $\hat{\mathbf{u}}$  into (6.32) leads to the following system:

$$\begin{cases} -\alpha\Delta\hat{\mathbf{u}} + \nabla\hat{\mathbf{u}} \cdot \hat{\mathbf{u}} + \nabla\hat{\mathbf{u}} \cdot \hat{\mathbf{g}} + \nabla\hat{\mathbf{g}} \cdot \hat{\mathbf{u}} + \nabla p = \mathbf{F}, & \text{in } \Omega, \\ \operatorname{div} \hat{\mathbf{u}} = 0, & \text{in } \Omega, \\ \hat{\mathbf{u}} = 0, & \text{on } \Gamma_{opt}, \\ -p + \alpha\mathbf{n} \cdot \nabla\hat{\mathbf{u}} \cdot \mathbf{n} = 0, \quad \alpha\mathbf{n} \cdot \nabla\hat{\mathbf{u}} \cdot \mathbf{t} = 0, & \text{on } (\Gamma_9), \\ \hat{\mathbf{u}} \cdot \mathbf{n} = 0, \quad \alpha\mathbf{n} \cdot \nabla\hat{\mathbf{u}} \cdot \mathbf{t} = 0, & \text{on } \Gamma_*, \\ \hat{\mathbf{u}} \cdot \mathbf{n} = 0, \quad (-p\mathbf{n} + \alpha\mathbf{n} \cdot \nabla\hat{\mathbf{u}}) = 0, & \text{on } \Gamma_2, \Gamma_7, \end{cases} \quad (6.54)$$

where  $\mathbf{F} := \mathbf{f} + \alpha\Delta\hat{\mathbf{g}} - \nabla\hat{\mathbf{g}} \cdot \hat{\mathbf{g}}$ .

**Theorem 6.2.2.** *Let us assume that  $\Omega$  is sufficiently smooth. Further more assume that the material derivatives  $\dot{\mathbf{u}}$  and  $\dot{p}$  exist, then the shape derivatives  $\hat{\mathbf{u}}' = \dot{\mathbf{u}} - \nabla\hat{\mathbf{u}} \cdot \mathbf{h}$  and  $p' = \dot{p} - \nabla p \cdot \mathbf{h}$  exist by formal arguments, and they are characterized as the solution of the system*

$$\begin{cases} -\alpha\Delta\hat{\mathbf{u}}' + \nabla\hat{\mathbf{u}} \cdot \hat{\mathbf{u}}' + \nabla\hat{\mathbf{u}}' \cdot \hat{\mathbf{u}} + \nabla\hat{\mathbf{u}}' \cdot \hat{\mathbf{g}} + \nabla\hat{\mathbf{g}} \cdot \hat{\mathbf{u}}' + \nabla p' = 0 & \text{in } \Omega, \\ \operatorname{div} \hat{\mathbf{u}}' = 0 & \text{in } \Omega, \\ \hat{\mathbf{u}}' = -(\nabla\hat{\mathbf{u}} \cdot \mathbf{n})(\mathbf{h}, \mathbf{n}) & \text{on } \Gamma_{opt}, \\ -p + \alpha\mathbf{n} \cdot \nabla\hat{\mathbf{u}}' \cdot \mathbf{n} = 0, \quad \alpha\mathbf{n} \cdot \nabla\hat{\mathbf{u}}' \cdot \mathbf{t} = 0, & \text{on } (\Gamma_9), \\ \hat{\mathbf{u}}' \cdot \mathbf{n} = 0, \quad \alpha\mathbf{n} \cdot \nabla\hat{\mathbf{u}}' \cdot \mathbf{t} = 0, & \text{on } \Gamma_*, \\ \hat{\mathbf{u}}' \cdot \mathbf{n} = 0, \quad (-p'\mathbf{n} + \alpha\mathbf{n} \cdot \nabla\hat{\mathbf{u}}') = 0, & \text{on } \Gamma_2, \Gamma_7. \end{cases} \quad (6.55)$$

Here  $\mathbf{h}$  denotes a velocity field which is considered zero on  $\Gamma \setminus \Gamma_{opt}$ .

*Proof.* Since  $\Omega$  is assumed to be sufficiently smooth,  $\Omega_t$  has the same regularity as  $\Omega$  for any  $t \in (0, \epsilon)$ . Then  $\hat{\mathbf{u}}$  satisfies

$$\int_{\Omega} \alpha \nabla \hat{\mathbf{u}} : \nabla \varphi + \nabla \hat{\mathbf{u}} \cdot \hat{\mathbf{u}} \cdot \varphi + \nabla \hat{\mathbf{u}} \cdot \hat{\mathbf{g}} \cdot \varphi + \nabla \hat{\mathbf{g}} \cdot \hat{\mathbf{u}} \cdot \varphi + \nabla p \varphi - \mathbf{F} \cdot \varphi = 0, \quad \text{for any } \varphi \in \mathcal{D}(\Omega, \mathbb{R}^2).$$

For  $t$  sufficiently small,  $\varphi$  belongs to  $\mathcal{D}(\Omega_t, \mathbb{R}^2)$  [Boisgérault 1993], and any solution  $(\hat{\mathbf{u}}_t, p_t)$  of the Navier-Stokes equations in  $\Omega_t$  satisfies:

$$\int_{\Omega_t} \alpha \nabla \hat{\mathbf{u}}_t : \nabla \varphi + \nabla \hat{\mathbf{u}}_t \cdot \hat{\mathbf{u}}_t \cdot \varphi + \nabla \hat{\mathbf{u}}_t \cdot \hat{\mathbf{g}} \cdot \varphi + \nabla \hat{\mathbf{g}} \cdot \hat{\mathbf{u}}_t \cdot \varphi + \nabla p_t \varphi - \mathbf{F} \cdot \varphi = 0. \quad (6.56)$$

Taking the derivative of (6.56) with respect to  $t$  at  $t = 0$ , and using Lemma 3.2.1 (see Chapter 3), we obtain

$$\begin{cases} \int_{\Omega} \alpha \nabla \hat{\mathbf{u}}' : \nabla \varphi + \nabla \hat{\mathbf{u}} \cdot \hat{\mathbf{u}}' \cdot \varphi + \nabla \hat{\mathbf{u}}' \cdot \hat{\mathbf{u}} \cdot \varphi + \nabla \hat{\mathbf{u}}' \cdot \hat{\mathbf{g}} \cdot \varphi + \nabla \hat{\mathbf{g}} \cdot \hat{\mathbf{u}}' \cdot \varphi + \nabla p' \varphi \\ + \int_{\Gamma_{opt}} (\alpha \nabla \hat{\mathbf{u}} : \nabla \varphi + \nabla \hat{\mathbf{u}} \cdot \hat{\mathbf{u}} \cdot \varphi + \nabla \hat{\mathbf{u}} \cdot \hat{\mathbf{g}} \cdot \varphi + \nabla \hat{\mathbf{g}} \cdot \hat{\mathbf{u}} \cdot \varphi + \nabla p \varphi - F \cdot \varphi)(\mathbf{h}, \mathbf{n}) ds = 0. \end{cases}$$

Since  $\varphi$  has compact support, the boundary integrals vanish. Using integration by parts, we obtain

$$\int_{\Omega} (-\alpha \Delta \hat{\mathbf{u}}' + \nabla \hat{\mathbf{u}} \cdot \hat{\mathbf{u}}' + \nabla \hat{\mathbf{u}}' \cdot \hat{\mathbf{u}} + \nabla \hat{\mathbf{u}}' \cdot \hat{\mathbf{g}} + \nabla \hat{\mathbf{g}} \cdot \hat{\mathbf{u}}' + \nabla p') \cdot \varphi = 0.$$

By density arguments, we obtain

$$-\alpha \Delta \hat{\mathbf{u}}' + \nabla \hat{\mathbf{u}} \cdot \hat{\mathbf{u}}' + \nabla \hat{\mathbf{u}}' \cdot \hat{\mathbf{u}} + \nabla \hat{\mathbf{u}}' \cdot \hat{\mathbf{g}} + \nabla \hat{\mathbf{g}} \cdot \hat{\mathbf{u}}' + \nabla p' = 0.$$

Since  $\hat{\mathbf{u}} = 0$  on  $\Gamma_{opt}$ , we have

$$\int_{\Gamma_{opt}} \hat{\mathbf{u}} \cdot \varphi \, ds = 0, \quad \text{for all } \varphi \in C^1(\overline{D}). \quad (6.57)$$

On  $\Gamma_{opt,t}$ , (6.57) becomes

$$\int_{\Gamma_{opt,t}} \hat{\mathbf{u}}_t \cdot \varphi \, ds_t = 0, \quad \text{for all } \varphi \in C^1(\overline{D}). \quad (6.58)$$

Taking the derivative of equation (6.58) with respect to  $t$  at  $t = 0$ , and using Lemma 3.2.1, we obtain

$$\int_{\Gamma_{opt}} \hat{\mathbf{u}}' \cdot \varphi + \varphi' \hat{\mathbf{u}} + \int_{\Gamma_{opt}} \left[ \frac{\partial}{\partial n} (\hat{\mathbf{u}} \varphi) + \kappa \hat{\mathbf{u}} \varphi \right] \mathbf{h} \cdot \mathbf{n} \, ds = 0, \quad (6.59)$$

where  $\kappa$  is the curvature of the boundary. If it is assumed in (6.59) that  $\frac{\partial \varphi}{\partial n} = 0$  on  $\Gamma_{opt}$ , and  $\varphi$  is

independent of the shape, i.e.,  $\varphi' = 0$ , then using (6.59) we obtain

$$\int_{\Gamma_{opt}} (\hat{\mathbf{u}}' \cdot \varphi + \frac{\partial \hat{\mathbf{u}}}{\partial \mathbf{n}} \varphi \mathbf{h} \cdot \mathbf{n}) = 0.$$

Again by density arguments, we have that

$$\hat{\mathbf{u}}' = -(\nabla \hat{\mathbf{u}} \cdot \mathbf{n})(\mathbf{h}, \mathbf{n}), \text{ on } \Gamma_{opt}.$$

Since  $\mathbf{h}$  is assumed to be zero on the other boundaries, derivation of the other boundary conditions easily follow in a similar way.  $\square$

Since  $\mathbf{g}$  is independent of the shape, the shape derivative  $\mathbf{u}'$  of the solution  $\mathbf{u}$  of the original Navier-Stokes system (6.32) is given by  $\hat{\mathbf{u}}' = \mathbf{u}'$ . Therefore we obtain the following corollary by substituting  $\hat{\mathbf{u}}' = \mathbf{u}'$  and  $\hat{\mathbf{u}} = \mathbf{u} - \hat{\mathbf{g}}$  into (6.55).

**Corollary 6.2.1.** *The shape derivative  $\mathbf{u}'$  of system (6.32) satisfies the following system*

$$\left\{ \begin{array}{l} -\alpha \Delta \mathbf{u}' + \nabla \mathbf{u} \cdot \mathbf{u}' + \nabla \mathbf{u}' \cdot \mathbf{u} + \nabla p' = 0 \text{ in } \Omega, \\ \operatorname{div} \mathbf{u}' = 0 \text{ in } \Omega, \\ \mathbf{u}' = -(\nabla(\mathbf{u} - \mathbf{g}) \cdot \mathbf{n})(\mathbf{h}, \mathbf{n}) \text{ on } \Gamma_{opt}, \\ -p' + \alpha \mathbf{n} \cdot \nabla \mathbf{u}' \cdot \mathbf{n} = 0, \quad \alpha \mathbf{n} \cdot \nabla \mathbf{u}' \cdot \mathbf{t} = 0, \quad \text{on } (\Gamma_9), \\ \mathbf{u}' \cdot \mathbf{n} = 0, \quad \alpha \mathbf{n} \cdot \nabla \mathbf{u}' \cdot \mathbf{t} = 0, \quad \text{on } \Gamma_*, \\ \mathbf{u}' \cdot \mathbf{n} = 0, \quad (-p' \mathbf{n} + \alpha \mathbf{n} \cdot \nabla \mathbf{u}') = 0, \quad \text{on } \Gamma_2, \Gamma_7. \end{array} \right. \quad (6.60)$$

The following lemma will become important in what follows

**Lemma 6.2.1.** *The shape derivative  $\mathbf{u}'$  in (6.60) satisfies*

$$\mathbf{u}' \cdot \mathbf{n} = 0, \text{ on } \Gamma_{opt}.$$

*Proof.* Using  $\mathbf{u}' = -(\nabla(\mathbf{u} - \mathbf{g}) \cdot \mathbf{n})(\mathbf{h}, \mathbf{n})$  on  $\Gamma_{opt}$ , using the tangential divergence formula (3.8), we have that:

$$\mathbf{u}' \cdot \mathbf{n} = (\nabla(\mathbf{u} - \mathbf{g}) \cdot \mathbf{n}) \cdot \mathbf{n}(\mathbf{h}, \mathbf{n}) = \operatorname{div}(\mathbf{u} - \hat{\mathbf{g}})(\mathbf{h}, \mathbf{n})|_{\Gamma_{opt}} - \operatorname{div}_{\Gamma_{opt}}(\mathbf{u} - \mathbf{g})(\mathbf{h}, \mathbf{n}). \quad (6.61)$$

Using  $\mathbf{u} - \mathbf{g} = 0$  on  $\Gamma_{opt}$ , as well as considering the fact that we are using divergence free fields, the expression in (6.61) vanishes.  $\square$

### 6.2.1.2 Gradients of cost functionals

This subsection is devoted to obtaining expressions for the optimality conditions. This is equivalent to the computation of the shape gradients of the 3 cost functionals introduced in Chapter 1, (see note 6.2.1). The goal is to find the Eulerian derivatives of  $J_i(\Omega, \mathbf{u})$ ,  $i = 1, \dots, 3$ , in the direction of the deformation vector field  $\mathbf{h}$ . If the mapping  $\mathbf{h} \mapsto dJ_i(\Omega, \mathbf{u})\mathbf{h}$  is linear and continuous, then we say that  $J_i$  is shape differentiable. If  $\Omega$  is sufficient smooth such that  $dJ_i(\Omega, \mathbf{u})\mathbf{h} = \int_{\Gamma_{opt}} \nabla J_i \mathbf{h} \cdot \mathbf{n}$ , then we call  $\nabla J_i \mathbf{n}$  the shape gradient of  $J_i$ .

**Theorem 6.2.3.** *Let  $\Omega$  be of class  $C^2$ ,  $\mathbf{u}_d$  the desired flow field, and  $\mathbf{h}$  a fixed vector field. Then the shape gradient  $\nabla J_1$  of the cost functional  $J_1$  can be expressed as*

$$\nabla J_1 = \left[ \frac{1}{2} |\mathbf{u} - \mathbf{u}_d|^2 + \alpha (\nabla(\mathbf{u} - \mathbf{g}) \cdot \mathbf{n}) \cdot (\nabla \mathbf{v} \cdot \mathbf{n}) \right] \mathbf{n}, \quad (6.62)$$

where all expressions are evaluated on  $\Gamma_{opt}$ , and the adjoint state  $\mathbf{v}$  satisfies (6.39) with  $J'_1(\mathbf{u}) = (\mathbf{u} - \mathbf{u}_d)$ .

*Proof.* Since  $J_1(\Omega, \mathbf{u})$  is differentiable with respect to  $\mathbf{u}$ , and the state  $\mathbf{u}$  is differentiable with respect to  $t$ , using Lemma 3.2.1 we obtain the Eulerian derivative of  $J_1(\Omega, \mathbf{u})$  with respect to  $t$ ,

$$dJ_1(\Omega, \mathbf{u})\mathbf{h} = \int_{\Omega} (\mathbf{u} - \mathbf{u}_d) \mathbf{u}' dx + \int_{\Gamma_{opt}} \frac{1}{2} |\mathbf{u} - \mathbf{u}_d|^2 \mathbf{h} \cdot \mathbf{n} ds. \quad (6.63)$$

From system (6.60), we have for the solution  $(\mathbf{v}, q)$  of the adjoint system (6.39)

$$0 = \int_{\Omega} \left( (-\alpha \Delta \mathbf{u}' + \nabla \mathbf{u} \cdot \mathbf{u}' + \nabla \mathbf{u}' \cdot \mathbf{u} + \nabla p') \cdot \mathbf{v} - (\operatorname{div} \mathbf{u}') \cdot q \right) dx. \quad (6.64)$$

Applying Greens formula (2.1.1) to equation (6.64) gives

$$\begin{aligned} 0 &= \int_{\Omega} \left( (-\alpha \Delta \mathbf{v} - \nabla \mathbf{v} \cdot \mathbf{u} + [\nabla \mathbf{u}]^t \cdot \mathbf{v} + \nabla q) \cdot \mathbf{u}' - (\operatorname{div} \mathbf{v}) \cdot p' \right) dx \\ &\quad - \int_{\Gamma} \mathbf{u}' (q \cdot \mathbf{n} - (\mathbf{u} \cdot \mathbf{n}) \mathbf{v} - \alpha \nabla \mathbf{v} \cdot \mathbf{n}) ds - \int_{\Gamma} (-p' \cdot \mathbf{n} + \alpha \nabla \mathbf{u}' \cdot \mathbf{n}) \mathbf{v} ds. \end{aligned} \quad (6.65)$$

Since  $(\mathbf{v}, q)$  satisfies the adjoint system (6.39), we have

$$\begin{aligned} 0 &= \int_{\Omega} (\mathbf{u} - \mathbf{u}_d) \cdot \mathbf{u}' dx - \int_{\Gamma} \mathbf{u}' (q \cdot \mathbf{n} - (\mathbf{u} \cdot \mathbf{n}) \mathbf{v} - \alpha \nabla \mathbf{v} \cdot \mathbf{n}) ds \\ &\quad - \int_{\Gamma} (-p' \cdot \mathbf{n} + \alpha \nabla \mathbf{u}' \cdot \mathbf{n}) \mathbf{v} ds. \end{aligned} \quad (6.66)$$

By writing the boundary terms in (6.66) in component form:

$$\begin{aligned} & \int_{\Gamma} (\mathbf{u}' \cdot \mathbf{n}) (q \cdot \mathbf{n} - (\mathbf{u} \cdot \mathbf{n}) \mathbf{v} - \alpha \nabla \mathbf{v} \cdot \mathbf{n}) \cdot \mathbf{n} + (\mathbf{u}' \cdot \mathbf{t}) (q \cdot \mathbf{n} - (\mathbf{u} \cdot \mathbf{n}) \mathbf{v} - \alpha \nabla \mathbf{v} \cdot \mathbf{n}) \cdot \mathbf{t} \, ds, \\ & \int_{\Gamma} (-p' \cdot \mathbf{n} + \alpha \nabla \mathbf{u}' \cdot \mathbf{n}) \cdot \mathbf{n} (\mathbf{v} \cdot \mathbf{n}) + (-p' \cdot \mathbf{n} + \alpha \nabla \mathbf{u}' \cdot \mathbf{n}) \cdot \mathbf{t} (\mathbf{v} \cdot \mathbf{t}) \, ds. \end{aligned} \quad (6.67)$$

Then it is easy to see that these terms in (6.67) vanish on  $\Gamma_9, \Gamma_*$  and  $\Gamma_f$ , due to (6.39) and (6.60). Therefore equation (6.66) becomes

$$\int_{\Omega} (\mathbf{u} - \mathbf{u}_d) \cdot \mathbf{u}' = - \int_{\Gamma_{opt}} (\alpha \nabla \mathbf{v} \cdot \mathbf{n} - q \cdot \mathbf{n}) \mathbf{u}' \, ds. \quad (6.68)$$

The term  $(q \cdot \mathbf{n}) \mathbf{u}'$  in (6.68) vanishes on  $\Gamma_{opt}$ , due to Lemma 6.2.1. Hence using (6.60), we obtain the Eulerian derivative from (6.63):

$$dJ_1(\Omega, \mathbf{u}) \mathbf{h} = \int_{\Gamma_{opt}} \left( \frac{1}{2} |\mathbf{u} - \mathbf{u}_d|^2 + (\nabla(\mathbf{u} - \mathbf{g}) \cdot \mathbf{n}) \cdot (\alpha \nabla \mathbf{v} \cdot \mathbf{n}) \right) \mathbf{h} \cdot \mathbf{n} \, ds. \quad (6.69)$$

Since the mapping  $\mathbf{h} \mapsto dJ_1(\Omega, \mathbf{u}) \mathbf{h}$  is linear and continuous, we get the expression for the shape gradient (6.62).  $\square$

**Theorem 6.2.4.** *Let  $\Omega$  be of class  $C^2$  and  $\mathbf{h}$  a fixed vector field. Then the shape gradient  $\nabla J_2$  of the cost functional  $J_2$  can be expressed as*

$$\nabla J_2 = \left[ \frac{1}{2} |\operatorname{curl} \mathbf{u}|^2 + \nabla(\mathbf{u} - \mathbf{g}) \cdot \mathbf{n} \cdot (\alpha \nabla \mathbf{v} \cdot \mathbf{n} - \operatorname{curl} \mathbf{u} \times \mathbf{n}) \right] \mathbf{n}, \quad (6.70)$$

where all expressions are evaluated on  $\Gamma_{opt}$ , and the adjoint state  $\mathbf{v}$  satisfies (6.39) with  $J'_2(\mathbf{u}) = -\Delta \mathbf{u}$ .

*Proof.* Since  $J_2(\Omega, \mathbf{u})$  is differentiable with respect to  $\mathbf{u}$ , and the state  $\mathbf{u}$  is differentiable with respect to  $t$ , using Lemma 3.2.1, we obtain the Eulerian derivative of  $J_2(\Omega, \mathbf{u})$  with respect to  $t$ ,

$$dJ_2(\Omega, \mathbf{u}) \mathbf{h} = \int_{\Omega} \operatorname{curl} \mathbf{u} \operatorname{curl} \mathbf{u}' \, dx + \int_{\Gamma_{opt}} \frac{1}{2} |\operatorname{curl} \mathbf{u}|^2 \mathbf{h} \cdot \mathbf{n} \, ds. \quad (6.71)$$

Utilizing (6.60) and  $J'_2(\mathbf{u}) = -\Delta \mathbf{u}$ , we obtain

$$\begin{aligned} 0 &= \int_{\Omega} -\Delta \mathbf{u} \cdot \mathbf{u}' \, dx - \int_{\Gamma} \mathbf{u}' (q \cdot \mathbf{n} - (\mathbf{u} \cdot \mathbf{n}) \mathbf{v} - \alpha \nabla \mathbf{v} \cdot \mathbf{n}) \, ds \\ &\quad - \int_{\Gamma} (-p' \cdot \mathbf{n} + \alpha \nabla \mathbf{u}' \cdot \mathbf{n}) \mathbf{v} \, ds. \end{aligned}$$

Using similar arguments as before, we have

$$\int_{\Omega} \Delta \mathbf{u} \cdot \mathbf{u}' dx = \int_{\Gamma_{opt}} (\alpha \nabla \mathbf{v} \cdot \mathbf{n} - q \cdot \mathbf{n}) \mathbf{u}' ds. \quad (6.72)$$

The term  $(q \cdot \mathbf{n}) \mathbf{u}'$  vanishes on  $\Gamma_{opt}$ , due to Lemma 6.2.1. Thus (6.72) becomes

$$\int_{\Omega} \Delta \mathbf{u} \cdot \mathbf{u}' dx = - \int_{\Gamma_{opt}} (\nabla(\mathbf{u} - \mathbf{g}) \cdot \mathbf{n}) \cdot (\alpha \nabla \mathbf{v} \cdot \mathbf{n}) \mathbf{h} \cdot \mathbf{n} ds. \quad (6.73)$$

Using Greens formula, see equation (3.83), we have that

$$\int_{\Omega} \operatorname{curl} \mathbf{u} \operatorname{curl} \mathbf{u}' dx = - \int_{\Omega} \Delta \mathbf{u} \cdot \mathbf{u}' dx + \int_{\Gamma} (\operatorname{curl} \mathbf{u} \times \mathbf{n}) \cdot \mathbf{u}' ds.$$

Utilizing (6.73) and (6.60), we obtain

$$\begin{aligned} \int_{\Omega} \operatorname{curl} \mathbf{u} \operatorname{curl} \mathbf{u}' dx &= \int_{\Gamma_{opt}} (\nabla(\mathbf{u} - \mathbf{g}) \cdot \mathbf{n}) \cdot (\alpha \nabla \mathbf{v} \cdot \mathbf{n}) \mathbf{h} \cdot \mathbf{n} ds \\ &\quad - \int_{\Gamma_{opt}} (\operatorname{curl} \mathbf{u} \times \mathbf{n}) (\nabla(\mathbf{u} - \mathbf{g}) \cdot \mathbf{n}) \mathbf{h} \cdot \mathbf{n} ds. \end{aligned}$$

Hence we obtain the Eulerian derivative from (6.71):

$$dJ_2(\Omega, \mathbf{u}) \mathbf{h} = \int_{\Gamma_{opt}} \left( \frac{1}{2} |\operatorname{curl} \mathbf{u}|^2 + \nabla(\mathbf{u} - \mathbf{g}) \cdot \mathbf{n} \cdot (\alpha \nabla \mathbf{v} \cdot \mathbf{n} - \operatorname{curl} \mathbf{u} \times \mathbf{n}) \right) \mathbf{h} \cdot \mathbf{n} ds. \quad (6.74)$$

Since the mapping  $\mathbf{h} \mapsto dJ_2(\Omega, \mathbf{u}) \mathbf{h}$  is linear and continuous, we get the expression for the shape gradient (6.70).  $\square$

**Theorem 6.2.5.** *Let  $\Omega$  be of class  $C^2$  and  $\mathbf{h}$  a fixed vector field. Then the shape gradient  $\nabla J_3$  of the cost functional  $J_3$  can be expressed as*

$$\nabla J_3 = [g_3(\det \nabla \mathbf{u}) + (\nabla(\mathbf{u} - \mathbf{g}) \cdot \mathbf{n}) \cdot (\alpha(\nabla \mathbf{v} \cdot \mathbf{n}) - P(\mathbf{u}))] \mathbf{n}, \quad (6.75)$$

where all expressions are evaluated on  $\Gamma_{opt}$ , and the adjoint state  $\mathbf{v}$  satisfies (6.39) with  $J'_3(\mathbf{u}) = R(\mathbf{u})$ , where

$$R(\mathbf{u}) = \begin{pmatrix} -\operatorname{curl} \left( g'_3(\det \nabla \mathbf{u}) \nabla u_2 \right) \\ \operatorname{curl} \left( g'_3(\det \nabla \mathbf{u}) \nabla u_1 \right) \end{pmatrix}, \quad (6.76)$$

and

$$P(\mathbf{u}) = \begin{pmatrix} g'_3(\det \nabla \mathbf{u}) \left( \frac{\partial u_2}{\partial x_2} - \frac{\partial u_2}{\partial x_1} \right) \\ g'_3(\det \nabla \mathbf{u}) \left( \frac{\partial u_1}{\partial x_1} - \frac{\partial u_1}{\partial x_2} \right) \end{pmatrix}.$$

*Proof.* Follows similar arguments as in the proof of Theorem 3.3.2 in combination with argu-

ments used in the previous 2 theorems in this subsubsection. So we skip the details here.  $\square$

**Remark 6.2.1.** Since the two conditions

$$\begin{aligned} (-p' \mathbf{n} + \alpha \mathbf{n} \cdot \nabla \mathbf{u}') &= 0 \text{ on } \Gamma_f, \\ \mathbf{u}' \cdot \mathbf{n} = 0, \quad \mathbf{u}' \cdot \mathbf{t} &= 0 \text{ on } \Gamma_f, \end{aligned} \tag{6.77}$$

exist simultaneously on  $\Gamma_f$ , the integrals in (6.67), evaluated on  $\Gamma_f$ , vanish irrespective of which boundary condition is posed on  $\Gamma_f$  for the adjoint problem. Therefore it suffices to consider only one of the conditions:

$$\begin{aligned} [q \cdot \mathbf{n} - (\mathbf{u} \cdot \mathbf{n})\mathbf{v} - \alpha \nabla \mathbf{v} \cdot \mathbf{n}] &= 0, \text{ on } \Gamma_f, \\ \mathbf{v} \cdot \mathbf{n} &= 0, \text{ on } \Gamma_f, \end{aligned} \tag{6.78}$$

for the adjoint problem, so that the optimality condition (6.74) is satisfied. In this work we chose to solve the following adjoint system

$$\left\{ \begin{array}{l} -\alpha \Delta \mathbf{v} - \nabla \mathbf{v} \cdot \mathbf{u} + [\nabla \mathbf{u}]^t \cdot \mathbf{v} + \nabla q = J'_i(\mathbf{u}), \text{ in } \Omega, \\ \operatorname{div} \mathbf{v} = 0, \text{ in } \Omega, \\ \mathbf{v} \cdot \mathbf{n} = 0, \quad \mathbf{t} \cdot [q \cdot \mathbf{n} - (\mathbf{u} \cdot \mathbf{n})\mathbf{v} - \alpha \nabla \mathbf{v} \cdot \mathbf{n}] = 0, \text{ on } \Gamma_*, \\ \mathbf{v} = 0, \text{ on } \Gamma_5, \\ q \cdot \mathbf{n} - (\mathbf{u} \cdot \mathbf{n})\mathbf{v} - \alpha \nabla \mathbf{v} \cdot \mathbf{n} = 0, \text{ on } \Gamma_f, \\ q \cdot \mathbf{n} - (\mathbf{u} \cdot \mathbf{n})\mathbf{v} - \alpha \nabla \mathbf{v} \cdot \mathbf{n} = 0, \text{ on } \Gamma_9. \end{array} \right. \tag{6.79}$$

## 6.2.2 Discretization of the optimization problem

The continuous formulations of the free-surface problem (6.10), adjoint free-surface problem (6.79), as well as the optimality conditions 6.62, 6.70, and 6.75 are discretized using finite element method. The discretization and numerical solution of (6.10) has been done in the previous section. The discretization of the adjoint system as well as optimality conditions follows the approach treated in Chapter 4, so we skip the details here. Now that we have everything at a discrete level, we proceed to analyze the method for solving the shape optimization problem.

## 6.2.3 Choice of descent direction and optimization algorithm

The optimization problem is solved in its original setting, i.e., we find a solution to (6.32) first, and then we proceed to the upper level represented by the minimization of the cost functional. On the minimization level, we use the boundary variation algorithm, described in detail in Chapter 3. We saw there that due to smoothness issues, one needs to solve an elliptic system to obtain

the deformation field  $\mathbf{h}$ , which not only has better smoothness properties, but also it is defined globally over the whole mesh. Further, such a deformation field was found to provide a descent direction for the cost functionals  $J_i(\Omega, \mathbf{u})$ . If we have the descent direction for the cost, then the overall optimization algorithm that we use in this chapter proceeds as shown in algorithm 5. In

---

**Algorithm 5** Free surface flow - shape optimization algorithm

---

- Choose initial shape  $\Omega_0$ ,  $tol$ ,  $N_{max}$ ;
- while** ( $(err > tol) \& (j < N_{max})$ ) **do**

  - Solve the free surface problem by algorithm 4 .
  - Compute the adjoint system (6.79).
  - Evaluate the descent direction  $\mathbf{h}_j$  by using

$$\begin{aligned} -\Delta \mathbf{h} + \mathbf{h} &= 0 \text{ in } \Omega, \\ \frac{\partial \mathbf{h}}{\partial \mathbf{n}} &= -\nabla J_i \mathbf{n} \text{ on } \Gamma_{opt}, \\ \mathbf{h} &= 0 \text{ on } \Gamma_{fixed} \equiv \Gamma_* \cup \Gamma_f \cup \Gamma_9, \end{aligned}$$

with  $\Omega = \Omega_j$  and  $\Gamma_{opt}$  is part of boundary to be optimized.

- Set  $\Omega_{j+1} = (Id + t_j \mathbf{h}_j) \Omega_j$ , where  $t_j$  is a small positive scalar, chosen using some step size rule .

**end while**

---

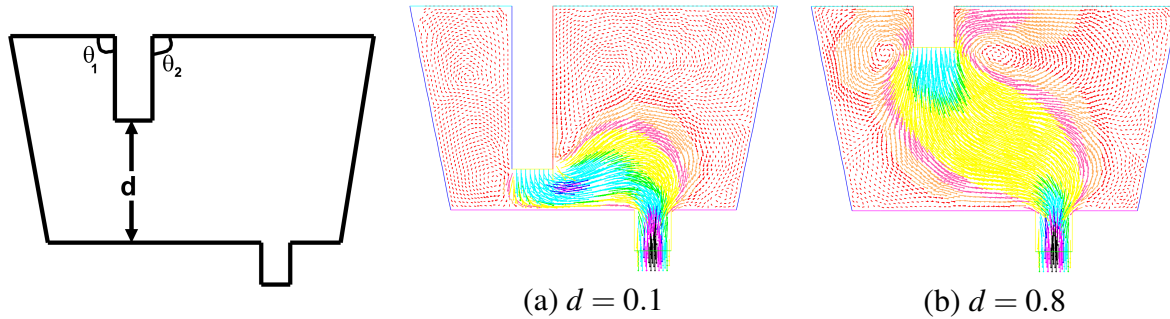
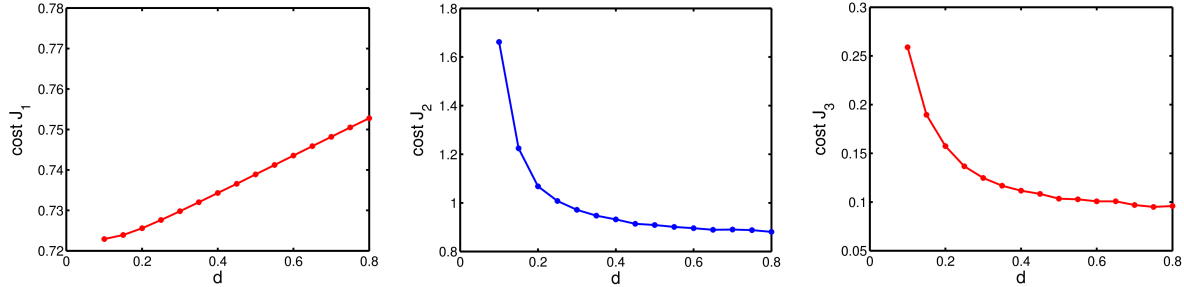
this algorithm, the outer optimization loop is indexed by  $j$ , the inner loop for the free surface flow solver by  $k$ , and the inner most loop within the free surface flow solver for the linearized Navier-stokes system by  $n$ .

#### 6.2.4 Direct numerical simulation

In order to obtain a priori knowledge about the behavior of the cost functionals with respect to changes in the geometrical configurations, at first the free surface part of the boundary is fixed and assumed to be flat. On the flat surface, we prescribe the following boundary conditions

$$\mathbf{u} \cdot \mathbf{n} = 0, \quad (-p \cdot \mathbf{n} + \frac{1}{Re} \nabla \mathbf{u} \cdot \mathbf{n}) \cdot \mathbf{t} = 0.$$

Different studies are considered at first. In the first study, we consider the variation of the spout with respect to the depth  $d$ . We start with  $d = 0.1$  (see Figure 6.6 (a)), and make increments of size 0.05 until we reach  $d = 0.8$  (see Figure 6.6 (b)). For each  $d$ , the value of the cost functional is computed, and the behavior is plotted in Figure 6.7. For  $J_1$ , we take  $\mathbf{u}_d = (0, -1)$ . Figure (6.7) suggests that both  $J_2$  and  $J_3$  decrease with increase in depth while the converse hold true for the cost  $J_1$ . Visual inspection of the streamline patterns corresponding to flows at different depths (see Figure 6.8) indicates that the big vortices in the containment are reduced as the depth

Figure 6.6: Flow field at different values for the depth  $d$ Figure 6.7: Variation of the cost functions with the depth  $d$ 

is increased to  $d = 0.99$ . This is consistent with the variations of the cost functions  $J_2$  and  $J_3$  in Figure 6.7. The physical explanation of these results is the following: By lowering the spout into the containment, a relatively small cross section area for the net flow occurs. This result in fairly large velocities in the containment as the stream turns, and consequently leads to an increase of the cost functionals  $J_2$  and  $J_3$ . In the second study, we consider the variation of the

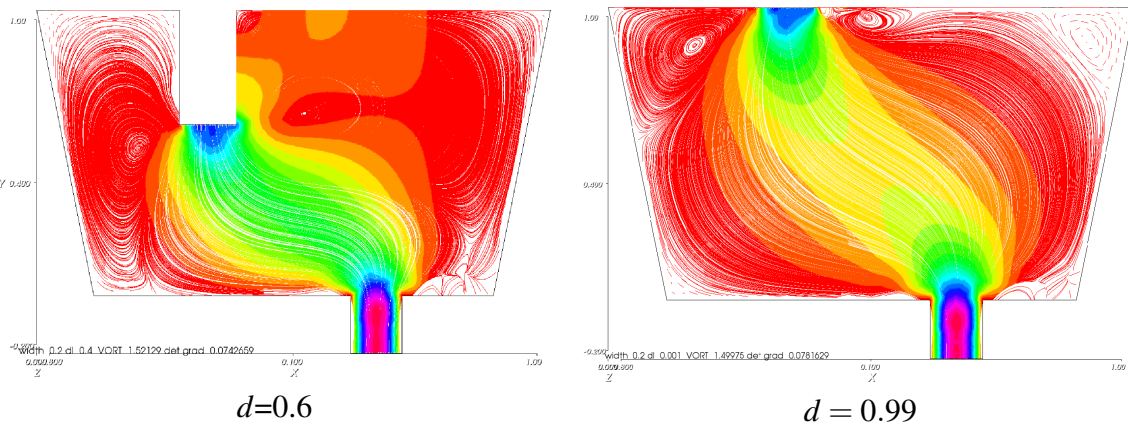


Figure 6.8: Streamlines corresponding to flows at different depths

spout with respect to the angles  $\theta_1$  and  $\theta_2$ . We start with  $\theta_1 = \theta_2 = 90^\circ$  (see Figure 6.9 (a)). In each iteration, the angles  $\theta_i$  are increased by  $\delta\theta_i = \tan^{-1}(\frac{\delta h_i}{1-d})$  where  $\delta h_i = 0.01$  and  $d = 0.6$  to obtain the flow field after nine iterations, depicted in Figure (6.9 (a)). Conversely, when the angles  $\theta_i$  are decreased in each iteration by  $\delta\theta_i$ , we obtain the flow field depicted in Figure (6.9(c)) after 9 iterations. For each iteration, the value of the cost functional is computed, and the

behaviors are depicted in Figures 6.10, 6.11. Visual inspection of the flow field patterns in Figure

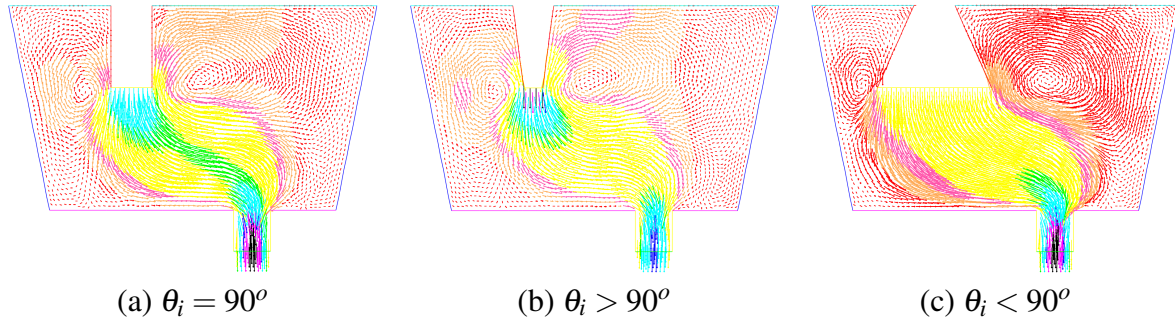


Figure 6.9: Flow field at different values for the angles  $\theta_i$

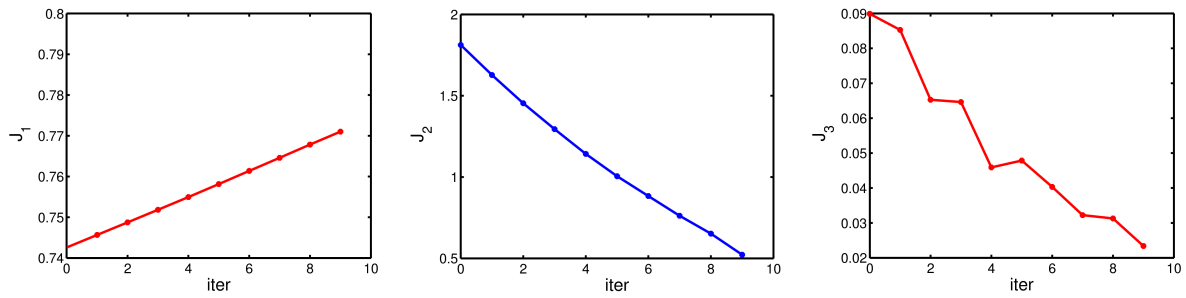


Figure 6.10: Variation of the cost functions with wall angles ( $\theta_i > 90^\circ$ )

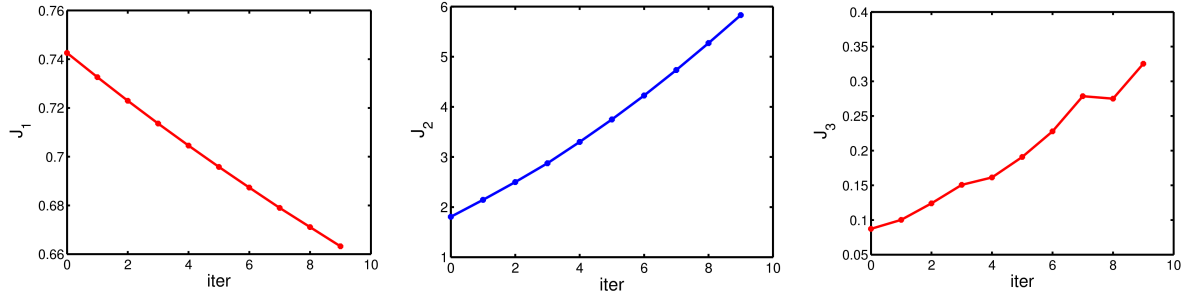


Figure 6.11: Variation of the cost functions with wall angles ( $\theta_i < 90^\circ$ )

6.9 indicates that the big vortices in the containment are reduced as the walls are made narrower. This is consistent with the variations of the cost functionals  $J_2$  and  $J_3$  in Figures 6.10, 6.11. A physical explanation of this phenomenon is the following. Momentum is transferred in a fluid by molecules in a slower-moving layer of fluid migrating to a faster-moving region of fluid and vice versa [Kesslerand 1999, Pg.26-28]. The rate of momentum transfer ( $I$ ) can mathematically be expressed as

$$I = \mathbf{u}^2 \rho A,$$

where  $\mathbf{u}$  is the velocity of the fluid,  $\rho$  the density and  $A$ , the cross section area of the flow region. By enlarging the inflow area  $A$  while keeping the velocity  $\mathbf{u}$  constant, the rate of momentum

transfer in the fluid is increased. This consequently leads to an increase in the magnitude of the velocity field as the stream turns giving results in Figures 6.11. The converse holds true when the inflow becomes narrower. Ideally, this explanation implies that the fluid enters into the containment with a bigger force when the inflow is broader, and with a small force, when narrower.

### 6.2.5 Optimization of inflow

In this subsection, we optimize the shape on the inflow portion  $\Gamma_5$  of the domain  $\Omega$ . Figure 6.12 shows the geometrical set up of this portion, not drawn to scale. To optimize this part, we need firstly to describe the set of admissible shapes. We shall therefore suppose that  $\Gamma_{opt}$  is represented

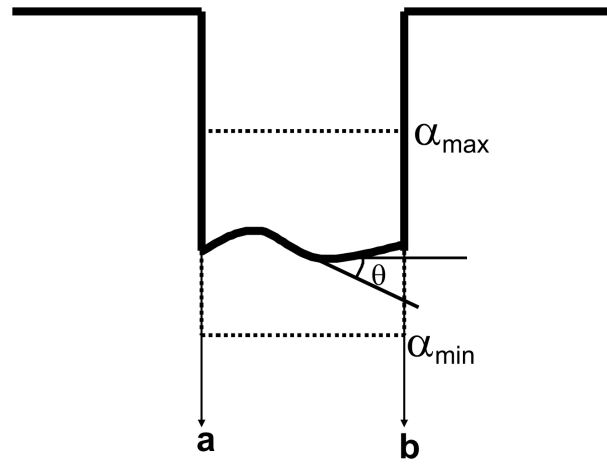


Figure 6.12: Admissible domains

by the graph of functions  $\alpha \in \mathcal{O}$ , where

$$\mathcal{O} = \{\alpha \in C^{1,1}([a, b]) \mid 0 < \alpha_{min} \leq \alpha(x_1) \leq \alpha_{max}, x_1 \in [a, b]\}. \quad (6.80)$$

Further we denote by

$$\mathcal{U}_{ad} = \{\Omega(\alpha) \mid \alpha \in \mathcal{O}\}, \quad (6.81)$$

the set of all admissible domains. To control the possible oscillations of  $\Gamma_{opt} \in \mathcal{O}$  that can result, we change the scalar product with which we compute the decent direction from  $L^2(\Omega)$  to  $H^1(\Omega)$ . See algorithm 5, and Chapter 3 for details. In what follows, we choose  $[a, b] = [-0.4, -0.2]$ ,  $\alpha_{max} = 0.65$ , and  $\alpha_{min} = 0.45$ , (see Figure 6.3). The form of the velocity field  $\mathbf{h}$  realizing shape variations depends on how shapes of admissible domains are parametrized. In our problem, we expect the  $h_{x_1}$  component of  $\mathbf{h}$  to be small and therefore it is natural to take a velocity field of the form  $\mathbf{h} = (0, h)$ . Moreover, see [Haslinger 2003, Chapter 3] for more details. The geometry of the

computed flow field in the previous section (see Figure 6.5 d), is used to initialize algorithm (5). During each optimization step, the step size  $t_j$  is chosen small. Since  $\Gamma_{opt}$  is perturbed by a small step, it is observed that we need on average only  $k = 2$  free surface flow solves per optimization step. This in fact leads to the convergence of the optimization algorithm. The geometries together

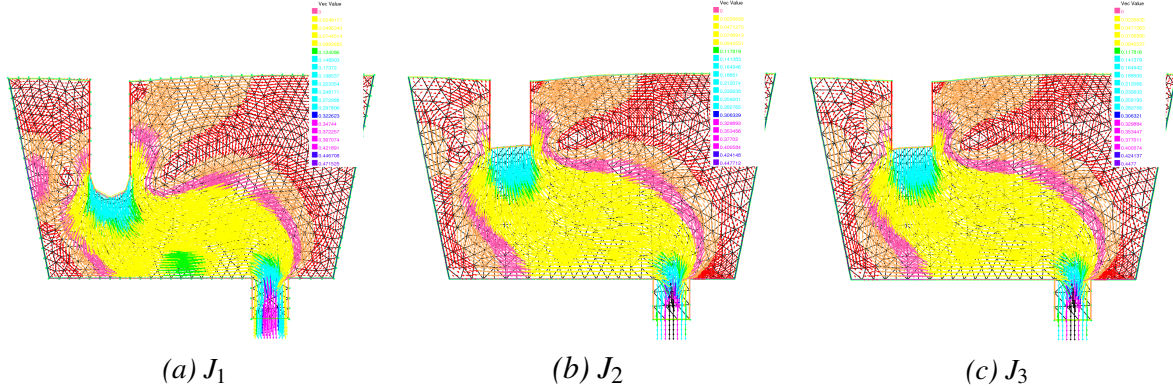


Figure 6.13: Snapshots of optimized geometries using the three costs  $J_1$ ,  $J_2$  and  $J_3$

with the flow field corresponding to the minimization of the three cost functionals are shown in Figure 6.13. The desired flow field for cost  $J_1$  is chosen to be  $\mathbf{u}_d = (0, -1)$ , which appears to be a natural choice. Moreover  $\mathbf{u}_d$  is chosen to be of the same magnitude as the inflow velocity. We observe that the optimal shape corresponding to the 3 cost functionals differ. For the cost functionals  $J_2$  and  $J_3$ , there is a slight difference. For both  $J_2$  and  $J_3$ , the depths  $d$  increase during the optimization (see Figure 6.14). The dashed line in Figure 6.14 indicates the location of the

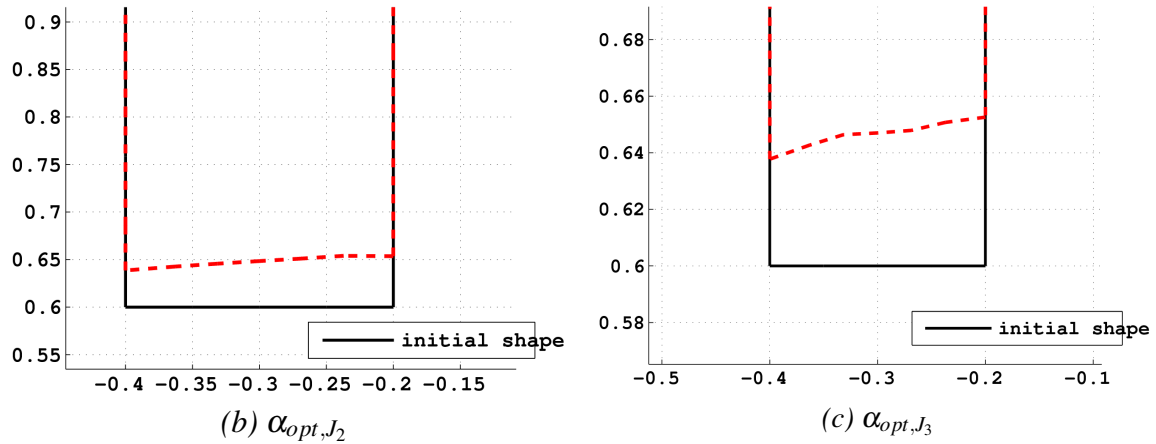


Figure 6.14: Zoom of  $\alpha_{opt}$  for  $J_2$  and  $J_3$

optimal boundary for the inflow. The right hand end point of  $\alpha_{opt}$  is active at the upper bound  $\alpha_{max}$  for the results in Figure 6.14. We compared the values for  $J_2$ ,  $J_3$  at  $\alpha_{opt,J_2}$ ,  $\alpha_{opt,J_3}$ , to the case where all of  $\Gamma_5$  is chosen to be active at  $\alpha_{max}$ . The corresponding values are  $J_2(\alpha_{opt,J_2}) = 1.011 < J_2(\alpha_{max}) = 1.02578$ ,  $J_3(\alpha_{opt,J_3}) = 0.0979 < J_3(\alpha_{max}) = 0.101275$ . Indeed the obtained shapes are optimal, and moreover their nature is possibly due to the asymmetry of the flow field.

The obtained results are consistent with the results from direct numerical simulation and hence leads to a reduction in the vortex in the flow field. A plot of the history of the 3 cost functionals in Figure 6.15 asserts the decrease of the 3 costs during the minimization.

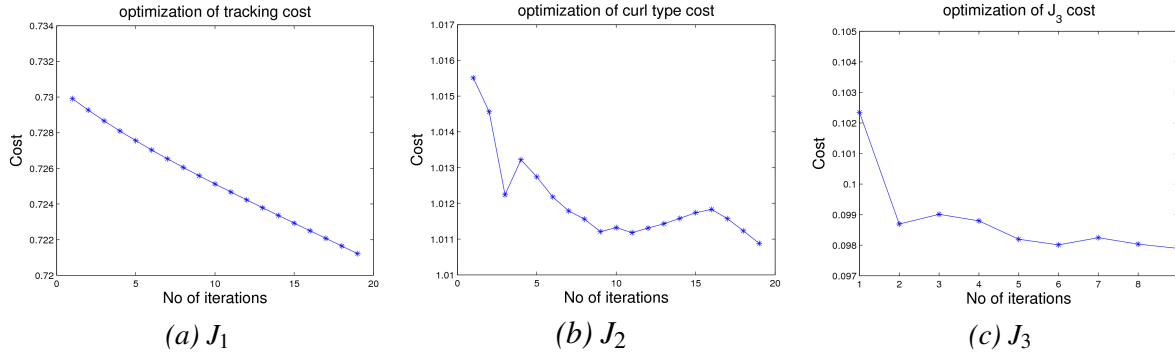


Figure 6.15: Convergence history using the three costs  $J_1$ ,  $J_2$  and  $J_3$

**Remark 6.2.2.** The optimal shape corresponding to the cost functional  $J_1$  depends choice of the desired flow  $\mathbf{u}_d$ . A different choice would yield a different optimal shape.

### 6.2.6 Optimization of inflow walls

In this subsection, we optimize the shape of the boundaries  $\Gamma_4$  and  $\Gamma_6$  of the domain  $\Omega$ . We shall therefore suppose that  $\Gamma_4$  and  $\Gamma_6$  are represented by the graphs of functions  $\alpha_i \in \mathcal{O}_i$ ,  $i = 1, 2$ , where

$$\begin{aligned}\mathcal{O}_1 &= \{\alpha_1 \in C^{1,1}([c, d]) \mid \alpha_{min,1} \leq \alpha_1(x_2) \leq \alpha_{max,1}, x_2 \in [c, d]\}, \\ \mathcal{O}_2 &= \{\alpha_2 \in C^{1,1}([c, d]) \mid \alpha_{min,2} \leq \alpha_2(x_2) \leq \alpha_{max,2}, x_2 \in [c, d]\}.\end{aligned}\quad (6.82)$$

Furthermore, we denote by

$$\mathcal{U}_{ad} = \{\Omega(\alpha) \mid \alpha_1 \in \mathcal{O}_1, \alpha_2 \in \mathcal{O}_2\} \quad (6.83)$$

the set of all admissible domains. Again, to control the possible oscillations of  $\alpha_i \in \mathcal{O}_i$  that can result, we change the scalar product with which we compute the decent direction from  $L^2(\Omega)$  to  $H^1(\Omega)$  as explained in the previous subsection. In what follows, we choose  $[c, d] = [0.6, 1]$ ,  $\alpha_{max,1} = -0.18$ ,  $\alpha_{min,1} = -0.22$ ,  $\alpha_{max,2} = -0.37$ , and  $\alpha_{min,2} = 0.43$ . The upper ends of  $\Gamma_4$  and  $\Gamma_6$  are fixed at the top and the lower ends are free. The geometries together with the flow field corresponding to the minimization of the three cost functionals are shown in Figure 6.16. The desired flow field for cost  $J_1$  is again chosen as in the previous subsection. We observe that the optimal shape corresponding to the 3 cost functionals differ. For the cost functionals  $J_2$  and  $J_3$ , there is a slight difference. For both  $J_2$  and  $J_3$ , their minimization leads to the narrowing of

the inflow tube (see Figure 6.16). The converse holds for the cost functional  $J_1$ . This is again consistent with the results from direct numerical simulation in section 6.2.4 and hence leads to a reduction in the vortex in the flow field.

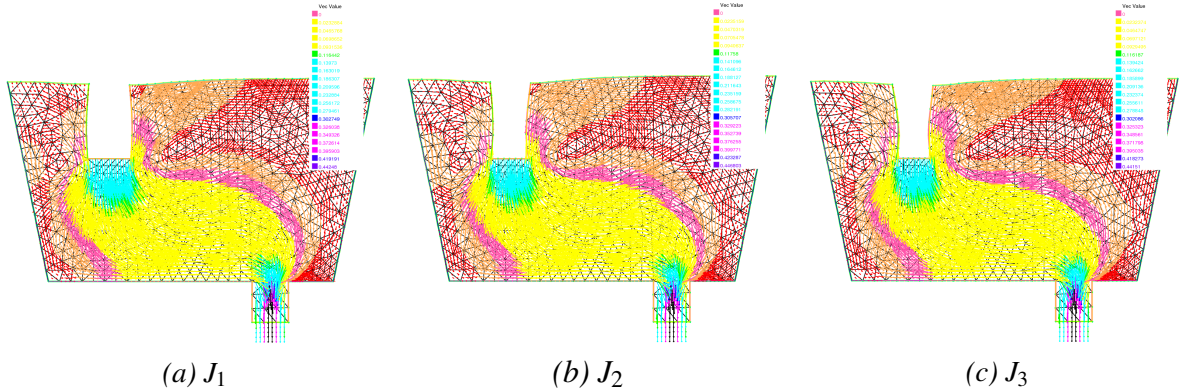


Figure 6.16: Snapshots of optimized geometries using the three costs  $J_1$ ,  $J_2$  and  $J_3$



# 7

## COMPUTATIONAL DETAILS

### 7.1 Componentwise splitting of vector matrices

As already mentioned in Chapter 4, in practice, the 2 components of velocity are always approximated using a single finite element space. Given scalar finite element basis functions  $\{\varphi_i\}_{i=1}^n$ , we set  $n_u = 2n$  where  $n_u = \dim(\mathbf{V}_{0h})$  and define the basis set

$$\{\vec{\varphi}_1, \dots, \vec{\varphi}_{2n}\} := \{(\varphi_1, 0)^T, \dots, (\varphi_n, 0)^T, (0, \varphi_1)^T, \dots, (0, \varphi_n)^T\}. \quad (7.1)$$

#### 7.1.1 The vector Laplacian matrix

Let  $\vec{\varphi}_i^1 = \begin{pmatrix} \varphi_i \\ 0 \end{pmatrix}, i = 1, \dots, n$  and  $\vec{\varphi}_j^2 = \begin{pmatrix} 0 \\ \varphi_j \end{pmatrix}, j = n+1, \dots, 2n$ , then we have

$$\nabla \vec{\varphi}_i^1 = \begin{pmatrix} \frac{\partial \varphi_i}{\partial x} & \frac{\partial \varphi_i}{\partial y} \\ 0 & 0 \end{pmatrix} \text{ and } \nabla \vec{\varphi}_j^2 = \begin{pmatrix} 0 & 0 \\ \frac{\partial \varphi_j}{\partial x} & \frac{\partial \varphi_j}{\partial y} \end{pmatrix}.$$

Let

$$\mathbf{A} = \int_{\Omega_h} \nabla \vec{\varphi}_i : \nabla \vec{\varphi}_j \, dx,$$

then

$$\begin{aligned} \mathbf{A}_{1,1} &= \int_{\Omega_h} \nabla \vec{\varphi}_i^1 : \nabla \vec{\varphi}_j^1 \, dx = \int_{\Omega_h} \frac{\partial \varphi_i}{\partial x} \frac{\partial \varphi_j}{\partial x} + \frac{\partial \varphi_i}{\partial y} \frac{\partial \varphi_j}{\partial y} \, dx = A, \quad i, j = 1 \dots n, \\ \mathbf{A}_{1,2} &= \int_{\Omega_h} \nabla \vec{\varphi}_i^1 : \nabla \vec{\varphi}_j^2 \, dx = 0, \text{ for } i = 1 \dots n, j = n+1, \dots, 2n, \\ \mathbf{A}_{2,1} &= \int_{\Omega_h} \nabla \vec{\varphi}_i^2 : \nabla \vec{\varphi}_j^1 \, dx = 0, \text{ for } i = n+1 \dots 2n, j = 1, \dots, n, \end{aligned}$$

and

$$\mathbf{A}_{2,2} = \int_{\Omega_h} \nabla \vec{\phi}_i^2 : \nabla \vec{\phi}_j^2 dx = \int_{\Omega_h} \frac{\partial \varphi_i}{\partial x} \frac{\partial \varphi_j}{\partial x} + \frac{\partial \varphi_i}{\partial y} \frac{\partial \varphi_j}{\partial y} dx = A, \quad i, j = n+1 \dots 2n.$$

Hence

$$\mathbf{A} = \begin{pmatrix} A & 0 \\ 0 & A \end{pmatrix} \in \mathbb{R}^{2n \times 2n}.$$

### 7.1.2 The convective linearized matrix

There are different alternatives for Picard linearization which are listed below

$$(\mathbf{u} \cdot \nabla \mathbf{u})^{k+1} \approx (\mathbf{u}^{k+1} \cdot \nabla) \mathbf{u}^k, \quad (7.2)$$

$$(\mathbf{u} \cdot \nabla \mathbf{u})^{k+1} \approx (\mathbf{u}^k \cdot \nabla) \mathbf{u}^{k+1}, \quad (7.3)$$

$$(\mathbf{u} \cdot \nabla \mathbf{u})^{k+1} \approx (\mathbf{u}^k \cdot \nabla) \mathbf{u}^k. \quad (7.4)$$

Of the last three possibilities, (7.3) is often preferred since it produces good convergence. Nevertheless we shall explain how to split componentwise the matrix resulting from the forms (7.2) and (7.3). The later appears in the linearized Picard or sometimes called Oseen equations that we use to solve the Navier-Stokes equations, and terms with similar structure as (7.2-7.3) appears in the adjoint of the Navier-Stokes equations. The parameter  $k$  in the above equations represents the iteration number.

#### 7.1.2.1 Case 1

We omit the superscript  $k$  and let

$$\mathbf{M}(\mathbf{w}) = \int_{\Omega_h} (\vec{\phi}_i \cdot \nabla) \mathbf{w} \vec{\phi}_j dx, \quad (7.5)$$

where  $\mathbf{w} = (w_1, w_2)$  is a known solution from the previous iteration step. Then

$$\begin{aligned} \mathbf{M}_{1,1} &= \int_{\Omega} \nabla \mathbf{w} \cdot \vec{\phi}_i^1 \cdot \vec{\phi}_j^1 dx = \int_{\Omega} \frac{\partial w_1}{\partial x} \varphi_i \varphi_j dx, \quad \text{for } i, j = 1 \dots n, \\ \mathbf{M}_{1,2} &= \int_{\Omega} \nabla \mathbf{w} \cdot \vec{\phi}_i^1 \cdot \vec{\phi}_j^2 dx = \int_{\Omega} \frac{\partial w_2}{\partial x} \varphi_i \varphi_j dx, \quad \text{for } i = 1 \dots n, j = n+1, \dots, 2n, \\ \mathbf{M}_{2,1} &= \int_{\Omega} \nabla \mathbf{w} \cdot \vec{\phi}_i^2 \cdot \vec{\phi}_j^1 dx = \int_{\Omega} \frac{\partial w_1}{\partial y} \varphi_i \varphi_j dx, \quad \text{for } i = n+1 \dots 2n, j = 1, \dots, n, \\ \mathbf{M}_{2,2} &= \int_{\Omega} \nabla \mathbf{w} \cdot \vec{\phi}_i^2 \cdot \vec{\phi}_j^2 dx = \int_{\Omega} \frac{\partial w_2}{\partial y} \varphi_i \varphi_j dx, \quad \text{for } i = n+1 \dots 2n, j = n+1, \dots, 2n. \end{aligned}$$

### 7.1.2.2 Case 2

Let

$$\mathbf{C}(\mathbf{w}) = \int_{\Omega_h} (\mathbf{w} \cdot \nabla) \vec{\phi}_i \vec{\phi}_j \, dx, \quad (7.6)$$

where  $\mathbf{w} = (w_1, w_2)$  is a known solution from the previous iteration step. Then

$$\begin{aligned} \mathbf{C}_{1,1} &= \int_{\Omega} \nabla \vec{\phi}_i^1 \cdot \mathbf{w} \cdot \vec{\phi}_j^1 \, dx = \int_{\Omega} \frac{\partial \phi_i}{\partial x} w_1 \phi_j \, dx + \frac{\partial \phi_i}{\partial y} w_2 \phi_j \, dx, \text{ for } i, j = 1 \dots n, \\ \mathbf{C}_{1,2} &= \int_{\Omega} \nabla \vec{\phi}_i^1 \cdot \mathbf{w} \cdot \vec{\phi}_j^2 \, dx = 0, \text{ for } i = 1 \dots n, j = n+1, \dots, 2n, \\ \mathbf{C}_{2,1} &= \int_{\Omega} \nabla \vec{\phi}_i^2 \cdot \mathbf{w} \cdot \vec{\phi}_j^1 \, dx = 0, \text{ for } i = n \dots 2n, j = 1, \dots, n, \\ \mathbf{C}_{2,2} &= \int_{\Omega} \nabla \vec{\phi}_i^2 \cdot \mathbf{w} \cdot \vec{\phi}_j^2 \, dx = \int_{\Omega} \frac{\partial \phi_i}{\partial x} w_1 \phi_j \, dx + \frac{\partial \phi_i}{\partial y} w_2 \phi_j \, dx, \text{ for } i, j = n \dots 2n. \end{aligned}$$

Hence  $\mathbf{C}(\mathbf{w})$  is a block diagonal matrix, which is reassembled for every solution  $\mathbf{w}$  at subsequent iterative steps.

**Remark 7.1.1.** *The discussion concerning the block matrix  $\mathbf{B}$  and right hand side vector  $\mathbf{f}$  follows similarly as above.*

**Remark 7.1.2.** *Solving the Navier-Stokes equations as well as their adjoint system therefore requires assembling scalar valued matrices  $A, B_x, B_y, C_{1,1}, C_{1,2}$  etc..*

## 7.2 Computation of the local stiffness matrices

In this section, we illustrate how to compute the necessary matrices required for the computation of the discrete solution without being exhaustive. Some of the ideas expressed here can be found in excellent texts about finite element method, for example [Schwarz 1991]. In finite element method, it is always convenient to work on the reference element. Therefore, over the element, reference element a complete quadratic “ansatz”

$$\begin{aligned} \phi_1 &= 1 - 3\xi - 3\eta + 2\xi^2 + 4\xi\eta + 2\eta^2, \\ \phi_2 &= -\xi + 2\xi^2, \\ \phi_3 &= -\eta + 2\eta^2, \\ \phi_4 &= 4\xi - 4\xi^2 - 4\xi\eta, \\ \phi_5 &= 4\xi\eta, \\ \phi_6 &= 4\eta - 4\xi\eta - 4\eta^2. \end{aligned} \quad (7.7)$$

for each of the velocity components and linear ansatz

$$\begin{aligned}\psi_1 &= 1 - \xi - \eta, \\ \psi_2 &= \xi, \\ \psi_3 &= \eta,\end{aligned}\tag{7.8}$$

for the pressure component are used. The relationship between the variables  $(x, y)$  on the real element and variables  $(\xi, \eta)$  on the reference element is as follows

$$\begin{aligned}x &= x_1 + (x_2 - x_1)\xi + (x_3 - x_1)\eta, \\ y &= y_1 + (y_2 - y_1)\xi + (y_3 - y_1)\eta.\end{aligned}\tag{7.9}$$

### 7.2.1 The stiffness matrix

The integral  $A = \int_{\Omega_h} \frac{\partial \varphi_i}{\partial x} \frac{\partial \varphi_j}{\partial x} + \frac{\partial \varphi_i}{\partial y} \frac{\partial \varphi_j}{\partial y} dx$  is expressed as a sum over each element such that

$$A = \sum_{k=1}^{Ne} \int_{T_k} \frac{\partial \varphi_i^k}{\partial x} \frac{\partial \varphi_j^k}{\partial x} + \frac{\partial \varphi_i^k}{\partial y} \frac{\partial \varphi_j^k}{\partial y} dxdy.$$

Transformation onto the reference element leads to

$$A = \sum_{k=1}^{Ne} J_k \int_{T_{ref}} \frac{\partial \phi_i}{\partial x} \frac{\partial \phi_j}{\partial x} + \frac{\partial \phi_i}{\partial y} \frac{\partial \phi_j}{\partial y} d\xi d\eta,$$

where the jacobian of transformation of element  $k$  is given by

$$J_k = (x_2^k - x_1^k)(y_3^k - y_1^k) - (x_3^k - x_1^k)(y_2^k - y_1^k).$$

Then the derivatives with respect to  $x$  are as follows:

$$\begin{aligned}\phi_{1x} &= \phi_{1\xi} \xi_x + \phi_{1\eta} \eta_x, & \phi_{1y} &= \phi_{1\xi} \xi_y + \phi_{1\eta} \eta_y, \\ \phi_{2x} &= \phi_{2\xi} \xi_x + \phi_{2\eta} \eta_x, & \phi_{2y} &= \phi_{2\xi} \xi_y + \phi_{2\eta} \eta_y, \\ \phi_{3x} &= \phi_{3\xi} \xi_x + \phi_{3\eta} \eta_x, & \phi_{3y} &= \phi_{3\xi} \xi_y + \phi_{3\eta} \eta_y, \\ \phi_{4x} &= \phi_{4\xi} \xi_x + \phi_{4\eta} \eta_x, & \phi_{4y} &= \phi_{4\xi} \xi_y + \phi_{4\eta} \eta_y, \\ \phi_{5x} &= \phi_{5\xi} \xi_x + \phi_{5\eta} \eta_x, & \phi_{5y} &= \phi_{5\xi} \xi_y + \phi_{5\eta} \eta_y, \\ \phi_{6x} &= \phi_{6\xi} \xi_x + \phi_{6\eta} \eta_x, & \phi_{6y} &= \phi_{6\xi} \xi_y + \phi_{6\eta} \eta_y.\end{aligned}\tag{7.10}$$

where  $\xi_x = \frac{y_3 - y_1}{J}$ ,  $\xi_y = \frac{y_1 - y_2}{J}$ ,  $\eta_x = \frac{x_1 - x_3}{J}$ ,  $\eta_y = \frac{x_2 - x_1}{J}$ , and the derivatives of the basis functions with respect to  $\xi$  and  $\eta$

$$\begin{aligned}\phi_{1\xi} &= -3 + 4\xi + 4\eta, & \phi_{1\eta} &= -3 + 4\eta + 4\eta, \\ \phi_{2\xi} &= -1 + 4\xi + 0\eta, & \phi_{2\eta} &= 0 + 0\eta + 0\eta, \\ \phi_{3\xi} &= 0 + 0\xi + 0\eta, & \phi_{3\eta} &= -1 + 0\eta + 4\eta, \\ \phi_{4\xi} &= 4 - 8\xi - 4\eta, & \phi_{4\eta} &= 0 - 4\eta + 0\eta, \\ \phi_{5\xi} &= 0 + 0\xi + 4\eta, & \phi_{5\eta} &= 0 + 4\eta + 0\eta, \\ \phi_{6\xi} &= 0 + 0\xi - 4\eta, & \phi_{6\eta} &= 4 - 4\eta - 8\eta.\end{aligned}\tag{7.11}$$

We can then proceed to compute the local  $6 \times 6$  stiffness matrix on the reference element and with the use of variables  $\xi_x, \xi_y, \eta_x, \eta_y$  and the Jacobian  $J_k$ , map this back onto the real local element  $k$ . Hence on an arbitrary triangle  $k$  we have

$$\begin{aligned}J_k \int_{T_{ref}} \frac{\partial \phi_i}{\partial x} \frac{\partial \phi_j}{\partial x} + \frac{\partial \phi_i}{\partial y} \frac{\partial \phi_j}{\partial y} d\xi d\eta &= a^k \int_{T_{ref}} \phi_{i\xi} \phi_{j\xi} d\xi d\eta \\ &\quad + b^k \int_{T_{ref}} (\phi_{i\xi} \phi_{j\eta} + \phi_{i\eta} \phi_{j\xi}) d\xi d\eta \\ &\quad + c^k \int_{T_{ref}} \phi_{i\eta} \phi_{j\eta} d\xi d\eta.\end{aligned}$$

Therefore over all indices  $i, j = 1, \dots, 6$ ,

$$\int_{T_k} \frac{\partial \varphi_i}{\partial x} \frac{\partial \varphi_j}{\partial x} + \frac{\partial \varphi_i}{\partial y} \frac{\partial \varphi_j}{\partial y} dx dy = a^k S_1 + b^k S_2 + c^k S_3,$$

where

$$S_1 = \frac{1}{6} \begin{bmatrix} 3 & 1 & 0 & -4 & 0 & 0 \\ 1 & 3 & 0 & -4 & 0 & 0 \\ 0 & 0 & 0 & 0 & 0 & 0 \\ -4 & -4 & 0 & 8 & 0 & 0 \\ 0 & 0 & 0 & 0 & 8 & -8 \\ 0 & 0 & 0 & 0 & -8 & 8 \end{bmatrix}, \quad S_2 = \frac{1}{6} \begin{bmatrix} 6 & 1 & 1 & -4 & 0 & -4 \\ 1 & 0 & -1 & -4 & 4 & 0 \\ 1 & -1 & 0 & 0 & 4 & -4 \\ -4 & -4 & 0 & 8 & -8 & 8 \\ 0 & 4 & 4 & -8 & 8 & -8 \\ -4 & 0 & -4 & 8 & -8 & 8 \end{bmatrix},$$

$$S_3 = \frac{1}{6} \begin{bmatrix} 3 & 0 & 1 & 0 & 0 & -4 \\ 0 & 0 & 0 & 0 & 0 & 0 \\ 1 & 0 & 3 & 0 & 0 & -4 \\ 0 & 0 & 0 & 8 & -8 & 0 \\ 0 & 0 & 0 & -8 & 8 & 0 \\ -4 & 0 & -4 & 0 & 0 & 8 \end{bmatrix},$$

and  $a^k = (x_{31}^k)^2 + (y_{31}^k)^2)/J_k$ ,  $b^k = -(x_{31}^k x_{21}^k + y_{31}^k y_{21}^k)/J_k$ ,  $c^k = (x_{21}^k)^2 + (y_{21}^k)^2)/J_k$ , and

$$x_{jl}^k = x_j^k - x_l^k, \quad y_{jl}^k = y_j^k - y_l^k, \quad j, l = 1, 2, 3.$$

**Remark 7.2.1.** The matrices  $S_1, S_2, S_3$  are computed once and stored. Only the coefficients  $a^k, b^k, c^k$ , and  $J_k$  change from element to element.

## 7.2.2 The div-grad matrices

Similarly the procedure is repeated for  $3 \times 6$  local stiffness matrices  $B_x|_{T_k}$  and  $B_y|_{T_k}$  defined as

$$\begin{aligned} B_x|_{T_k} &= -\sum_{k=1}^{Nel} J_k \int_{T_{ref}} \psi_k \frac{\partial \phi_i}{\partial x} dx, \quad k = 1, 2, 3, \quad i = 1, \dots, 6, \\ B_y|_{T_k} &= -\sum_{k=1}^{Nel} J_k \int_{T_{ref}} \psi_k \frac{\partial \varphi_i}{\partial y} dx, \end{aligned}$$

and over each local element and one can show that

$$B_x|_{T_k} = y_{31}^k C_1^T - y_{21}^k C_2^T, \quad B_y|_{T_k} = x_{21}^k C_2^T - x_{31}^k C_1^T,$$

where

$$C_1 = \begin{bmatrix} -1 & 0 & 0 \\ 0 & 1 & 0 \\ 0 & 0 & 0 \\ 1 & -1 & 0 \\ 1 & 1 & 2 \\ -1 & -1 & -2 \end{bmatrix}, \quad C_2 = \begin{bmatrix} -1 & 0 & 0 \\ 0 & 0 & 0 \\ 0 & 0 & 1 \\ -1 & -2 & -1 \\ 1 & 2 & 1 \\ 1 & 0 & 1 \end{bmatrix}.$$

### 7.2.3 The convective matrices

Suppose  $\mathbf{u}$  is known from the previous iteration step, then as we saw in Chapter 4, the convective matrices can be written as

$$\begin{aligned} C_{1,1}(\mathbf{u}) &= [c(\mathbf{u})_{i,j}], \quad c_{1,1}(\mathbf{u})_{i,j} = \int_{\Omega} \frac{\partial \phi_i}{\partial x} u_1 \phi_j + \frac{\partial \phi_i}{\partial y} u_2 \phi_j \, dx, \quad \text{for } i, j = 1 \dots n, \\ C_{2,2}(\mathbf{u}) &= [c(\mathbf{u})_{i,j}], \quad c_{2,2}(\mathbf{u})_{i,j} = \int_{\Omega} \frac{\partial \phi_i}{\partial x} u_1 \phi_j + \frac{\partial \phi_i}{\partial y} u_2 \phi_j \, dx, \quad \text{for } i, j = n \dots 2n. \end{aligned} \quad (7.12)$$

From (7.10-7.11),

$$\Phi_x = \Phi_\xi \xi_x + \Phi_\eta \eta_x,$$

where  $\Phi_\xi = A_1^T + A_2^T \xi + A_3^T \eta$ ,  $\Phi_\eta = B_1^T + B_2^T \xi + B_3^T \eta$  and

$$\begin{aligned} A_1 &= \begin{bmatrix} -3 & -1 & 0 & 4 & 0 & 0 \end{bmatrix}, \quad B_1 = \begin{bmatrix} -3 & 0 & -1 & 0 & 0 & 4 \end{bmatrix}, \\ A_2 &= \begin{bmatrix} 4 & 4 & 0 & -8 & 0 & 0 \end{bmatrix}, \quad B_2 = \begin{bmatrix} 4 & 0 & 0 & -4 & 4 & -4 \end{bmatrix}, \\ A_3 &= \begin{bmatrix} 4 & 0 & 0 & -4 & 4 & -4 \end{bmatrix}, \quad B_3 = \begin{bmatrix} 4 & 0 & 4 & 0 & 0 & -8 \end{bmatrix}, \end{aligned}$$

If  $\mathbf{U} = (U_1, U_2)$  is a vector field on an arbitrary triangle  $k$  with  $U_i \in \mathbb{R}^6$ . Then one can show as before, that the local convective matrix for each component can be evaluated as follows:

$$\sum_{k=1}^{Nel} J_k \int_{T_k} \frac{\partial \phi_i}{\partial x} u_1 \phi_j + \frac{\partial \phi_i}{\partial y} u_2 \phi_j \, dx = \mathcal{A} + \mathcal{B},$$

where

$$\begin{aligned} \mathcal{A} &= J_k M(U_1^T A_1 \xi_x + U_1^T B_1 \eta_x) + J_k P(U_1^T A_2 \xi_x + U_1^T B_2 \eta_x) + J_k Q(U_1^T A_3 \xi_x + U_1^T B_3 \eta_x), \\ \mathcal{B} &= J_k M(U_2^T A_1 \xi_y + U_2^T B_1 \eta_y) + J_k P(U_2^T A_2 \xi_y + U_2^T B_2 \eta_y) + J_k Q(U_2^T A_3 \xi_y + U_2^T B_3 \eta_y), \end{aligned}$$

and the  $6 \times 6$  matrices  $M, P, Q$  are defined as

$$M = \int_{T_{ref}} \phi_i \phi_j \, d\xi \, d\eta, \quad P = \int_{T_{ref}} \xi \phi_i \phi_j \, d\xi \, d\eta \quad \text{and} \quad Q = \int_{T_{ref}} \eta \phi_i \phi_j \, d\xi \, d\eta.$$

These matrices can be easily computed on the reference element, e.g., one can show that

$$M = \frac{1}{360} \begin{bmatrix} 6 & -1 & -1 & 0 & -4 & 0 \\ -1 & 6 & -1 & 0 & 0 & -4 \\ -1 & -1 & 6 & -4 & 0 & 0 \\ 0 & 0 & -4 & 32 & 16 & 16 \\ -4 & 0 & 0 & 16 & 32 & 16 \\ 0 & -4 & 0 & 16 & 16 & 32 \end{bmatrix}.$$

## 7.3 Derivative of a finite element solution

Since our sensitivity information involve derivatives of the finite element solution with respect to Cartesian coordinates  $x$  and  $y$ . It is therefore important to illustrate how such information can be obtained. If  $u_h$  denoted the approximation of  $u$  by the  $N$  dimensional basis  $\{\phi_i\}_{i=1}^N$  such that

$$u_h = \sum_{i=1}^N u_i \phi_i(x, y),$$

then

$$\frac{\partial u_h}{\partial x} = \sum_{i=1}^N u_i \frac{\partial \phi_i(x, y)}{\partial x}, \quad \frac{\partial u_h}{\partial y} = \sum_{i=1}^N u_i \frac{\partial \phi_i(x, y)}{\partial y}. \quad (7.13)$$

Since each basis  $\phi_i$  has a local support in element  $K$  of the triangulation, we can express (7.13) as follows,

$$\begin{pmatrix} (u_x)_1 \\ (u_x)_2 \\ \vdots \\ (u_x)_k \end{pmatrix} = \begin{pmatrix} u(x_1^1)\phi_{1x}^1 + u(x_2^1)\phi_{2x}^1 + u(x_3^1)\phi_{3x}^1 \\ u(x_1^2)\phi_{1x}^2 + u(x_2^2)\phi_{2x}^2 + u(x_3^2)\phi_{3x}^2 \\ \vdots \\ u(x_1^k)\phi_{1x}^k + u(x_2^k)\phi_{2x}^k + u(x_3^k)\phi_{3x}^k \end{pmatrix}. \quad (7.14)$$

where  $x_i^k$  means  $x_i$  in element  $K$  and similarly  $\phi_{ix}^k$  means derivative of  $\phi_i$  with respect to  $x$  in element  $k$ . In equation (7.14), a piecewise linear basis is with degree of freedom in the nodes of the triangulation is chosen. As an example let us consider the following triangulation .

It is convenient to work on the reference element with the  $P_2$  basis functions expressed in (7.7). The relationship between the variables  $(x, y)$  on the real element and variables  $(\xi, \eta)$  on the reference element is given in (7.9). We obtain the derivatives of the basis functions with respect to  $\xi$  and  $\eta$  which is expressed in (7.11). Then the derivatives with respect to  $x$  follows as shown in (7.10). Then with respect to the triangulation in Figure 7.1, we have on element 1 with local

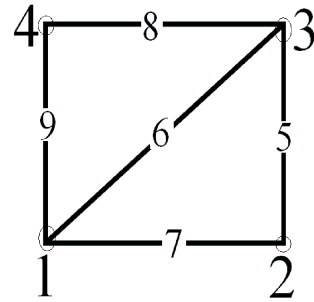


Figure 7.1: Typical triangulation

index numbering  $I = [1, 2, 3, 5, 6, 7]$ ,

$$\begin{aligned} \mathbf{u}_x^1 &= \left( (u_x)_1^1 \quad (u_x)_2^1 \quad (u_x)_3^1 \quad (u_x)_5^1 \quad (u_x)_6^1 \quad (u_x)_7^1 \right)^T \\ &= u(x_1, y_1) \begin{pmatrix} \phi_{1x}(x_1, y_1) & \phi_{1x}(x_2, y_2) & \phi_{1x}(x_3, y_3) & \phi_{1x}(x_5, y_5) & \phi_{1x}(x_6, y_6) & \phi_{1x}(x_7, y_7) \end{pmatrix}^T \\ &+ u(x_2, y_2) \begin{pmatrix} \phi_{2x}(x_1, y_1) & \phi_{2x}(x_2, y_2) & \phi_{2x}(x_3, y_3) & \phi_{2x}(x_5, y_5) & \phi_{2x}(x_6, y_6) & \phi_{2x}(x_7, y_7) \end{pmatrix}^T \\ &+ u(x_3, y_3) \begin{pmatrix} \phi_{3x}(x_1, y_1) & \phi_{3x}(x_2, y_2) & \phi_{3x}(x_3, y_3) & \phi_{3x}(x_5, y_5) & \phi_{3x}(x_6, y_6) & \phi_{3x}(x_7, y_7) \end{pmatrix}^T \\ &+ u(x_5, y_5) \begin{pmatrix} \phi_{4x}(x_1, y_1) & \phi_{4x}(x_2, y_2) & \phi_{4x}(x_3, y_3) & \phi_{4x}(x_5, y_5) & \phi_{4x}(x_6, y_6) & \phi_{4x}(x_7, y_7) \end{pmatrix}^T \\ &+ u(x_6, y_6) \begin{pmatrix} \phi_{5x}(x_1, y_1) & \phi_{5x}(x_2, y_2) & \phi_{5x}(x_3, y_3) & \phi_{5x}(x_5, y_5) & \phi_{5x}(x_6, y_6) & \phi_{5x}(x_7, y_7) \end{pmatrix}^T \\ &+ u(x_7, y_7) \begin{pmatrix} \phi_{6x}(x_1, y_1) & \phi_{6x}(x_2, y_2) & \phi_{6x}(x_3, y_3) & \phi_{6x}(x_5, y_5) & \phi_{6x}(x_6, y_6) & \phi_{6x}(x_7, y_7) \end{pmatrix}^T. \end{aligned}$$

Similarly on element 2 with local index numbering  $I = [1, 3, 4, 8, 9, 6]$ , we can obtain

$$\mathbf{u}_x^2 = \left( (u_x)_1^2 \quad (u_x)_3^2 \quad (u_x)_4^2 \quad (u_x)_8^2 \quad (u_x)_9^2 \quad (u_x)_6^2 \right)^T,$$

as illustrated above. Therefore the approximation to the derivative is given by

$$\mathbf{u}_x = \begin{pmatrix} (u_x)_1 \\ (u_x)_2 \\ (u_x)_3 \\ (u_x)_4 \\ (u_x)_5 \\ (u_x)_6 \\ (u_x)_7 \\ (u_x)_8 \\ (u_x)_9 \end{pmatrix} = \begin{pmatrix} \frac{1}{2}((u_x)_1^1 + (u_x)_1^2) \\ (u_x)_2^1 \\ \frac{1}{2}((u_x)_3^1 + (u_x)_3^2) \\ (u_x)_4^2 \\ (u_x)_5^1 \\ \frac{1}{2}((u_x)_6^1 + (u_x)_6^2) \\ (u_x)_7^1 \\ (u_x)_8^2 \\ (u_x)_9^2 \end{pmatrix}.$$

## 7.4 Numerical integration

All finite element methods, with the exception of point collocation-based ones, are based on weak forms that are expressed as integrals over the domain  $\Omega$  and its boundary  $\partial\Omega$  (or parts of it). Let us consider here the integral

$$\int_{\Omega_h} f(x, y) \, dx dy.$$

This integral is ultimately evaluated as a sum of integrals over the single element domain  $T_j$  to obtain

$$\int_{\Omega_h} f(x, y) \, dx dy = \sum_{j=1}^{Nel} \int_{T_j} f(x, y) \, dx dy.$$

The linear mapping

$$\begin{aligned} x &= x_1 + (x_2 - x_1)\xi + (x_3 - x_1)\eta, \\ y &= y_1 + (y_2 - y_1)\xi + (y_3 - y_1)\eta, \end{aligned} \tag{7.15}$$

transforms an arbitrary triangle  $T_j$  with coordinates  $(x_1, y_1), (x_2, y_2), (x_3, y_3)$  to one with coordinates  $(\xi_1, \eta_1), (\xi_2, \eta_2), (\xi_3, \eta_3)$  respectively, where  $(\xi_1, \eta_1) = (0, 0)$ ,  $(\xi_2, \eta_2) = (1, 0)$  and  $(\xi_3, \eta_3) = (0, 1)$ . If we denote by  $I_j$  the transformation of integral  $\int_{T_j} f(x, y) \, dx dy$  onto the reference triangle  $T_{ref}$  such that

$$I_j = J_j \int_{T_{ref}} f(\xi, \eta) \, d\xi d\eta, \tag{7.16}$$

where  $J_j$  is the jacobian of transformation of element  $T_j$ . Approximating (7.16) using Gauss-quadrature gives

$$I_j \approx J_j \sum_{k=1}^n W_k f(\xi_k, \eta_k), \quad (7.17)$$

where  $(\xi_k, \eta_k)$  are evaluation points for the quadrature,  $W_k$  are the weights of the evaluation points, and  $n$  is the total number of the evaluation points. Hence

$$\int_{\Omega_h} f(x, y) dx dy \approx \sum_{j=1}^{Nel} J_j \sum_{k=1}^n W_k f(\xi_k, \eta_k). \quad (7.18)$$

Gauss integration rules designed for triangular elements are tabulated in [Hughes 1987, pp. 173-174].

#### 7.4.1 Integration of a finite element solution

In our work, the discrete objective functionals are expressed as integrals of a discrete finite element solution. Therefore provided that we have computed the solution, we can evaluate, for example

$$\int_{\Omega_h} u_h dx, \quad (7.19)$$

as follows:

$$\int_{\Omega_h} u_h dx = \sum_{i=1}^N u_i \int_{\Omega_h} \phi_i(x, y) dx dy. \quad (7.20)$$

Using (7.18)

$$\int_{\Omega_h} \phi_i(x, y) dx dy = \sum_{j=1}^{Nel} J_j \sum_{k=1}^n W_k \phi_i^j(\xi_k, \eta_k), \quad (7.21)$$

where  $i = 1, 2, 3$  for  $P_1$  ansatz functions and  $i = 1, 2, \dots, 6$  for  $P_2$  ansatz functions. Over all the degrees of freedom in the triangulation, we have

$$\int_{\Omega_h} \phi_i(x, y) dx dy = \mathbf{I} \in \mathbb{R}^N, \beta = 1 \dots, N. \quad (7.22)$$

Therefore

$$\int_{\Omega_h} u_h dx = \mathbf{I}^T \mathbf{U}, \text{ where } \mathbf{U} = [u_1, \dots, u_N]^T. \quad (7.23)$$



## BIBLIOGRAPHY

- [Adams 1975] R. A. Adams. Sobolev spaces. Academic Press, New York, 1975.
- [Allaire 2006] G. Allaire and O. Pantz. *Shape optimization with Freefem++*. Structural and Multidisciplinary Optimization, vol. 32, 2006.
- [Ameur 2004] H. B. Ameur, M. Burger and B. Hackl. *Level set methods for geometric inverse problems in linear elasticity*. Inverse Problems, vol. 20, no. 3, pages 673–696, 2004.
- [Bach 1998] M. Bach, C. Constanda, G. C. Hsiao, A. M. Sandig and P. Werner. Analysis, numerics and applications of differential and integral equations, vol. 379. Research Notes in Mathematics Series. Addison Wesley Longman Limited, USA, 1998.
- [Benzi ] M. Benzi, G. H. Golub and J. Liesen. *Numerical Solution of Saddle Point Problems*. Acta Numerica, vol. 32.
- [Blackburn 1996] H. M. Blackburn, N. N. Mansour and B. J. Cantwell. *Topology of fine-scale motions in turbulent channel flow*. Journal of Fluid Mechanics, vol. 310, pages 269–292, 1996.
- [Boisgérault 1993] S. Boisgérault and J. P. Zolésio. Shape derivative of sharp functionals governed by navier-stokes flow. In W. Jäger, J. Necás, O. Johh, K. Najzar, and J stará, editors. Partial Differential Equations: Theory and Numerical Solution, pages 49–63. Chapman & Hall/CRC Reseach Notes in Mathematics, 1993.
- [Boland 1983] J. Boland and R. Nicolaides. *The Stability of Finite Elements Under Divergence Constraints*. SIAM Journal on Numerical Analysis, vol. 20, no. 4, pages 722–731, 1983.
- [Boulkhemair 2007] A. Boulkhemair and A. Chakib. *On the Uniform Poincaré Inequality*. Communications in Partial Differential Equations, vol. 32, no. 9, pages 1439–1447, 2007.

- [Chenais 1975] D. Chenais. *On the existence of a solution in a domain identification problem.* J. Math. Anal and Appl., vol. 52, pages 189–219, 1975.
- [Chong 1990] M. S. Chong, A. E. Perry and B. J. Cantwell. *A general classification of three-dimensional flow fields.* Physics of Fluids, vol. 2, no. 5, pages 765–777, May 1990.
- [Cuvelier 1986] C. Cuvelier, A. Segal and A. A. Van Steenhoven. Finite element methods and navier-stokes. D. Reidel publishing company, 1986.
- [Cuvelier 1990] C. Cuvelier and R. M. S. M. Schulkes. *Some numerical methods for the computation of capillary free boundaries governed by the Navier-Stokes equations.* SIAM Rev., vol. 32, no. 3, pages 355–423, 1990.
- [Davis 1999] T. A. Davis and I. S. Duff. *A combined unifrontal/multifrontal method for unsymmetric sparse matrices.* ACM Trans. Math. Softw., vol. 25, no. 1, pages 1–20, 1999.
- [Davis 2004] T. A. Davis. *Algorithm 832: UMFPACK V4.3—an unsymmetric-pattern multifrontal method.* ACM Trans. Math. Softw., vol. 30, no. 2, pages 196–199, 2004.
- [Delfour 2001] M. C. Delfour and J. P. Zolésio. Shapes and geometries: analysis, differential calculus, and optimization. Society for Industrial and Applied Mathematics, Philadelphia, PA, USA, 2001.
- [Elman 1994] H. C. Elman and G. H. Golub. *Inexact and preconditioned Uzawa algorithms for saddle point problems.* SIAM J. Numer. Anal., vol. 31, no. 6, pages 1645–1661, 1994.
- [Evans 1998] L. C. Evans. Partial differential equations. American Mathematical Society, 1998.
- [Fulmanski 2008] P. Fulmanski, A. Laurain, J. F Scheid and J. Sokolowski. *Level set method with topological derivatives in shape optimization.* Int. J. Comput. Math., vol. 85, no. 10, pages 1491–1514, 2008.
- [Gartling 1994] D. K. Gartling and J. N. Reddy. The finite element method in heat transfer and fluid dynamics. Taylor & Francis Inc, 1994.
- [Girault 1986] V. Girault and P. A. Raviart. Finite element methods for navier-stokes. Springer-Verlag, Berlin, 1986.
- [Grisvard 1985] P. Grisvard. Elliptic problems in nonsmooth domains, monographs and studies in mathematics, vol. 24. Pitman, Massachusetts, 1985.
- [Gunzburger 1989] M. D. Gunzburger. Finite element methods for viscous incompressible flows. Academic Press, San Diego, 1989.

- [Hadamard ] J. Hadamard. Mémoire sur le problème d'analyse relatif à l'équilibre des plaques élastiques encastrées, Mémoires des Savants Etrangers vol. 33 (1908).
- [Haller 2001] G. Haller. *Lagrangian structures and the rate of strain in a partition of two-dimensional turbulence*. Physics of Fluids, vol. 13, no. 11, pages 3365–3385, 2001.
- [Haller 2005] G. Haller. *An objective definition of a vortex*. Journal of Fluid Mechanics, vol. 525, pages 1–26, 2005.
- [Haslinger 2003] J. Haslinger and R. A. E. Mäkinen. Introduction to shape optimization: Theory, approximation, and computation. Society for Industrial and Applied Mathematics, Philadelphia, PA, USA, 2003.
- [Haslinger 2009] J. Haslinger, K. Ito, T. Kozubek, K. Kunisch and G. Peichl. *On the shape derivative for problems of Bernoulli type*. Interfaces and Free Boundaries, vol. 11, no. 2, pages 317–330, 2009.
- [Hecht a] F. Hecht. BAMG: Bidimensional anisotropic mesh generator, <http://www.rocq.inria.fr/gamma/cdrom/www/bamg/eng.html>, 1998.
- [Hecht b] F. Hecht and O. Pironneau. FreeFEM++ Manual, Laboratoire Jacques Louis Lions, 2005, FreeFem++ is a free software available at: <http://www-rocq.inria.fr/Frederic.Hecht/freefem++.html>.
- [Henrot 2009] A. Henrot and Y. Privat. *What is the optimal shape of a pipe?* Archive for Rational Mechanics and Analysis, vol. 196, no. 1, pages 281–302, 2009.
- [Heywood 1996] J. G. Heywood, R. Rannacher and S. Turek. *Artificial boundaries and flux and pressure conditions for the incompressible Navier-Stokes equations*. International Journal for Numerical Methods in Fluids, vol. 22, no. 5, pages 325–352, 1996.
- [Hintermüller 2004] M. Hintermüller, K. Kunisch, Y. Spasov and S. Volkwein. *Dynamical systems based optimal control of incompressible fluids*. Int. J. Numer. Methods in Fluids, vol. 4, pages 345–359, 2004.
- [Hughes 1987] T. J. R. Hughes. The finite element method. New Jersey, USA, 1987.
- [Ito 2006] K. Ito, K. Kunisch and G. Peichl. *Variational approach to shape derivatives for a class of Bernoulli problems*. Journal of Mathematical Analysis and Applications, vol. 314, no. 1, pages 126–149, 2006.

- [Jenny ] M. Jenny and M. Souhar. *Numerical simulation of a film coating flow at low capillary numbers*. Computers & Fluids, vol. 38.
- [Jeong 1995] J. Jeong and F. Hussain. *On the identification of a vortex*. Journal of Fluids Mechanics, vol. 285, pages 69–94, 1995.
- [Juntunen 2009] M. Juntunen and R. Stenberg. *Nitsche’s method for general boundary conditionsn*. Mathematics of Computation, vol. 78, no. 267, pages 1353–1374, 2009.
- [Kaplan 1967] W. Kaplan. Ordinary differential equations. Addison-Wesley, Reading, Mass, 1967.
- [Karakashian 1982] O. Karakashian. *On a Galerkin-Lagrange Multiplier Method for the Stationary Navier-Stokes Equations*. SIAM J. Numer. Anal., vol. 19, no. 5, pages 909–923, 1982.
- [Kärkkäinen 1999] K. T. Kärkkäinen and T. Tiihonen. *Free surfaces: shape sensitivity analysis and numerical methods*. Int. J. Numer. Meth. Engrg., vol. 44, no. 8, pages 1079–1098, 1999.
- [Kawahara 1984] M. Kawahara and T. Miwa. *Finite element analysis of wave motion*. International Journal for Numerical Methods in Engineering, vol. 20, no. 7, pages 1193–1210, 1984.
- [Kawahara 1987] M. Kawahara and B. Ramaswamy. *Lagrangian finite element analysis applied to viscous free surface fluid flow*. International Journal for Numerical Methods in Engineering, vol. 953, no. 7, 1987.
- [Kesslerand 1999] D. P. Kesslerand and R. A. Greenkorn. Momentum, heat, and mass transfer fundamentals. Marcel Dekker, Inc, 1999.
- [Kundu 1990] P. Kundu. Fluid mechanics. Academic Press, New York,, 1990.
- [Kunisch 2007] K. Kunisch and B. Vexler. *Optimal Vortex Reduction for Instationary Flows Based on Translation Invariant Cost Functionals*. SIAM J. Control Optim., vol. 46, no. 4, pages 1368–1397, 2007.
- [Ladyzhenskaya 1969] O. A. Ladyzhenskaya. The mathematical theory of viscous incompressible flow. Gordon and Breach, New York, 1969.
- [Laumen 1999] M. Laumen. *Newton’s Method for a Class of Optimal Shape Design Problems*. SIAM J. on Optimization, vol. 10, no. 2, pages 503–533, 1999.

- [Lehnhäuser 2005] T. Lehnhäuser and M. Schäfer. *A numerical approach for shape optimization of fluid flow domains*. Computer Methods in Applied Mechanics and Engineering, vol. 194, no. 50-52, pages 5221 – 5241, 2005.
- [Li ] J. Li, M. Hesse, J. Ziegler and A. W. Woods. *An arbitrary Lagrangian Eulerian method for moving-boundary problems and its application to jumping over water*. Journal of Computational Physics, vol. 208.
- [Liu 2007] Z. Liu and J. G. Korvink. *Structural Shape Optimization Using Moving Mesh Method*. European Comsol Conference, 2007.
- [Losasso 2006] F. Losasso, R. Fedkiw and S. Osher. *Spatially adaptive techniques for level set methods and incompressible flow*. Computers and Fluids, vol. 35, no. 10, pages 995 – 1010, 2006.
- [Martinec ] D. Martinec. *Lecture notes on Continuum Mechanics*. [PDF document] Retrieved from Lecture Notes Online. Web site: <http://geo.mff.cuni.cz/vyuka/Martinec-ContinuumMechanics.pdf>.
- [Monk 2003] P. Monk. Finite element methods for maxwell's equations. Oxford University Press, 2003.
- [Nocedal 1999] J. Nocedal and S. J. Wright. Numerical optimization. Springer, 1999.
- [Osher 1988] S. Osher and J. A. Sethian. *Fronts propagating with curvature-dependent speed: algorithms based on Hamilton-Jacobi formulations*. J. Comput. Phys., vol. 79, no. 1, pages 12–49, 1988.
- [Peterson 1999] R. C. Peterson, P. K. Jimack and M. A. Kelmanson. *The solution of two-dimensional free-surface problems using automatic mesh generation*. International Journal for Numerical Methods in Fluids, vol. 31, no. 6, pages 937–960, 1999.
- [Pironneau 1984] O. Pironneau. Optimal shape design for elliptic systems. Springer-Verlag, Berlin, 1984.
- [Pironneau 2001] O. Pironneau and B. Mohammadi. Applied shape optimization in fluids. Oxford University Press Inc, Newyork, 2001.
- [Quarteroni 1997] A. Quarteroni and A. Valli. Numerical approximation of partial differential equations. Springer-Verlag, Berlin, 1997.
- [Schwarz 1991] H. R. Schwarz. Methode der finiten elemente. Teubner, Stuttgart, 1991.

- [Sethian 1999] J. A. Sethian. level set methods and fast matching methods. Cambridge University Press, USA, 1999.
- [Simon 1980] J. Simon. *Differentiation with respect to the domain in boundary value problems*. Numer. Funct. Anal. Optim., vol. 2, no. 7-8, pages 649–687 (1981), 1980.
- [Sokolowski 1992] J. Sokolowski and J. P. Zolésio. Introduction to shape optimization. shape sensitivity analysis. Springer-Verlag, 1992.
- [Temam 1977] R. Temam. Navier stokes equations: Theory and numerical analysis (studies in mathematics and its applications 2. North-Holland, 1977.
- [Toivanen 2008] J. I. Toivanen, J. Haslinger and R. A. E. Mäkinen. *Shape optimization of systems governed by Bernoulli free boundary problems*. Computer Methods in Applied Mechanics and Engineering, vol. 197, no. 15, pages 3803–3815, 2008.
- [Tropea 2007] C. Tropea, A. L. Yarin and J. F. Foss. Springer handbook of experimental fluid mechanics. Springer-Verlag, New York, USA, October 2007.
- [VanLohuizen 1996] E. P. VanLohuizen, P. J. Slikkerveer and S. B. G. O'Brien. *An implicit surface tension algorithm for picard solvers of surface-tension-dominated free and moving boundary problems*. International Journal for Numerical Methods in Fluids, vol. 22, no. 9, pages 851–65, 1996.
- [Wei 1996] S. Wei, R. W. Smith, H. S. Udaykumar and M. M. Rao. Computational fluid dynamics with moving boundaries. Taylor & Francis, Inc., Bristol, PA, USA, 1996.